CHIRAL SULFURIZATION FOR SYNTHESIS OF ANTISENSE OLIGONUCLEOTIDES

by

JOSHUA ANDREW MUKHLALL

A dissertation submitted to the Graduate Faculty in Chemistry in partial fulfillment of the requirements for the degree of Doctor of Philosophy, The City University of New York

2010

This manuscript has been read and accepted for the Graduate Faculty in Chemistry in satisfaction of the dissertation requirement for the degree of Doctor of Philosophy.

_____	_____
Date	Professor William H. Hersh Chair of Examining Committee
_____	_____
Date	Professor Mahesh K. Lakshman Executive Officer
	_____
	Professor Robert Bittman
	_____
	Professor David R. Mootoo Supervisory Committee

THE CITY UNIVERSITY OF NEW YORK

Abstract

CHIRAL SULFURIZATION FOR SYNTHESIS OF ANTISENSE OLIGONUCLEOTIDES

by

Joshua Andrew Mukhlall

Research Advisor: Professor William H. Hersh

Chapter 1: Antisense and RNA interference (RNAi) reagents are two of the most widely studied oligonucleotide-based therapeutics. Phosphorothioate oligonucleotide, an antisense reagent, has a stereogenic center at the phosphorothioate linkage and in the absence of enantioselective synthesis, a mixture of diastereomers results. Stereodefined phosphorothioates have shown greater antisense activity; however, only a few research groups have successfully designed methods for enantioselective synthesis of phosphorothioates with >98% de, albeit in low yields. This dissertation presents a conceptually different method for enantioselective synthesis of phosphorothioate oligonucleotides via a Curtin-Hammett system that requires epimerization of the phosphite triester on the reaction time scale and selective sulfurization of one of the equilibrating epimers with a chiral sulfurizing reagent.

Chapter 2: 2-Cyanoethyl[5'-*O*-acetyl-2'-deoxythymylyl]-(3',5')-3'-*O*-(acetyl)-2'-deoxythymidine phosphite triester was found to invert at 150 ºC with $\Delta G^{\dagger} = 33.0 \pm 0.2$ kcal/mol. Separation of the two diastereomers of the phosphite triester was successfully achieved via its 2-cyanoethyl[5'-*O*-(*p,p*'-dimethoxytrityl)-2'-deoxythymylyl]-(3',5')-3'-*O*-(*tert*-butyldimethylsilyl)-

2'-deoxythymidine boranophosphate analogue. For the inversion study the *p,p*'-dimethoxytrityl and *tert*-butyldimethylsilyl groups were substituted with acetyl groups to reduce decomposition during heating. Attempts to induce inversion at lower temperature with acidic and radical species failed.

Chapter 3: Chiral analogues of phenylacetyl disulfide (PADS) and 5-methyl-3*H*-1,2,4-dithiazol-3-one (MEDITH) were synthesized from the same α-alkylated carboxylic acids to give products with enantiomeric purities of 99.0 to >99.9% and 86.1-99.4%, respectively. X-ray diffraction results for one pair of enantiomers unequivocally establish the absolute configurations of two disulfides, and density functional theory (DFT) calculations suggest that the observed high specific rotations could be due to preferred retention of helicity about the S–S bond in solution.

Chapter 4: Phosphite triesters with varying degrees of steric hindrance around the phosphorus atom (β-cyanoethyl, TMS, TBDMS, and TPS derivatives) were screened against chiral analogues of PADS and MEDITH. The R_{PS}:S_{PS} diastereomeric ratios of the resulting phosphite sulfides or phosphorothioates were determined by reverse-phase HPLC, and a numerical procedure was developed to express the diastereoselectivity of the reactions. The best selectivities to give R_{PS} enriched and S_{PS} enriched phosphorothioates were achieved with MEDITH analogues (*S*)-**6d** (naproxen derivative) (14.7% de) and (*S*)-**6c** (isopropyl group at the α position) (-7.9% de), respectively, when reacted with the phosphite triester bearing the TMS group.

Table of Contents

List of Schemes

Chapter 1

Chapter 2

Chapter 3

Chapter 4

List of Tables

Chapter 2

Chapter 3

Chapter 4

List of Figures and Charts

Chapter 1

Chapter 2

Chapter 3

Chapter 4

Abbreviations

BSA	*N*,*O*-bis(trimethylsilyl)acetamide
CPG	controlled pore glass
DABCO	1,4-diazabicyclo[2.2.2]octane
DBU	1,4-diazabicyclo[5.4.0]undec-7-ene
de	diastereomeric excess
DFT	density functional theory
DMTr	dimethoxytrityl
DNA	deoxyribonucleic acid
ds	diastereoselectivity
equiv	equivalent
HRMS	high resolution mass spectrometry
MEDITH	5-methyl-3*H*-1,2,4-dithiazol-3-one
mRNA	messenger ribonucleic acid
NMI	N-methylimidazole
NMR	nuclear magnetic resonance
Nucleobases:	
A	adenine
T	thymine
U	uracil
G	guanine
C	cytosine
PADS	phenylacetyl disulfide

PTFA	pyridinium trifluoroacetate
RP HPLC	reverse phase high pressure liquid chromatography
RNAi	ribonucleic acid interference
rt	room temperature
siRNA	short interfering RNA
TBAF	tetra-*n*-butylammonium fluoride
TBDMSCl	*t*-butyldimethylsilylchloride
TEAA	triethylammonium acetate
TEAB	triethylammonium bicarbonate
TLC	thin-layer chromatography
TMG	1,1,3',3'-tetramethylguanidine
TMSCl	trimethylsilylchloride
TPS	triphenylsilylchloride
tRNA	transfer ribonucleic acid

Chapter 1

Oligonucleotides as therapeutics

1.1 General introduction

Pharmaceutical treatment of diseases can in principle be handled by two approaches: (1) synthesis of active compounds (small molecules) to target specific proteins e.g. enzymes or receptors, that are responsible for certain diseases, and (2) therapeutic intervention at the level of the nucleic acids which are responsible for the synthesis of the disease-causing proteins.[1] The latter approach has attracted immense interest over the last 30 years since the discovery made in 1978 by Zemecnik and Stephenson that the growth of the Rous sarcoma virus could be inhibited in cell culture by a single-stranded 13-mer oligodeoxynucleotide that was complementary to the RNA of the virus.[2, 3] With this revelation and the improvements made over the years in the methods of DNA sequencing and oligonucleotide synthesis, there have been vast amounts of research done to produce single-stranded oligodeoxynucleotides for clinical testing on a variety of diseases such as cancer, HIV infections, asthma, and diabetes. [4, 5] These single-stranded compounds used in clinical trials are typically in the range of 15 – 25 nucleotides in length and are called antisense oligonucleotides based on their binding to the target sequence (sense strand).[1, 6]

RNA interference (RNAi) is another more recently discovered oligonucleotide-based therapeutic, which resulted in the award of the Nobel Prize in Medicine in 2006 to A. Fire and C. Mello.[7-10] RNAi is an evolved mechanism for genome defense in many organisms,[10] but its activity was discovered only about 15 years ago and since then has been investigated as a potential nucleotide-based therapeutic for numerous diseases. Unlike antisense reagents, RNAi

involves double-stranded oligonucleotides which have also been shown to inhibit protein expression in a sequence-specific manner in cell culture.[11]

The precise mechanisms for the activity of antisense and RNAi oligonucleotides are not fully understood. However, they are both post-transcriptional gene silencing methods that occur in the cytoplasm of the cell and entail the binding (hybridization) of the heterocyclic bases of the antisense DNA or the antisense (guide) strand of the double-stranded RNA to the complementary target mRNA by Watson-Crick base pairing (Figure 1). Cellular enzymes are then activated that selectively degrade mRNA, releasing the antisense DNA or RNA to bind to more mRNA, leading to catalytic use of the reagent.

Figure 1. Watson – Crick base pairing

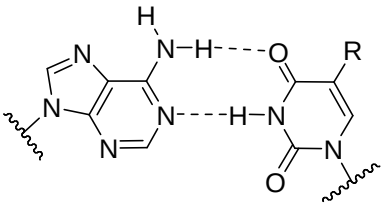

Hydrogen bonding in

A·T (R = CH_3) or A·U (R = H) base pair

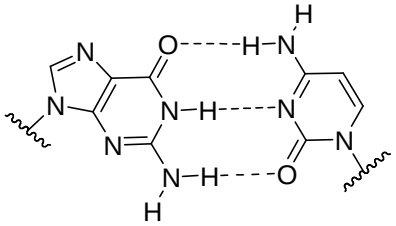

Hydrogen bonding in

a G·C base pair

Scheme 1 illustrates a simple representation of the proposed mechanism of an antisense reagent. The usual pathway for protein synthesis begins in the nucleus.[12] The template strand of the DNA is transcribed by RNA polymerases to give mRNA which then goes through a splicing process. This process is mediated by a RNA/protein complex called a spliceosome that removes introns (noncoding sequences) and stitches together the exons (coding sequences) to give the mature mRNA. The single-stranded matured mRNA migrates out into the cytoplasm where

Scheme 1. Possible mechanism by which antisense oligonucleotides block protein synthesis

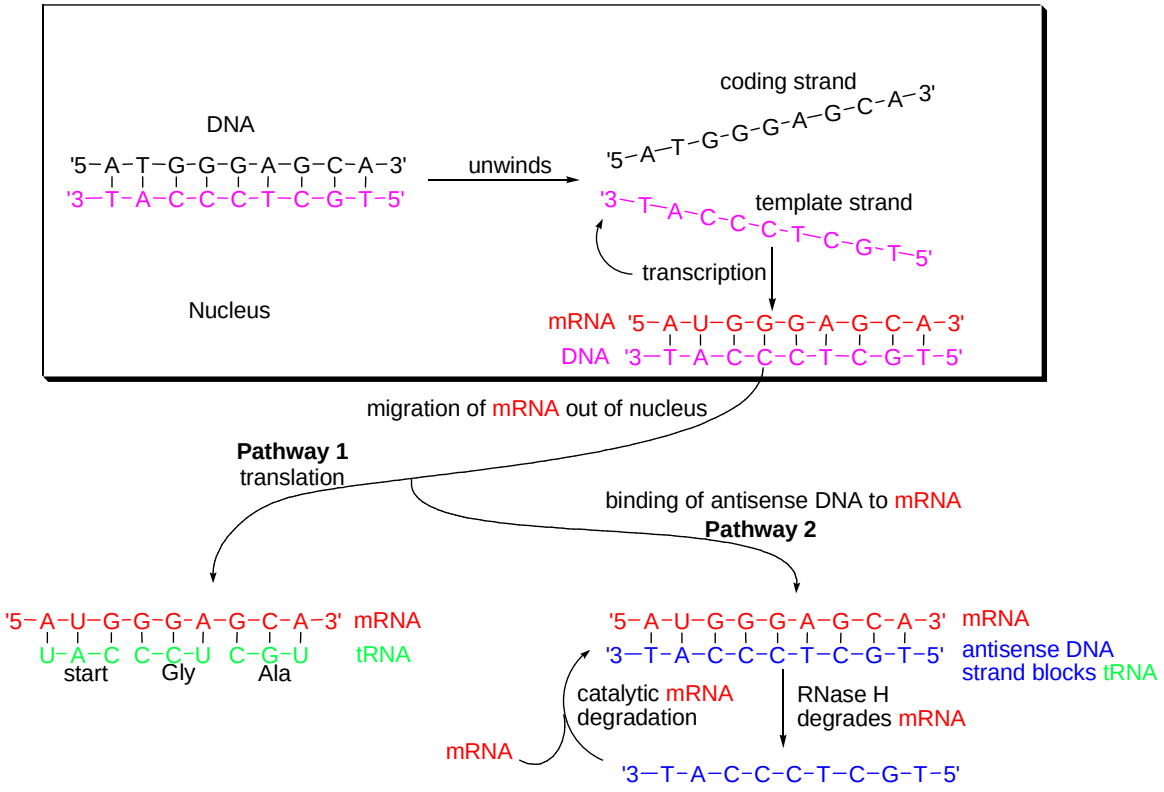

protein synthesis occurs (pathway 1) by translation, which is mediated by ribosomes. Translation involves complementary base pairing of each three-nucleotide codon on the mRNA with the three-nucleotide anticodon on the tRNA, which brings a specific amino acid. The process starts at the start codon AUG, and the ribosome moves along the mRNA, translating the nucleotide sequence one codon at a time eventually giving the polypeptide (protein) encoded in the mRNA. At the end of this process, a release factor binds to the stop codon, terminating translation and releasing the protein from the ribosome. However, in the presence of an antisense reagent, inhibition of protein synthesis can occur (pathway 2). By processes still unknown, the antisense strand comes into close proximity and binds to the mRNA. The duplex formed blocks the ribosome from binding and thus prevents translation of the protein encoded in

the mRNA sequence. The antisense DNA-RNA duplex formed can activate the cellular enzyme RNase H which degrades the mRNA strand in the hybrid duplex and releases the antisense strand so that it can be used catalytically for binding to more mRNA. Although the precise mechanism is not known, physical blockage and activation of RNase H are the two most widely accepted mechanisms for the inhibition of protein expression by antisense oligonucleotides.[13]

The proposed mechanism of RNA interference (RNAi) is illustrated in scheme 2.[14] The mechanism involves cleavage of double-stranded RNA (ds RNA) present in the cytoplasm by cellular enzymes called "Dicer" (a RNase III-family enzyme) at specific sites to give shorter double-stranded fragments of 21-25 nucleotides called short interfering RNA (siRNA).[15] These naturally generated siRNA fragments, which can also be synthesized and introduced into the cytoplasm,[11, 16] consist of the guide strand (antisense strand) and the passenger strand (sense strand) with overhanging nucleotides on one or both strands. The siRNA is incorporated into an inactive ribonucleoprotein complex that unwinds the duplex and degrades the sense strand to give an active RNA-induced silencing complex (RISC). The complex facilitates the binding of the guide strand to the target mRNA, which is then cleaved at defined positions by a component of RISC called the Argonaute-2 protein (Ago-2). The resulting mRNA fragments are subsequently degraded by several cellular nucleases, thus releasing the active RISC-antisense complex to incorporate and bind to other mRNA molecules.

There are currently over thirty antisense oligonucleotides[13, 17] and only a few RNAi reagents in clinical trials. However, the fact that only one antisense reagent (Fomivirsen) has been approved by the FDA suggests that there may be physiological problems with these approaches.[13] That is, although both approaches have shown promising results in vitro, they both appear to suffer some major problems when used in vivo, and this has been detrimental for

Scheme 2. Possible mechanism by which RNAi oligonucleotides block protein synthesis

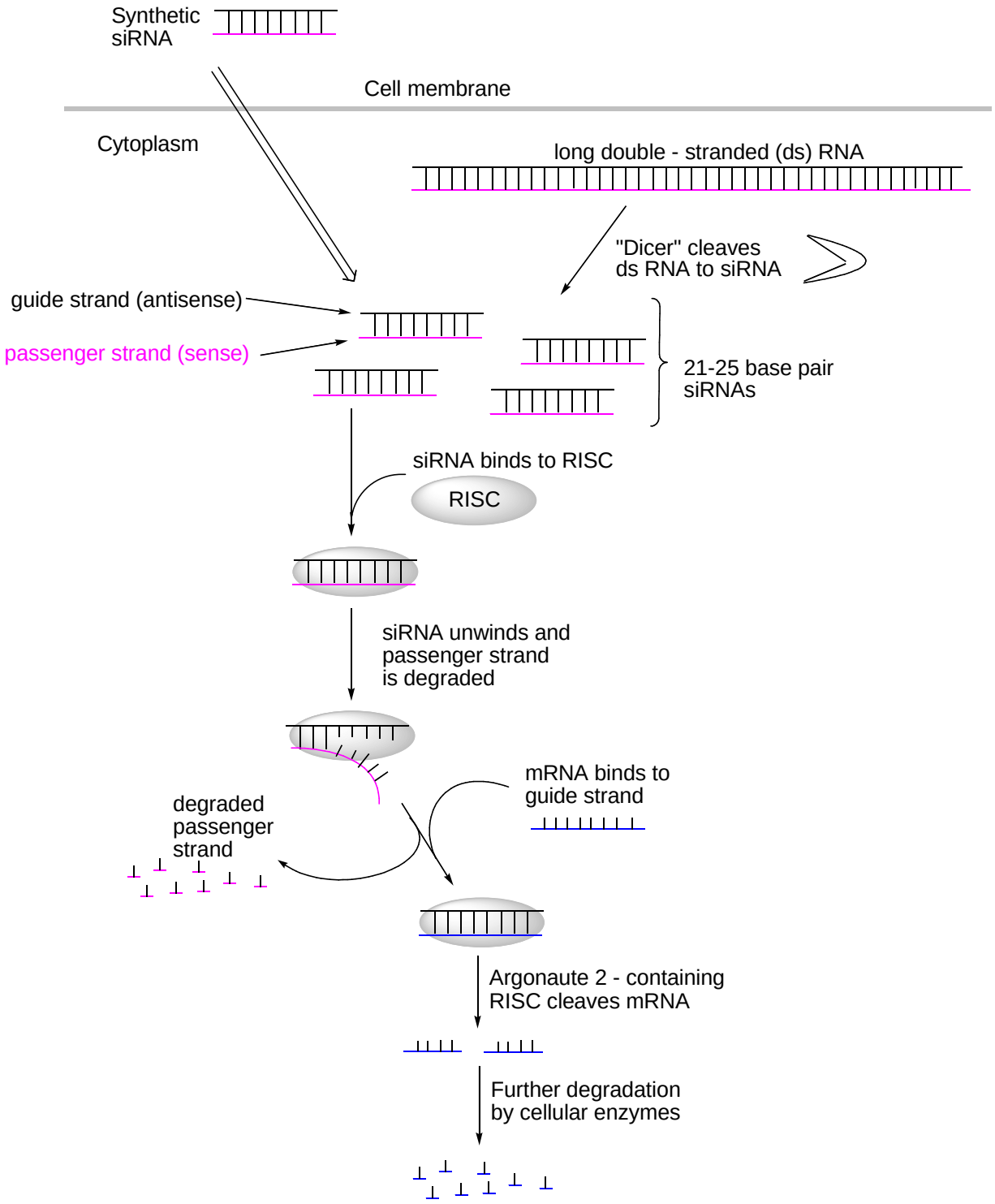

their success as compounds for drug use. Some of the problems include difficulty in the delivery of the large polyanionic single-stranded antisense DNA (~5034 Da for 15-mer, T) or double-stranded RNA (~16164 Da for 23-mer, A·U) into the target cells, structure-specific (sequence-independent) effects due to protein binding, and "irrelevant cleavage" of mRNA by coincidental homology to a short sequence of the full antisense reagent.[18] Sequence-specific effects were also observed where the mere presence of motifs such as CG and GGGG in the antisense reagents and CG in RNAi reagents were found to stimulate the immune system via Toll-like receptors (TLRs),[13, 19, 20] a system that protects cells from bacterial and viral infections by recognition of non-mammalian sequence patterns. These immunostimulatory effects have since been taken advantage of and there are several oligonucleotides with the CG motif currently being tested in clinical trials for the sole purpose of stimulating the immunue system for treatment of diseases such as cancer, asthma, and allergies.[19] However, to harness antisense activity from antisense oligonucleotides for clinical studies, the TLR effect must be avoided by excluding the CG motif from the oligonucleotides.[13, 19, 21]

Because RNAi activity is an evolutionarily conserved gene silencing mechanism, its therapeutic activity in vitro has been found to be more specific than antisense oligodeoxynucleotides, which most likely bind to the target mRNA by a diffusion-controlled, non-enzymatic process. While this might account for the apparent increase in popularity of RNAi over antisense DNA in the last 5-8 years (based on the number publications cited in PubMed),[13] there are several advantages of the antisense approach that make it attractive for continued research. Antisense oligonucleotides are half the molecular weight (single-stranded reagents) and potentially will be delivered more efficiently into the target cells in vivo, do not require the hybridization step during synthesis and so large-scale preparation of the compound is

simplified, and have been vigorously studied for over 30 years, proving a wealth of data on its failures and successes for future progress. There have also been examples where the activities of some antisense oligonucleotides have been comparable or better than those obtained with RNAi.

1.2 Phosphorothioate oligonucleotides as antisense reagents

While natural phosphodiester DNA possesses some desirable properties for antisense use, it undergoes rapid degradation in the presence of nucleases. A number of modifications on the nucleobase, the sugar ring, and the phosphate backbone of natural oligonucleotides have been proposed (Figure 2).[1] However, because hydrogen bonding is needed to elicit antisense activity,

Figure 2. Proposed position for modification of natural DNA for antisense reagents

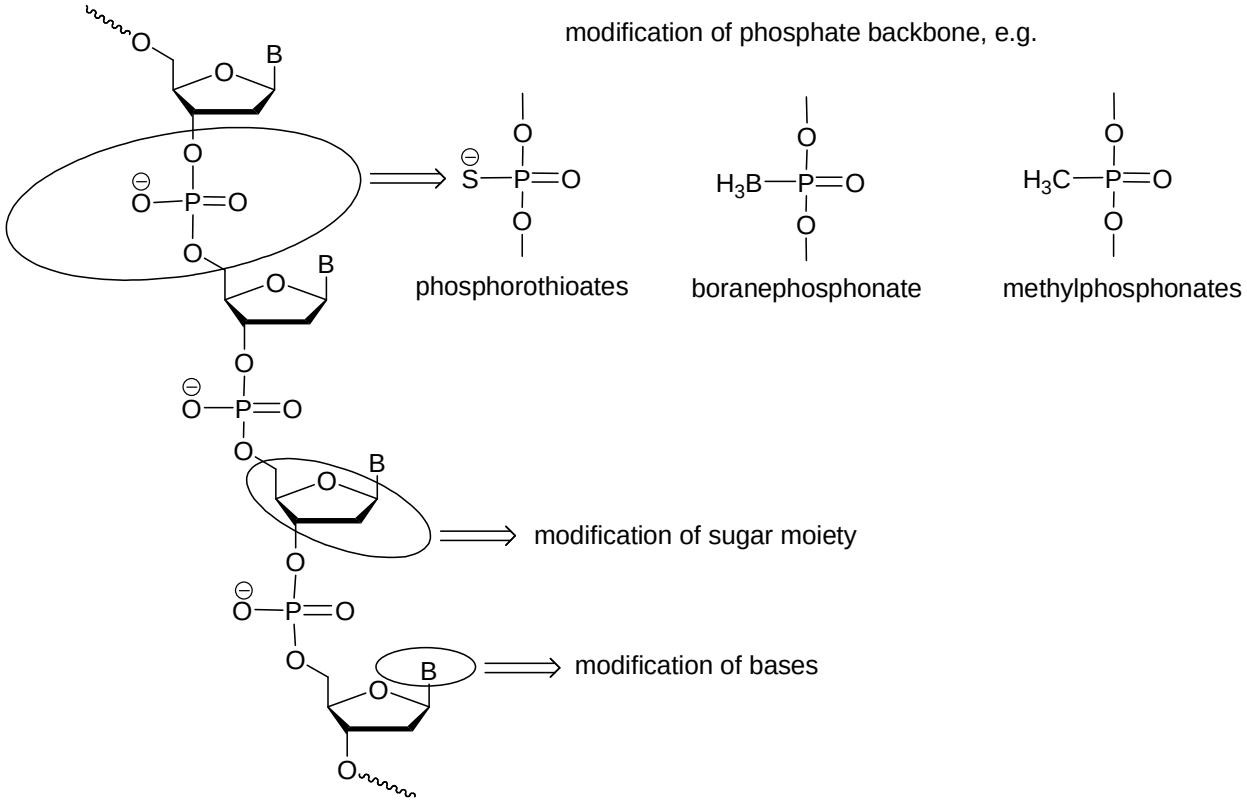

modifications made on the phosphate backbone, rather than on the bases or sugar ring, to generate compounds such as phosphorothioates, boranephosphonate, and methylphosphonates

have been studied extensively. The one modified oligonucleotide that has been most widely studied for the last 30 years is the phosphorothioate oligonucleotide. It binds efficiently to mRNA, is nuclease-resistant, and can activate RNase H for selective degradation of the target mRNA. Phosphorothioates differ from natural DNA by replacement of one of the phosphodiester oxygen atoms not involved in the bridge by a sulfur atom. Substitution of an oxygen atom with a sulfur atom creates a new stereogenic center, which results in a mixture of diastereomers in the absence of an enantioselective synthesis.

The synthesis of phosphorothioate oligonucleotides can be carried out as easily as that of DNA oligonucleotides via solid phase synthesis by the phosphoramidite (Scheme 3)[22-25] or H-phosphonate method (Scheme 4).[26, 27] The phosphoramidite method begins with the addition of a phosphoramidite molecule to a growing DNA strand bound to a solid support via tetrazole-induced coupling. The phosphite triester obtained is oxidized with I_2/H_2O for the natural DNA cycle, or sulfurized with a disulfide reagent such as Beaucage's reagent[28] to give the phosphite sulfide in ~ 50:50 ratios (R_P and S_P diastereomers) for the phosphorothioate cycle. The sulfurizing step is followed by the capping step (acylation), which stop chain elongation of any 5'-hydroxyl nucleoside that failed the coupling step. The dimethoxytrityl (DMTr) group at the 5' position of the phosphite sulfide is removed with dichloroacetic acid to give the free 5'-hydroxyl nucleotide, which restarts the cycle by undergoing coupling with another phosphoramidite molecule. This is followed with another sulfurization, capping, and detritylation step. This procedure is repeated until the desired length of nucleotide is attained. At the conclusion of the synthesis, reaction with ammonium hydroxide simultaneously cleaves the strand from the solid support, cleaves all the protecting groups on the bases, and cleaves the β-cyanoethoxy group to

release acrylonitrile and give the phosphorothioate. A typical yield for phosphorothioate obtained by the phosphoramidite method is ~72% for a 20-mer nucleotide.[29]

Scheme 3. Phosphoramidite method for synthesis of phosphorothioate oligonucleotides

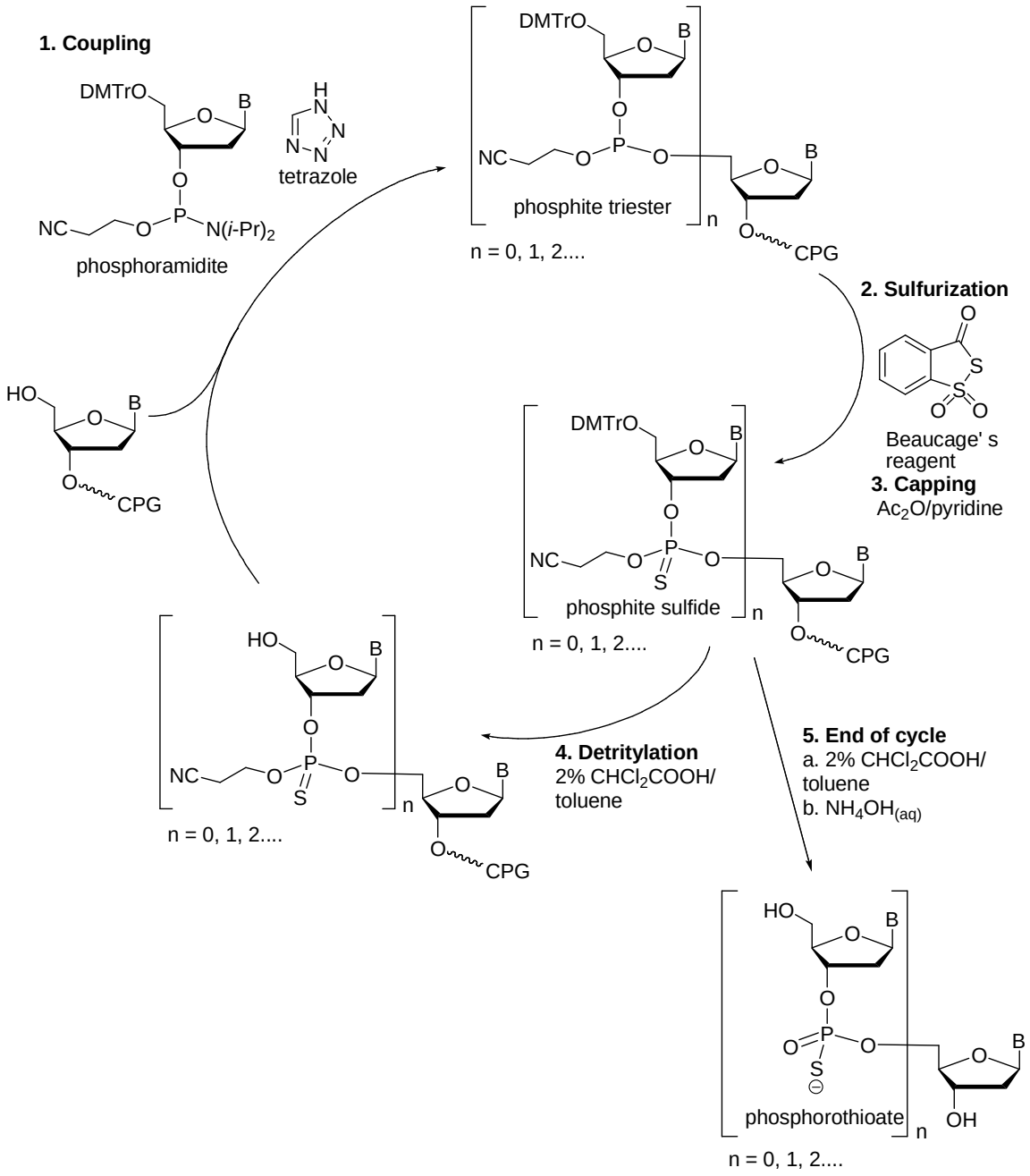

For the H-phosphonate method (Scheme 4), the mononucleoside H-phosphonate is coupled (using pivaloyl chloride) to the growing DNA strand bound to a solid support to give the

Scheme 4. H-Phosphonate method for synthesis of phosphorothioate oligonucleotides

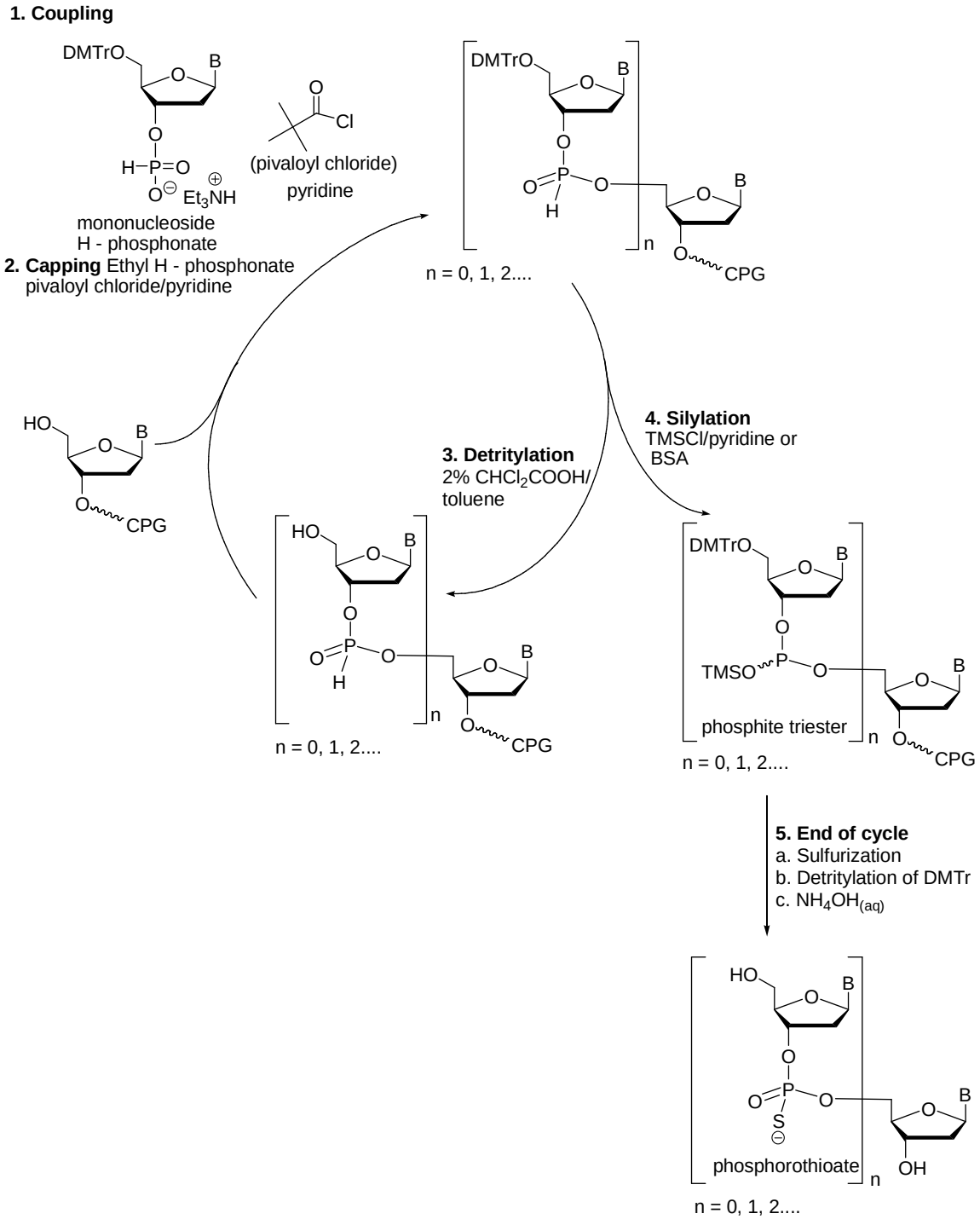

dinucleoside H-phosphonate in a ~ 60:40 ratio. After the coupling step, capping is done with ethyl H-phosphonate (i.e., another coupling reaction), followed by detritylation of the DMTr group. The procedure is repeated until the desired length of nucleotide is attained. Unlike the phosphoramidite method, the sulfurization reaction is done once at the end of the synthesis of the oligonucleoside. For this step, the H-phosphonate is first converted to the phosphite triester with *N,O*-bis(trimethylsilyl)acetamide (BSA) and then reacted with a sulfurizing reagent such as sulfur to give the phosphite sulfide. After the removal of the DMTr group with dichloroacetic acid, release of the nucleotide from the solid support and deprotection of the bases are accomplished with ammonium hydroxide.

Currently all phosphorothioate oligonucleotides in clinical trials are synthesized by the phosphoramidite method as a random mixture of diastereomers. For instance, Fomivirsen, a 21-mer oligonucleotide for the treatment of cytomegalovirus (CMV) retinitis, would consist of a mixture of 2^{20} = 1048576 diastereomers when prepared without an enantioselective synthesis. Although Fomivirsen and other phosphorothioates have been tested as a mixture of diastereomers, several in vitro studies have used stereodefined phosphorothioates obtained from a low yield chemical synthesis and enzymatic-assisted method.[30-32] The latter method allows for stereoselective synthesis of only [all-R_P] phosphorothioates. The studies have shown that many properties of phosphorothioates, such as binding affinity to the complementary RNA, stability to nucleases, and RNase H activity, are affected by the configuration of the phosphorous atoms and that phosphorothioates with properly arranged R_P and/or S_P internucleotidic linkages might have a better potential as antisense molecules.[33] One can imagine that the cell might be conducting gene-silencing by combinatorial chemistry, where only a small sub-set of the mixture of diastereomers present is effective, and of course if that sub-set could be found and synthesized, a

significantly smaller dose could be used; Stec and co-workers pointed this out in the 1990's,[30, 34] albeit without the language of combinatorial chemistry. In addition, it was recently discovered that DNA from *Streptomyces lividans* and related bacteria that was degraded during electrophoresis gave stereodefined phosphorothioate dinucleotides with the R_P configurations of $G_{PS}A$ and $G_{PS}G$.[35, 36]

1.3 Stereodefined phosphorothioate oligonucleotides

For a more extensive study of stereodefined phosphorothioates as antisense reagents, a practical method that permits their large scale preparation is highly desired. Several groups have developed methods with varying degrees of success but those designed by Stec,[37, 38] Beaucage,[39] and Wada[40] gave stereodefined phosphorothioates of greater than 98% diastereomeric excess on solid phase synthesis.

1.3.1 Stec's method for synthesis of stereodefined phosphorothioate oligonuclotides

Stec's tetracoordinate phosphorus synthons **1**-**3**[37, 38] (Scheme 5) were designed so that the two diastereomers of each compound differed sufficiently in asymmetry for them to be separated by column chromatography. The R_P and S_P diastereomers of compounds **1**-**3** were obtained in an approximately 1:1 mixture, and after tedious silica gel chromatography the separated diastereomers were obtained in ~15-17% yields for **1**-**2** (with nucleosides Thy, Ade^{Bz}, Cyt^{Bz}, and Gua^{iBu}) and 78-86% yields for **3** with nucleosides Thy, Ade^{Bz}, and Cyt^{Bz}. Diastereomerically pure compounds (**1**-**3**) were used for solid-phase synthesis, in which the coupling step required a large excess of precursor (**1**-**3**) and DBU. The yields of the phosphorothioates obtained varied between 5 and 26% depending on the nucleobase and the length of the nucleotide.

Scheme 5. Stec's method for stereoselective synthesis of phosphorothioates

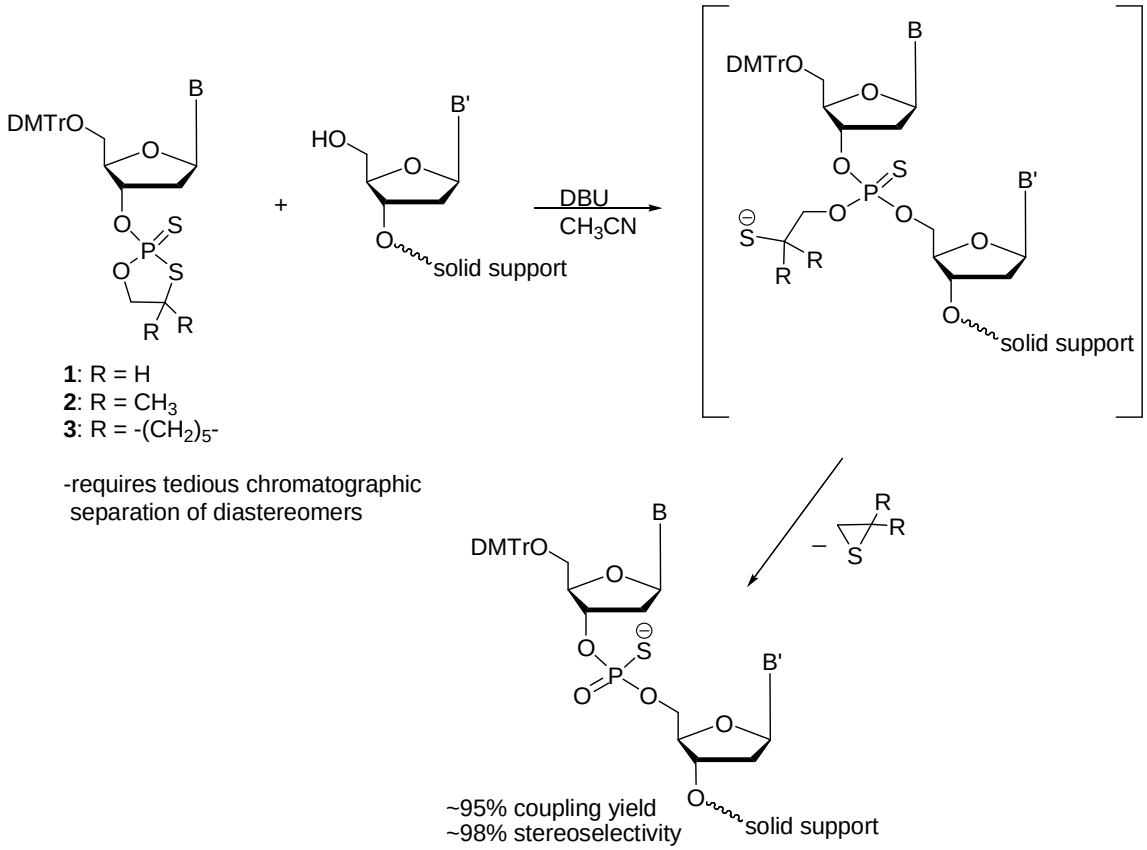

1.3.2 Beaucage's method for synthesis of stereodefined phosphorothioate oligonuclotides

Beaucage's method[39] (Scheme 6) begins by treating racemic 1,2-amino alcohol **4** with ethyl fluoroacetate, followed by hexaethylphosphorus triamide to give cyclic compound **5**. 5'-*O*-(4,4'-Dimethoxytrityl)-2'-deoxythymidine **6** was then coupled to **5** using 1*H*-tetrazole to give a mixture of the S_P and R_P configurations of *N*-acyl phosphoramidites **7**. Compound **7** was relatively unstable on silica gel, and only low yields of ~23% of each diastereomer were obtained after silica gel chromatography. After S_P-**7** was coupled to a 5'-hydroxyl nucleoside with 1,1,3,3-tetramethylguanidine, the resulting phosphite triester **8** was sulfurized to give a nearly quantitative yield and total P-stereospecificity. Solid-phase syntheses were carried out to

prepared [R_P, R_P] and [S_P, S_P]-d($C_{PS}C_{PS}C_{PS}$) and [R_P, S_P, R_P]-d($C_{PS}C_{PS}C_{PS}C_{PS}$) with total P-stereospecificity.[39]

Scheme 6. Beaucage's method for stereoselective synthesis of phosphorothioates

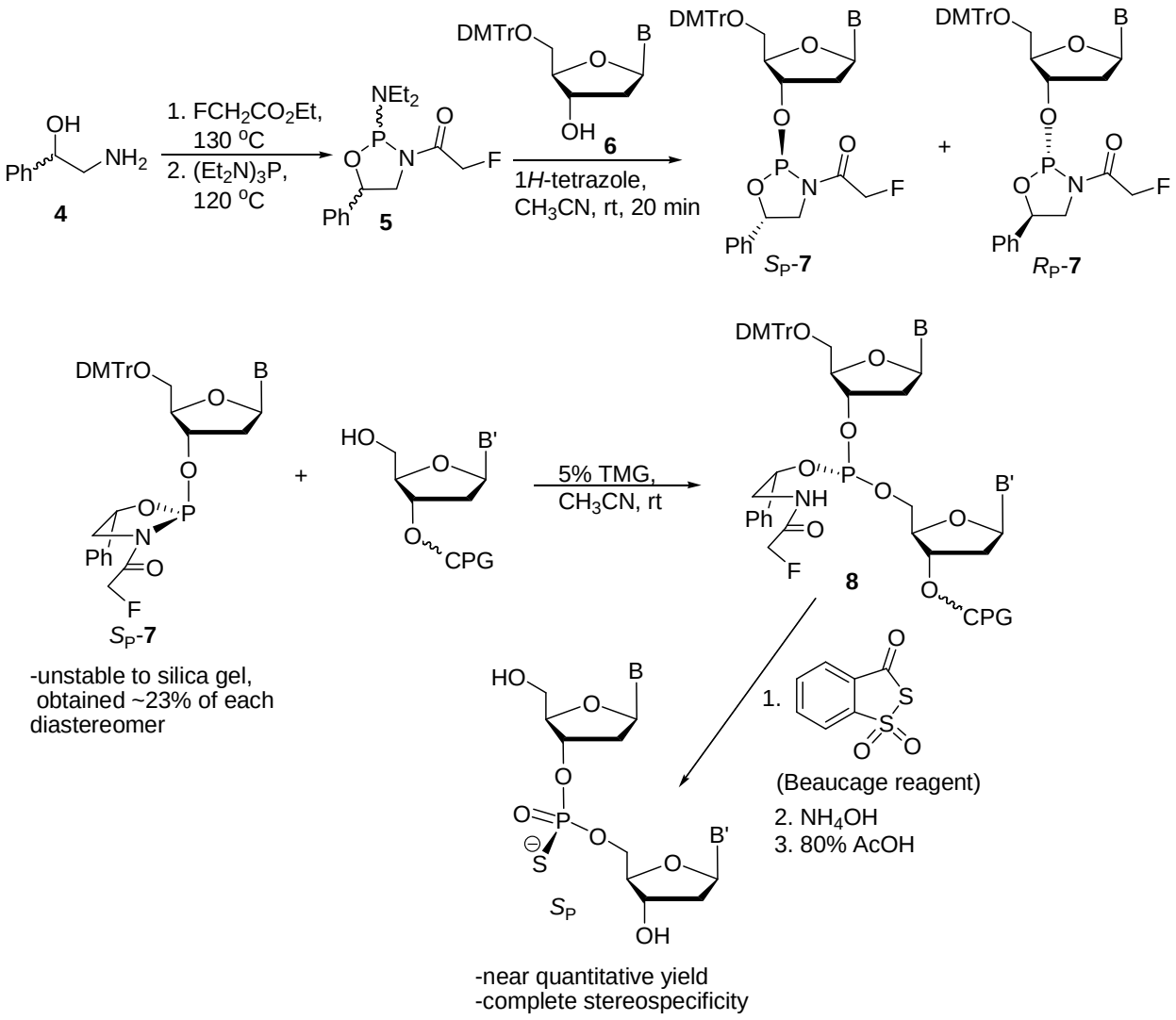

1.3.3 Wada's method for synthesis of stereodefined phosphorothioate oligonuclotides

Using Wada's method[40] (Scheme 7), a dinucleotide phosphorothioate oligonucleotide with the S_P configuration was prepared from 1,2-amino alcohol (1*R*, 2*S*)-**9** (Scheme 7); the R_P configuration

Scheme 7. Wada's method for stereoselective synthesis of phosphorothioates

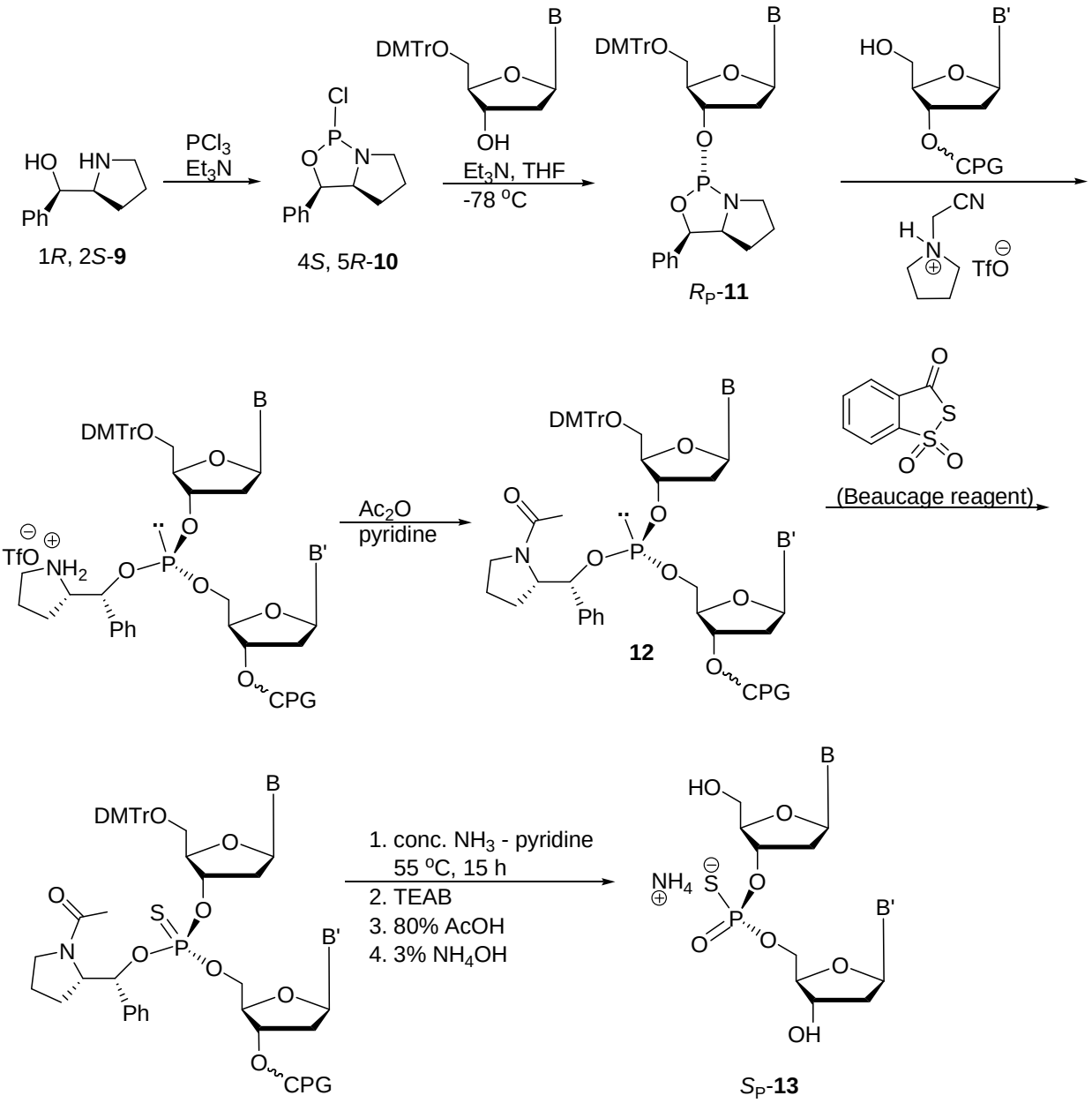

was obtained from 1,2-amino alcohol (1*S*, 2*R*)-**9**. For instance, the synthesis of a S_P phosphorothioate dinucleotide begins by treating 1,2-amino alcohol (1*R*, 2*S*)-**9** with PCl_3 to give (4*S*, 5*R*)-**10**. Compound (4*S*, 5*R*)-**10** could then be treated with a 5'-*O*-(4,4'-dimethoxytrityl)-2'-

deoxynucleoside to give R_P-**11** as a mixture of trans:cis diastereomers in the ratio of >99:1; trans signifies that the Ph group is trans to the nucleoside. The product was found to be unstable on silica gel and was obtained in only ~50% yield after silica gel chromatography. After coupling of R_P-**11** to a 5'-hydroxyl nucleoside, the resulting phosphite triester **12** was sulfurized to give S_P-**13** in 97% yield and S_P:R_P stereospecificity of >99:1. However, synthesis of longer phosphorothioate oligonucleotides resulted in lower yields; for example a 10-mer was obtained in 32% yield and a 12-mer in only 12% yield.

Although the three methods described above gave products with excellent diastereomeric excess, none of the methods have been used for large-scale preparation of stereodefined phosphorothioates. The reasons might be a combination of the difficulty in obtaining the two diastereomers of the phosphorylating reagents and the low yields of the phosphorothioate oligonucleotides obtained from solid-phase synthesis. Therefore, the development of an improved method for enantioselective phosphorothioate synthesis is still needed.

1.4 A conceptually new method for enantioselective synthesis of phosphorothioates

We propose in this thesis a conceptually different method that involves the use of chiral sulfurizing reagents for enantioselective synthesis of stereodefined phopshorothioates. The method we propose will retain most of the features of current oligonucleotide synthesis that are amenable to large-scale synthesis. The method is a classic Curtin-Hammett system[41] that requires the following two parts (Figure 3): (1) rapid epimerization of the phosphite triester **14** and (2) selective sulfurization of one of the equilibrating epimers with a chiral sulfurizing reagent. If epimerization at the phosphorus is fast enough so that both P-epimers (R_P and S_P) are made available on a synthetic time-scale, then it would be possible to convert all the phosphite triester (R_P and S_P) to a single phosphorothioate by addition of the selective sulfurizing reagent.

Figure 3. Curtin-Hammett sulfurization of epimerizing phosphite

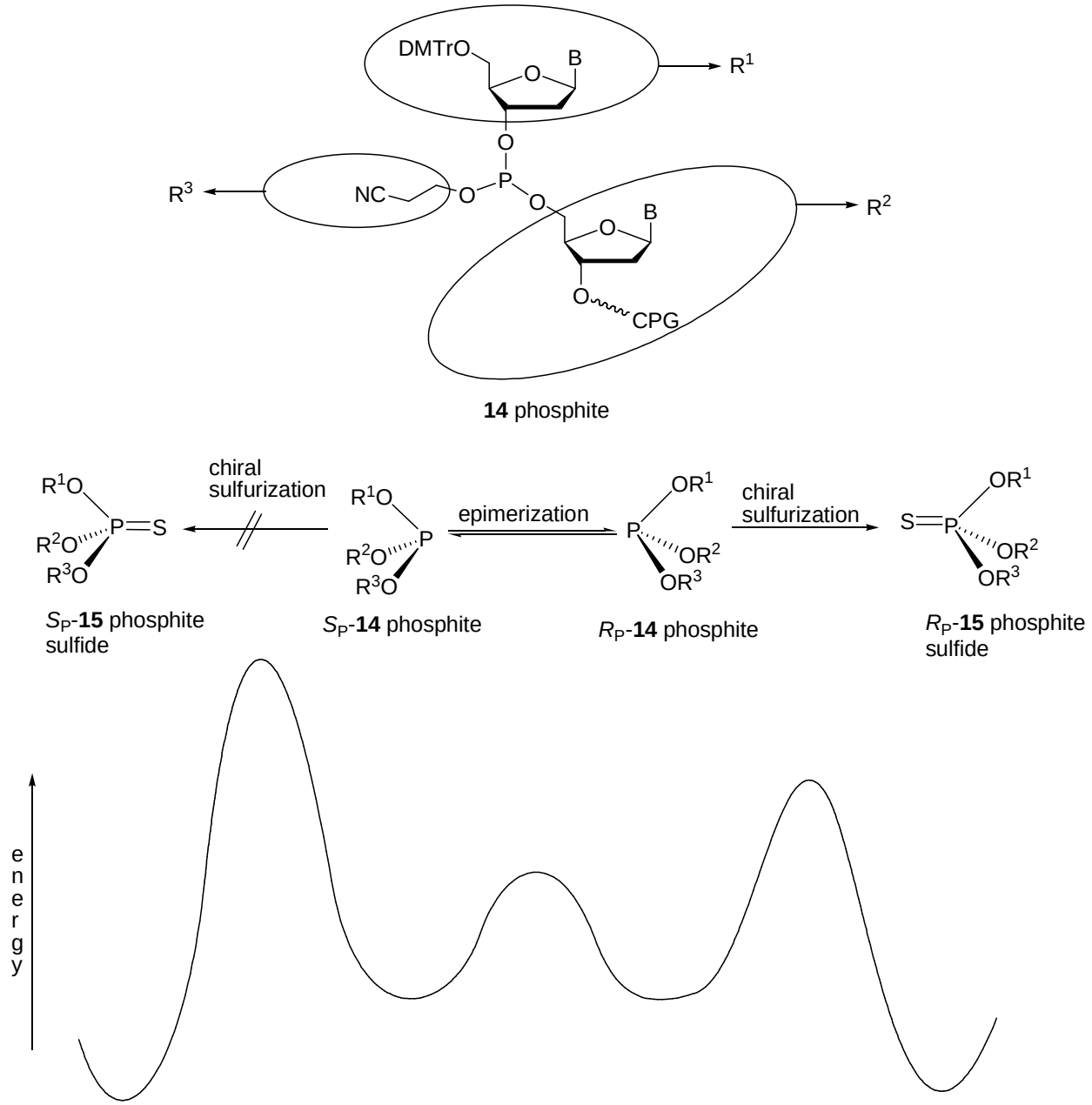

In principle, since phosphite **14** is a mixture of diastereomers, a chiral sulfurizing reagent is not needed for selective sulfurization, but in practice use of a chiral reagent seems to be the most reasonable way to achieve selectivity.

A precedent for our proposal comes from work by Mikolajczyk et al. on chiral oxidation and sulfurization of phosphines (Scheme 8).[42, 43] For example, oxidation of racemic P-chiral

Scheme 8. Kinetic resolution of phosphines by stoichiometric oxidation and sulfurization; Curtin-Hammett oxidation of a chlorophosphine

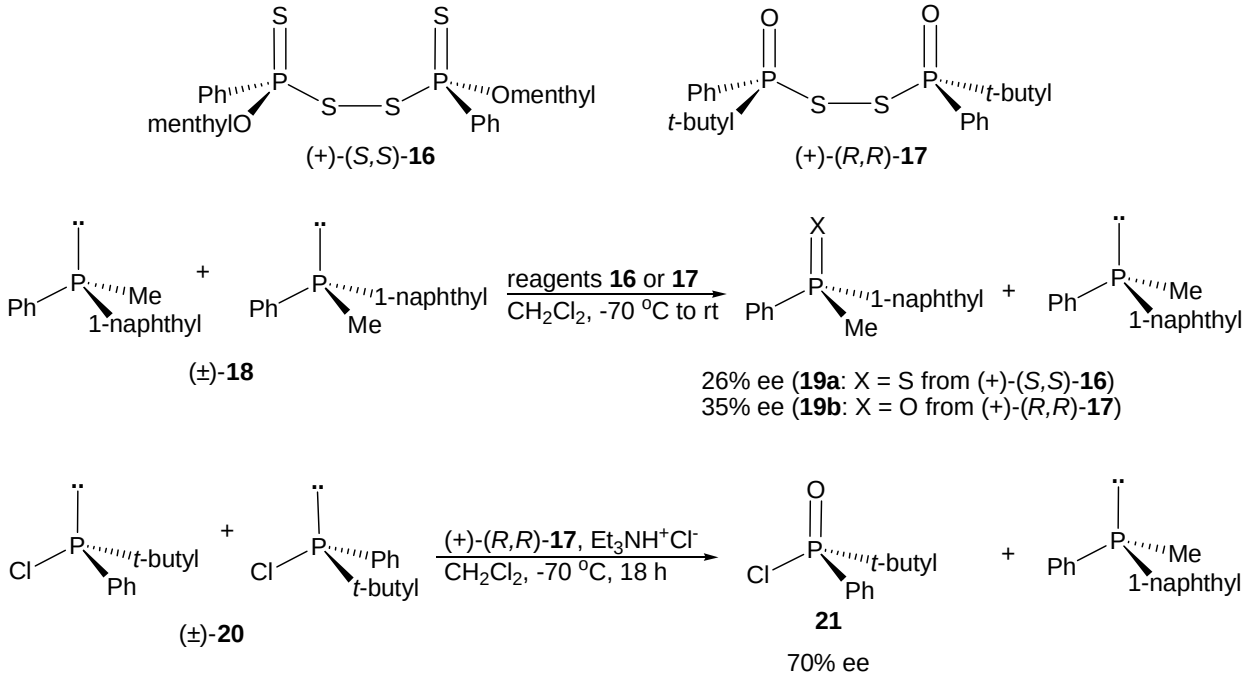

phosphine (±)-**18** by reaction with ~0.5 equiv of chiral disulfide (+)-(*S*,*S*)-**16** gave, via kinetic resolution, the product phosphine sulfide (-)-(*S*)-**19a** in up to 26% ee; reaction with (+)-(*R*,*R*)-**17** gave phosphine oxide (-)-(*S*)-**19b** in up to 35% ee[43] Reaction of chlorophosphine (±)-**20** with (+)-(*R*,*R*)-**17** in the presence of $Et_3NH^+Cl^-$ to promote epimerization (by addition/elimination of Cl^-) gave chlorophosphine oxide (-)-(*S*)-**21** with 70% ee in 80% yield, showing that one of the equilibrating epimers could be selectively trapped.[42] Thus our proposed Curtin-Hammett sulfurization has precedent in this oxidation example.

Chapter 2

Configurational stability of acyclic phosphite triesters

2.1 Abstract

Separation of the S_P and R_P configurations of 2-cyanoethyl[5'-*O*-(*p*,*p*'-dimethoxytrityl)-2'-deoxythymylyl]-(3',5')-3'-*O*-(*tert*-butyldimethylsilyl)-2'-deoxythymidine was achieved via the compound's boranophosphate analogue. For an inversion study of the phosphite triester, the *p*,*p*'-dimethoxytrityl and *tert*-butyldimethylsilyl groups had to be substituted with acetyl groups to reduce decomposition during the heating cycle at 150 ± 0.2 ºC. Using a computer modeling program (dubbed CRK2005), we found that the rates of epimerization were similar for both diastereomers, and good fits of the data to first-order epimerization coupled with an "impurity"-induced decomposition pathway were found. Regardless of the decomposition pathway, rate constants for epimerization gave an activation barrier of $\Delta G^{\dagger} = 33.0 \pm 0.2$ kcal/mol. Attempts to induce inversion of a single diastereomer of 2-cyanoethyl[5'-*O*-(*p*,*p*'-dimethoxytrityl)-2'-deoxythymylyl]-(3',5')-3'-*O*-(*tert*-butyldimethylsilyl)-2'-deoxythymidine phosphite triester at lower temperature with acidic and radical species failed.

2.2 Introduction

Figure 1 shows the difference between a phos*phine* and a phos*phite*, i.e. phosphines are trivalent species with P-C bonds, whereas phosphites are trivalent species with P-O-C bonds. Because these are trivalent compounds, they can undergo inversion at the phosphorus center, and several P-chiral phosphines were found to invert at temperatures over 130 ºC with barriers of 30-36 kcal/mol.[44] There are numerous examples in which P-stereogenic phosphines have been used as ligands for asymmetric hydrogenation.[45] Asymmetric hydroformylations have been achieved using chiral phosphites in which the chirality was introduced by a biphenyl or binaphthyl

Figure 1. Phosphine and phosphite (phosphite triester)

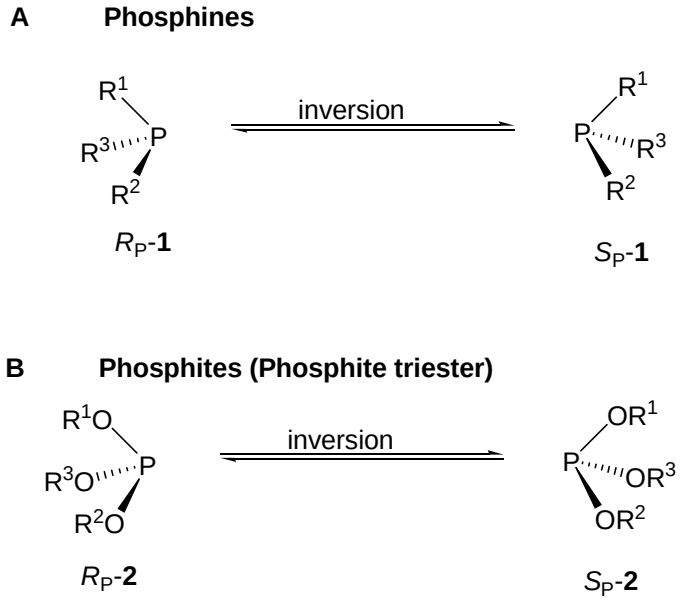

moiety,[46, 47] but to our knowledge never by P-chiral phosphites.

To our knowledge, no inversion barriers have been measured for an acyclic phosphite. However, there are hints in the literature on the configurational stability of phosphites, specifically P-chiral phosphites, such as those synthesized by Beaucage and Wada (Chapter 1, compound **8** in Scheme 6 and compound **12** in Scheme 7, respectively). These phosphites were not isolated but were immediately sulfurized to give the phosphite sulfides, which were then converted to the phosphorothioates. Therefore, these reactions suggest that the acylic phosphites formed after the coupling steps do not epimerize rapidly at room temperature.

Similar to Beaucage's and Wada's phosphite triesters (Chapter 1, compound **8** in Scheme 6 and compound **12** in Scheme 7, respectively), an example was reported by Hata et al., who demonstrated the configurational stability of a phosphite triester (Scheme 1) obtained via a novel deacylation of S_P-**3** to give phosphite triester **4** (absolute configuration unknown).[48, 49] In this

case the diastereomers of the alkoxycarbonyl phosphonate **3** were separated by preparative HPLC. The conversion of S_P-**3** to phosphite triester **4** was carried out over a period of 1 h, which was then treated in situ with sulfur for another 1 h to give **5**. Unlike the methods described by Beaucage and Wada, which used diastereomerically pure mononucloside synthons for chain-elongation to synthesize stereodefined phosphorothioates, the diastereomerically pure phosphonate **3** prepared by Hata et al. is a dinucleoside and was not intended to be used for stereodefined synthesis of phosphorothioates.

Scheme 1. Deacylation of a P-stereogenic acylphosphonate followed by stereospecific sulfurization

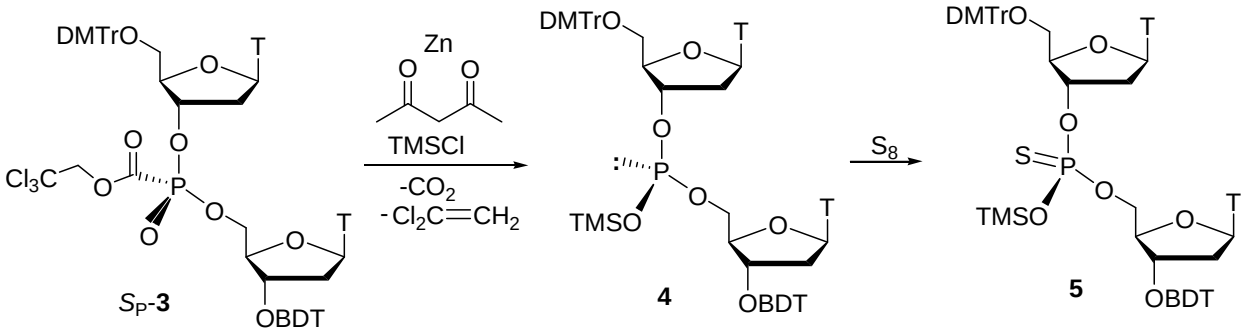

Mixture of R_P-**3** (not shown) and S_P-**3** diastereomers separated by preparative HPLC

not isolated but configurationally stable

BDT = 1,3-benzodithiol-2-yl = 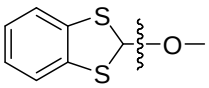

Makino et al. showed (Scheme 2) that selected phosphite triesters could be chromatographically separated to give ~100 mg quantities of S_P and R_P-**7**,[50, 51] which are the only isolated stereopure acyclic P-stereogenic phosphites of which we are aware. While not fully characterized (elemental analysis of the mixture, but no elemental analysis for the individual

Scheme 2. Isolated P-stereogenic phosphites

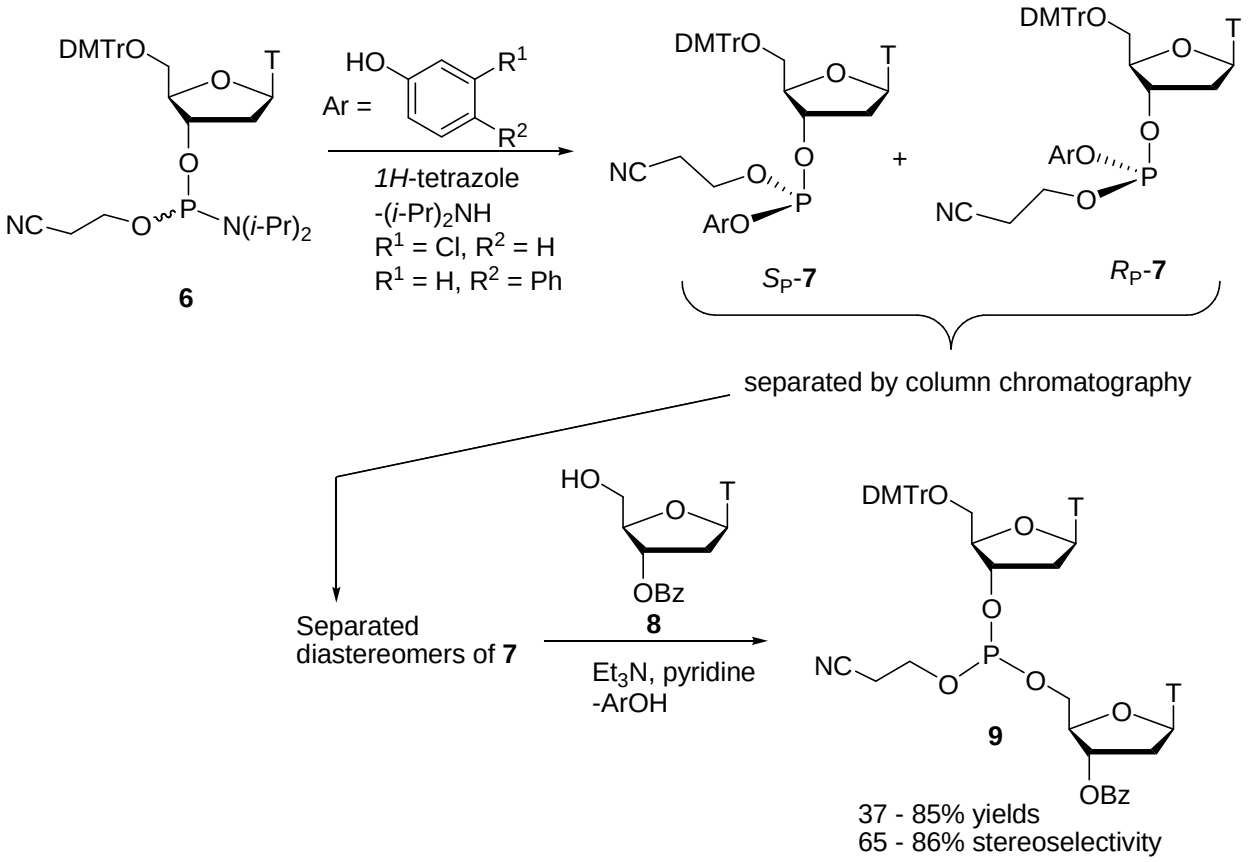

diastereomers), evidence was presented that showed the epimers to be configurationally stable at room temperature. S_P and R_P-**7** can undergo substitution of the phenol by **8** to give phosphite triester **9** in moderate to good yields (determined by RP HPLC) and with moderate stereoselectivety (determined by ^{31}P NMR). The selectivity of the reaction was determined by ^{31}P NMR, but full characterization was not carried out on phosphite triester **9**.

2.2.1 Apparent inversion of cyclic phosphites

There are a few examples in the literature of the apparent inversion of phosphites, specifically *cyclic* phosphites (Scheme 3). In the first example (Scheme 3 A), Bentrude et al. first prepared 3', 5'-cyclic thymidine phosphoramidite **10** by combining thymidine with hexamethylphosphorus triamide at room temperature,[52] then treated **10** with methanol in the

presence of excess pyridinium hydrochloride to give a 40/60 ratio of the **11-ax**/**11-eq** isomers.[53] However, heating for 30 min at approximately 60 ºC in the presence of pyridinium chloride gave a ratio of 95/5 of **11-ax**/**11-eq**. In a later report by Hayakawa et al., a cyclic phosphite similar to **11** (Scheme 3 B) was prepared by combining thymidine with diaminophosphine **12** in the presence of excess *1H*-tetrazole to give a 1:1 mixture of isomers (**13-eq** and **13-ax**) at room temperature.[54] However, after heating at 55 °C for 36 h in the presence of tetrazole, the mixture was converted to **13-ax** exclusively. It is well known that the P-axial isomers are thermodynamically preferred[55] while at the same time the thermodynamic preference for substituents on the carbon atoms remains equatorial.

Scheme 3. Apparent inversion of cyclic phosphites

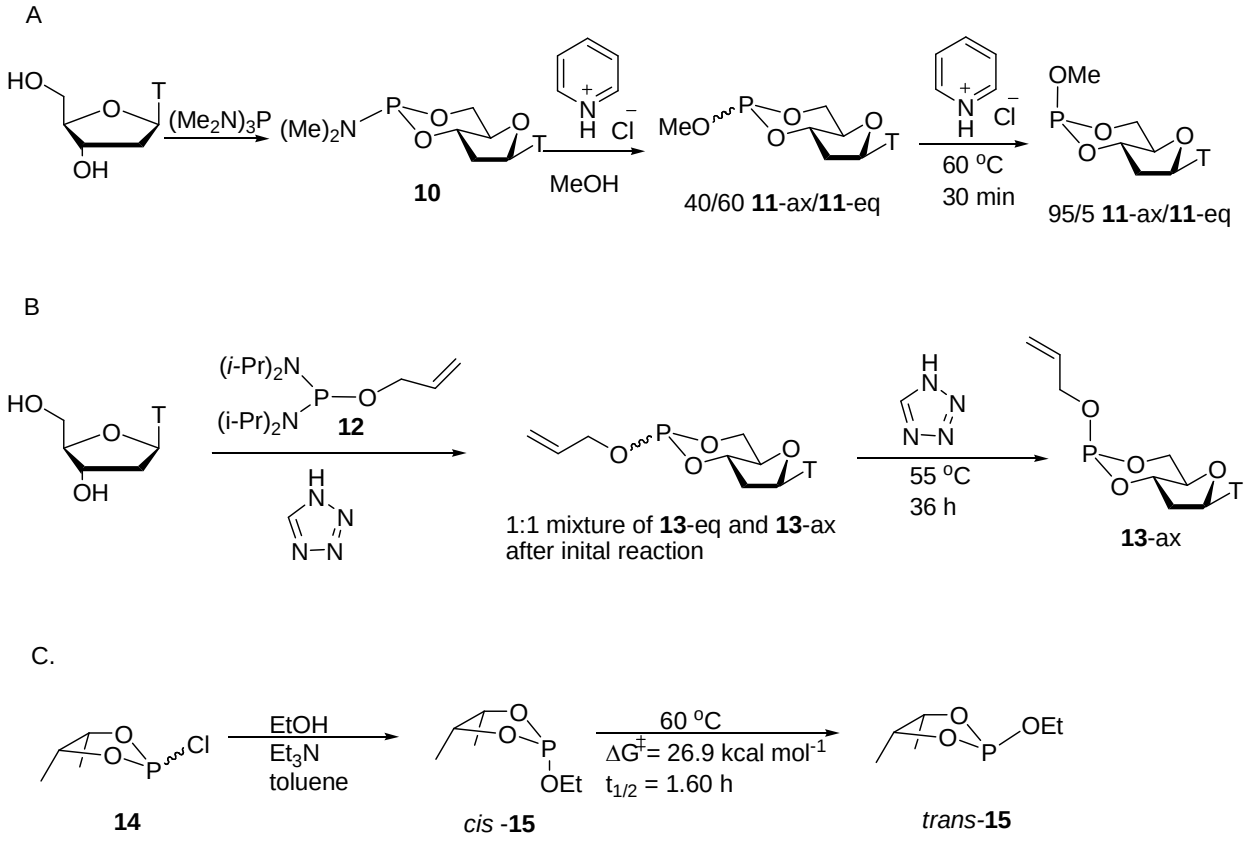

In the last example (Scheme 3 C) of epimerization of a cyclic phosphite, Hommer and Gordillo prepared achiral cyclc phosphite **15** in order to measure the rate of phosphite inversion.[56] Although a $\Delta G^{\dagger}$ of 26.9 kcal mol^{-1} was obtained from the study, the results are suspect because the rate of cis/trans isomerization was measured using impure *cis*-**15**, which was not fully separated from the $Et_3NH^+Cl^-$ by-product. In fact, the isomerization proceeded at a reasonable rate at 60 °C, not unlike that seen for **11** with pyridinium chloride and **13** with tetrazole.

2.3 Results and discussion

2.3.1 Configurational stability of an epimeric phosphite triester

In order to study the acyclic phosphite epimerization required for our chiral sulfurization method (described in Chapter 1, Section 1.4), our goal was the synthesis and separation of the diastereomers of a dithymidine phosphite triester related to **8** or **12** (see Chapter 1, Schemes 6 and 7) and the determination of their barriers of inversion. Dithymidine phosphite triester **16** (Scheme 2 A) was chosen because the nucleobases (i.e. thymines) do not require any protecting

Figure 2. A: Phosphite triester for epimerization study; B: Protection of nucleobases for DNA synthesis

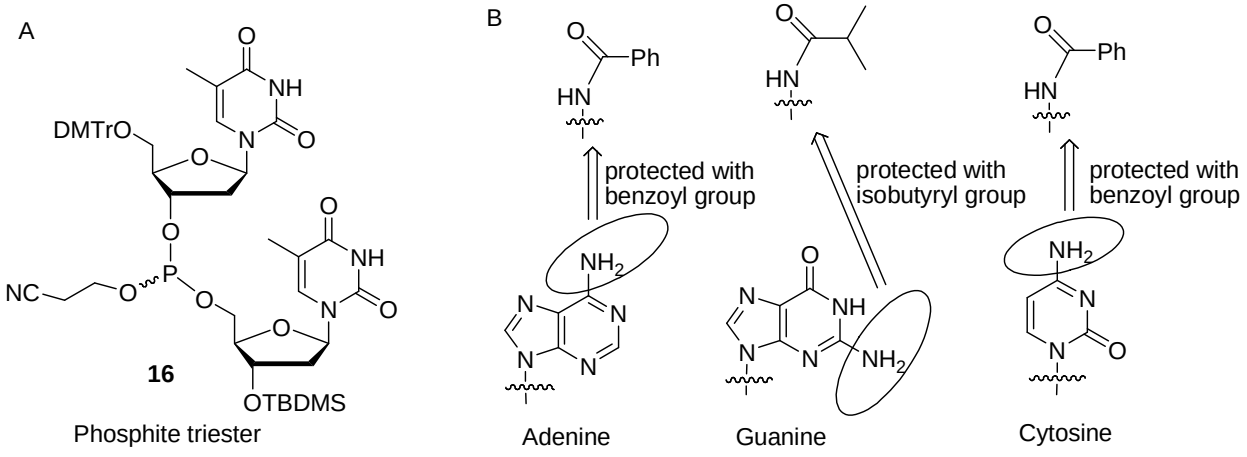

groups during the synthetic pathway, unlike the other nucleobases such as adenine, guanine, and cytosine, which have to be protected with a benzoyl or isobutyryl group (Figure 2 B).[57]

2.3.1.1 Synthesis of 2-cyanoethyl[5'-*O*-(*p,p*'-dimethoxytrityl)-2'-deoxythymylyl]-(3',5')-3'-*O*-(*tert*-butyldimethylsilyl)-2'-deoxythymidine phosphite triester 16

The complete synthesis is shown in Scheme 4. Under nitrogen, β-cyanoethanol **17** was treated with PCl_3 to give 2-cyanoethylphosphorodichloridite **18** as a clear oil,[58] which was then combined with 2 equiv of *i*Pr_2NH to afford 2-cyanoethyl monochlorophosphoramidite **19**[59] as a

Scheme 4. Synthesis of 2-cyanoethyl[5'-*O*-(*p,p*'-dimethoxytrityl)-2'-deoxythymylyl]-(3',5')-3'-*O*-(*tert*-butyldimethylsilyl)-2'-deoxythymidine phosphite triester (**16**)

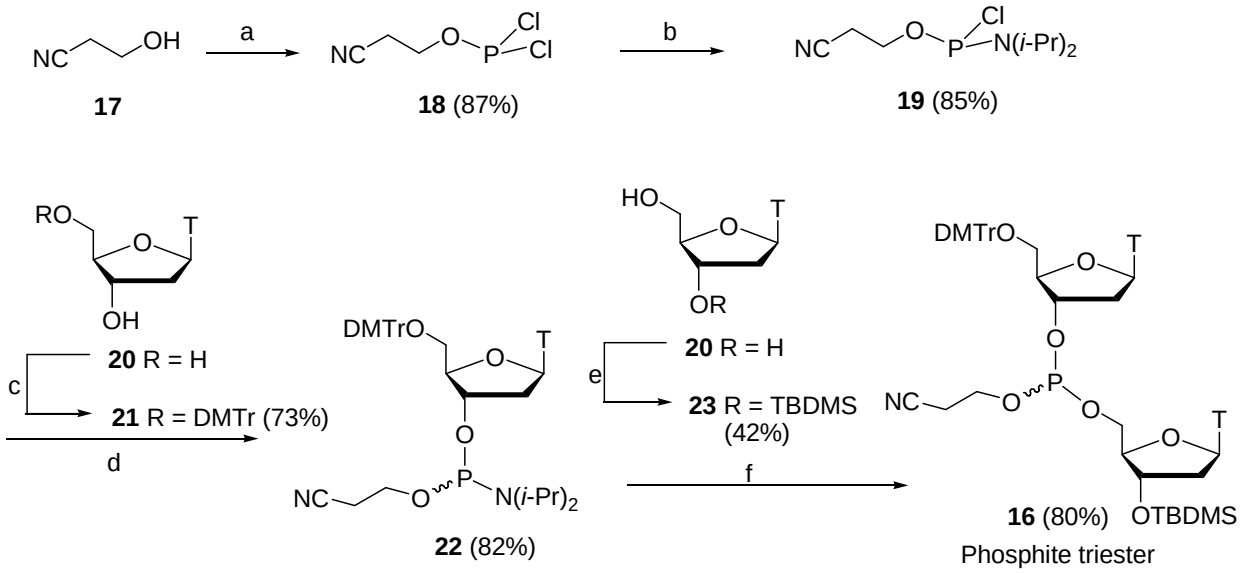

Reagents and conditions: (a) PCl_3 (6.0 equiv), CH_3CN, rt, 15 min; (b) *i*Pr_2NH (2.0 equiv), Et_2O, rt, 1.5 h; (c) DMTrCl (1.1 equiv), pyridine, rt, 4 h; (d) **21** (1.0 equiv), **19** (1.2 equiv), *i*Pr_2NEt (1.5 equiv), THF, -78 ºC to rt, 1.5 h; (e) (i) TBDMSCl (2.2 equiv), imidazole (4.4 equiv), DMF, rt, 1.5 h, (ii) 80% AcOH, 80 ºC, 6 h; (f) **23** (1.0 equiv), **22** (1.1 equiv), pyridinium trifluoroacetate (2.2 equiv), *N*-methylimidazole (1.1 equiv), CH_3CN, rt, 1.0 h.

slightly yellow oil. Compound **19** was then treated with 5'-*O*-(4,4' dimethoxytrityl)thymidine **21**[60] in the presence of *i*Pr_2NEt at -78 ºC to give 5'-*O*-(4,4'-dimethoxytrityl)-2'-deoxythymidine 3'-(2-cyanoethyl *N*,*N*-diisopropylphosphoramidite **22**[61] as a white powder in 82% yield. For the synthesis of dinucleoside **16**, instead of using tetrazole as the activator, a mixture of PTFA and *N*-methylimidazole[62] was used to induce the coupling of **22** and **23**[63, 64] to give product **16** as a white foam in 80% yield. Since a single diastereomer of the phosphite triester **16** was needed for the inversion, attempts were made to separate the diastereomers by column chromatography. No solvent system was found to give any separation on TLC, and attempts to split the eluting band in fractions by column chromatography also failed.

2.3.1.2 Separation of S_P and R_P diastereomers of 16 via its boranophosphate analogue

The synthesis and separation of boranophosphates S_P-**24** and R_P-**24** were reported by Just and coworkers (Scheme 5).[65] Therefore, this approach was taken to isolate the two diastereomers of phosphite triester **16**. For the boronation of the phosphite triester **16**, the authors claimed that $Me_2S{\cdot}BH_3$ also removed the DMTr group, which had to be reinstalled before the separation of the diastereomers could be accomplished. Since the reaction of BH_3 with the phosphite was reported to occur "within 5-10 minutes," we tried both a short reaction time and rapid work-up. In fact, we found that carrying out the reaction at 0 ºC for 15 min and then quickly passing the reaction solution through a pad of silica gel with the aid of THF allowed for phosphite boronation without deprotection of the DMTr group in 95% yield. The diastereomers of boranophosphate **24** were then separated by silica gel column chromatography to give a 25% yield of S_P-**24** and 23% yield of R_P-**24**, each on the basis of the total amount of **24**.

For our initial attempt at the inversion study, the phosphite triester of one diastereomer (S_P-**16**) was obtained by removing the BH_3 group of the boranophosphate (S_P-**24**) with 10 equiv

Scheme 5. Separation of S_P and R_P diastereomers of phosphite triester **16** via its boranophosphate analogue

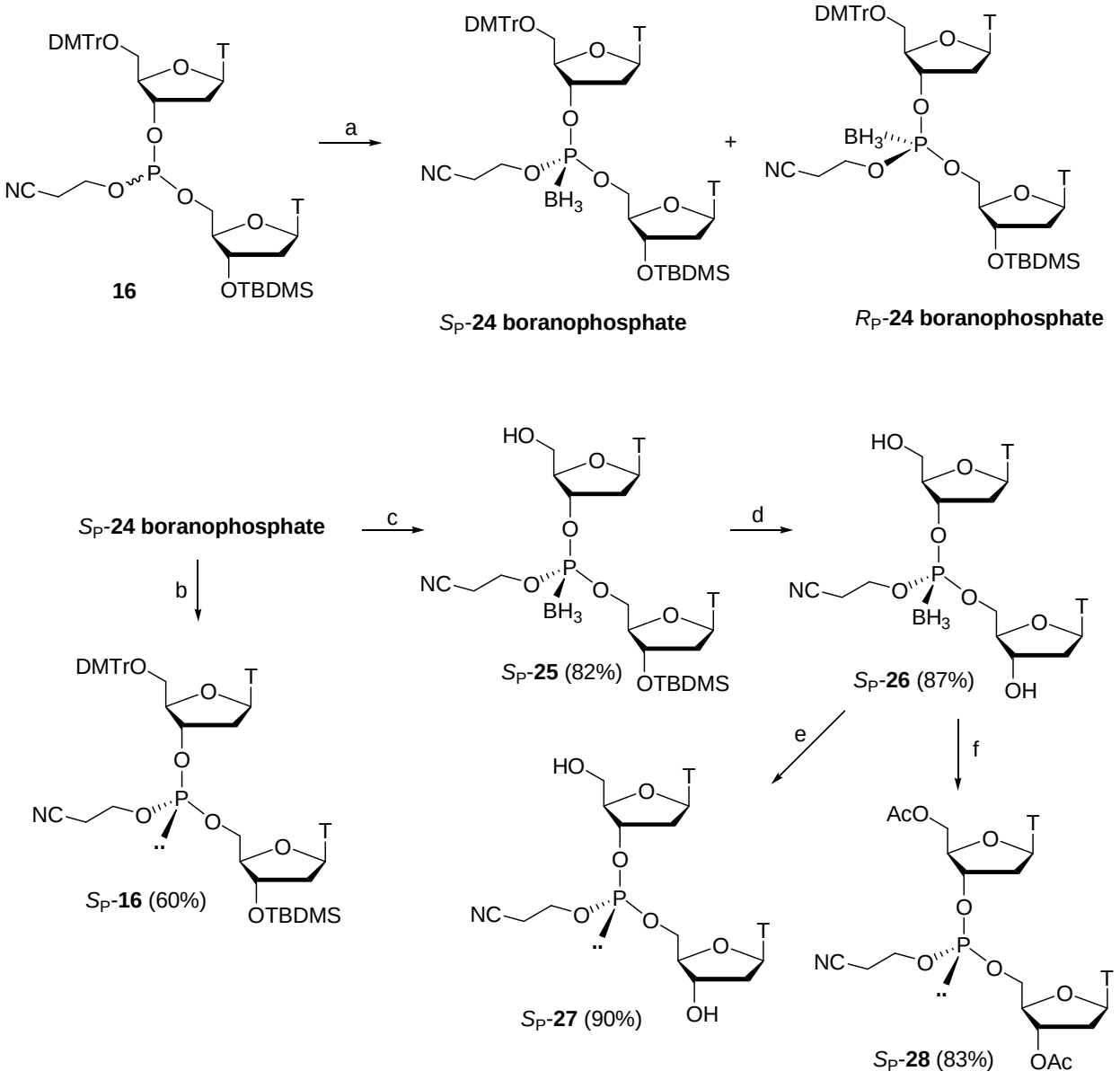

Reagents and conditions: (a) $BH_3 \cdot Me_2S$ (3.0 equiv), THF, 0 ºC to rt, 15 min; (b) DABCO (10 equiv), THF, rt, 37 h; (c) 2% $CHCl_2COOH/CH_2Cl_2$, rt, 20 min; (d) HF-pyridine (25 equiv), THF, rt, 24 h; (e) pyridine, rt, 36 h; (f) Ac_2O (15 equiv), pyridine, rt, 24 h.

of DABCO at rt for 37 h. TLC of the crude solution showed movement of the product with the solvent front (THF) and some UV-active material at the origin of the plate. After the crude material was filtered through a pad of silica gel, a modest yield of 60% was obtained for S_P-**16**. This low yield might be due to the conversion of tetravalent boranophosphates **24** to the pentavalent boranophosphate species, possibly caused by elimination of the β-cyanoethyl group by DABCO. The ^{31}P NMR spectrum of S_P-**16** in toluene-d_8 at rt exhibited a broad peak at 139.7 ppm, but a sharp peak at 140.0 ppm when the NMR spectrum was acquired at 40 ºC; ^{1}H NMR spectra also exhibited broad peaks at rt but sharp peaks at 40 ºC.

A sample of the phosphite triester S_P-**16** (16 mg) dissolved in approximately 0.5 mL of toluene-d_8 was sealed in an NMR tube under vacuum, and then was heated at 150 ºC in an oil bath. After ~7 h of heating, the ^{31}P NMR spectrum of the sample showed ~ 2.7% decomposition to an unknown species at ~27 ppm, and two peaks at 140.0 and 139.4 ppm corresponding to the two diastereomers of compound **16**. The NMR spectra were recorded at 40 ºC to get sharper peaks. Inversion of 4.7% was calculated from the integral ratio of the two diastereomers using the following equation: [R_P-**16**/(S_P-**16** + R_P-**16**)] x 100%. Longer periods of heating the sample resulted in extensive decomposition of the phosphite triester.

Since the decomposition at 150 ºC might be due to the DMTr and TBDMS groups, the next candidate for inversion to be tried was the deprotected dithymidine. The DMTr group of S_P-**24** and R_P-**24** was removed with 2% $CHCl_2CO_2H/CH_2Cl_2$ over 20 min to give compounds S_P-**25** and R_P-**25** in approximately 80% yields. For the deprotection of the TBDMS group, Just and coworkers used TBAF (1equiv)/AcOH (24 equiv) in THF,[65] but we found that this mixture resulted in a very slow deprotection with decomposition of the compound over the reaction time. Using TBAF exclusively (without AcOH) caused extensive decomposition to unknown

compounds as indicated by TLC; one possible side reaction might be a β-cyanoethyl elimination. HF·Et_3N and HF·pyridine were tried next, and while HF·Et_3N resulted in slow deprotection with some decomposition of the compound (observed by TLC), the latter reagent was found to be much more efficient in the deprotection of the TBDMS group, giving yields of 87% and 85% for compounds S_P-**26** and R_P-**26** respectively.

To remove the BH_3 group of compounds S_P-**26** and R_P-**26** for inversion studies of their corresponding phosphite triesters, we have found that instead of using DABCO, a large excess of pyridine (~130 equiv) gave a ~90% yield of S_P-**27** and 80% of R_P-**27** after purification by silica gel chromatography. ^{31}P NMR spectra of S_P-**26** and R_P-**26**, acquired at rt in CD_3CN, exhibited sharp peaks at 140.78 and 140.37 ppm, respectively. A sample of ~5 mg each of S_P-**27** and R_P-**27** was dissolved in CD_3CN, sealed in an NMR tube and placed in an oil bath maintained at 150 ± 0.2 ºC. After the solution of S_P-**27** heated for 1 h, the ^{31}P NMR spectrum of the solution exhibited peaks at 140.78 and 140.37 ppm, corresponding to S_P-**27** and R_P-**27**, respectively, and peaks at 140.67 and 140.13 ppm corresponding to ~2.3% decomposition. Using the integral ratio of S_P-**27** and R_P-**27**, inversion of 24% was calculated using the following equation: [R_P-**27**/(S_P-**27** + R_P-**27**)] x 100%. Longer periods of heating the sample resulted in decomposition of the phosphite triester to unknown species with chemical shifts adjacent to those of the phosphite triester – possibly due to cyclization of either one of the thymidine residues with simultaneous elimination of 2-cyanoethanol. This side reaction made monitoring of the inversion difficult because the ^{31}P NMR peaks of two diastereomers of phosphite triester **27** and the unknown species were too close to be integrated with accuracy.

Since the two free hydroxyl groups in dinucleotides **27** were most likely causing the observed decomposition, they were protected with acetyl groups by reaction with acetic

anhydride in pyridine. After 24 h of stirring at rt, complete acetylation of the two hydroxyl groups and removal of the BH_3 group was achieved to afford diacyldinucleosides S_P-**28** and R_P-**28**, which were purified by flash chromatography under nitrogen to give an approximately 85% yield of each compound.

2.4 Epimerization of diacyldithymidine S_P-28 and R_P-28

A total of six experiments were carried out, each in pairs of two in order to compare the inversion of S_P-**28** and R_P-**28** (Table 1). One pair was carried out with Ph_3P as an internal

Table 1. Solutions prepared for the inversion studies of phosphite triesters S_P-**28** and R_P-**28**

Exp	Amount of compound/~0.5 mL of CD_3CN[a]	Internal standard (Ph_3P)	External standard (Ph_3P)[b] in sealed capillary
1	5.2 mg S_P-**28** (0.00779 mmol)	0.2 mg (0.00076 mmol)	
2	5.1 mg R_P-**28** (0.00764 mmol)	0.2 mg (0.00076 mmol)	
3	5.4 mg S_P-**28** (0.00809 mmol)		50 µL (0.00103 mmol)
4	5.3 mg R_P-**28** (0.00794 mmol)		50 µL (0.00103 mmol)
5[c]	5.1 mg S_P-**28** (0.00764 mmol)		50 µL (0.00103 mmol)
6[c]	5.1 mg R_P-**28** (0.00764 mmol)		50 µL (0.00103 mmol)

[a] The solutions were prepared in a glove box and then sealed under vacuum; [b] an internal standard was made in CH_3CN (0.0206 M); [c] the tubes were silanized.

standard (exp. 1 and 2), while two pairs were carried out with Ph_3P as an external standard in acetonitrile solution in a sealed capillary tube; for one of the external standard pairs, all glassware contacted by the phosphites was silanized with $(CH_3)_2SiCl_2$ (exp. 5 and 6).[66] The sealed tubes containing the solutions in Table 1 were heated in a thermostatted oil bath kept at 150.0 ± 0.2 ºC with approximately 1″ of the tube above the level of the oil. The tubes were taken out every 30 min and immediately submerged in a water bath kept at ~20 ºC for ~5 min, and then ^{31}P NMR spectra were recorded.

During the period of heating the solutions, in addition to inversion of the phosphite triester, ^{31}P NMR spectra also showed decomposition of the phosphite triester to unknown

phosphorus species with chemical shifts mainly between 7-9 ppm. Examples of ^{31}P NMR spectra representative of before and after the heating cycle are shown in Figure 3 (exp. 6 in Table 1).

Figure 3. ^{31}P NMR spectrum before heating R_P-**28** (A); ^{31}P NMR spectrum after heating R_P-**28** for 4 h at 150 °C

A.

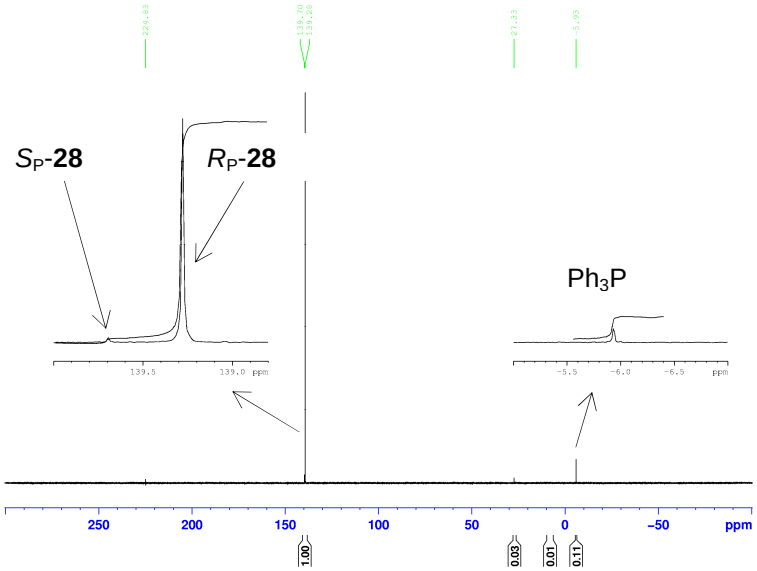

B.

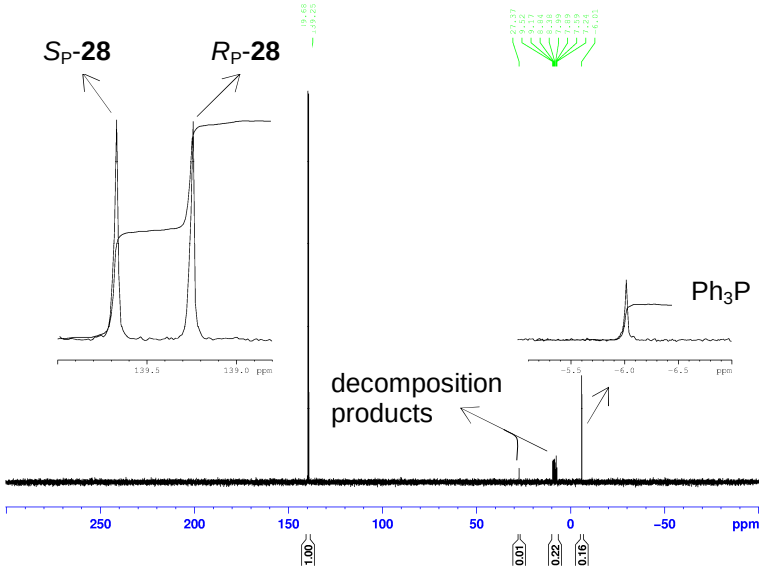

Examination of plots of concentration versus time showed that equilibration occurred within about 3 h, after which the concentrations declined slowly. Examination of the total phosphite concentration versus time made it clear that decomposition was relatively rapid during the first ~2 h and slowed down after that. In order to separate the epimerization from decomposition, it was clear that standard kinetic plots would not suffice. We had previously developed a computer program called CRK2005 ("Complex Reaction Kinetics")[67] that allows one to fit rate constants to observed data in multiple kinetic runs for any set of coupled differential equations. It was written to quantitatively model a kinetic system using known numerical routines to: (1) numerically integrate the coupled set of differential equations, using a fourth-order Runge – Kutta method with adaptive step-size control, (2) calculate the deviation of the values of the calculated time points from the observed, which is reported as the reduced chi square function χ_v^2 (where a "perfect" fit will give $\chi_v^2 \approx 1$), and (3) iteratively adjust the rate constants using a simplex minimization algorithm to give the best-fit set of rate constants simultaneously for all the runs. At the end of all runs, a % error was also calculated by dividing the standard deviation of the calculated concentrations by the average concentration. The program requires input of (1) the differential equations, (2) the observed species, (3) the concentrations of all species whose initial values could be allowed to vary to give the best fit, and (4) guesses for each rate constant.

A number of kinetic mechanisms of decomposition were considered before one was found that allowed a good fit to the observed kinetic data. These are described in detail now.

2.4.1 Rate of decomposition of S_P-28 and R_P-28 using CRK2005 computer modeling

We started by using the data from the silanized experiments (exp. 5 and 6 in Table 1), which gave the smoothest results, and were virtually superimposable for the two experiments

starting from the same concentrations of S_P-**28** and R_P-**28**, respectively. In order to model phosphite decomposition, we followed total concentration of the two epimers versus time, before adding in the complication of epimerization. The rate equations that were fitted are shown in Chart 1. As shown in Figure 4, experiment 5 was followed for 8 h (i.e. 28800 sec) while

Chart 1. Rate equations of phosphite triester **28** decomposition

(A) 1st order decomposition of **28**:

$$\text{rate} = -k([S_P\text{-}\mathbf{28}] + [R_P\text{-}\mathbf{28}])$$

(B) 2nd order decomposition of **28**:

$$\text{rate} = -k([S_P\text{-}\mathbf{28}] + [R_P\text{-}\mathbf{28}])^2$$

(C) "impurity" induced decomposition:

$$d([S_P\text{-}\mathbf{28}] + [R_P\text{-}\mathbf{28}])/dt = -k([S_P\text{-}\mathbf{28}] + [R_P\text{-}\mathbf{28}])[\text{impurity}]$$

$$d[\text{impurity}]/dt = -k([S_P\text{-}\mathbf{28}] + [R_P\text{-}\mathbf{28}])[\text{impurity}]$$

experiment 6 was followed only for 4 h (14,400 sec). Simple first-order decomposition of the phosphites gave a poor fit to the observed data points, and second-order decomposition (for which we had no rational mechanism) gave only a marginally better fit, as seen. Clearly both sets of calculated data showed that any mechanism that required the phosphite concentrations to approach zero would not fit the observed data, in which the phosphite concentrations appear to level out. One can imagine some adventitious species that might react with the phosphites resulting in decomposition, but after that species is consumed, the decomposition would end. In order to model this, CRK2005 allows the concentration of any initial species to be varied, within limits, to give the best fit, since the numerical integration method for calculating the outcomes of coupled rate equations depends on the values of the initial starting points. This was done by allowing the concentration of an initial "impurity" to vary, along with the second-order rate

Figure 4. Phosphite triester **28** decomposition, silanized experiments 5 and 6

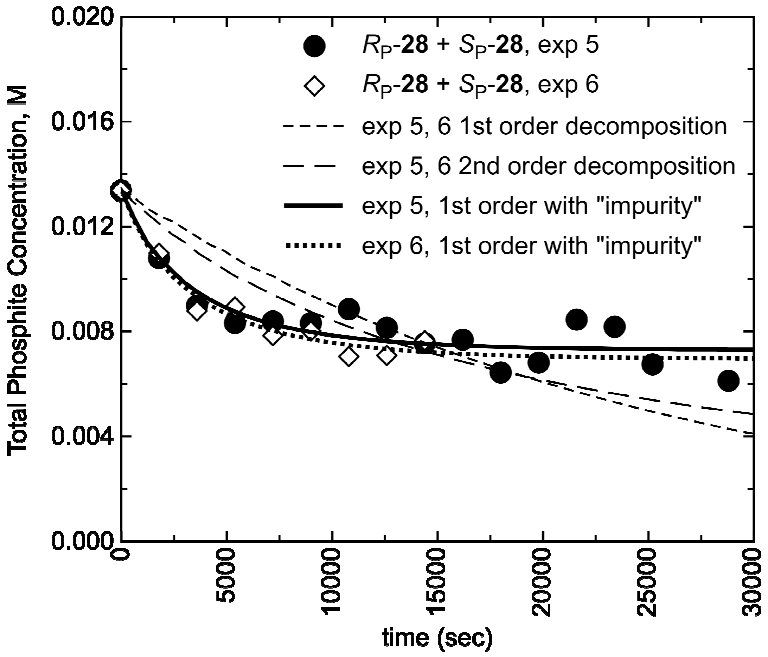

constant, and as seen this gave an excellent fit to the data. Similarly, all six experiments could be fit to this mechanism, and while the overall fit is not as good, the fact that six experiments can be fit to the same rate constant (and comparable "impurity" concentrations) lends confidence that the mechanism is reasonable. Calculated rate constants and error estimates are collected in Table 2. It should be noted that, not surprisingly, multiple sets of rate constant and "impurity" concentrations give comparable fits to individual experiments (as seen for runs 5 and 6), but when all experiments are considered simultaneously it is less likely that more than one set will fit.

Table 2. Phosphite triester **28** decomposition

Experiment	χ_v^2	%error	*k*	[impurity]
5, 6: 1st order decomposition	11.2	19.3	3.95 ± 0.19 E-5	
5, 6: 2nd order decomposition	6.9	15.1	4.93 ± 0.21 E-3	
5, 6: "impurity" decomposition	1.5	6.8	2.55 ± 0.13 E-2	0.00608 M 0.00642 M
Exp 1-6: "impurity" decomposition	2.4	9.4	7.79 ± 0.50 E-3	*

*for exp 1-6, [impurity] = 0.00484, 0.00390, 0.00442, 0.00433, 0.00844, 0.0113 M (see Chart 5 in Experimental Section for graphs)

2.4.2 Rate of phosphite epimerization using CRK2005 computer modeling

As before, the two silanized experiments were considered first. The kinetic pathways to be fit are shown in Charts 1, 2, and 3; even though we found that the "impurity" mechanism was best, it seemed reasonable to check how much the best fit rate constants for epimerization would vary with the decomposition pathway chosen. As seen in Figure 5, the best-fit lines for the first-

Chart 2. Kinetic pathway for first order epimerization and decomposition of S_P-**28** and R_P-**28**

A.

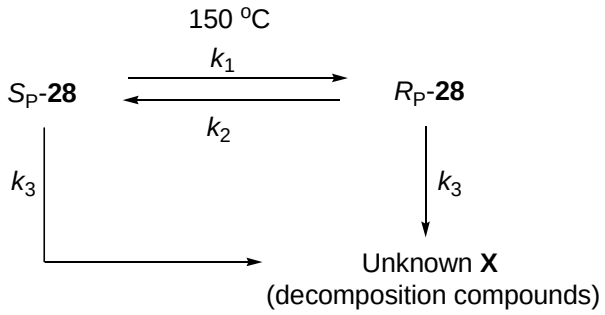

The differential equations describing Chart 2 are as follows:

$$d[S_P\text{-}\mathbf{28}]/dt = -(k_1 + k_3)[S_P\text{-}\mathbf{28}] + k_2[R_P\text{-}\mathbf{28}] \quad (1)$$

$$d[R_P\text{-}\mathbf{28}]/d = -(k_2 + k_3)[R_P\text{-}\mathbf{28}] + k_1[S_P\text{-}\mathbf{28}] \quad (2)$$

$$d[\text{Unknown } \mathbf{X}]/dt = k_3([R_P\text{-}\mathbf{28}] + [S_P\text{-}\mathbf{28}]) \quad (3)$$

Chart 3. Kinetic pathway for second order epimerization and decomposition of S_P-**28** and R_P-**28**

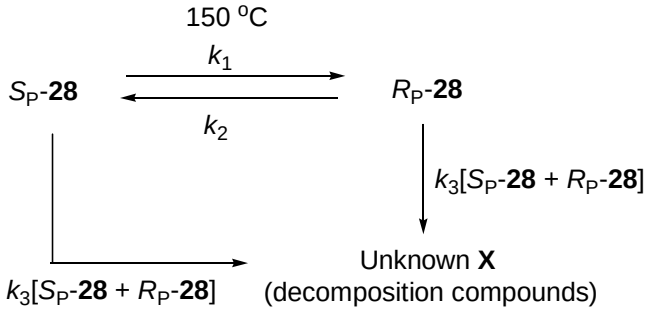

The differential equations describing Chart 3 are as follows:

$$d[S_P\text{-}\mathbf{28}]/dt = -(k_1 + k_3[S_P\text{-}\mathbf{28} + R_P\text{-}\mathbf{28}]) \times [S_P\text{-}\mathbf{28}] + k_2[R_P\text{-}\mathbf{28}] \quad (1)$$

$$d[R_P\text{-}\mathbf{28}]/d = -(k_2 + k_3[S_P\text{-}\mathbf{28} + R_P\text{-}\mathbf{28}]) \times [R_P\text{-}\mathbf{28}] + k_1[S_P\text{-}\mathbf{28}] \quad (2)$$

$$d[\text{Unknown } \mathbf{X}]/dt = k_3([S_P\text{-}\mathbf{28} + R_P\text{-}\mathbf{28}])^2 \quad (3)$$

Chart 4. Kinetic pathway for first order epimerization with "impurity" induced decomposition of S_P-**28** and R_P-**28**

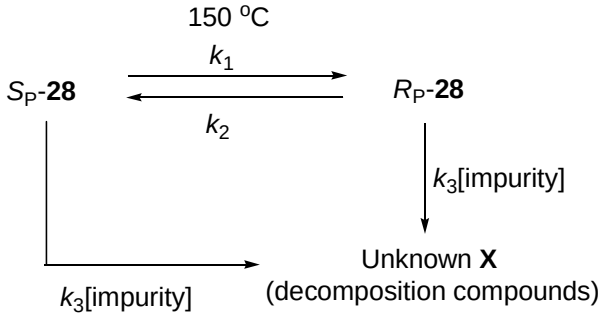

The differential equations describing Chart 4 are as follows:

$$d[S_P\text{-}\mathbf{28}]/dt = -(k_1 + k_3[\text{impurity}]) \times [S_P\text{-}\mathbf{28}]) + k_2[R_P\text{-}\mathbf{28}] \quad (1)$$

$$d[R_P\text{-}\mathbf{28}]/d = -(k_2 + k_3[\text{impurity}]) \times [R_P\text{-}\mathbf{28}]) + k_1[S_P\text{-}\mathbf{28}] \quad (2)$$

$$d[\text{Unknown } \mathbf{X}]/dt = k_3[\text{impurity}]([S_P\text{-}\mathbf{28} + R_P\text{-}\mathbf{28}]) \quad (3)$$

$$d[\text{impurity}]/dt = -k_3[\text{impurity}]([S_P\text{-}\mathbf{28} + R_P\text{-}\mathbf{28}]) \quad (4)$$

and second-order decomposition mechanisms are very similar (for simplicity only the fit for experiment 5 is shown, but that for experiment 6 is nearly coincident). However, once again the fit for the "impurity" mechanism is seen to be significantly better, and as seen in Table 3, the analytical error estimates (χ_v^2 and % error) are much better.

Fitting the epimerization and decomposition rates to all six experiments again yields slightly different rate constants, but again the fact that all the data can be simultaneously fit provides strong support for the calculated rate constants.

Figure 5. Phosphite triester **28** epimerization, silanized experiments 5 and 6

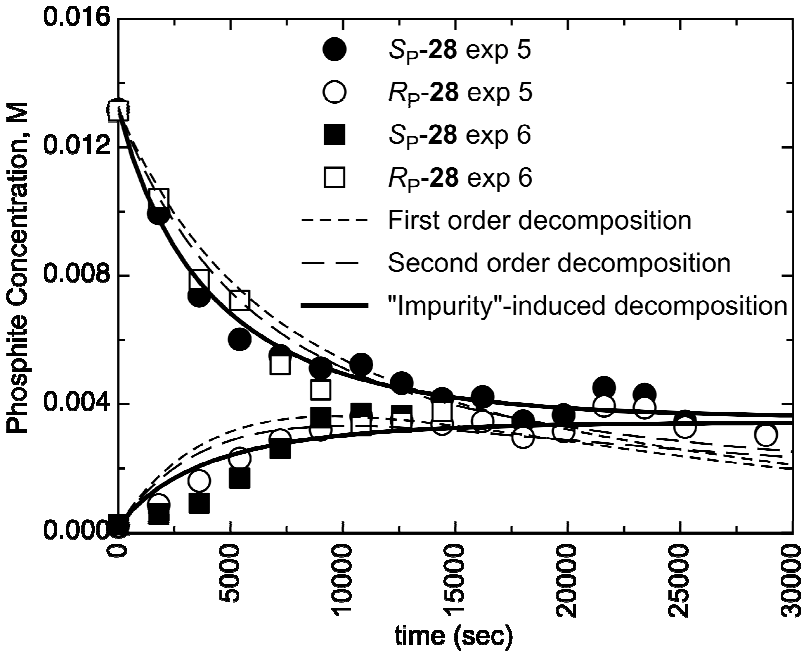

Table 3. Phosphite triester **28** epimerization

Experiment	χ_v^2	%error	k_1 ($\Delta G^\dagger$)	k_2 ($\Delta G^\dagger$)	k_3	[impurity]
5, 6: 1st order epim. and decomp.	3.3	20.7	8.36 ± 0.45 E-5 (33.0 kcal/mol)	8.86 ± 0.48 E-5 (32.9 kcal/mol)	3.95 ± 0.20 E-5	
5, 6: 2nd order epim. and decomp.	2.2	16.9	7.92 ± 0.37 E-5 (33.0 kcal/mol)	8.42 ± 0.39 E-5 (33.0 kcal/mol)	4.36± 0.23 E-3	
5, 6: 1st order epim. and "impurity" decomp.	1.1	11.8	7.16 ± 0.23 E-5 (33.1 kcal/mol)	7.46 ± 0.26 E-5 (33.1 kcal/mol)	1.95 ± 0.13 E-2	0.00637 M 0.00681 M
Exp 1-6: epim. and "impurity" decomp.	1.5	16.9	6.73 ± 0.29 E-5 (33.1 kcal/mol)	6.89 ± 0.31 E-5 (33.1 kcal/mol)	1.29 ± 0.13 E-2	*

* for epimerization exp 1-6, [impurity] = 0.00390, 0.00422, 0.00400, 0.00348, 0.00711, 0.00833 M (see Chart 6 in Experimental Section for graphs)

2.4.3 Calculated inversion barrier

The critical result of the above fitting procedures is not the precise value of the epimerization or decomposition rate constants, but rather the derived value of the activation barrier for phosphite inversion. The best estimates for the epimerization rates, those obtained from all six experiments in Table 3, were the lowest rate constants, while the calculated results for the two silanized experiments assuming first-order phosphite decomposition gave the highest values. As shown in Table 3, the modest deviations in the rate constants have little effect on $\Delta G^\dagger$, and so the details of the decomposition pathways really have no impact on the calculated inversion barrier.

2.5 Attempts to invert diastereomerically pure phosphite triester 16

Since the phosphite triester **16** did not epimerize at a temperature that is suitable for our sulfurization method, a means for inverting the phosphite at lower temperatures was sought. There is a report in the literature on the inversion of a phosphine with 10% I_2, possibly through a pseudorotation mechanism via a pentavalent intermediate.[68] The proposed mechanism of the inversion of the phosphine by I_2 is shown in Figure 6. It starts with the reaction of an iodine

molecule with the lone pair electrons on the phosphorus atom of S_P-**29** to give a tetravalent species, which can then combine with the anionic I^- to give the pentavalent species **30**; the iodine atoms are labeled I_a and I_b so that their movement can be followed easily. The mechanism that represents one pseudorotation involves rotation of two equatorial atoms (in this case R^2 and R^3) to apical positions and the apical atoms (I_a and I_b) to equatorial positions. The pentavalent species **30** could then undergo a few more pseudorotations to give species **31**, followed by an initial elimination of I_b to give tetravalent species **32**, and then I_2 elimination to give R_P-**29**.

Figure 6. Possible pseudorotation mechanism of a phosphine with iodine

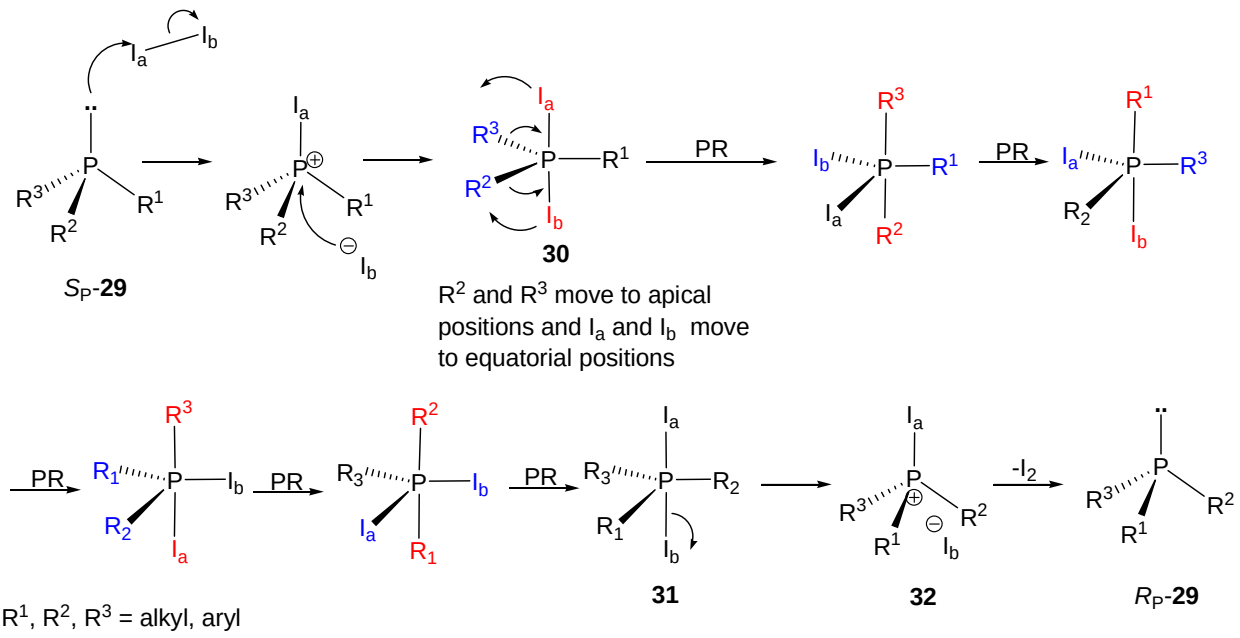

PR = pseudorotation: the mechanism is illustrated on pentavalent species **30** - i.e. the atoms colored blue move to apical positions and the atoms colored red move to equatorial positions.

In order to test I_2 as a inversion catalyst, a sample of $(EtO)_3P$ was treated with 1 equiv of I_2 in CD_3CN. During the time it took to obtain the ^{31}P NMR spectrum, the $(EtO)_3P$ had already decomposed to a single unknown compound with a chemical shift of -41 ppm. The ^1H NMR

spectrum showed that ethyl iodide could be present in solution because peaks corresponding to two ethyl groups are in the NMR spectrum. The splitting of the peaks of the ethyl group of the major compound is a triplet and multiplet (due to coupling of C*H*$_2$ with the phosphorus atom) and the splitting of the ethyl peaks of the minor compound is a well-resolved triplet and quartet. This decomposition of $(EtO)_3P$ could be due to an Arbuzov-type reaction (Figure 7), and therefore no further work was carried out with I_2.

Figure 7. Reaction of phosphite with iodine through an Arbuzov-type reaction

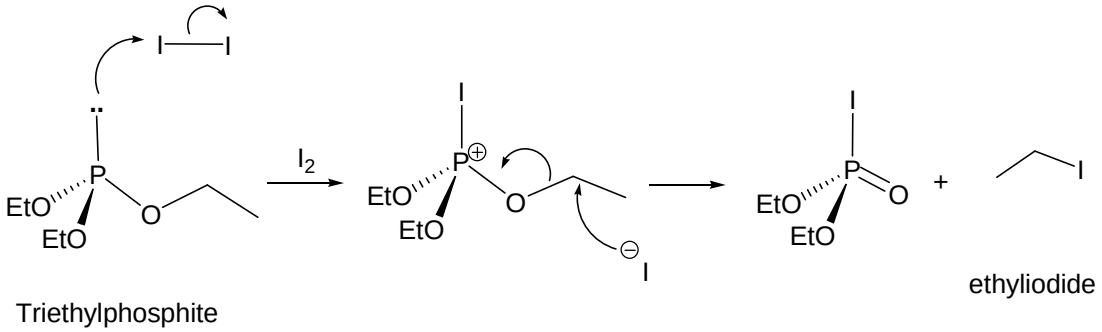

Chlorophosphines[42, 43, 69, 70] have been observed to undergo rapid inversion at the phosphorus in the presence of $Et_3NH^+Cl^-$, possibly by a mechanism involving addition followed by elimination of HCl via a pentavalent intermediate.[71] Therefore, a variety of reagents that could deliver HCl or related species to invert phosphite triester **16** were tried, including tetrazole (**33**), triethylammonium chloride (**34**), dimethyl(cyanomethyl)ammonium chloride (**35**), methyldiphenylphosphonium chloride (**36**), pyridinium chloride (**37**), and *N*-methylimidazolium chloride (**38**). All reagents were tested with the idea that they might undergo the same pseudorotation mechanism as I_2 to give the other epimer. Two other reagents that were tested for potential inversion were $(p\text{-}BrC_6H_4)_3N^+ SbCl_6^-$ and galvinoxyl, both stable free radicals. Since

(p-$BrC_6H_4)_3N^+$ $SbCl_6^-$ has been used for cation-radical catalyzed Diels-Alder reactions,[72] we considered that it might remove one of the lone pair electrons from the phosphorus atom, and thus might lower the inversion barrier because this is the orbital that is likely to rise in energy during inversion.

To monitor the inversion, the chemical shifts of the two diastereomers of phosphite triester **16** were first determined in the solvents used for the experiments (Table 4). However, after carrying out the experiments in the solvents and at the temperatures shown in Table 5, we found no inversion for any of the reagents tested except decomposition of the phosphite triester to unknown species.

Table 4. ^{31}P Chemical shifts for the diastereomeric mixture of phosphite triester **16**

Diastereomer	Toluene-d_8	$CDCl_3$	Nitrobenzene-d_5 [a]	Dimethylformamide (DMF) [a]
S_P-**16**	139.75 ppm	140.13 ppm	139.71 ppm	139.60 ppm
R_P-**16**	139.43 ppm	138.87 ppm	139.36 ppm	139.49 ppm

[a] A sealed capillary tube of C_6D_6 in NMR tube was used as lock signal.

Treating phosphite triester S_P-**16** with 1.45 equiv of methyldiphenylphosphonium chloride (exp. 7) in $CDCl_3$ resulted in a reaction solution that gave a ^{31}P NMR spectrum showing broad peaks at ~139 ppm and a single broad ^{31}P peak for methyldiphenylphosphine at -26 ppm. Heating the sample to 50 ºC in the NMR probe did not show any change in the ^{31}P NMR spectrum. To neutralize the acidity of the solution, approximately 7 equiv of Et_3N were added to the mixture, but ^{31}P NMR analysis of the solution did show any change in the spectrum. The NMR solution was passed through a pad of silica gel in a Pasteur pipet using THF. The UV-active material moving with the solvent front was collected, and the solvent was removed on a

vacuum line to give material identified as compound S_P-**16** (^{31}P NMR show a single peak at 139.51 ppm). This result, therefore, suggests that the broad peaks at ~139 ppm resulting from the mixture of methyldiphenylphosphonium chloride and phosphite triester S_P-**16** in CD_3Cl

Table 5. Experiments attempted to induce inversion of phosphite triester **16**[a]

Exp.[b]	Reagent (pK_a)	Solvent	Phosphite: reagent ratio	Temp(℃) /time
1	Galvinoxyl free radical	Toluene-d_8	1.00 : 1.00	rt/~17 h 94ºC/~1h
2[c]	(pBrC$_6$H$_4$)$_3$N$^+$SbCl$_6$	CD_3CN	1.00 : 0.21	rt/~20 h
3[c]	1*H*-tetrazole (**33**) (pk_a = 4.8)[d]	CD_3CN	1.00 : 1.03	rt/~17 h 67℃/~6 h
4	Et_3NH^+Cl (**34**) (pk_a = 10.7)[e]	Nitrobenzene-d_5	1.00 : 0.88	rt/~1 hr 65℃/~17 h
5	**35**	Nitrobenzene-d_5/ DMF (1/1). Mixture used to dissolve salt	1.00 : 0.50	rt/~17 h 50ºC/~ 2 h
6	**36** (pk_a = 4.57)[f]	Nitrobenzene-d_5	1.00 : 0.25	rt/~24 h
7	**36**	$CDCl_3$	1.00 : 1.45	rt/~12 h
8	**37** (pk_a = 5.2)[e]	$CDCl_3$	1.00 : 1.16	rt/~5 ¼ h
9	**38**	$CDCl_3$	1.00 : 1.06	rt/~4 ½ h 55ºC/~2 h

[a] For all experiments, S_P-**16** was used with the exception for experiment 9 (R_P-**16** was used instead); [b] monitor inversion by ^{31}P NMR unless indicated; [c] monitor inversion by ^{1}H NMR (TBDMS and anomeric hydrogen of deoxyribose ring) because ^{31}P peaks of the two diastereomers coincided in CD_3CN; [d] ref.[73]; [e] ref.[74] ; [f] ref.[75].

might be due to a random protonation of the nucleobases (thymine) and/or coordination of the dinuclosides through H-bonding of the thymines. The broadening of the ^{31}P and ^{1}H peaks with methyldiphenylphosphonium chloride did not occur with any of the other reagents shown in

Table 5, and might be because it is more acidic (pK_a of 4.57) than the other reagents.

Treating phosphite triester S_P-**16** with ~1 equivalent of pyridinium chloride (exp. 8) for ~1 day at rt resulted in a reaction solution that gave a ^{31}P NMR spectrum showing peaks at 139.52 (S_P-**16**) and 139.35 ppm in ratio of 20:80, and an unknown phosphorus species at ~29 ppm. The compound that corresponded to the major fraction at 139.35 ppm was separated by silica gel chromatography using a Pasteur pipet with a solvent system of 10% MeOH/CH_2Cl_2. The solvent was removed on a vacuum line and the material was identified possibly as the DMTr-free analogue of S_P-**16**.

2.6 Conclusion

Unlike Mislow's study of phosphine inversion, where first-order phosphine racemization was observed without detectable decomposition, the dinucleoside phosphite triesters used in the present study did undergo decomposition. However, the use of acyl protecting groups on the deoxyribose ring minimized the decomposition pathways, and allowed epimerization to be observed from both P-epimers. The rates of epimerization were similar from both diastereomers, and good fits of the data to first-order epimerization coupled with an "impurity" induced-decomposition pathway were found. Rate constants for epimerization, regardless of the decomposition pathway, yielded an activation barrier $\Delta G^{\dagger} = 33.0 \pm 0.2$ kcal/mol, comparable to that seen for phosphines. A variety of acidic and radical reagents failed to induce any epimerization, although decomposition did occur. Even if one were to worry that such a reagent might nevertheless exist and be responsible for our observed epimerization, the results obtained here clearly establish a lower limit for phosphite inversion. In fact, we would argue that the simplest mechanism is indeed inversion, and that all previous reports of epimerization of cyclic phosphites and related species at low temperature are not due to inversion. While the use of such

cyclic phosphites as ligands for catalytic asymmetric reactions is therefore problematic, the use of P-stereogenic phosphites, which we have shown here to be comparable to phosphines in configurational stability, should now be considered.

2.7 Experimental Section

General information. ^{1}H and ^{13}C NMR specra were recorded on a Bruker 400-MHz spectrometer with tetramethylsilane as an external standard. High-resolution mass spectrometry was performed on an Agilent G6520A Q-TOF instrument. ^{31}P NMR spectra were recorded on a Bruker 400-MHz spectrometer with an external capillary containing 85% H_3PO_4 in CD_3CN. β-Cyanoethylphosphodichloridite **18**[58] and 5'-*O*-(4,4'-dimethoxytrityl)-2'-deoxythymidine **21**[57] were synthesized according to literature procedures. *N*,*N*-Diisopropylamine, *N*,*N*-diisopropylethylamine, *N*-methylimidazole, and pyridine were distilled from calcium hydride and collected under nitrogen. Thymidine, *tert*-butyldimethylsilyl chloride, trifluoroacetic acid, borane-methyl sulfide complex (2 M solution in THF), dichloroacetic acid, hydrogen fluoride-pyridine (65-70%), methyldiphenyl phosphine, dimethyl(cyanomethyl)amine, DABCO, citric acid, hydrochloric acid (12 M), and acetic acid were used directly from suppliers. Acetonitrile and *N*,*N*-dimethylformamide were distilled under nitrogen from calcium hydride. Diethyl ether and tetrahydrofuran were dried prior to use by distillation from sodium-benzophenone. Dichloromethane, ethyl acetate, and hexanes were used directly from suppliers. Flash column chromatography was carried out on 230-400 mesh silica gel purchased from Silicycle. Thin-layer chromatography was carried out on Analtech aluminum-backed silica gel F (200-μm) plates.

Synthesis of (2-cyanoethyl) (*N*,*N*-diisopropylamino)chlorophosphine (19). Compound **19** was synthesized by a modification of the literature procedure.[25] Instead of carrying out the reaction at -20 ºC and purifying the product by distillation, the reaction was done

at rt and the crude product was used for the next step. Under nitrogen, *i*Pr_2NH (4.95 g, 48.88 mmol) was added dropwised over 1.5 h to a solution of **18** (4.20 g, 24.42 mmol) dissolved in 25 mL of Et_2O. The reaction mixture was stirred for an additional 5 min, then filtered through Celite and evaporated on a vacuum line to afford **19** (4.80 g, 85%) as a slightly yellow oil. ^1H NMR (400 MHz, CD_3CN): δ 4.00 (m, 2H), 3.83 (m, 2H), 2.76 (t, *J* = 5.98 Hz, 2H), 1.24 (d, *J* = 6.87 Hz, 12H). ^{13}C NMR (100 MHz, CD_3CN): δ 118.9, 61.8 (d, *J* = 19.83 Hz), 47.0 (d, *J* = 12.70 Hz), 23.9 (d, *J* = 8.02 Hz), 20.5 (d, *J* = 7.22 Hz). ^{31}P NMR (161 Mz, CD_3CN): δ 118.9

Synthesis of 5'-*O*-(4,4'dimethoxytrityl)-2'-deoxythymidine 3'-(2-cyanoethyl *N*,*N*-diisopropylphosphoramidite (22). 5'-*O*-(4,4'-Dimethoxytrityl)-2'-deoxythymidine 3'-(2-cyanoethyl *N*,*N*-diisopropylphosphoramidite was synthesized by following the literature procedure used for the synthesis of the adenosine analogue of compound **22**.[58, 61]

Under nitrogen, *i*Pr_2NEt (1.09 g, 8.45 mmol) was added to a solution of **21** (3.02 g, 5.55 mmol) dissolved in 15 mL of THF and the reaction mixture cooled to -78 ^oC. A solution of **19** (1.58 g, 6.69 mmol) dissolved in 2 mL of THF was then added to the cooled solution over 10 min. The reaction solution was allowed to warm to rt and stirred for 1.5 h. The solution was then washed with 30 mL of saturated aqueous $NaHCO_3$ solution and then with 30 mL of brine. The organic layer was dried with anhydrous $MgSO_4$, filtered, and evaporated on a vacuum line to give a white foam. The product was purified by silica gel chromatography using EtOAc/hexanes (2/1) – 50 g silica gel in a column with a diameter of 30 mm. All fractions with R_f of 0.51 (2:1 EtOAc/hexanes) were combined and evaporated on a vacuum line to afford compound **22** as a white powder. Yield = 3.40 g (82%). ^1H NMR (400 MHz, CD_3CN, ~1:1 S_P-**22**:R_P-**22**; peaks could not be assigned to the two diastereomers; integrals are combined where peaks for the diastereomers overlap): δ 9.03 (br s, 2 x N*H*), 7.48-7.23 (m, 18H, DMTr, 2 x H-6), 6.88-6.85 (m,

8H, DMTr), 6.25 (m, 2 x H-1'), 4.63 (m, 2 x H-3'), 4.07 (m, 2 x H-4'), 3.76 (s, C*H*$_3$O, 6 H), 3.75 (s, C*H*$_3$O, 6 H), 3.84-3.50 (m, 2 x C*H*$_2$OP, 4 x N*H*(CH$_3$)$_2$, 8H), 3.31 (m, 2 x H-5', 2 x H-5''), 2.64 (t, *J* = 5.94 Hz, C*H*$_2$CN), 2.51 (t, *J* = 5.94 Hz, C*H*$_2$CN), 2.38 (m, 2 x H-2', 2 x H-2''), 1.50 (d, *J* = 1.03 Hz, C*H*$_3$C-5), 1.48 (d, *J* = 1.03 Hz, C*H*$_3$C-5), 1.17-1.03 (m, 24 H, NH(C*H*$_3$)$_2$). ^{31}P NMR (161 Mz, CD_3CN, two diastereomers): δ 148.97, 148.91 (51.4/48.6%).

3'-*O*-(*tert*-Butyldimethylsilyl)-thymidine (23). This compound was synthesized by modification of literature procedures.[63, 64] At rt, TBDMSCl (5.56 g, 36.86 mmol) was added to a suspension of thymidine **20** (4.05 g, 16.70 mmol) and imidazole (5.00 g, 73.49 mmol) in 15 mL of dry DMF. After the reaction solution was stirred at rt for 1.5 h, the solvent was evaporated on a vacuum line to give crude 3', 5'-di-*O*-(*tert*-butyldimethylsilyl)-thymidine as a gel (R_f = 0.88, EtOAc). Acetic acid (80%, 100 mL) was added to the gel, and the reaction solution heated on a steam bath. The reaction was monitored by TLC over 6 h until the 3', 5'-di-*O*-(*tert*-butyldimethylsilyl)-thymidine was converted to the 3'-*O*-(*tert*-butyldimethylsilyl)-thymidine. Two other UV-active by-products were also formed during the reaction time, possibly 5'-*O*-(*tert*-butyldimethylsilyl)-thymidine and thymidine. The reaction solution was evaporated on a vacuum line to give a gum, which was dissolved in 100 mL of CH_2Cl_2 and washed with 30 mL of water. The organic layer was dried with $MgSO_4$, filtered, and evaporated on a vacuum line to give a slightly yellow gum. The gum was dissolved in 30 mL of EtOH and 300 mL of distilled water was added gently, resulting in the precipitation of **23** as a white solid. The compound was filtered and dried on a vacuum line (2.49 g, 42%, R_f = 0.64, eluent = EtOAc). ^{1}H NMR (400 MHz, CD_3CN): δ 9.52 (br s, 1H), 7.56 (br s, 1H), 6.09 (t, *J* = 6.7 Hz, 1H), 4.45 (m, 1H), 3.82 (m, 1H), 3.67 (m, 1H), 3.22 (br s, 1H), 2.16 (m, 2H), 1.82 (d, *J* = 4.0 Hz, 3H), 0.89 (s, 9H), 0.09 (s,

6H). ^{31}C NMR (100 MHz, CD_3CN): δ 165.1, 151.7, 137.4, 111.1, 88.6, 85.8, 72.9, 62.3, 41.1, 26.1, 18.6, 12.7, -4.53, -4.67.

Synthesis of pyridinum trifluoroacetate (PTFA). Trifluoroacetic acid (7.10 g, 62.28 mmol) was added slowly to a vigorously stirred solution of pyridine (4.90 g, 61.88 mmol) in 75 mL of Et_2O. After ~10 min, the precipitate was filtered and dried on a vacuum line to afford the title compound (10.56 g, 88%) as white crystals. ^{1}H NMR (400 MHz, $CDCl_3$): δ 8.89-8.87 (m, 2H), 8.33-8.28 (m, 1H), 7.86-7.83 (m, 2H). ^{13}C NMR (100 MHz, $CDCl_3$): δ 162.4 (q, J = 36.6 Hz), 143.4, 143.2, 126.4, 116.4 (d, J = 290.9 Hz).

Synthesis and separation of 2-cyanoethyl-[5'-*O*-(4,4'dimethoxytrityl)-2'-deoxythymylyl]-(3',5')-3'-*O*-(*tert*-butyldimethylsilyl)-2'-deoxythymidine boranophosphate S_P-24 and R_P-24. Under nitrogen, a solution of pyridinum trifluoroacetate (PTFA) (0.8524 g, 4.4138 mmol) and *N*-methylimidazole (NMI) (0.1919 g, 2.3371 mmol) in 8 mL of CH_3CN was added dropwise over ~5 min to a magnetically stirred solution of compound **22** (1.6514 g, 2.2172 mmol) and compound **23** (0.7191 g, 2.0171 mmol) in 20 mL of CH_3CN. After 1 h, the reaction solution was evaporated on a vacuum line to give a gum. The gum was dissolved in 60 mL of CH_2Cl_2 and then was washed with 20 mL of saturated aqueous $NaHCO_3$ solution. The organic layer was dried with anhydrous $MgSO_4$, and the solvent was evaporated on a vacuum line to give a foam. The foam was dissolved in 25 mL of dry THF and the solution was placed under N_2 in an ice-water bath. To the stirred solution $BH_3{\cdot}Me_2S$ (3.4 mL of a 2.0 M solution in THF, 6.8 mmol) was added dropwise over ~3-4 min. The ice-water bath was removed after addition of the $BH_3{\cdot}Me_2S$ solution and then the solution was allowed to stir for an additional 10 min, after which it was immediately eluted through a pad of silica gel (~100 g in a 150 mL coarse frit) with THF. All of the UV-active material moving with the solvent front was collected and evaporated on a

vacuum line to give crude compound **24** as a white foam (1.94 g, 95%). The two diastereomers of **24** were separated by silica gel chromatography using EtOAc/hexanes 4:1 (120 g silica gel in a column with a diameter of 30 mm). The fractions corresponding to R_f = 0.56 and 0.44 were combined separately and evaporated on a vacuum line to give white foams. Since the ^{1}H NMR spectra of both samples showed that *N*-methylimidazole was present, each sample was dissolved in 50 mL of EtOAc/hexanes (2:1), and then washed with 25 mL of 0.5 M citric acid. The organic layer was dried with $MgSO_4$ and evaporated on a vacuum line to afford S_P-**24** (0.49 g, 25%) and R_P-**24** (0.44 g, 23%) as white foams. S_P-**24** (R_f = 0.56, in EtOAc/hexanes (4:1), peaks assigned by 2D NMR: ^{1}H NMR (400 MHz, CD_3CN): δ 9.36 (br s, NH, 2H), 7.47-7.27 (m, ArH, 2 x H-6, 11H), 6.91-6.90 (m, ArH, 4H), 6.28 (dd, *J* = 6.8, 8.1 Hz, ^{T1}H-1', 1H), 6.14 (t, *J* = 6.8 Hz, ^{T2}H-1', 1H), 5.20 (m, ^{T1}H-3', 1H), 4.41 (m, ^{T2}H-3', 1H), 4.80-3.91 (m, ^{T1}H-4', ^{T2}H-5', ^{T2}H-5'', C*H*$_2$OP, 5H), 3.94 (m, ^{T2}H-4', 1H), 3.76 (s, C*H*$_3$O, 6H), 3.33 (m, ^{T1}H-5', ^{T1}H-5'', 2H), 2.72 (t, *J* = 5.8 Hz, C*H*$_2$CN, 2H), 2.48 (m, ^{T1}H-2', ^{T1}H-2'', 2H), 2.18 (m, ^{T2}H-2', ^{T2}H-2'', 2H), 1.82 (s, C*H*$_3$C-5, 3H), 1.45 (s, C*H*$_3$C-5, 3H), 0.89 (s, (C*H*$_3$)CSi, 9H), 0.45 (br, B*H*$_3$, 3H), 0.099 (s, C*H*$_3$Si, 3H), 0.096 (s, C*H*$_3$Si, 3H). ^{13}C NMR (100 MHz, CD_3CN): δ 164.7, 159.9, 151.5, 151.4, 145.7, 137.0, 136.6, 136.39, 136.37, 131.1, 131.0, 129.03, 128.98, 128.1, 118.3, 114.2, 111.8, 111.6, 87.8, 85.7, 85.5 (d, *J* = 6.5 Hz), 85.31 (d, *J* = 5.1 Hz), 85.28, 79.4, 72.4, 67.0 (d, *J* = 5.0 Hz), 64.2, 62.6 (d, *J* = 3.0 Hz), 56.0, 40.4, 39.6 (d, *J* = 3.0 Hz), 26.1, 20.4 (d, *J* = 6.0 Hz), 18.6, 12.7, 12.2, -4.5, -4.6. ^{31}P NMR (161 Mz, CD_3CN): δ 116.89. HRMS (ESI): Calcd for $C_{50}H_{64}BN_5O_{13}PSi$ $[M-H]^-$: 1012.4101, found 1012.4100.

R_P-**24** (R_f = 0.44, in EtOAc/hexanes (4:1), peaks assigned by 2D NMR: ^{1}H NMR (400 MHz, CD_3CN): δ 9.31 (br s, NH, 1H), 9.28 (br s, NH, 1H), 7.47-7.27 (m, ArH, 2 x H-6, 11H), 6.91-6.90 (m, ArH, 4H), 6.28 (dd, *J* = 6.0, 8.1 Hz, ^{T1}H-1', 1H), 6.12 (t, *J* = 6.8 Hz, ^{T2}H-1', 1H), 5.21

(m, ^{T1}H-3', 1H), 4.38 (m, ^{T2}H-3', 1H), 4.80-3.91 (m, ^{T1}H-4', ^{T2}H-5', ^{T2}H-5", C*H*$_2$OP, 5H), 3.93 (m, ^{T2}H-4', 1H), 3.75 (s, C*H*$_3$O, 6H), 3.32 (m, ^{T1}H-5', ^{T1}H-5", 2H), 2.74 (t, *J* = 5.8 Hz, C*H*$_2$CN, 2H), 2.50 (m, ^{T1}H-2', ^{T1}H-2", 2H), 2.18 (m, ^{T2}H-2', ^{T2}H-2", 2H), 1.80 (s, C*H*$_3$C-5, 3H), 1.45 (s, C*H*$_3$C-5, 3H), 0.88 (s, (C*H*$_3$)CSi, 9H), 0.44 (br, B*H*$_3$, 3H), 0.076 (s, (C*H*$_3$)$_2$Si, 6H). ^{13}C NMR (100 MHz, CD_3CN): δ 164.7, 159.9, 151.5, 151.4, 145.7, 137.0, 136.6, 136.42, 136.41, 131.07, 131.03, 129.03, 128.97, 128.0, 118.3, 114.2, 111.7, 111.5, 87.8, 86.0, 85.6 (d, *J* = 6.6 Hz), 85.30 (d, *J* = 5.1 Hz), 85.33, 79.3, 72.6, 67.3 (d, *J* = 5.0 Hz), 64.2, 63.0 (d, *J* = 3.0 Hz), 56.0, 40.4, 39.6 (d, *J* = 3.0 Hz), 26.1, 20.4 (d, *J* = 6.0 Hz), 18.5, 12.7, 12.2, -4.5, -4.6. ^{31}P NMR (161 Mz, CD_3CN): δ 116.83. HRMS (ESI): Calcd for $C_{50}H_{64}BN_5O_{13}PSi$ $[M-H]^-$: 1012.4101, found 1012.4104.

2-Cyanoethyl[5'-*O*-(*p,p*'-dimethoxytrityl)-2'-deoxythymylyl]-(3',5')-3'-*O*-(*tert*-butyldimethylsilyl)-2'-deoxythymidine phosphite triester (*S*$_P$-16). In the glove box, a solution of *S*$_P$-**24** (0.31 g, 0.31 mmol) and DABCO (0.35 g, 3.10 mmol) in 15 mL of CH_2Cl_2 was stirred for 37 h at rt. The solvent was evaporated on a vacuum line to give crude *S*$_P$-**16** as a gum. The gum was applied to a short column of silica gel (~30 g in a coarse frit), and was then eluted with THF. All of the UV-active material moving with the solvent front was collected and the solvent was evaporated on a vacuum line to afford *S*$_P$-**16** as a white foam (0.184 g, 60%). ^{31}P NMR (161 Mz, toluene-d_8): δ 139.36.

2-Cyanoethyl [2'-deoxythymylyl]-(3',5')-3'-*O*-(*tert*-butyldimethylsilyl)-2'-deoxythymidine boranophosphate *S*$_P$-25. A cooled solution of 2% $CHCl_2CO_2H/CH_2Cl_2$ (15 mL) was added to compound *S*$_P$-**24** (0.32 g, 0.32 mmol) with stirring for 20 min at rt. The reaction solution was then diluted further with 15 mL of CH_2Cl_2 and washed with 10 mL of 5% aqueous $NaHCO_3$. The organic layer was extracted and the aqueous layer was washed with 3 x

10 mL of CH_2Cl_2. The combined organic layer was dried with anhydrous $MgSO_4$, filtered, and evaporated on a vacuum line to give crude S_P-**25** as a gum. The crude material was dissolved in EtOAc/hexanes (2:1) and applied to a short column of silica gel (~30 g in a column with a diameter of 20 mm). The material was first eluted with EtOAc/hexanes (2:1), then with EtOAc/hexanes (4:1), and finally with EtOAc. The appropriate fractions with R_f of 0.5 (EtOAc) were combined, and the solvent was evaporated on a vacuum line to afford compound S_P-**25** as a white foam (0.18 g, 82%). Peak assignments for compound S_P-**25** were determined by 2D NMR. ^{1}H NMR (400 MHz, CD_3CN): δ 9.23 (br s, NH, 2H), 7.53 (d, *J* = 1.2 Hz, H-6, 1H), 7.27 (d, *J* = 1.2 Hz, H-6, 1H), 6.20 (m, ^{T1}H-1', ^{T2}H-1', 2H), 5.06 (m, ^{T1}H-3', 1H), 4.44 (m, ^{T2}H-3', 1H), 4.23 (m, ^{T2}H-5', ^{T2}H-5", C*H*$_2$OP, 4H), 4.14 (m, ^{T1}H-4', 1H), 3.98 (m, ^{T2}H-4', 1H), 3.71 (m, ^{T1}H-5', ^{T1}H-5", 2H), 3.33 (br t, *J* = 5.2 Hz, O*H*), 2.79 (t, *J* = 6.0 Hz, C*H*$_2$CN, 2H), 2.38 (m, ^{T1}H-2', ^{T1}H-2", 2H), 2.21 (m, ^{T2}H-2', ^{T2}H-2", 2H), 1.85 (d, *J* = 1.2 Hz, C*H*$_3$C-5, 3H), 1.82 (d, *J* = 1.2 Hz, C*H*$_3$C-5, 3H), 0.90 (s, (C*H*$_3$)CSi, 9H), 0.46 (br, B*H*$_3$, 3H), 0.110 (s, C*H*$_3$Si, 3H), 0.105 (s, C*H*$_3$Si, 3H). ^{13}C NMR (100 MHz, CD_3CN): δ 164.7, 151.54, 151.46, 137.0, 136.9, 118.5, 111.6, 111.5, 86.5 (d, *J* = 4.0 Hz), 85.8, 85.7, 85.5 (d, *J* = 7.0 Hz), 79.4 (d, *J* = 2.0 Hz), 72.5, 67.0 (d, *J* = 4.0 Hz), 62.9 (d, *J* = 3.0 Hz), 62.3, 40.4, 39.3 (d, *J* = 3.0 Hz), 26.1, 20.4 (d, *J* = 6.0 Hz), 18.6, 12.7, 12.6, -4.5, -4.7. ^{31}P NMR (161 Mz, CD_3CN): δ 116.47. HRMS (ESI): Calcd for $C_{29}H_{48}BN_5O_{11}PSi$ $[M+H]^+$: 712.2950, found 712.2962.

2-Cyanoethyl [2'-deoxythymylyl]-(3',5')-3'-*O*-(*tert*-butyldimethylsilyl)-2'-deoxythymidine boranophosphate R_P-25. The procedure above was used to prepare R_P-**25** (0.12 g, 87%). Peak assignments for compound R_P-**25** were determined by 2D NMR. ^{1}H NMR (400 MHz, CD_3CN): δ 9.27 (br s, NH, 1H), 9.26 (br s, NH, 1H), 7.54 (d, *J* = 1.2 Hz, H-6, 1H), 7.27 (d, *J* = 1.2 Hz, H-6, 1H), 6.20 (m, ^{T1}H-1', ^{T2}H-1', 2H), 5.08 (m, ^{T1}H-3', 1H), 4.43 (m, ^{T2}H-3',

1H), 4.23 (m, ^{T2}H-5', ^{T2}H-5", C*H*$_2$OP, 4H), 4.13 (m, ^{T1}H-4', 1H), 3.98 (m, ^{T2}H-4', 1H), 3.71 (m, ^{T1}H-5', ^{T1}H-5", 2H), 3.35 (br t, *J* = 5.2 Hz, O*H*), 2.79 (t, *J* = 6.0 Hz, C*H*$_2$CN, 2H), 2.38 (m, ^{T1}H-2', ^{T1}H-2", 2H), 2.20 (m, ^{T2}H-2', ^{T2}H-2", 2H), 1.85 (d, *J* = 1.2 Hz, C*H*$_3$C-5, 3H), 1.82 (d, *J* = 1.2 Hz, C*H*$_3$C-5, 3H), 0.90 (s, (C*H*$_3$)CSi, 9H), 0.49 (br, B*H*$_3$, 3H), 0.112 (s, C*H*$_3$Si, 3H), 0.104 (s, C*H*$_3$Si, 3H). ^{13}C NMR (100 MHz, CD_3CN): δ 164.74, 164.71, 151.6, 151.5, 137.1, 137.0, 118.5, 111.6, 111.5, 86.5 (d, *J* = 4.0 Hz), 85.9, 85.8, 85.5 (d, *J* = 6.0 Hz), 79.2 (d, *J* = 4.0 Hz), 72.5, 67.1 (d, *J* = 4.0 Hz), 63.1 (d, *J* = 3.0 Hz), 62.3, 40.4, 39.3 (d, *J* = 4.0 Hz), 26.1, 20.4 (d, *J* = 7.0 Hz), 18.6, 12.7, 12.6, -4.5, -4.7. ^{31}P NMR (161 Mz, CD_3CN): δ 116.25. HRMS (ESI): Calcd for $C_{29}H_{48}BN_5O_{11}PSi$ $[M+H]^+$: 712.2950, found 712.2957.

2-Cyanoethyl-2'-deoxythymylyl-(3',5')-2'-deoxythymidine boranophosphate *S*$_P$-26. Compound *S*$_P$-**25** (0.17 g, 0.24 mmol) was dissolved in 8 mL of THF and then HF-pyridine (0.54 mL, 5.99 mmol) was added to the magnetically stirred solution. After ~20 h at rt, TLC indicated complete conversion to the product. The reaction solution was evaporated on a vacuum line to dryness, then redissolved in 10 mL of MeOH and evaporated on 1 g of silica gel. The material was applied to a silica gel column (~20 g in a column with a diameter of 20 mm) and eluted with 10% MeOH/EtOAc. The appropriate fractions with R_f 0.42 (10% MeOH/EtOAc) were combined and the solvent was evaporated on a vacuum line to afford compound *S*$_P$-**26** as a white foam (0.123 g, 87%). Peak assignments for compound *S*$_P$-**26** were determined by 2D NMR. ^{1}H NMR (400 MHz, CD_3CN): δ 9.27 (br s, NH, 2H), 7.54 (d, *J* = 1.2 Hz, H-6, 1H), 7.28 (d, *J* = 1.2 Hz, H-6, 1H), 6.21 (m, ^{T1}H-1', ^{T2}H-1', 2H), 5.07 (m, ^{T1}H-3', 1H), 4.37 (m, ^{T2}H-3', 1H), 4.25 (m, ^{T2}H-5', ^{T2}H-5", C*H*$_2$OP, 4H), 4.14 (m, ^{T1}H-4', 1H), 3.99 (m, ^{T2}H-4', 1H), 3.71 (m, ^{T1}H-5', ^{T1}H-5", 2H), 3.66 (br t, *J* = 5.2 Hz, ^{T1}O*H*), 3.60 (br s, ^{T2}O*H*), 2.80 (t, *J* = 6.0 Hz, C*H*$_2$CN, 2H), 2.37 (m, ^{T1}H-2', ^{T1}H-2", 2H), 2.18 (m, ^{T2}H-2', ^{T2}H-2", 2H), 1.85 (d, *J* = 1.2 Hz, C*H*$_3$C-5, 3H), 1.82 (d, *J* =

1.2 Hz, C*H*$_3$C-5, 3H), 0.46 (br, B*H*$_3$, 3H). ^{13}C NMR (100 MHz, CD_3CN): δ 164.7, 151.6, 151.5, 137.1, 136.8, 118.6, 111.64, 111.55, 86.5 (d, *J* = 5.0 Hz), 85.9, 85.5, 85.2 (d, *J* = 7.0 Hz), 79.4 (d, *J* = 2.0 Hz), 71.3, 67.3 (d, *J* = 5.0 Hz), 62.9 (d, *J* = 3.0 Hz), 62.3, 39.9, 39.3 (d, *J* = 3.0 Hz), 20.4 (d, *J* = 7.0 Hz), 12.7, 12.6. ^{31}P NMR (161 Mz, CD_3CN): δ 116.21. HRMS (ESI): Calcd for $C_{23}H_{34}BN_5O_{11}P$ $[M+H]^+$: 598.2086, found 598.2095.

2-Cyanoethyl-2'-deoxythymylyl-(3',5')-2'-deoxythymidine boranophosphate *R*$_P$-26. The procedure above was used to prepare *R*$_P$-**26** (78 mg, 85%). Peak assignments for compound *R*$_P$-**26** were determined by 2D NMR. ^{1}H NMR (400 MHz, CD_3CN): δ 9.19 (br s, NH, 2H), 7.53 (d, *J* = 1.2 Hz, H-6, 1H), 7.28 (d, *J* = 1.2 Hz, H-6, 1H), 6.20 (m, ^{T1}H-1', ^{T2}H-1', 2H), 5.08 (m, ^{T1}H-3', 1H), 4.35 (m, ^{T2}H-3', 1H), 4.25 (m, ^{T2}H-5', ^{T2}H-5", C*H*$_2$OP, 4H), 4.14 (m, ^{T1}H-4', 1H), 3.99 (m, ^{T2}H-4', 1H), 3.72 (m, ^{T1}H-5', ^{T1}H-5", 2H), 3.56 (br s, ^{T2}O*H*), 3.36 (br s, ^{T1}O*H*), 2.80 (t, *J* = 6.0 Hz, C*H*$_2$CN, 2H), 2.39 (m, ^{T1}H-2', ^{T1}H-2", 2H), 2.20 (m, ^{T2}H-2', ^{T2}H-2", 2H), 1.85 (d, *J* = 1.2 Hz, C*H*$_3$C-5, 3H), 1.83 (d, *J* = 1.2 Hz, C*H*$_3$C-5, 3H), 0.46 (br, B*H*$_3$, 3H). ^{13}C NMR (100 MHz, CD_3CN): δ 164.7, 151.6, 151.5, 137.1, 136.8, 118.5, 111.7, 111.5, 86.50 (d, *J* = 4.0 Hz), 85.9, 85.6, 85.3 (d, *J* = 6.0 Hz), 79.3 (d, *J* = 3.0 Hz), 71.3, 67.4 (d, *J* = 5.0 Hz), 63.0 (d, *J* = 3.0 Hz), 62.3, 40.0, 39.3 (d, *J* = 3.0 Hz), 20.4 (d, *J* = 7.0 Hz), 12.68, 12.65. ^{31}P NMR (161 Mz, CD_3CN): δ 115.90. HRMS (ESI): Calcd for $C_{23}H_{34}BN_5O_{11}P$ $[M+H]^+$: 598.2086, found 598.2099.

2-Cyanoethyl-2'-deoxythymylyl-(3',5')-2'-deoxythymidine phosphite triester *S*$_P$-27. In the glove box, a solution of *S*$_P$-**26** (0.115 g, 0.192 mmol) in 2 mL of pyridine was stirred for 36 h at rt. The solution was then evaporated over 1 g of silica gel on a vacuum line. The material was applied to a short column of silica gel (~10 g in a coarse frit), then eluted with 5% MeOH/EtOAc, followed by 5% MeOH/THF. All fractions with R_f = 0.54 (5% MeOH/THF) were combined and the solvent was evaporated on a vacuum line to afford *S*$_P$-**27** as a white foam

(0.10 g, 90%). ^{1}H NMR (400 MHz, CD_3CN): δ 9.07 (br s, 2H), 7.53 (d, *J* = 1.2 Hz, 1H), 7.40 (d, *J* = 1.2 Hz, 1H), 6.23-6.15 (m, 2H), 4.88 (m, 1H), 4.35 (m, 1H), 4.09-4.01 (m, 5H), 3.75 (m, 1H), 3.71 (m, 2H), 3.50 (br s, 1H), 3.26 (br s, 1H), 2.70 (t, *J* = 6.0 Hz, 2H), 2.37-2.23 (m, 2H), 2.20-2.14 (m, 2H), 1.84 (d, *J* = 1.2 Hz, 3H), 1.82 (d, *J* = 1.2 Hz, 3H). ^{31}P NMR (161 Mz, CD_3CN): δ 140.79.

2-Cyanoethyl-2'-deoxythymylyl-(3',5')-2'-deoxythymidine phosphite triester *R*$_P$-27. The procedure above was used to prepare *R*$_P$-**27** (90 mg, 80%). ^{1}H NMR (400 MHz, CD_3CN): δ 9.07 (br s, 2H), 7.63 (s, 1H), 7.39 (s, 1H), 6.21-6.17 (m, 2H), 4.91 (m, 1H), 4.34 (m, 1H), 4.04-4.01 (m, 5H), 3.94 (m, 1H), 3.71 (m, 2H), 3.48 (br s, 1H), 3.26 (br s, 1H), 2.70 (t, *J* = 6.0 Hz, 2H), 2.38-2.25 (m, 2H), 2.20-2.14 (m, 2H), 1.84 (s, 3H), 1.82 (s, 3H). ^{31}P NMR (161 Mz, CD_3CN): δ 140.37.

2-Cyanoethyl-[5'-*O*-(acetyl)-2'-deoxythymylyl]-(3',5')-3'-*O*-(acetyl)-2'-deoxythymidine phosphite triester *S*$_P$-28. In the glove box a solution of *S*$_P$-**26** (80.3 mg, 0.1376 mmol) and acetic anhydride (2.0892 mg, 0.2133 mmol) in 4 mL of pyridine was stirred for 24 h at rt. Approximately 0.5 g of silica gel was added to the flask and the excess pyridine was evaporated on a vacuum line. The silica gel containing the crude product was applied to a short column of silica gel (~10 g in a 15 mL coarse frit), and the product was eluted with EtOAc followed by EtOAc/THF (2:1), then THF. The fractions with R_f 0.41 (2:1 EtOAc/THF) were combined and the solvent was evaporated on a vacuum line to afford compound *S*$_P$-**28** as a white foam (76.3 mg, 83% yield). Peak assignments for compound *S*$_P$-**28** were determined by 2D NMR. ^{1}H NMR (400 MHz, CD_3CN): δ 9.34 (br s, NH, 2H), 7.45 (d, *J* = 1.2 Hz, H-6, 1H), 7.33 (d, *J* = 1.2 Hz, H-6, 1H), 6.24 (m, ^{T1}H-1', ^{T2}H-1', 2H), 5.26 (m, ^{T1}H-3', 1H), 4.87 (m, ^{T2}H-3', 1H), 4.28-4.05 (m, ^{T2}H-5', ^{T2}H-5", ^{T1}H-5', ^{T1}H-5", ^{T1}H-4', ^{T2}H-4',C*H*$_2$OP, 8H), 2.74 (t, *J* = 6.0 Hz,

CH_2CN, 2H), 2.46-2.28 (m, ^{T1}H-2', ^{T1}H-2", ^{T2}H-2', ^{T2}H-2", 4H), 2.08 (s, CH_3), 2.07 (s, CH_3), 1.88 (d, J = 1.2 Hz, CH_3C-5, 3H), 1.87 (d, J = 1.2 Hz, CH_3C-5, 3H). ^{13}C NMR (100 MHz, CD_3CN): δ 170.41, 170.36, 164.7 (br s), 150.6, 150.4, 135.7, 135.6, 118.3, 110.7, 110.6, 84.7, 84.5, 83.1 (d, J = 5.0 Hz), 83.0 (d, J = 4.0 Hz), 73.9, 73.0 (d, J = 13.1 Hz), 63.2, 62.5 (d, J = 8.9 Hz), 57.7 (d, J = 9.7 Hz), 38.5 (br s), 36.4, 20.2, 20.1, 19.9 (d, J = 4.5 Hz), 11.7, 11.6. ^{31}P NMR (161 Mz, CD_3CN): δ 140.78. HRMS (ESI): Calcd for $C_{27}H_{33}N_5O_{13}P$ $[M-H]^-$: 666.1813, found 666.1828.

2-Cyanoethyl[5'-*O*-(acetyl)-2'-deoxythymylyl]-(3',5')-3'-*O*-(acetyl)-2'-deoxythymidine phosphite triester R_P-28. The procedure above was used to prepare R_P-**28** (67 mg, 84%). Peak assignments for compound R_P-**28** were determined by 2D NMR. ^{1}H NMR (400 MHz, CD_3CN): δ 9.24 (br s, NH, 2H), 7.44 (d, J = 1.2 Hz, H-6, 1H), 7.34 (d, J = 1.2 Hz, H-6, 1H), 6.24 (m, ^{T1}H-1', ^{T2}H-1', 2H), 5.27 (m, ^{T1}H-3', 1H), 4.93 (m, ^{T2}H-3', 1H), 4.28-4.05 (m, ^{T2}H-5', ^{T2}H-5", ^{T1}H-5', ^{T1}H-5", ^{T1}H-4', ^{T2}H-4', CH_2OP, 8H), 2.74 (t, J = 6.0 Hz, CH_2CN, 2H), 2.46-2.28 (m, ^{T1}H-2', ^{T1}H-2", ^{T2}H-2', ^{T2}H-2", 4H), 2.08 (s, CH_3), 2.07 (s, CH_3), 1.88 (d, J = 1.2 Hz, CH_3C-5, 3H), 1.87 (d, J = 1.2 Hz, CH_3C-5, 3H). ^{13}C NMR (100 MHz, CD_3CN): δ 170.39, 170.37, 164.7 (br s), 150.5, 150.4, 135.63, 135.57, 118.2, 110.6, 110.5, 84.6 (br s), 83.11 (d, J = 6.0 Hz), 83.06 (d, J = 4.0 Hz), 74.0, 72.5 (d, J = 9.9 Hz), 63.2, 62.5 (d, J = 9.2 Hz), 58.2 (d, J = 13.8 Hz), 38.5 (br s), 36.5, 20.2, 20.1, 19.9 (d, J = 4.9 Hz), 11.7, 11.6. ^{31}P NMR (161 Mz, CD_3CN): δ 140.32. HRMS (ESI): Calcd for $C_{27}H_{33}N_5O_{13}P$ $[M-H]^-$: 666.1813, found 666.1831.

Dimethyl(cyanomethyl)ammonium chloride (35). To a solution of dimethyl(cyanomethyl)amine (1.00 g, 11.88 mmol) in 15 mL of benzene was added 12 M HCl (2.00 mL, 24.00 mmol). The solution was stirred at rt for 30 min and, was then evaporated on a vacuum line to give an oil. The oil was co-evaporated with 5 mL of EtOH to give the product as a white solid (1.3 g, 91% yield). The NMR spectrum of the product indicated that the sample

was pure enough to be used. ^{1}H NMR (400 MHz, DMSO-d_6, internal standard): δ 4.54 (s, 2H), 2.82 (s, 6H). ^{13}C NMR (100 MHz, DMSO-d_6, internal standard): δ 112.9, 43.2, 42.0.

Methyldiphenyl phosphonium chloride (36). To a solution of methyldiphenylphosphine (1.0105 g, 5.0470 mmol) in 10 mL of benzene was added 12 M HCl (0.8 mL, 9.6 mmol). The solution was stirred at rt for 30 min, and was then evaporated on a vacuum line to give a gum. The gum was co-evaporated with 5 mL of EtOH to afford the product as a white solid (1.02 g, 86% yield). ^{1}H NMR (400 MHz, $CDCl_3$): δ 10.76 (br s, 1H), 7.86-7.81 (m, 4H), 7.64-7.52 (m, 6H), 2.36 (d, J = 10.5, 3H). ^{31}P NMR (161 Mz, $CDCl_3$): δ -9.91.

Pyridinium hydrochloride (37). To a solution of pyridine (1.00 g, 12.64 mmol) in 12 mL of benzene was added 12 M HCl (1.20 mL, 14.40 mmol). The solution was stirred at rt for 30 min, and then was evaporated on a vacuum line to give a gum. The gum was taken into the glove box, dissolved in 20 mL of CH_2Cl_2, and the solution was dried with anhydrous $MgSO_4$. The solution was filtered and then evaporated on a vacuum line to afford the product as a white solid (1.21 g, 83% yield). ^{1}H NMR (400 MHz, $CDCl_3$): δ 8.93-8.92 (m, 2H), 8.51 (m, 1H), 8.04 (m, 2H). ^{13}C NMR (100 MHz, $CDCl_3$): δ 145.7, 141.1, 127.2.

***N*-Methylimidazolium hydrochloride (38).** To a solution of *N*-methylimidazole (1.01 g, 12.23 mmol) in 10 mL of benzene was added 12 M HCl (1.20 mL, 14.40 mmol). The solution was stirred at rt for 30 min, and was then evaporated on a vacuum line to give a gum. The gum was taken into the glove box, dissolved in 20 mL CH_2Cl_2, and the solution was dried with anhydrous $MgSO_4$. The solution was filtered and then evaporated on the vacuum line to afford the product as a white solid (1.22 g, 84% yield). ^{1}H NMR (400 MHz, $CDCl_3$): δ 15.68 (br s, 1H),

9.72 (s, 1H), 7.38 (m, 1H), 7.21 (m, 1H), 4.10 (s, 3H). ^{13}C NMR (100 MHz, $CDCl_3$): δ 136.0, 121.9, 119.8, 36.2.

Chart 5. Experiments 1-6: "impurity" decomposition

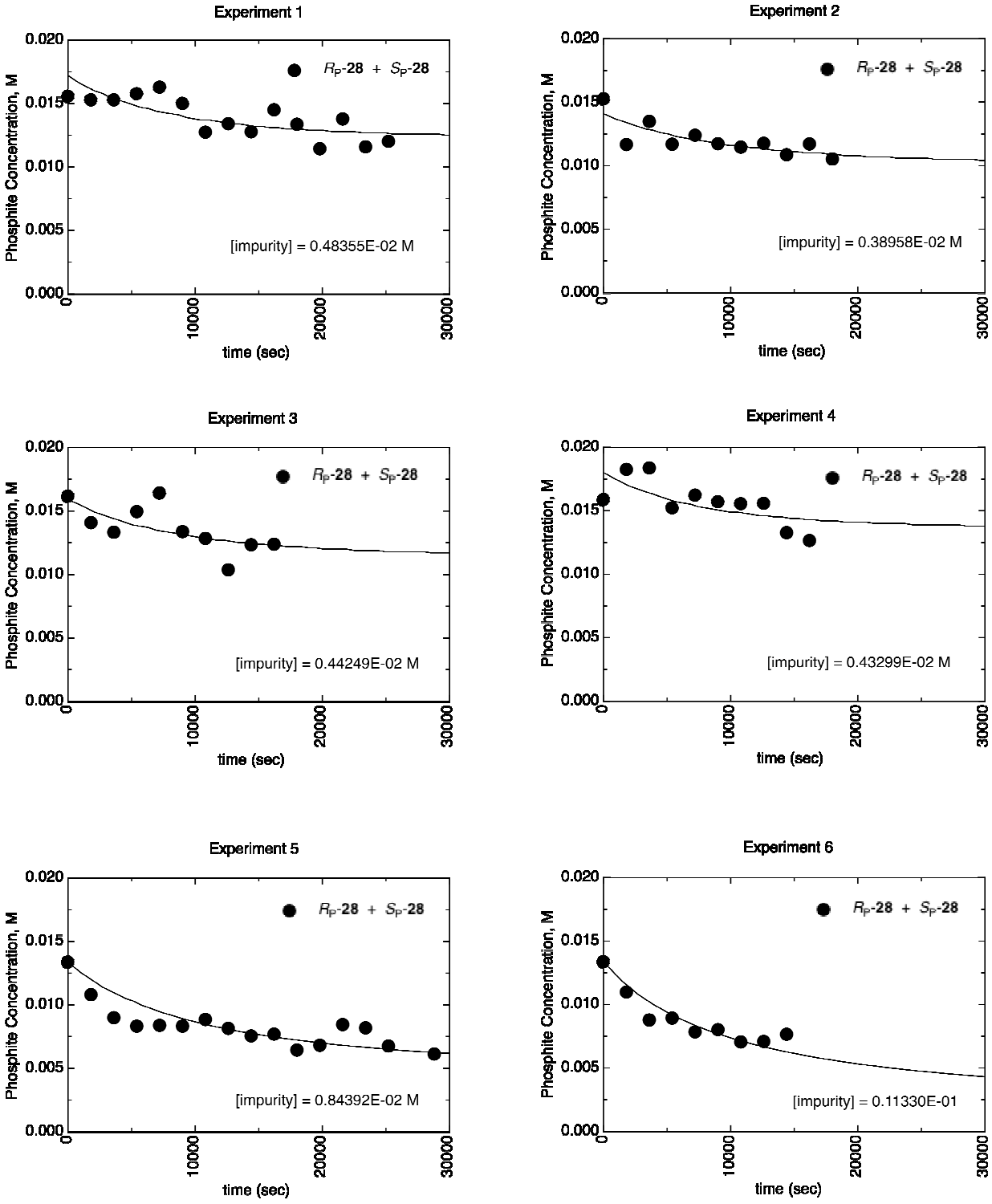

Chart 6. Experiments 1-6: epimerization and "impurity" decomposition

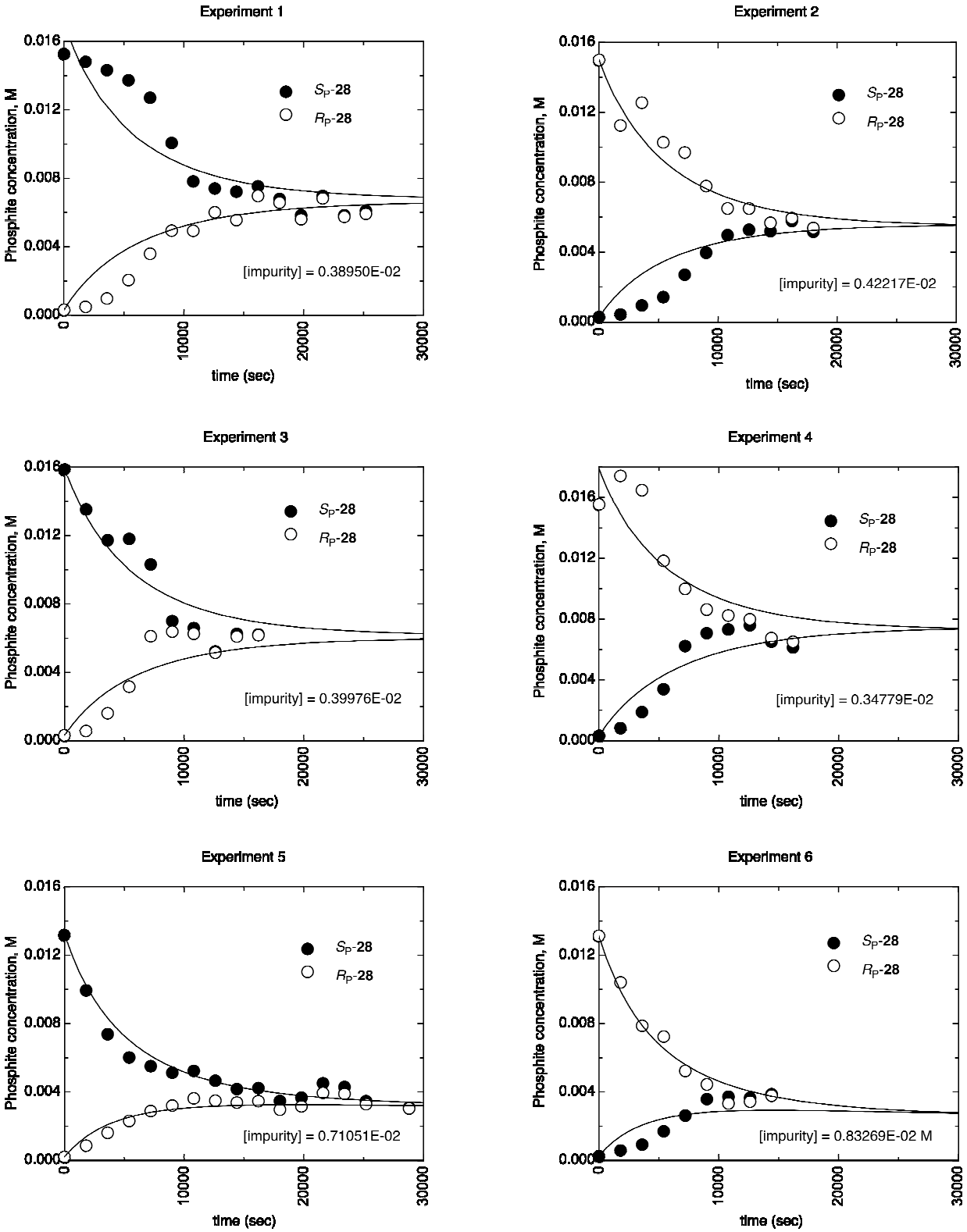

Chapter 3

Chiral analogues of PADS and MEDITH

3.1 Abstract

Chiral analogues of phenylacetyl disulfide (PADS) and of 5-methyl-3*H*-1,2,4-dithiazol-3-one (MEDITH) can be synthesized from the same set of 2-arylalkanoic acids. For the PADS analogues, conversion of the acids to acid chlorides was followed by phase-transfer catalyzed reaction with Na_2S_2 to give the desired compounds in 50-63% yield. Chiral HPLC showed that the final products were formed with enantiomeric purities of from 99.0 to >99.9%. The X-ray crystal structures of the disulfides derived from (*R*) and (*S*)-2-phenylpropionic acid establish the stereochemistry and the helicity of these materials, and DFT calculations suggest that the high specific rotations can be due to preferred retention of this helicity in solution. For the MEDITH analogues, conversion of the acid chlorides to the thioamides was accomplished in high enantiomeric purity and yield only by avoidance of acidic conditions and chromatography. The final conversion to the desired heterocycles failed using the literature procedure, which gave relatively low yields of racemic product; optimization of the base (pyridine) and reactant solvent (ether) solved both problems. Analysis by chiral HPLC showed the enantiomeric purities to range from 86.1–99.4%.

3.2 Introduction

Sulfurization of phosphorus is a key step in the synthesis of phosphorothioate oligonucleotides, reagents which can be used as DNA analogues for antisense applications.[4, 13, 76, 77] While elemental sulfur can be used, it was noted long ago that it is relatively slow and, when used in an automated DNA synthesizer, "led to instrument failure as a result of the insolubility of S_8 in most organic solvents."[28] Beaucage et al. solved this problem in 1990 with the report of a

soluble reagent, now popularly known as Beaucage reagent (Figure 1), that rapidly delivered sulfur to the phosphorus of the phosphite triester in the phosphoramidite method of solid-phase DNA synthesis.[28, 66] While effective, many reports have noted its poor stability in solution

Figure 1. Examples of sulfurizing reagents

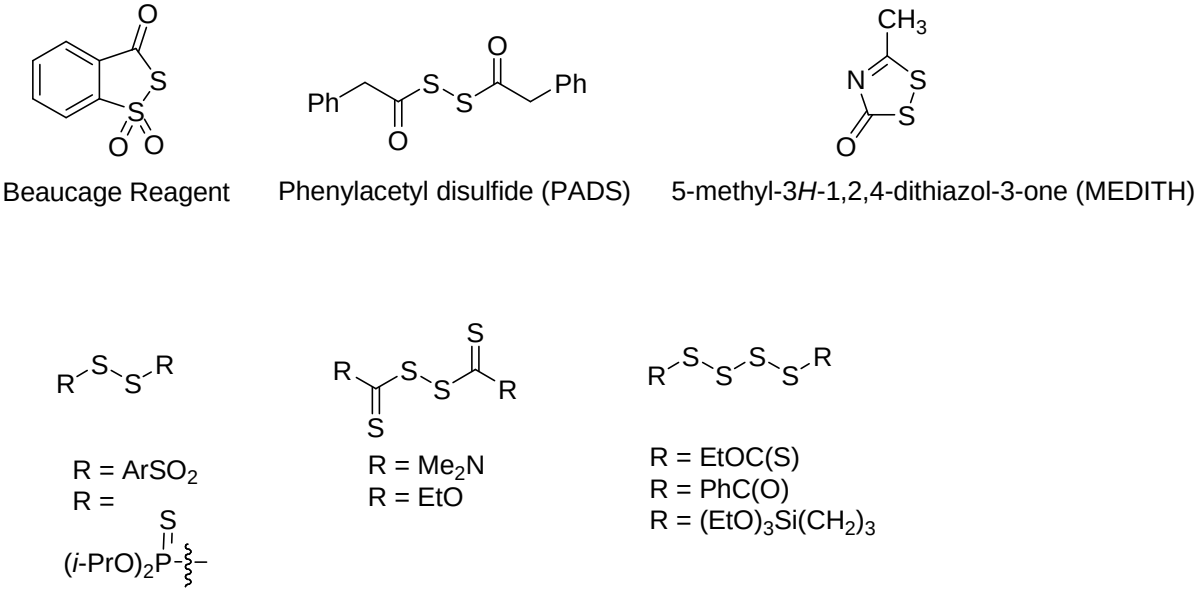

(necessitating its use in silylated glass[66]), difficult synthesis resulting in high cost, and formation of an oxidizing reagent as a byproduct, which may account for small amounts of phosphate impurity linkages.[29, 78-80] In order to overcome these problems, a wide variety of sulfurizing reagents, a selection of which is shown in Figure 1, has been investigated.[29, 78-97]

For one reagent that has been successfully used by Isis Pharmaceuticals, phenylacetyl disulfide (PADS), it was shown that the diastereomer ratio was indistinguishable from that obtained using Beaucage reagent.[98, 99] Beaucage reagent itself does not appear to be a good choice for synthesis of a chiral analogue, but both PADS and 5-methyl-3*H*-1,2,4-dithiazol-3-one[100] (MEDITH), another highly reactive sulfurizing reagent, presented ready opportunities for

convergent synthesis of chiral reagents; the other reagents would place centers of chirality farther from the reactive disulfide linkage. We report here (1) the synthesis of enantiomerically pure chiral analogues of PADS starting with known α-alkylated carboxylic acids, (2) X-ray diffraction results for one pair of enantiomers that unequivocally establish the absolute configurations of two disulfides and are in accord with the reported configurations of the starting carboxylic acids, (3) density functional theory (DFT) calculations that support the observed helicity about the S–S bond, (4) conversion of the enantiomerically pure chiral acids to chiral thioamides with no epimerization in cases where there is relatively little steric encumbrance, (5) conversion of the thioamides to acid-sensitive enantiomerically pure chiral analogues of MEDITH, and (6) chiral HPLC results in support of the enantiomeric purity of the new disulfides.

3.3 Results and Discussion

3.3.1 Chiral analogues of phenylacetyl disulfide (PADS)

The synthesis of PADS from phenylacetyl chloride has been reported by several groups.[82, 101-103] Since enantiomerically pure 2-aryl carboxylic acids are well known, this seemed to be a straightforward route to the desired chiral disulfides. The method developed by Kodomari and coworkers,[101] which gave PADS in 95% yield, was carried out by the addition of an aqueous solution of Na_2S_2 to a benzene solution of phenylacetyl chloride and hexadecyltributylphosphonium bromide as a phase-transfer catalyst. When this method was used for the synthesis of the chiral analogues of PADS using chiral carboxylic acid chlorides,[104] crude yields of only ~60-70% were obtained. This could be improved to ~80-90% simply by addition of the acid chloride to a vigorously stirred mixture of aqueous Na_2S_2 and the phase-transfer catalyst in toluene (Scheme 1). A single crystallization of **2a**–**c** in methanol and of **2d** in

benzene/petroleum ether gave the enantiomers in 50-63% isolated yields. The specific rotations of the disulfides are unusually high, ranging from an average of ±366 for **2a** to ±541 for **2c**.

Scheme 1. Synthesis of chiral analogues of phenylacetyl disulfides

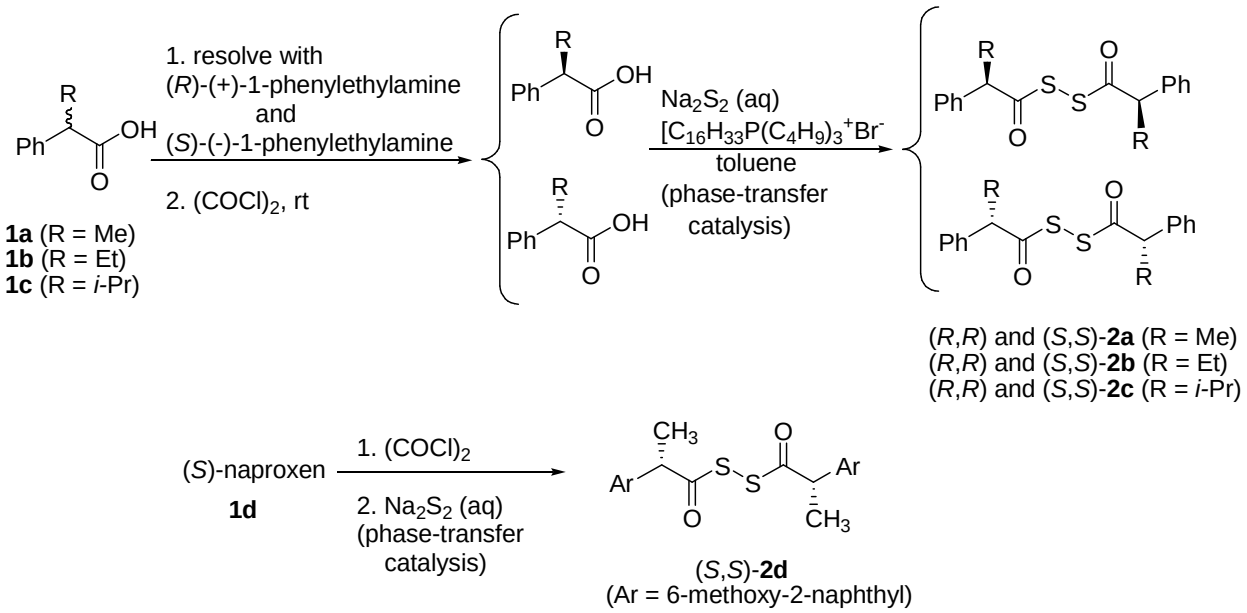

3.3.2 X-ray structure of 2a and DFT calculations

Single crystals of (*R*,*R*)- and (*S*,*S*)-**2a** were grown by a single crystallization from hot methanol with cooling to rt. The X-ray structure determinations confirmed both the overall structures and on the basis of Flack parameters[105, 106] unequivocally established the absolute stereochemistry of the α-stereocenters of the carboxylic acids, namely, (*R*)-(–)-**1a**[107-109] giving rise to (*R*,*R*)-(–)-**2a** and (*S*)-(+)-**1a** giving rise to (*S*,*S*)-(+)-**2a** (see Figure 2 for a representative ORTEP drawing). The absolute configurations of the starting carboxylic acids were reported in 1956 without the use of a single-crystal X-ray diffraction structure,[107] and other workers have reported results in agreement with this determination: each of the (+)-enantiomers of **1a**–**e** is

Figure 2. ORTEP drawing of (*S*,*S*)-**2a**

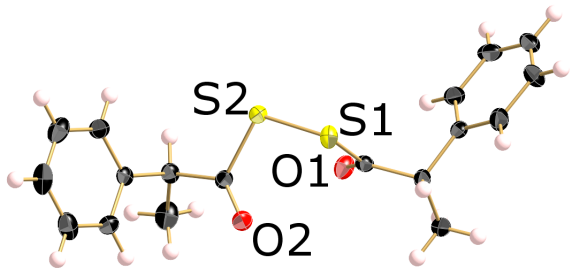

accepted as having the *S*-configuration.[107-111] In some cases X-ray structures of diastereomeric salts of α-alkyl carboxylic acids have been reported, but without optical rotations to connect the configurations with the specific rotations.[112, 113] A search of the Cambridge Structural Database for structures of 2-phenylpropionic acid (**1a**) turned up several structures of the pure enantiomers and cocrystals, but the absolute configurations were all assumed to be correct and no attempts to crystallographically confirm the *R* and *S* configurations were made.[114, 115] However, we did find one other case comparable to those of (*R*,*R*) and (*S*,*S*)-**2a** in which an ester derived from (*S*)-(+)-**1a** was subjected to a Flack analysis and the absolute configuration confirmed.[116]

Returning now to the disulfides themselves, a search of the Cambridge Structural Database for disulfides having carbonyl groups on the disulfide linkage resulted in finding eight neutral acyclic compounds of the form RC(O)SSC(O)R' (Table 1). Most of the R groups are aromatic (i.e. R = R' = Ph (**3a**),[117, 118] 4-chlorophenyl (**3b**),[119] 2-methoxyphenyl (**3c**),[120] 1-indolyl (**3d**),[121] ferrocenyl (**3e**)),[122] one has R = R' = $(cyclohexyl)_2N$ (**3f**),[123] and two have R = F and R' = CF_3 (**3g**), CF_2Cl (**3h**).[124, 125] The disulfide bond lengths fall in a fairly tight range (2.013 Å for **3d** to 2.039(2) Å for **3c**), so those for (*R*,*R*)-**2a** (2.0381(9), 2.037(1) Å - there are two independent molecules in the unit cell, differing slightly in the tilt of the phenyl rings) - and for

Table 1. Structural data (X-ray and DFT calculations) for dicarbonyl disulfides, RC(O)SSC(O)R'

Cmpd	R, R′[a]	S-S (Å)	∠(CSSC) (°)	∠($SSCO_1$) (°)	∠($SSCO_2$) (°)	Space Group/DFT[b]
3a[117, 118]	Ph	2.021(2)	80.8(3)	7.8(5)	-9.2(5)	$P2_1/a$[c]
3b[119]	4-ClC_6H_4	2.021(8)	79.1(1)	-2.9(3)	-10.3(3)	$P\bar{1}$
3c[120]	2-$MeOC_6H_4$	2.039(2)	84.7(3)	-3.5(5)	-10.7(6)	*Pbca*
3d[121]	1-indolyl[d]	2.013(1)	85.4	-2.0	-12.4	$P2_1/c$
3e[122]	$(C_5H_5)Fe(C_5H_4)$	2.022(2)	92.2(3)	-0.6(5)	-9.4(5)	$P2_12_12_1$
3f[123]	$(C_6H_{12})_2N$	2.014(1)	89.7(1)	-3.2(2)	-3.2(2)	$C2/c$
3g[124]	F, CF_3	2.017(2)	77.7(2)	-6.1(4)	8.0(5)	$P2_1/n$
3h[125]	F, CF_2Cl	2.029(1)	84.2(2)	0.8(4)	4.8(3)	$P2_1/n$
(*R,R*)-**2a**	Ph(CH_3)CH	2.0381(9)	-77.5(1)	4.3(2)	-5.0(2)	$P12_11$
		2.037(1)	-81.2(1)	0.4(2)	6.7(2)	
(*S,S*)-**2a**	Ph(CH_3)CH	2.0408(6)	77.29(8)	-4.4(2)	5.5(2)	$P12_11$
		2.0416(7)	81.24(8)	-0.1(2)	-6.9(2)	
(*S,S*)-**2a**, DFT		2.069	81.78	-3.47	-3.49	gas phase
		2.070	-84.52	0.87	0.88	gas phase, 0.72 kcal/mol
		2.070	90.10	-5.18	-5.81	CH_2Cl_2
		2.072	-90.04	-0.36	-0.50	CH_2Cl_2, 0.84 kcal/mol

[a]R = R′ where only one R group is given. [b]structures at local minima, and energies relative to the preceding structure. [c]Data from ref 115; see text. [d]Data from Cambridge Structural Database.

(*S,S*)-**2a** (2.0408(6), 2.0416(7) Å) are relatively long. The C-S-S-C dihedral angles range from 77.7(2)° for **3g** to 92.2(3)° for **3e**, averaging 84.2 ± 4.7°. Here, the dihedral angles for (*R,R*)-**2a** (–77.5(1)°, –81.2(1)°) and *(S,S)*-**2a** (+77.29(8)°, +81.24(8)°) fall at the acute end of the range. Finally, we note that in all cases the CO bonds of the carbonyl groups very nearly eclipse the disulfide bond; the absolute values of the O-C-S-S dihedral angles range from 0.1(2)° (**2a**) to 10.7(6)° (3**c**). Overall, the bond lengths and dihedral angles in **2a** are comparable to those in a variety of disulfides, not just the above dicarbonyl disulfides.[118, 126] As discussed by Harpp and Colman,[127] the near 90° dihedral angle can be understood as arising from a gauche conformation about the S-S bond to minimize lone pair-lone pair repulsion of the electron pair that resides in the 3p orbital on each sulfur atom.

The solid-state structures of **2a** exhibit opposite helicity about the S–S bond, namely $S_{S–S}$ (or *P*, i.e. "plus" signs for the dihedral angles) for (*S,S*)-**2a** and $R_{S–S}$ (or *M*, for "minus") for (*R,R*)-**2a**.[128] The major difference between **2a** and the compounds **3a-h** above is that only **2a** is non-racemic, and so only for **2a** are the signs of the dihedral angles important. That is, for **3a-h**, either both the *R* and *S* forms must be present in the crystal, or if the compound crystallizes in a chiral space group, we presume both enantiomorphs of the crystals were present. In fact the latter must be the case for **3e**, which crystallizes in the chiral space group $P2_12_12_1$, and by chance two structures have been reported. While the authors did not comment on this, one is *S*[122] and the other is *R*,[129] and data for the structure with the smaller R-Factor value are given in Table 1. In addition, one structure, that of **3a**, was refined in a centrosymmetric space group ($P2_1$/c), yet was described as having "right-handed chirality", which would imply a single enantiomer; the published packing diagram, in fact, showed identical chiral molecules, which would not be possible in $P2_1$/c.[118] Another group had previously published this structure (refined in $P2_1/a$)

and reported essentially the same molecular structure,[117] but no packing diagram was published. While the data are in line with the other structures, the values must be viewed with caution.

While it seems most unlikely that (*R*,*R*) and (*S*,*S*)-**2a** are atropisomers – that is, that they do not interconvert with respect to rotation about the S–S bond – the high specific rotations noted for each of the disulfides could be due to a preferred helicity in solution driven by the stereogenic centers. Density functional theory calculations[130] were carried out to assess the relative energies of S_{S-S}-(*S*,*S*)-**2a** and R_{S-S}-(*S*,*S*)-**2a**. The (*S*,*S*)-isomer was first optimized (6-31+G(d), B3LYP) starting from the x-ray coordinates of molecule 1, to give a structure that was little changed (S–S 2.069 Å, ∠(C-S-S-C) +81.8°; see Table 1). Rotation about the S-S bond followed by reoptimization (6-31+G(d), B3LYP) gave a local minimum with virtually the same S-S bond length (2.070 Å) and a C-S-S-C dihedral angle of –84.5°. The energies of the optimized structures were calculated at the 6-311+G(2d,p) level again using the B3LYP functional, and the energy of this R_{S-S} conformation of (*S*,*S*)-**2a** was calculated to be 0.72 kcal/mol higher than that of S_{S-S}-(*S*,*S*)-**2a**. The optimizations were then repeated using solvation (PCM model) in methylene chloride, since that solvent was used to measure the optical rotations. The two minima were located but with modest changes in the dihedral angles (~ ±90°), and there was a small predicted increase (to 0.84 kcal/mol) in the change in energy upon rotation. The S_{S-S} minimum was difficult to find because the potential energy surface appeared to be quite flat, with another minimum at ∠(C-S-S-C) = 83.47° that was 0.18 kcal/mol higher in energy than the 90.10° minimum, but the calculation kept optimizing to an apparent local energy maximum found at ∠(C-S-S-C) ≈ 87.7° that was energetically 0.01 kcal/mol higher. Nevertheless, both in the gas phase and in solution, the ~0.8 kcal/mol energy difference between the rotamers is in agreement with the observed solid state structure. However, it confirms the supposition that

these are not likely to be true atropisomers, but the difference could certainly give a preference in solution and account for the high optical rotations of the disulfides.

3.3.3 Synthesis of chiral analogues of 5-methyl-3*H*-1,2,4-dithiazol-3-one (MEDITH)

Chiral sulfurizing reagents based on the MEDITH structure (Figure 1) are attractive for a number of reasons. First, MEDITH and a related ethoxy (in place of the methyl) substituted analogue are particularly reactive.[89, 90] In our hands, for instance, MEDITH sulfurized the phosphorus of a chiral *N*-sulfonylvaline-derived oxazaphospholidinone[69] while the Beaucage reagent did not react.[131] Second, the structure of MEDITH is arguably the most different from those of the acyclic di- and tetrasulfides shown in Figure 1, and therefore chiral analogues provide the greatest opportunities for different results from the PADS analogues. Third, the starting materials for synthesis of the MEDITH analogues are the same as the chiral carboxylic acids **1a**–**d** used for the PADS analogues.

The chiral carboxylic acids shown in Scheme 2 were converted to the acid chlorides[104] and then treated with concentrated NH_4OH[108] to give the chiral amides (**4a**–**e**), for which literature data are available albeit from alternate synthetic routes that generally did not give both enantiomers.[110, 111, 132, 133]

The conversions of the chiral amides to the thioamides were initially attempted with Lawesson's reagent,[134] but only racemic products were isolated. The problem was traced to racemization of the thioamides on silica gel,[135] even on silica gel treated with 1% Et_3N. Since the use of Lawesson's reagent required purification by column chromatography, other methods were tried, including P_4S_{10} alone,[136] P_4S_{10} on basic alumina,[136] and P_4S_{10}/Na_2CO_3.[137] The P_4S_{10}/Na_2CO_3 procedure gave the highest yields and it did not require column chromatography, the purification of the products instead being carried out by an aqueous work-up followed by

Scheme 2. Synthesis of MEDITH analogues

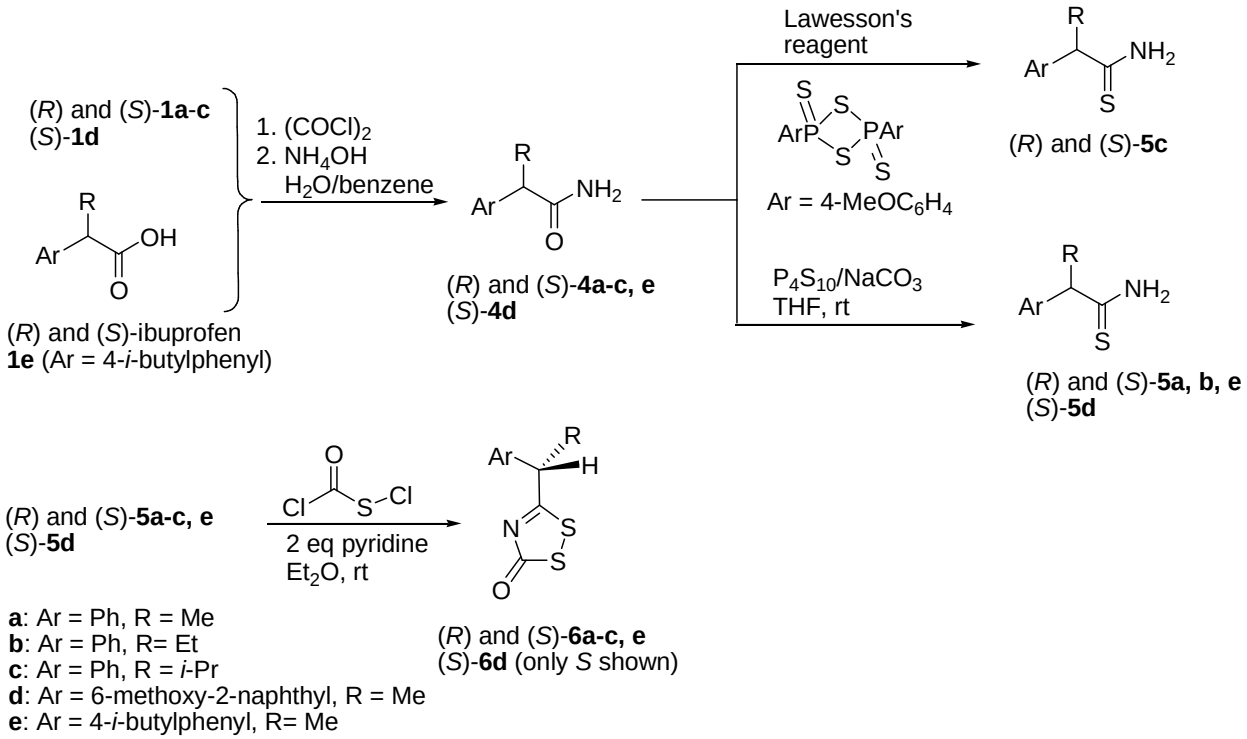

crystallization. The α-methyl- and ethyl- substituted chiral amides **4a**,**b**,**d**,**e** were converted in this way to the new thioamides **5a**,**b**,**d**,**e** in 85-95% yield. Only the *i*-Pr substituted **4c** failed to react with P_4S_{10}/Na_2CO_3, even after stirring for longer times or at reflux. It is reasonable to suppose that the "adamantane-like" structure of P_4S_{10} gives too much steric hindrance with the relatively bulky isopropyl group. For the conversion to the thioamide, Lawesson's reagent was used followed by chromatography on neutral alumina (rather than silica) treated with 1% Et_3N, and modest 43–48% yields of the enantiomers of **5c** were obtained following crystallization. Not surprisingly, however, as will be seen below, the enantiomeric purities of **5c** were lower than those of the other thioamides.

The synthesis of 5-methyl-3*H*-1,2,4-dithiazol-3-one (MEDITH) or analogues with different substituents at the 5-position has been reported previously,[138-142] and we chose Barany's

procedure[141] since it was used to prepare material for phosphite triester sulfurization.[90] This method only gave a ~10% yield when applied to the synthesis of (*S*)-**6d**, so optimization of the reaction was attempted using achiral 2-phenylethanethioamide. It immediately became apparent that Barany's procedure using thioacetamide essentially fails for the 2-phenyl-substituted analogue - only traces of product were detected by NMR following the initial reaction, which gave a dark gum. The use of methylene chloride or acetonitrile as the solvent instead of dimethoxyethane gave the same result. Racemic 2-phenylpropanethioamide was tried next, both at rt and –35 °C (the literature conditions were <10 °C), with both normal and inverse addition of reactants, but again only traces of product formed.

During the course of these experiments we observed that a mixture of triethylamine and chlorocarbonylsulfenyl chloride in dimethoxyethane appeared to react and gave a dark solution, so a room temperature reaction of 2-phenylpropanethioamide and chlorocarbonylsulfenyl chloride was run in the absence of the base. To our surprise, the reaction was complete within 5 minutes, as judged by ^{1}H NMR and TLC. When this method was used starting with (*S*)-**5d**, the product **6d** was in fact isolated in ~95% yield, but it was found to be racemic. Evidently the two equiv of HCl produced must be sequestered to prevent racemization, but a milder base than triethylamine was required to prevent reaction with the chlorocarbonylsulfenyl chloride. Pyridine was found to be effective, and ether was used as the solvent to facilitate removal of the pyridinium chloride salt; in this way optically active material was formed in ~95% crude yield. Compounds (*S*)-**6d** and both enantiomers of **6a** were isolated in 92 and 60% yields, respectively, following crystallization, while both enantiomers of each of **6b**,**c**,**e** were obtained as viscous oils that did not solidify, in 85-92% yield.

The acid sensitivity of the MEDITH analogues towards racemization was not anticipated, and would not be seen in the parent compound unless one were looking (for instance) for deuterium incorporation in the methyl group. We presume that the enol tautomer is relatively stable and that this accounts for the observed racemization, although even without enol formation related epimerization in acid has been observed at a stereocenter attached to the C=N moiety of a five-membered oxazole heterocycle.[143]

3.3.4 Enantiomeric purity of disulfides

The starting materials for the new disulfides described here, the chiral carboxylic acids **1a**–**e**, have all been reported, along with their enantiomeric purities and a variety of optical rotations for some of the individual acids. Determination of the optical purity of the starting acids on the basis of optical rotation was therefore somewhat uncertain; our values and literature values are shown in Table 2, along with data for the diastereomeric salts (Table 3) and amides

Table 2. Observed and literature specific rotations of acids **1a**–**e**

Compound	[α] (obs[a])	[α] (lit[b])
(*R*)-**1a**	-60.6 (*c* 1.15, $CHCl_3$, 25 °C)	
(*S*)-**1a**	+72.5 (*c* 1.05, $CHCl_3$, 25 °C)	+76.5 (*c* 2, $CHCl_3$, 25 °C)[108] +61.8 (*c* 4.27, $CHCl_3$, 25 °C, 90% ee)[110]
(*R*)-**1b**	-66.3 (*c* 1.20, $CHCl_3$, 26 °C)	
(*S*)-**1b**	+70.3 (*c* 1.20, $CHCl_3$, 26 °C)	+61.3 (*c* 4.97, $CHCl_3$, 25 °C, >99% ee)[110]
(*R*)-**1c**	-59.0 (*c* 1.05, $CHCl_3$, 27 °C)	-62.4 (*c* 4.46, $CHCl_3$, 24 °C)[108]
(*S*)-**1c**	+60.0 (*c* 1.05, $CHCl_3$, 27 °C)	+62.5 (*c* 2, $CHCl_3$, 25 °C)[108] +60 (*c* 1.95, $CHCl_3$, 25 °C, >99% ee)[110]
(*S*)-**1d**	+65.2 (*c* 1.02, $CHCl_3$, 25 °C)	+64.9 (*c* 1.8, $CHCl_3$, 26 °C)[111] *(R)*-**1d**: -67.2 (*c* 1.096, $CHCl_3$, 20 °C)[144]
(*R*)-**1e**	-53.4 (*c* 1.47, EtOH, 25 °C)	-53 (*c* 2, EtOH, 25 °C, 98% ee)[133] -57.5 (*c* 1.0, EtOH, 25 °C, 96.4% ee)[145]
(*S*)-**1e**	+51.4 (*c* 1.15, EtOH, 25 °C)	+54 (*c* 2, EtOH, 25 °C, 99% ee)[133]

[a]589 nm, 1.00 dm cell length. [b]For values that list ee, these are the ee values listed in the literature reports as measured by HPLC, but the specific rotations are the measured (not extrapolated) values.

(Table 4). Regardless of the starting material purity, chiral HPLC is necessary for determining the enantiomeric purity of the disulfide products, and as will be seen below in at least some cases, high enantiomeric purity can be achieved.

Table 3. Observed and literature specific rotations of α-methylbenzylamine (MBA) salts of **1a**–**e**

Compound	[α] (obs[a])	[α] (lit)
(*S*)-(-)-MBA-*(R)*-(-)-**1a**	–18.7 (*c* 1.00, EtOH, 27 °C)	
(*R*)-(+)-MBA-*(S)*-(+)-**1a**	+20.1 (*c* 1.05, EtOH, 28 °C)	–19.0 (*c* 1.0, EtOH, 25°C)[145,b]
(*R*)-(+)-MBA-*(R)*-(-)-**1b**	-4.6 (*c* 1.00, EtOH, 29 °C)	-7.3 (*c* 1, EtOH, 27 °C)[146]
(*S*)-(-)-MBA-*(S)*-(+)-**1b**	+9.76 (*c* 1.25, EtOH, 30 °C)	+12.3 (*c* 1, EtOH, 25 °C)[146]
(*R*)-(+)-MBA-*(R)*-(-)-**1c**	-5.3 (*c* 1.04, MeOH, 26 °C)	-5.2 (*c* 2.62, MeOH, 26 °C)[108]
(*S*)-(-)-MBA-*(S)*-(+)-**1c**	+5.26 (*c* 1.07, MeOH, 23.3 °C)	
(*R*)-(+)-MBA-*(R)*-(-)-**1e**	~0 (*c* 1.13, EtOH, 25 °C)	
(*S*)-(-)-MBA-*(S)*-(+)-**1e**	~0 (*c* 1.23, EtOH, 25 °C)	

[a]589 nm, 1.00 dm cell length. [b]The literature value is presumably a typographical error, and should be +19.0.

Table 4. Observed and literature specific rotations of amides **4a**–**e**

Compound	[α] (obs[a])	[α] (lit[b])
(*R*)-(-)-**4a**	–48.6 (*c* 1.10, $CHCl_3$, 28 °C)	–56.8 (*c* 4.31, $CHCl_3$, 25 °C, >99% ee)[110]
(*S*)-(+)-**4a**	+55.6 (*c* 1.0, $CHCl_3$, 27 °C)	
(*R*)-(-)-**4b**	–68.0 (*c* 1.05, $CHCl_3$, 26 °C)	–56.5 (*c* 6.99, $CHCl_3$, 25 °C, 96% ee)[110]
(*S*)-(+)-**4b**	+74.3 (*c* 1.00, $CHCl_3$, 29 °C)	
(*R*)-(-)-**4c**	–69.0 (*c* 1.05, $CHCl_3$, 25 °C)	–72.9 (*c* 1.32, $CHCl_3$, 25 °C, >99% ee)[110]
(*S*)-(+)-**4c**	+70.6 (*c* 1.00, $CHCl_3$, 25 °C)	
(*S*)-(+)-**4d**	+48.6 (*c* 0.22, $CHCl_3$, 25 °C)	+20 (*c* 1, $CHCl_3$, 25 °C)[132,c]
(*R*)-(-)-**4e**	–27.0 (*c* 1.04, EtOH, 27 °C)	–35 (*c* 1, EtOH, 25 °C)[133]
(*S*)-(+)-**4e**	+26.0 (*c* 1.00, EtOH, 27 °C)	+33 (*c* 1, EtOH, 25 °C)[133]

[a]589 nm, 1.00 dm cell length. [b]For values that list ee (enantiomeric excess), these are the ee values listed in the literature reports as measured by HPLC, but the specific rotations are the measured (not extrapolated) values. [c]We believe this specific rotation is in error because we could not dissolve **4e** in $CHCl_3$ at this high concentration.

For disulfides **2a**–**d**, it is necessary to separate the meso and racemic mixture by chiral HPLC. In all cases it was necessary to prepare this mixture by synthesis of the disulfides from

the racemic acid. For naproxen-derived **2d** where the racemic acid was not the starting material, the mixture was prepared by racemization of **1d** with DBU at 120 °C.[145] We found these mixtures could be separated on the new Chiral Technologies bonded CHIRALPAK® IB column, but the separation for **2a**–**c** was remarkably sensitive to minor changes in the percentage of 2-propanol in hexane (0.25% at 25 °C gave excellent results); for **2d**, the mixture was separated by eluting with 8% acetone in hexanes. Figure 3 shows an example of the chromatogram of a mixture of meso and racemic **2a**, and Figure 4 shows the chromatogram of (*R*,*R*)-**2a**. In two cases we have detected 0.09% and 0.03% of the wrong enantiomer or the meso isomer as impurities, so we conservatively estimate a detection limit of >0.1%; these values are uncorrected for any potential differences in the absorbance of the meso diastereomers. The enantiomeric purities of the PADS analogues ranged from 98.99% for (*S*,*S*)-**2c** to >99.9% for

Figure 3. Chromatogram of mixture of meso and racemic **2a**[a]

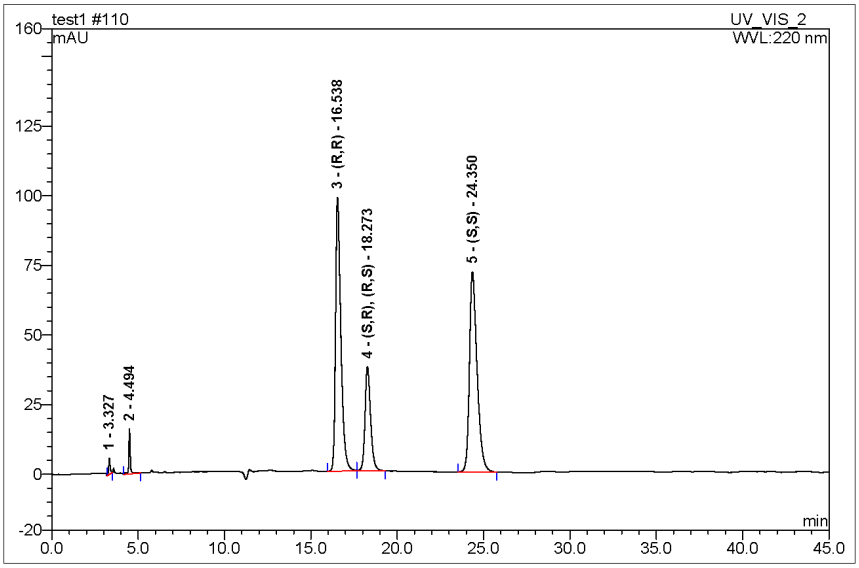

[a] Analyzed on a Chiral Technologies bonded CHIRALPAK® IB column (5 µ particle size, 4.6 mm x 250 mm) at 25 °C, eluting at 1 mL/min with 0.25% 2-propanol in hexanes and detected at 220 nm.

Figure 4. Chromatogram of the (*R*,*R*)-**2a**[a]

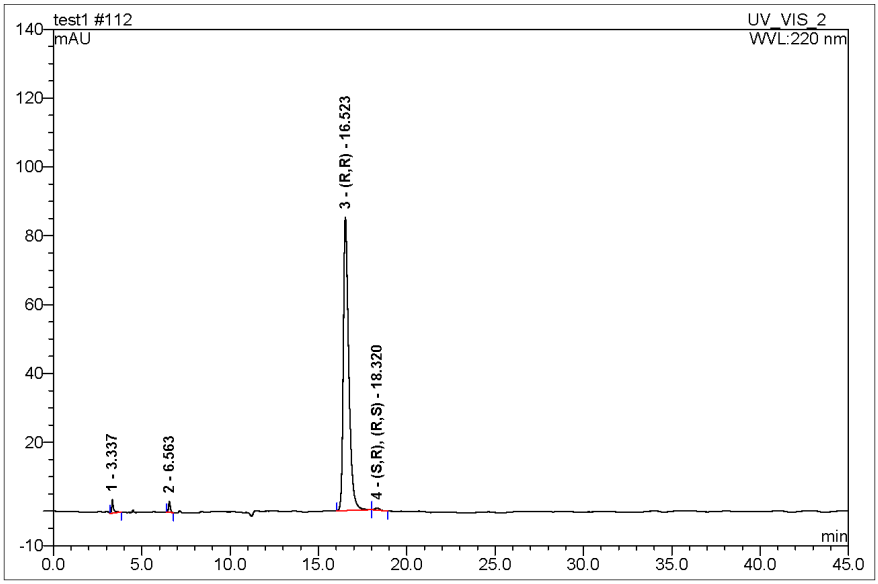

[a] Analyzed on a Chiral Technologies bonded CHIRALPAK® IB column (5 μ particle size, 4.6 mm x 250 mm) at 25 °C, eluting at 1 mL/min with 0.25% 2-propanol in hexanes and detected at 220 nm.

(*S*,*S*)-**2a** and (*S*,*S*)-**2b**. Each of the PADS analogues is a solid, and can benefit from purification by removal of the "wrong" enantiomer of the chiral acid chlorides in the disulfide reaction by removal of any of the meso diastereomer that forms.

Both the new chiral thioamides **5a**–**e** and the MEDITH analogues **6a**–**e** were similarly analyzed by chiral HPLC. The racemic mixtures were prepared by simply mixing the enantiomers for all but the naproxen-derived compounds **5d** and **6d**; for **5d** the racemic mixture was prepared by stirring a mixture of *(S)*-**5d** and silica gel in CH_2Cl_2 for 1 h, and for **6d** the racemic mixture was prepared by reaction of *(S)*-**5d** and ClSC(O)Cl in the absence of pyridine. Figure 5 shows an example of the chromatogram of the racemic mixture of **5a**, and Figure 6 shows the chromatogram of (*R*)-**5a**. The enantiomeric purities of the thioamides ranged from

Figure 5. Chromatogram of racemic **5a**[a]

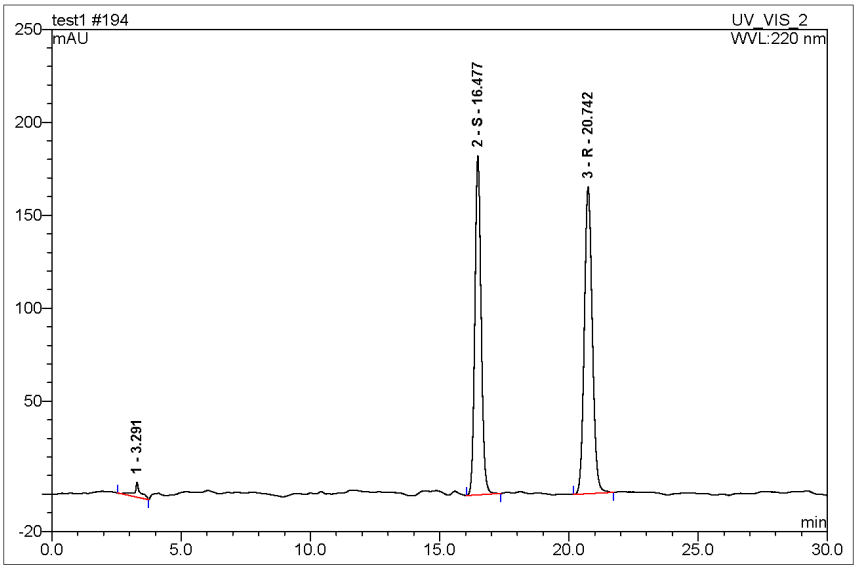

[a] Analyzed on a Chiral Technologies bonded CHIRALPAK® IB column (5 μ particle size, 4.6 mm x 250 mm) at 20 °C, eluting at 1 mL/min with 10% acetone/90% hexanes and detected at 220 nm.

Figure 6. Chromatogram of (*R*)-**5a**[a]

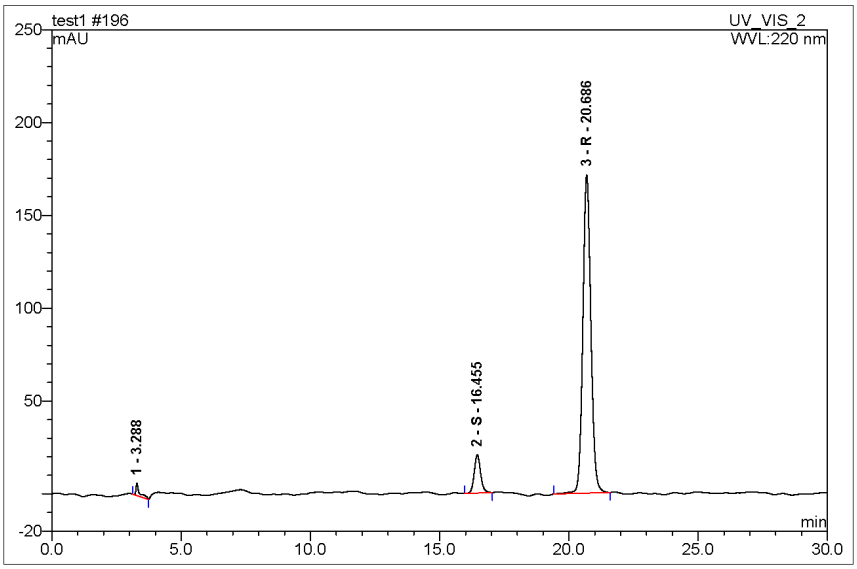

[a] Analyzed on a Chiral Technologies bonded CHIRALPAK® IB column (5 μ particle size, 4.6 mm x 250 mm) at 20 °C, eluting at 1 mL/min with 10% acetone/90% hexanes and detected at 220 nm.

88.9% and 85.8% for (*R*) and *(S)*-**5c** to >99.9% for (*R*) and (*S*)-**5b**; enantiomer separations were easily achieved for **5a**,**b**,**c**,**e** on CHIRALPAK® IB eluting with 10% acetone in hexanes at 20 °C. However, for **5d** we were unable to find any conditions for separation of the enantiomers on any of CHIRALPAK® IA, B, or C.

For the final MEDITH analogues, the enantiomeric purities ranged from 88.5% and 86.1% for (*R*) and (*S*)-**6c** to 99.1% and 99.4% for (*R*) and (*S*)-**6a**. Separation of these enantiomers was much more difficult, and was achieved on CHIRALPAK® IA or IB eluting with 0.25–1% methanol or ethanol in hexanes at temperatures from 12–25 °C except for **6d**, which was carried out with 8% acetone in hexanes at 20 °C on CHIRALPAK® IC. Figure 7 shows an example of the chromatogram of the racemic mixture of **6a**, and Figure 8 shows the chromatogram of (*R*)-**6a**. While we were concerned that racemization might be occurring on-

Figure 7. Chromatogram of racemic **6a**[a]

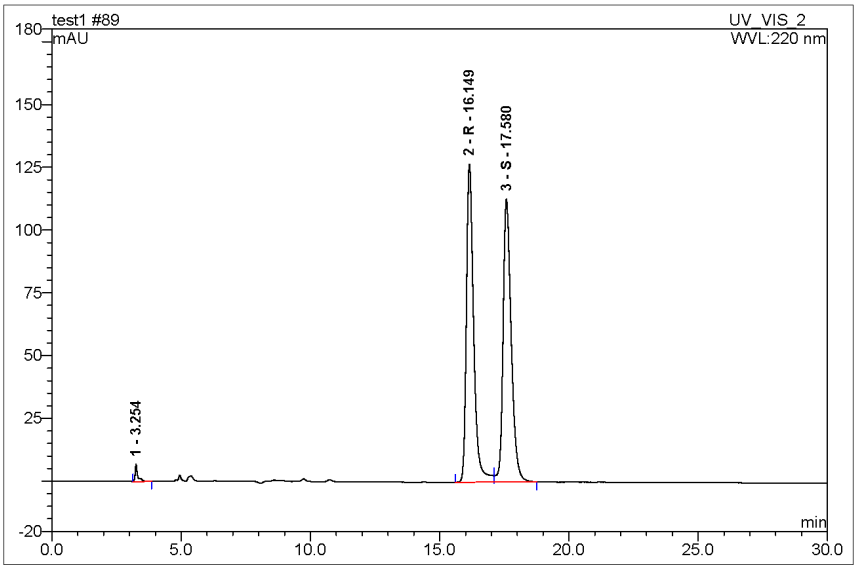

[a] Analyzed on a Chiral Technologies bonded CHIRALPAK® IA column (5 μ particle size, 4.6 mm x 250 mm) at 25 °C, eluting at 1 mL/min with 0.5% MeOH/99.5% hexanes and detected at 220 nm.

Figure 8. Chromatogram of (*R*)-**6a**[a]

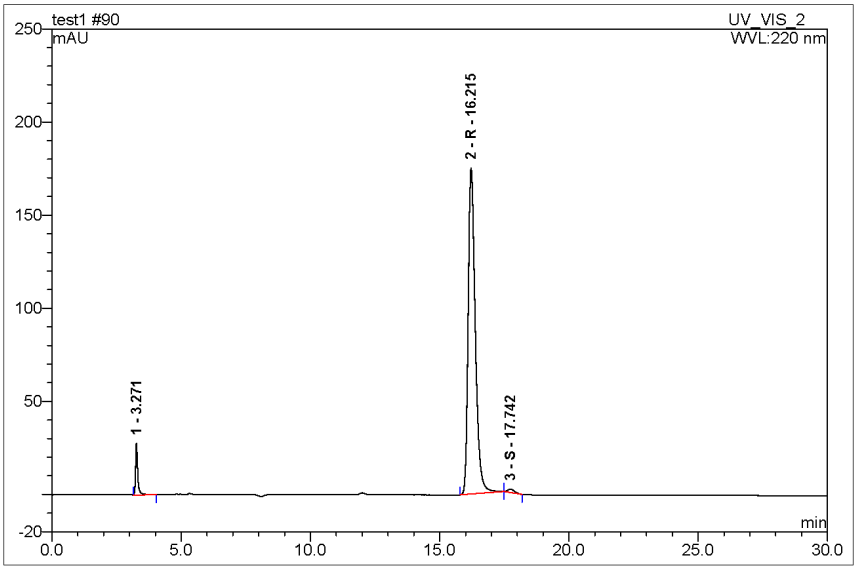

[a] Analyzed on a Chiral Technologies bonded CHIRALPAK® IA column (5 μ particle size, 4.6 mm x 250 mm) at 25 °C, eluting at 1 mL/min with 0.5% MeOH/99.5% hexanes and detected at 220 nm.

column during the HPLC runs, no change in enantiomer ratios was detected when we decreased the column contact-time by eluting at higher flow rates.

In order to evaluate the enantioselectivities of the disulfide-forming syntheses, enantiomeric purity data are collected in Table 5. Values for each compound were determined either by comparison of observed specific rotation to literature values (for **1** and **4**) or by HPLC as described above (for **2**, **5**, and **6**). The comparison of the PADS analogues to the precursor chiral carboxylic acids shows that each of the disulfides has equal or greater enantiomeric purity, so not only is there no evidence of epimerization, but as expected, the enantiomeric purity can be enhanced by removal of the meso (and racemate) by crystallization, as particularly seems to be the case for (*R*)-**1a** conversion to (*R*,*R*)-**2a**. The conversions of the acids to the amides consistently gave similar enantiomeric purities (average deviation ±0.5%) except for **1e** to **4e**, but given the higher enantiomeric purities for **5e** and **6e**, it is more likely that the specific

Table 5. Enantiomeric purity[a] of chiral precursors and disulfides

Compd	Acid (**1**)[b]	PADS (**2**)[c]	Amide (**4**)[b]	Thioamide (**5**)[c]	MEDITH (**6**)[c]
(*R*)-**a**	91.7	99.4	92.8	91.3	99.1
(*S*)-**a**	99.9	>99.9	98.9	98.2	99.4
(*R*)-**b**	97.2	99.4	95.8	>99.9	91.3
(*S*)-**b**	>99.9	>99.9	>99.9	>99.9	91.2
(*R*)-**c**	97.9	99.9	97.3	88.9	88.5
(*S*)-**c**	98.7	99.0	98.4	85.8	86.1
(*S*)-**d**	99.4	99.4	100		94.9
(*R*)-**e**	97.6		89.7	98.7	96.3
(*S*)-**e**	95.8		88.2	93.5	96.5

[a]Enantiomeric purity = [major configuration]/[(*R*) + (*S*) + meso] × 100. [b]Evaluated from observed $[\alpha]_D$ by comparison to literature values; see Table 2 and 4 for data used. Literature data were averaged if more than one value was available, (*R*) and (*S*) values were combined where available and included in the average, and corrected for HPLC % ee when available. In cases where our observed $[\alpha]_D$ was higher than the literature value, it was taken as 100% enantiomeric purity and $[\alpha]_D$ for the opposite configuration was compared to this new 100% value. [c]Evaluated from chiral HPLC data.

rotations are in error. The HPLC values for the thioamides are, with two exceptions remarkably similar to the $[\alpha]_D$ values for the acids (average deviation ±1.4%); the exceptions are for the α-isopropyl compounds where the thioamide syntheses necessitated the use of Lawesson's reagent, which gave a significant drop in enantiomeric purity on going from the amides (**4c**) to the thioamides (**5c**). The P_4S_{10}/Na_2CO_3 method, in contrast, clearly proceeded with high retention of enantiopurity, as seen for overall conversion of **1a**, **b**, **e** to **4a**, **b**, **e**. Last, the conversions of the thioamides to the MEDITH analogues proceeded with comparable (or better) enantiomeric purity for **5a**, **c**, **e** to **6a**, **c**, **e**; for **5a** to **6a**, the purity improved suggesting that like the PADS case,

crystallization must serve to remove some racemate. On the other hand, there was a drop in purity on going from the α-2-phenylbutane case **5b** to **6b**, and a smaller but still noticeable drop for the naproxen case **4d** to **6d**. In the naproxen case, we were unable to resolve the thioamide enantiomers, so we can only guess that the loss occurred at this stage, rather than the acid to amide stage. In any case, there is no explanation for these modest differences. For instance, while **6b** is an oil and presents no opportunity for crystallization-enhanced purity, **6e** is also an oil and formed in high enantiomeric purity; **6d** on the other hand is a solid, just like **6a**, which gave the highest enantiomeric purity.

3.4 Conclusion

Conversion of α-alkyl-substituted phenyl acetic acids to diacyl disulfides is readily carried out to give the desired compounds in >99.0% enantiomeric purity. The absolute configurations of the methyl-substituted compounds (*R*) and (*S*)-**2a** were unequivocally established by single-crystal X-ray diffraction. The high specific rotations ($[\alpha]_D \approx 360–540$) suggest that the helicity about the S-S bond observed in the solid state may be preferentially retained in solution. Conversion of the same set of chiral carboxylic acids to thioamides without racemization could best be carried out by avoidance of both acidic conditions and chromatography; specific rotation and HPLC data showed this could be accomplished using P_4S_{10} under basic conditions but not with Lawesson's reagent. Conversion of the thioamides to the MEDITH analogues was carried out in much higher yield than previously described, by using pyridine rather than triethylamine to sequester the HCl generated during the reaction. The heterocycles, which were formed in up to ~99% enantiomeric purity, were quite sensitive toward acid-induced racemization, and while six of the cases proceeded with comparable enantiomeric purity upon conversion of the thioamides, three gave up to 9% lower enantiomeric purities.

3.5 Experimental Section

^{1}H and ^{13}C NMR specra were recorded on a Bruker 400 MHz spectrometer with tetramethylsilane as an internal standard. High-resolution mass spectrometry was performed on an Agilent G6520A Q-TOF instrument. X-ray structure determination of (*S*,*S*)- and (*R*,*R*)-**2a** was measured on a Bruker SMART BREEZE CCD diffractometer using graphite-monochromated Mo Kα radiation (0.71073 Å) at 200 K. Optical rotations were determined on a Rudolph Autopol III automatic polarimeter at 589 nm with a cell length of 1.0 dm. IR spectra were recorded on a 4020 Galaxy series FT-IR spectrometer. (±)-2-Phenylpropanoic acid (**1a**), sodium carbonate (anhydrous), oxalyl chloride, phosphorus pentasulfide, hexadecyltributylphosphonium bromide, chlorocarbonylsulfenyl chloride, Lawesson's reagent, sodium sulfide nonahydrate, and sulfur were used directly from suppliers. Toluene and benzene were used directly from suppliers. Diethyl ether and tetrahydrofuran was dried prior to use by distillation from sodium-benzophenone. Pyridine was distilled from calcium hydride. Ethanol (Aaper Alcohol, USP 200 proof) and chloroform were used directly from suppliers for recording optical rotations. Petroleum ether refers to the fraction of petroleum ether boiling between 35 and 60 °C. Flash column chromatography was done using neutral alumina Brockman activity l.

Carboxylic acids, acid chlorides, and amides. Resolutions of racemic **1a**,[107] **1b**,[107] **1c**,[108] and **1e**[145] were carried out as described in the referenced papers, except that for **1e** the starting point was the racemate rather than the partially enriched material. Racemic **1b** was synthesized using the method described for **1c**,[108] and **1c** was prepared using the literature procedure.[108] Racemic **1e** was obtained by ether extraction from commercial ibuprofen tablets, and *(S)*-**1d** was isolated from commercial sodium naproxen tablets by ether extraction from an aqueous acidic solution of the powdered material. In all cases the procedure used for **1e**[145] was

employed to regenerate the acid from the diastereomeric α-methylbenzylamine salts (i.e. by hydrolysis with 0.5 M H_2SO_4). Enantiomeric purities were evaluated by comparison to literature values of specific rotations for the salts[108, 145, 146] used for the resolutions and for the final acids.[108, 110, 111, 133, 144, 145] A few cautions need to be included here: there is a typo for the rotation of the salt of (*S*)-**1a**[145] (it should be +19.0, not –19.0); the rotations for the salts of **1a** and **1b** given by Mosher in his Table I are completely in error[108] (the values given are in fact Pettersson's values for the acids[107]); and while not published (to our knowledge), the specific rotation of the salts of **1e** are ~0, so the resolution procedure described in the literature[145] is accurate but does not mention the reason one must monitor the progress of the successive crystallizations by hydrolysis of a small fraction of the salt – it is necessary to measure the specific rotation of the enantio-enriched **1e** since the rotation of the crystallized salt remains ~0 throughout the successful resolution procedure. The acids were converted to the acid chlorides by reaction with neat oxalyl chloride[104] rather than with thionyl chloride[108] because the usual thionyl chloride procedure failed with naproxen (**1d**), while oxalyl chloride gave complete (and much cleaner) reaction in 30 min. The other carboxylic acids required 2 h for complete conversion. Following removal of the excess oxalyl chloride and volatiles on a vacuum line, the acid chlorides were used without further isolation in the next step.[104] Conversions to the amides **4a**–**e** were carried out as previously described for **1c**,[108] and specific rotations have all been reported;[110, 132, 133] however, work-up details differed significantly from that described[108] and may be found on pages 83-85.

Synthesis of 2-phenylbutanoic acid (1b). This procedure follows that for **1c**.[108] Under a nitrogen atmosphere, sodium naphthalenide was prepared by stirring a mixture of sodium (4.041 g, 175.7 mmol) and naphthalene (22.39 g, 174.7 mmol) in 150 mL of THF for about 20 h.

This solution was rapidly added to a vigorously stirred solution of phenylacetic acid (10.47 g, 76.93 mmol) in 150 mL of THF. After the mixture had stirred for 4 h, ethyl bromide (13.14 g, 120.6 mmol) was added over a 1¼ h period and the reaction mixture was stirred with a mechanical stirrer overnight. Water (100 mL) was added and the mixture was extracted with 10% Na_2CO_3 solution (100 mL) and then with water (150 mL). The basic aqueous extracts were washed with Et_2O (2 x 60 mL) and then acidified with 1 M HCl (300 mL). The acid was extracted with Et_2O (4 x 60 mL) which was then dried with $MgSO_4$. The solvent was evaporated under reduced pressure to give **1b** (12.3 g, 98%) as a slightly yellow oil. ^{1}H NMR (400 MHz, $CDCl_3$): δ 11.99 (br, 1H), 7.21-7.31 (m, 5H), 3.45 (t, $^3J_{HH}$ = 7.70 Hz, 1H), 2.09 (m, 1H), 1.81 (m, 1H), 0.89 (t, $^3J_{HH}$ = 7.3, 3H); ^{13}C NMR (100 MHz, $CDCl_3$): 180.8, 138.3, 128.6, 128.1, 127.4, 53.3, 26.3, 12.1 ppm.

Resolution of 2-(4-isobutylphenyl)propanoic acid (1e). Details of this procedure (i.e. quantities of solvents) have not been published so we provide our method here. Racemic **1e** (5.85 g, 28.4 mmol) and (*R*)-(+)-α-methylbenzylamine (3.45 g, 28.5 mmol) were dissolved in 50 mL of hot isopropanol. The solution was allowed to cool slowly to rt. The salt that separated out was recrystallized four more times from 2-propanol to give 2.40 g of a white salt. Since the optical rotation of the salt was ~0°, the only way that the diastereomeric purity of the material could be monitored was to treat a small sample with 0.5 M H_2SO_4 and then check the specific rotation of the free acid **1e**. Once a constant rotation was observed, the acid was regenerated by stirring the salt with 20 mL of 0.5 M H_2SO_4 at rt for 30 min. The acid was extracted with 3 x 50 mL CH_2Cl_2. The organic extracts were washed with 50 mL of brine, dried with $MgSO_4$ and evaporated under reduced pressure to give (*R*)-(-)-**1e** (1.61 g, 55%) as a white solid, $[\alpha]^{26}_D$ -53.4 (*c* 1.47, EtOH). The mother liquors were concentrated, and the partially active acid regenerated

in the same way to give 2.10 g of enriched (*S*)-(+)-**1e**. This acid (2.10 g, 10.2 mmol) was treated with (*S*)-(-)-α-methylbenzylamine (1.27 g, 10.5 mmol) in 25 mL hot 2-propanol. The salt that separated was recrystallized two more times from 2-propanol to give 1.87 g white salt. The same regeneration process was repeated to give (*S*)-(+)-**1e** (1.25 g, 43%) as a white solid, $[\alpha]^{25}_{D}$ +51.44 (*c* 1.14, EtOH).

Synthesis of PADS analogues: (*S,S*)-Di-2-phenylpropanoyl disulfide ((*S,S*)-**2a).** The following procedure is representative of the method used for **2a**–**d**. An aqueous solution of sodium disulfide was prepared by heating a mixture of sulfur (0.050 g, 1.6 mmol) and sodium sulfide nonahydrate (0.375 g, 1.56 mmol) in water (1.5 mL) at 90 °C for 15 min with stirring. After the aqueous solution was cooled, hexadecyltributylphosphonium bromide (0.071 g, 0.14 mmol) and 4 mL of toluene were added. With vigorous stirring at room temperature a solution of (*S*)-2-phenylpropanoyl chloride (0.350 g, 2.08 mmol) dissolved in 1 mL toluene was added dropwise over 2-3 min. After 20 min of stirring, the reaction solution was transferred to a separatory funnel with an additional 5 mL of toluene. The aqueous layer was separated and the organic layer was washed with 5 mL H_2O, and then dried with $MgSO_4$. The solvent was removed on a rotary evaporator and the crude product was passed through a pad of silica gel eluting with CH_2Cl_2. The UV-active material moving with the solvent front was collected and the solvent evaporated to afford the product as a pale white solid (0.31 g, 90% yield). The compound was crystallized from hot methanol to give white crystals of **2a** (0.18 g, 53% yield). mp 57-58 °C; $[\alpha]_D^{26}$ +370.2 (*c* 0.55, CH_2Cl_2); HPLC >99.9% (*S,S*), <0.1% (*R,R*), <0.1% meso; IR (KBr, cm^{-1}): 1735, 1720; ^{1}H NMR (400 MHz, $CDCl_3$): δ 7.38-7.25 (m, 5H), 4.06 (q, $^3J_{HH}$ = 7.1 Hz, 1H), 1.58 (d, $^3J_{HH}$ = 7.1, 3H); ^{13}C NMR (100 MHz, $CDCl_3$): 195.2, 138.4, 129.0, 128.3,

128.0, 53.6, 18.6 ppm; HRMS (ESI): Calcd for $C_{18}H_{22}NO_2S_2$ $[M+NH_4]^+$: 348.1092, found 348.1090.

Data for 2a–d:

HPLC conditions for determination of enantiomeric purity. Each of **2a**–**d** was analyzed on a Chiral Technologies bonded CHIRALPAK® IB column (5 μ particle size, 4.6 mm x 250 mm) at 25 °C eluting at 1 mL/min with 0.25% 2-propanol in hexanes (**1a**–**c**) or 8% acetone/92% hexanes (**1d)**.

(*R*,*R*)-Di-2-phenylpropanoyl disulfide ((*R*,*R*)-**2a)** was obtained as white crystals (0.17 g, 50% yield); mp 56-57 °C; $[\alpha]_D^{25}$ -362.8 (*c* 0.50, CH_2Cl_2); HPLC 99.4% (*R*,*R*), <0.1% (*S*,*S*), 0.6% meso; IR, NMR same as (*S*,*S*)-**2a**); HRMS (ESI): Calcd for $C_{18}H_{22}NO_2S_2$ $[M+NH_4]^+$: 348.1092, found 348.1092.

(*R*,*R*)-Di-2-phenylbutanoyl disulfide ((*R*,*R*)-**2b)** was obtained as a white solid (0.165 g, 50% yield); mp 74-75 °C; $[\alpha]_D^{24}$ -426.4 (*c* 0.55, CH_2Cl_2); HPLC 99.4% (*R*,*R*), 0.3% (*S*,*S*), 0.3% meso; IR (KBr, cm^{-1}): 1732, 1713; ^{1}H NMR (400 MHz, $CDCl_3$): δ 7.36-7.26 (m, 5H), 3.83 (t, $^3J_{HH}$ = 7.5 Hz, 1H), 2.23 (m, 1H), 1.88 (m, 1H), 0.93 (t, $^3J_{HH}$ = 7.4, 3H); ^{13}C NMR (100 MHz, $CDCl_3$): 194.6, 136.9, 128.9, 128.5, 128.0, 61.3, 26.9, 12.0 ppm; HRMS (ESI): Calcd for $C_{20}H_{26}NO_2S_2$ $[M+NH_4]^+$: 376.1405, found 376.1397.

(*S*,*S*)-Di-2-phenylbutanoyl disulfide ((*S*,*S*)-**2b)** was obtained as a white solid (0.313 g, 55% yield); mp 73-74 °C; $[\alpha]_D^{26}$ +422.6 (*c* 0.65, CH_2Cl_2); HPLC >99.9% (*S*,*S*), <0.1% (*R*,*R*), <0.1% meso; IR, NMR same as (*R*,*R*)-**2b**; HRMS (ESI): Calcd for $C_{20}H_{26}NO_2S_2$ $[M+NH_4]^+$: 376.1405, found 376.1401.

(*R*,*R*)-Di-3-methyl-2-phenylbutanoyl disulfide ((*R*,*R*)-**2c)** was obtained as a white solid (0.33 g, 61% yield); mp 111.5-112.5 °C; $[\alpha]_D^{25}$ –540.6 (*c* 0.515, CH_2Cl_2); HPLC 99.9% (*R*,*R*),

0.1% (*S,S*), <0.1% meso; IR (KBr, cm^{-1}): 1737, 1711; ^{1}H NMR (400 MHz, $CDCl_3$): δ 7.34-7.25 (m, 5H), 3.57 (d, $^3J_{HH}$ = 10.1 Hz, 1H), 2.46 (m, 1H), 1.16 (d, $^3J_{HH}$ = 6.5 Hz, 3H), 0.73 (d, $^3J_{HH}$ = 6.7, 3H); ^{13}C NMR (100 MHz, $CDCl_3$): 194.4, 136.3, 128.8, 128.7, 127.8, 67.6, 32.6, 21.3, 20.5 ppm; HRMS (ESI): Calcd for $C_{22}H_{30}NO_2S_2$ $[M+NH_4]^+$: 404.1718, found 404.1707.

(*S,S*)-Di-3-methyl-2-phenylbutanoyl disulfide ((*S,S***)-2c)** was obtained as a white solid, (0.32 g, 60%); mp 112-113 °C; $[\alpha]_D^{26}$ +541.2 (*c* 0.59, CH_2Cl_2); HPLC 99.0% (*S,S*), 1.0% (*R,R*), <0.1% meso; IR, NMR same as (*R,R*)-**2c**); HRMS (ESI): Calcd for $C_{22}H_{30}NO_2S_2$ $[M+NH_4]^+$: 404.1718, found 404.1715.

(*S,S*)-Di-2-(6-methoxynaphthalen-2-yl)propanoyl disulfide ((*S,S***)-2d)** was obtained as a white solid (0.346 g, 63% yield); mp 128-129 °C; $[\alpha]_D^{31}$ +381.6 (*c* 0.50, CH_2Cl_2); HPLC 99.4% (*S,S*), <0.1% (*R,R*), 0.6% meso; IR (KBr, cm^{-1}): 1728, 1713; ^{1}H NMR (400 MHz, $CHCl_3$): δ 7.73-7.11 (m, 6H), 4.18 (q, $^3J_{HH}$ = 7.0 Hz, 1H), 3.91 (s, 3H), 1.64 (d, $^3J_{HH}$ = 7.0 Hz, 3H); ^{13}C NMR (100 MHz, $CDCl_3$): 195.5, 158.0, 134.1, 133.4, 129.4, 128.9, 127.6, 127.4, 126.4, 119.3, 105.6, 55.3, 53.6, 18.6 ppm; HRMS (ESI): Calcd for $C_{28}H_{30}NO_4S_2$ $[M+NH_4]^+$: 508.1616, found 508.1608.

Synthesis and data, 4a-e:

(*S*)-2-Phenylpropanamide ((*S*)-4a). The following is representative of the procedures for the syntheses of **4a-c**, **e**; specific rotations are collected in Table 4 on page 70. (*S*)-2-Phenylpropanoic acid ((*S*)-**1a**, 0.450 g, 3.00 mmol) was stirred with oxalyl chloride ($(COCl)_2$, 2.60 mL, 30.3 mmol) for 2 h at rt. The excess $(COCl)_2$ was removed on a vacuum line to give the acid chloride as an oil. The oil was dissolved in 5 mL benzene and then treated with cool concentrated NH_4OH (1.00 mL, 15.0 mmol). The reaction solution was stirred for 15 min, and then 10 mL benzene and 5 mL distilled water were added to the reaction flask. The solution was

transferred to a separatory funnel and the aqueous layer removed. The benzene layer was washed with 3 x 2 mL water, and then dried with $MgSO_4$. The solution was filtered and the solvent was removed on a rotary evaporator to give (*S*)-**4a** as white solid (0.38 g, 84% yield from (*S*)-**1a**). ^{1}H NMR (400 MHz, $CHCl_3$): δ 7.26-7.38 (m, 5H), 5.48 (br s, 1H), 5.31 (br s, 1H), 3.61 (q, $^3J_{HH}$ = 7.2 Hz, 1H), 1.53 (d, $^3J_{HH}$ = 7.2, 3H); ^{13}C NMR (100 MHz, $CHCl_3$): 176.5, 141.3, 129.0, 127.6, 127.4, 46.6, 18.3 ppm.

(*R*)-2-Phenylpropanamide ((*R*)-**4a**) was obtained as a white solid (0.57 g, 89% yield from (*R*)-**1a**); NMR same as (*S*)-**4a**.

(*R*)-2-Phenylbutanamide ((*R*)-**4b**) was obtained as a white solid (0.69 g, 79% yield from (*R*)-**1b**); ^{1}H NMR (400 MHz, $CDCl_3$): δ 7.25-7.36 (m, 5H), 5.78 (br s, 1H), 5.43 (br s, 1H), 3.28 (t, $^3J_{HH}$ = 7.6 Hz, 1H), 2.18 (m, 1H), 1.80 (m, 1H), 0.89 (t, $^3J_{HH}$ = 7.4, 3H); ^{13}C NMR (100 MHz, $CDCl_3$): 176.1, 139.8, 128.9, 128.0, 127.3, 54.6, 26.1, 12.3 ppm.

(*S*)-2-Phenylbutanamide ((*S*)-**4b**) was obtained as a white solid (0.74 g, 74% yield from (*S*)-**1b**); NMR same as (*R*)-**4b**.

(*R*)-3-Methyl-2-phenylbutanamide ((*R*)-**4c**) was obtained as a white solid (1.40 g, 95% yield from (*R*)-**1c**); ^{1}H NMR (400 MHz, $CDCl_3$): δ 7.23-7.34 (m, 5H), 5.78 (br s, 2H), 5.59 (br s, 2H), 2.92 (d, $^3J_{HH}$ = 10.2 Hz, 1H), 2.39 (m, 1H), 1.07 (d, $^3J_{HH}$ = 6.5 Hz, 3H), 0.71 (d, $^3J_{HH}$ = 6.7, 3H); ^{13}C NMR (100 MHz, $CDCl_3$): 175.9, 139.2, 128.6, 128.3, 127.2, 61.1, 31.2, 21.6, 20.3 ppm.

(*S*)-3-Methyl-2-phenylbutanamide ((*S*)-**4c**) was obtained as a white solid (1.48 g, 90% yield from (*S*)-**1c**); NMR same as (*R*)-**4c**.

(*R*)-2-(4-Isobutylphenyl)propanamide ((*R*)-**4e**) was obtained as a white solid (0.92 g, 60% yield from *(R)*-**1e**); ^{1}H NMR (400 MHz, $CHCl_3$): δ 7.10-7.25 (m, 5H), 5.59 (br s, 1H), 5.35 (br s, 1H), 3.57 (q, $^3J_{HH}$ = 7.2 Hz, 1H), 2.45 (d, $^3J_{HH}$ = 7.2 Hz, 2H), 1.88 (m, 1H), 1.51 (d, $^3J_{HH}$ =

7.2 Hz, 3H), 0.89 (d, $^3J_{HH}$ = 6.8, 6H); ^{13}C NMR (100 MHz, $CDCl_3$): 177.0, 140.9, 138.4, 129.7, 127.3, 46.3, 45.0, 30.2, 22.4, 18.3 ppm.

(*S*)-2-(4-Isobutylphenyl)propanamide ((*S*)-**4e**) was obtained as a white solid (0.92 g, 74% yield from (*S*)-**1e**); NMR same as (*R*)-**4e**.

(*S*)-2-(6-Methoxynaphthalen-2-yl)propanamide ((*S*)-**4d).** (*S*)-2-(6-Methoxynapthalen-2-yl)propanoic acid ((*S*)-**1d**, 1.02 g, 4.43 mmol) was stirred with $(COCl)_2$ (4.00 mL, 46.6 mmol) at rt for 30 min. The excess $(COCl)_2$ was removed on a vacuum line to give the acid chloride as a slightly yellow solid. The acid chloride was dissolved in 15 mL benzene and then treated with cold concentrated NH_4OH (1.20 mL, 18.0 mmol). After the reaction mixture was stirred for 15 min, the product precipitated out of solution. The precipitate was filtered, washed with 10 mL water and 10 mL benzene and then dried on the vacuum line. The product was obtained as white solid (0.88 g, 87% yield from (*S*)-**1d**). ^{1}H NMR (400 MHz, $CHCl_3$): δ 7.11-7.74 (m, 6H), 5.44 (br s, 1H), 5.35 (br s, 1H), 3.91 (s, 3H), 3.73 (q, $^3J_{HH}$ = 7.2 Hz, 1H), 1.60 (d, $^3J_{HH}$ = 7.2 Hz, 3H); ^{13}C NMR (100 MHz, $CDCl_3$): 179.7, 157.8, 136.3, 133.8, 129.2, 129.0, 127.7, 126.2, 126.1, 119.3, 105.6, 55.3, 46.6, 18.3 ppm.

Synthesis of thioamides. 1. (*S*)-2-Phenylpropanethioamide ((*S*)-**5a).** The following procedure is representative of the method used for **5a**, **5b**, **5d**, and **5e**. Under a nitrogen atmosphere, a mixture of P_4S_{10} (0.647 g, 1.46 mmol) and Na_2CO_3 (0.156 g, 1.47 mmol) in 70 mL dry THF was stirred at rt for 1.5 h. To the resulting clear yellow solution was added a solution of (*S*)-**4a** (0.320 g, 2.14 mmol) dissolved in 10 mL THF. The reaction solution was stirred at rt for ~24 h and then the solvent was removed on a rotary evaporator to give a gum. The gum was then dissolved in 50 mL CH_2Cl_2 and washed in a separatory funnel with 10 mL 5% $NaHCO_3$ and then 20 mL brine. The organic layer was removed, dried with anhydrous $MgSO_4$, and the

solvent was again removed on a rotary evaporator to give a gum. The gum was taken up in 6 mL benzene and then 30 mL petroleum ether (30-60°) was added to give a turbid solution which was cooled in a freezer at –18 °C to give (*S*)-**5a** as a white solid (0.33 g, 93% yield). mp 76-78 °C; $[\alpha]_D^{27}$ +80.0 (*c* 0.59, C_6H_6); HPLC 98.2% (*S*), 1.8% (*R*); IR (KBr, cm^{-1}): 3489, 3419, 3371, 3276, 3158, 1620, 1594; ^{1}H NMR (400 MHz, CD_3CN): δ 7.94 (br s, 1H), 7.70 (br s, 1H), 7.42-7.24 (m, 5H), 4.04 (q, $^3J_{HH}$ = 8.0 Hz, 1H), 1.54 (d, $^3J_{HH}$ = 8.0, 3H); ^{13}C NMR (100 MHz, CD_3CN): 213.7, 143.5, 129.5, 128.4, 128.1, 53.2, 21.7 ppm; HRMS (ESI): Calcd for $C_9H_{12}NS$ $[M+H]^+$: 166.0690, found 166.0684.

Synthesis of thioamides. 2. (*R*)-3-Methyl-2-phenylbutanethioamide ((*R*)-5c). Under a nitrogen atmosphere, a solution of (*R*)-**4c** (0.507 g, 2.86 mmol) in 10 mL THF was added to a solution of Lawesson's reagent (see Scheme 2; 1.16 g, 2.87 mmol) in 30 mL THF. The reaction mixture was stirred at rt for ~24 h and then the solvent was evaporated on a vacuum line. The resulting gum was dissolved in 50 mL EtOAc and washed in a separatory funnel with 10 mL 5% $NaHCO_3$. The organic layer was removed, dried with anhydrous $MgSO_4$, and the solvent was removed on a rotary evaporator to give a gum. The gum was dissolved in 3:1:0.01 EtOAc/hexanes/Et_3N and passed through a pad of neutral alumina (Brockmann I) pre-washed with the same solvent mixture. All the UV-active material moving with the solvent front was collected and crystallized from 1:9 benzene/petroleum ether to afford (*R*)-**5c** as a white solid (0.26 g, 48%). mp 99-101 °C; $[\alpha]_D^{30}$ –84.0 (*c* 0.62, C_6H_6); HPLC 88.9% (*R*), 11.1% (*S*); IR (KBr, cm^{-1}): 3497, 3445, 3380, 3279, 3164, 1622, 1595; ^{1}H NMR (400 MHz, $CDCl_3$): δ 7.87 (br s, 2H,), 7.48-7.23 (m, 5H), 3.38 (d, $^3J_{HH}$ = 11.0 Hz, 1H), 2.62-2.49 (m, 1H), 1.03 (d, $^3J_{HH}$ = 6.5 Hz, 3H), 0.695 (d, $^3J_{HH}$ = 6.7 Hz, 3H); ^{13}C NMR (100 MHz, $CDCl_3$): 212.7, 141.6, 129.5, 129.2,

128.1, 68.2, 33.4, 21.5, 20.7 ppm; HRMS (ESI): Calcd for $C_{11}H_{16}NS$ $[M+H]^+$: 194.1003, found 194.0996.

Data for 5a–e:

HPLC conditions for determination of enantiomeric purity. Each of **5a**–**e** was analyzed on a Chiral Technologies bonded CHIRALPAK® IB column (5 μ particle size, 4.6 mm x 250 mm) at 20 °C eluting at 1 mL/min with 10% acetone/90% hexanes; **5d** was analyzed on the analogous IA and IC columns as well, in all cases using various combinations of acetone, methanol, ethanol, 2-propanol, and hexanes, without achieving any separation.

(*R*)-2-Phenylpropanethioamide ((*R*)-**5a)** was obtained as a white solid using method 1 (0.53 g 92% yield); mp 77.0-78.5 °C; $[\alpha]_D^{29}$ –67.7 (*c* 0.75, C_6H_6); HPLC 91.3% (*R*), 8.7% (*S*); NMR same as (*S*)-**5a**; HRMS (ESI): Calcd for $C_9H_{12}NS$ $[M+H]^+$: 166.0690, found 166.0683.

(*R*)-2-Phenylbutanethioamide ((*R*)-**5b)** was obtained as a white solid using method 1 (0.59 g, 87% yield); mp 83-84 °C; $[\alpha]_D^{30}$ –116.0 (*c* 0.64, C_6H_6); HPLC >99.9% (*R*), <0.1% (*S*); ^{1}H NMR (400 MHz, $CDCl_3$): δ 7.56 (br s, 1H), 6.72 (br s, 1H), 7.39-7.26 (m, 5H), 3.73 (dd, $^3J_{HH}$ = 6.3, 8.9 Hz, 1H), 2.40 (m, 1H), 1.97 (m, 1H), 0.91 (t, $^3J_{HH}$ = 8.0, 3H); ^{13}C NMR (100 MHz, $CDCl_3$): 211.9, 139.5, 129.1, 127.9, 127.8, 61.4, 28.6, 12.4 ppm; HRMS (ESI): Calcd for $C_{10}H_{14}NS$ $[M+H]^+$: 180.0847, found 180.0838.

(*S*)-2-Phenylbutanethioamide ((*S*)-**5b)** was obtained as a white solid using method 1 (0.71 g, 95% yield); mp 84-85 °C; $[\alpha]_D^{31}$ +113.6 (*c* 0.58, C_6H_6); HPLC >99.9% (*S*), <0.1% (*R*); NMR same as (*R*)-**5b**; HRMS (ESI): Calcd for $C_{10}H_{14}NS$ $[M+H]^+$: 180.0847, found 180.0837.

(*S*)-3-Methyl-2-phenylbutanethioamide ((*S*)-**5c)** was obtained as a white solid using method 2 (0.24 g, 43% yield); mp 97-99 °C; $[\alpha]_D^{30}$ +79.0 (*c* 0.55, C_6H_6); HPLC 85.8% (*S*),

14.2% (*R*); NMR same as (*R*)-**5c**; HRMS (ESI): Calcd for $C_{11}H_{16}NS$ $[M+H]^+$: 194.1003, found 194.0995.

(*S*)-2-(6-Methoxynaphthalen-2-yl)propanethioamide ((*S*)-5d) was obtained as a white solid using method 1 (0.67 g, 71% yield); mp 140.5-142.0 °C; $[\alpha]_D^{27}$ +59.1 (*c* 0.55, C_6H_6); ^{1}H NMR (400 MHz, CD_3CN): δ 7.96 (br s, 2H), 7.13-7.78 (m, 6H), 4.17 (q, $^3J_{HH}$ = 7.0 Hz, 1H), 3.88 (s, 3H), 1.63 (d, $^3J_{HH}$ = 7.0 Hz, 3H); ^{13}C NMR (100 MHz, CD_3CN): 213.8, 158.7, 138.6, 134.9, 130.2, 129.8, 127.9, 127.3, 126.7, 119.8, 106.7, 56.0, 53.3, 21.6 ppm; HRMS (ESI): Calcd for $C_{14}H_{16}NOS$ $[M+H]^+$: 246.0953, found 246.0946.

(*R*)-2-(4-Isobutylphenyl)propanethioamide ((*R*)-5e) was obtained as a white solid using method 1 (0.84 g, 85% yield); mp 85.0-86.5 °C; $[\alpha]_D^{26}$ –62.0 (*c* 0.55, C_6H_6); HPLC 98.7% (*R*), 1.3% (*S*); ^{1}H NMR (400 MHz, CD_3CN): δ 7.91 (br s, 1H), 7.67 (br s, 1H), 7.32-7.11 (m, 5H), 4.00 (q, $^3J_{HH}$ = 8.0 Hz, 1H), 2.45 (d, $^3J_{HH}$ = 8.0 Hz, 2H), 1.83 (m, 1H), 1.52 (d, $^3J_{HH}$ = 8.0 Hz, 3H), 0.88 (d, $^3J_{HH}$ = 8.0, 6H); ^{13}C NMR (100 MHz, $CDCl_3$): 214.0, 141.7, 140.8, 130.2, 128.1, 53.0, 45.5, 31.1, 22.6, 21.7 ppm; HRMS (ESI): Calcd for $C_{13}H_{20}NS$ $[M+H]^+$: 222.1316, found 222.1309.

(*S*)-2-(4-Isobutylphenyl)propanethioamide ((*S*)-5e) was obtained as a white solid using method 1 (0.84 g, 85% yield); mp 83-85 °C; $[\alpha]_D^{27}$ +54.0 (*c* 0.64, C_6H_6); HPLC 93.5% (*S*), 6.5% (*R*); NMR same as (*R*)-**5e**; HRMS (ESI): Calcd for $C_{13}H_{20}NS$ $[M+H]^+$: 222.1316, found 222.1307.

Synthesis of MEDITH analogues: (*S*)-5-(1-(6-methoxynapthalen-2-yl)ethyl)-*3H*-1,2,4-dithiazol-3-one ((*S*)-6d). In a nitrogen-filled glove box, a solution of thioamide (*S*)-**5d** (0.1019 g, 0.4153 mmol) and pyridine (0.0748 g, 0.946 mmol) in 10 mL ether was added at rt to a solution of chlorocarbonylsulfenyl chloride (0.0695 g, 0.531 mmol) in 4 mL ether. After

stirring for ~2 min, TLC (3:1 hexane/EtOAc) indicated complete conversion of **5d** to **6d**. The pyridinium chloride was filtered out and the solvent was removed using a vacuum pump to give a gum. The gum was dissolved in ~2 mL ether and hexane was added until the solution became turbid (~6 mL). The resulting turbid solution was placed in the glove box freezer (–32 °C) overnight to give **6d** as a white solid after filtration and rinsing with hexane (0.12 g, 92% yield). mp 84-86 °C; $[\alpha]_D^{28}$ +54.0 (*c* 0.50, C_6H_6); HPLC 94.9% (*S*), 5.1% (*R*); IR (KBr, cm^{-1}): 1713, 1536; ^{1}H NMR (400 MHz, CD_3CN): δ 7.17-7.87 (m, 6H), 4.57 (q, $^3J_{HH}$ = 7.1 Hz, 1H), 3.90 (s, 3H), 1.83 (d, $^3J_{HH}$ = 7.1 Hz, 3H); ^{13}C NMR (100 MHz, $CDCl_3$): 201.2, 188.3, 159.3, 135.63, 135.55, 130.5, 129.7, 128.6, 128.5, 127.7, 120.4, 106.8, 56.1, 48.0, 20.9 ppm; HRMS (ESI): Calcd for $C_{15}H_{14}NO_2S_2$ $[M+H]^+$: 304.0466, found 304.0466.

Data for 6a-e:

HPLC conditions for determination of enantiomeric purity. Each compound required different conditions for adequate separations. Each used elution at 1 mL/min and a CHIRALPAK® IA, IB, or IC column (5 μ particle size, 4.6 mm x 250 mm). For **6a**: IA, 0.5% MeOH/99.5% hexanes at 25 °C; for **6b**: IB, 1% EtOH/99% hexanes at 12 °C; for **6c**: IA, 0.25% MeOH/99.75% hexanes at 25 °C; **6d**: IC, 8% acetone/92% hexanes at 20 °C; **6e**: IA, 2% acetone/98% hexanes at 20 °C.

(*R*)-5-(1-Phenylethyl)-3*H*-1,2,4-dithiazol-3-one ((*R*)-6a) was obtained as a white solid (0.083 g, 59% yield); mp 42-43 °C; $[\alpha]_D^{24}$ –68.7 (*c* 0.52, C_6H_6); HPLC 99.1% (*R*), 0.9% (*S*); IR (KBr, cm^{-1}): 1713, 1537; ^{1}H NMR (400 MHz, CD_3CN): δ 7.45-7.36 (m, 5H), 4.45 (q, $^3J_{HH}$ = 7.2 Hz, 1H), 1.76 (d, $^3J_{HH}$ = 7.2, 3H); ^{13}C NMR (100 MHz, CD_3CN): 200.9, 188.2, 140.8, 130.1, 129.49, 129.46, 48.0, 20.9 ppm; HRMS (ESI): Calcd for $C_{10}H_{10}NOS_2$ $[M+H]^+$: 224.0204, found 224.0201.

(*S*)-5-(1-Phenylethyl)-3*H*-1,2,4-dithiazol-3-one ((*S*)-6a) was obtained as a white solid (0.083 g, 60% yield); mp 42-43 °C; $[\alpha]_D^{24}$ +67.0 (*c* 0.56, C_6H_6); HPLC 99.4% (*S*), 0.6% (*R*); IR and NMR same as (*R*)-**6a**; HRMS (ESI): Calcd for $C_{10}H_{10}NOS_2$ $[M+H]^+$: 224.0204, found 224.0199.

(*R*)-5-(1-Phenylpropyl)-3*H*-1,2,4-dithiazol-3-one ((*R*)-6b) was obtained as a gum (0.12 g, 90% yield); $[\alpha]_D^{23}$ –60.0 (*c* 0.50, C_6H_6); HPLC 91.3% (*R*), 8.7% (*S*); IR (KBr, cm^{-1}): 1714, 1538; ^{1}H NMR (400 MHz, $CDCl_3$): δ 7.45-7.34 (m, 5H), 4.19 (dd, $^3J_{HH}$ = 6.5, 8.8 Hz, 1H), 2.35 (m, 1H), 2.12 (m, 1H), 0.90 (t, $^3J_{HH}$ = 7.4, 3H); ^{13}C NMR (100 MHz, $CDCl_3$): 199.7, 188.2, 139.4, 130.1, 129.8, 129.4, 55.5, 29.2, 12.4 ppm; HRMS (ESI): Calcd for $C_{11}H_{12}NOS_2$ $[M+H]^+$: 238.0360, found 238.0359.

(*S*)-5-(1-Phenylpropyl)-3*H*-1,2,4-dithiazol-3-one ((*S*)-6b) was obtained as a gum (0.12 g, 90% yield); $[\alpha]_D^{25}$ +59.8 (*c* 0.55, C_6H_6); HPLC 91.2% (*S*), 8.8% (*R*); IR and NMR same as (*R*)-**6b**; HRMS (ESI): Calcd for $C_{11}H_{12}NOS_2$ $[M+H]^+$: 238.0360, found 238.0361.

(*R*)-5-(2-Methyl-1-phenylpropyl)-3*H*-1,2,4-dithiazol-3-one ((*R*)-6c) was obtained as a gum (0.11 g, 85% yield); $[\alpha]_D^{27}$ –85.4 (*c* 0.52, C_6H_6); HPLC 88.5% (*R*), 11.5% (*S*); IR (KBr, cm^{-1}): 1719, 1549; ^{1}H NMR (400 MHz, CD_3CN): δ 7.47-7.31 (m, 5H), 3.88 (d, $^3J_{HH}$ = 10.3 Hz, 1H), 2.63 (m, 1H), 1.02 (d, $^3J_{HH}$ = 6.5 Hz, 3H), 0.80 (d, $^3J_{HH}$ = 6.6 Hz, 3H); ^{13}C NMR (100 MHz, $CDCl_3$): 198.6, 188.2, 139.4, 129.9, 129.8, 129.3, 62.2, 34.9, 21.4, 21.0 ppm; HRMS (ESI): Calcd for $C_{12}H_{14}NOS_2$ $[M+H]^+$: 252.0517, found 252.0514.

(*S*)-5-(2-Methyl-1-phenylpropyl)-3*H*-1,2,4-dithiazol-3-one ((*S*)-6c) was obtained as a gum (0.12 g, 89% yield); $[\alpha]_D^{24}$ = +75.8 (*c* 0.55, C_6H_6); HPLC 86.1% (*S*), 13.9% (*R*); IR and NMR same as (*R*)-**6c**; HRMS (ESI): Calcd for $C_{12}H_{14}NOS_2$ $[M+H]^+$: 252.0517, found 252.0516.

(*R*)-5-(1-(4-Isobutylphenyl)ethyl)-3*H*-1,2,4-dithiazol-3-one ((*R*)-**6e)** was obtained as a gum (0.12 g, 92% yield); $[\alpha]_D^{29}$ –43.1 (*c* 0.58, C_6H_6); HPLC 96.3% (*R*), 3.7% (*S*); IR (KBr, cm^{-1}): 1713, 1536; ^{1}H NMR (400 MHz, CD_3CN): δ 7.35-7.20 (m, 4H), 4.42 (q, $^3J_{HH}$ = 7.1 Hz, 1H), 2.49 (d, $^3J_{HH}$ = 7.2 Hz, 2H), 1.85 (m, 1H), 1.74 (d, $^3J_{HH}$ = 7.2 Hz, 3H), 0.89 (d, $^3J_{HH}$ = 6.6, 6H); ^{13}C NMR (100 MHz, $CDCl_3$): 201.3, 188.3, 143.3, 137.9, 130.7, 129.3, 47.7, 45.5, 31.1, 22.6, 20.9 ppm; HRMS (ESI): Calcd for $C_{14}H_{18}NOS_2$ $[M+H]^+$: 280.0830, found 280.0831.

(*S*)-5-(1-(4-Isobutylphenyl)ethyl)-3*H*-1,2,4-dithiazol-3-one ((*S*)-6e) was obtained as a gum (0.11 g, 90% yield); $[\alpha]_D^{30}$ +43.0 (*c* 0.70, C_6H_6); HPLC 96.5% (*S*), 3.5% (*R*); IR and NMR same as (*R*)-**6e**; HRMS (ESI): Calcd for $C_{14}H_{18}NOS_2$ $[M+H]^+$: 280.0830, found 280.0830.

Chapter 4

Screening of chiral analogues of phenylacetyl disulfide (PADS) and 5-methyl-3*H*-1,2,4-dithiazol-3-one (MEDITH)

4.1 Abstract

Dinucleosides, prepared from the phosphoramidite and H-phosphonate methods of DNA synthesis, were used for screening chiral analogues of phenylacetyl disulfide (PADS) and 5-methyl-3*H*-1,2,4-dithiazol-3-one (MEDITH). To attain different steric hindrance around the phosphorus atom, dinucleoside H-phosphonate was successfully converted to phosphite triesters with different silyl groups using BSA (5 equiv), TBDMSCl/Et_3N (5 equiv/10 equiv) and Ph_3SiCl/Et_3N (5 equiv/10 equiv). Screening of the phosphite triesters was carried out with less than ½ equiv of the sulfurizing reagents, and the R_{PS}:S_{PS} diastereomeric ratios of the resulting phosphite sulfides or phosphorothioates were determined by reverse-phase HPLC (RP HPLC). A numerical routine was developed to express the diastereoselectivity ($ds_{R(PS)}$ and $ds_{S(PS)}$) of the reactions, regardless of the source of stereochemistry and the de (i.e, $ds_{R(PS)} - ds_{S(PS)}$) of the reactions were used to compare the selectivities of the reaction. It was found that, through a match with the S_P diastereomer of the phosphite triesters (to give the R_{PS} phosphorothioate) that have the TMS group around the phosphorous atom, the highest de of 14.7%, followed by 12.5% were achieved with MEDITH analogues (*S*)-**6d** (naproxen derivative) and (*S*)-**6e** (ibuprofen derivative), respectively. Through a match with the R_P diastereomer of the same phosphite triester (to give the S_{PS} phosphorothioate), MEDITH analogue (*S*)-**6c** (isopropyl group at α position) gave the highest de of -7.9%.

4.2 Introduction: Phosphite triesters for chiral sulfurization

Since phosphite triester **1** (Scheme 1) has an inversion barrier of 33.0 ± 0.2 kcal/mol at 150 ºC and no reagent was found to induce inversion at lower temperature, it is not a suitable compound for our Curtin-Hammett method for stereoselective synthesis of phosphorothioates. However, there is still a need to determine the selectivity of the chiral sulfurizing reagents made in Chapter 3, and so **1** or the more readily available phosphite triester **2** are suitable model compounds that can be used for this purpose. In this chapter the more readily available phosphite **2** will be used.

Scheme 1. Phosphite triester for chiral sulfurization

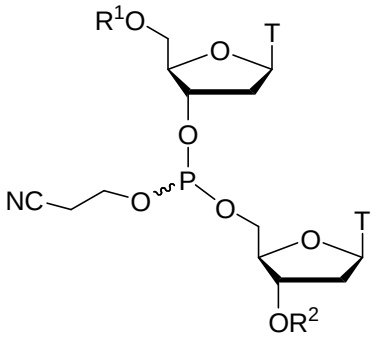

1 $R^1 = R^2 = Ac$
2 $R^1 = DMTr$, $R^2 = TBDMS$

Another model compound that will be used for the sulfurization reactions is phosphite triester **6**, prepared from H-phosphonate **3** (Scheme 2). The conversion of H-phosphonate **3** to phosphite triester **6** has been achieved with reagents such as *N*,*O*-bis(trimethylsilyl)acetamide (BSA),[147, 148] *N*,*O*-bis(trimethylsilyl)trifluoroacetamide (BSTFA),[149] heptamethyldisilazane (HMDS)[149] or a mixture of chlorotrimethylsilane (TMSCl)/Et_3N solution.[48, 149] B. R. Shaw et al. have tested the efficiency of these reagents at room temperature in anhydrous THF on 5'-

Scheme 2. Phosphite triesters via the H-phosphonate method for chiral sulfurization

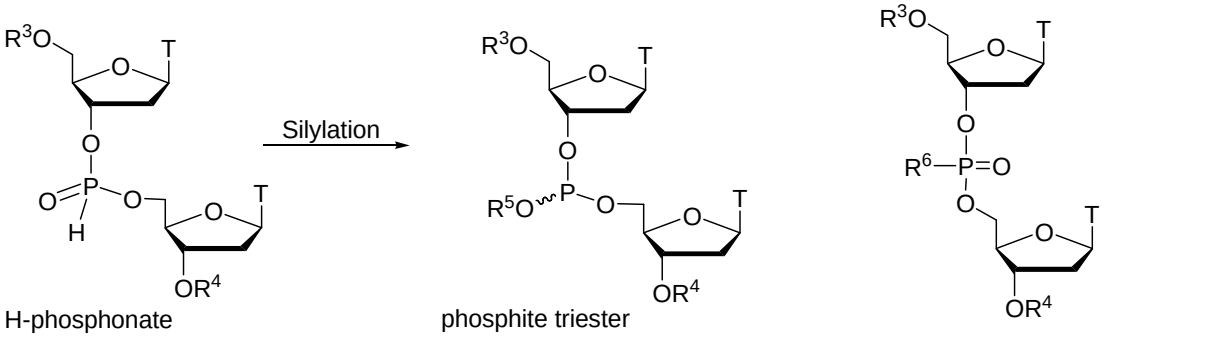

H-phosphonate

3 R^3 = DMTr, R^4 = TBDMS
4 R^3 = OH, R^4 = CPG
5 R^3 = R^4 = TBDMS

phosphite triester

6 R^3 = DMTr, R^4 = TBDMS, R^5 = TMS
7 R^3 = TMS, R^4 = CPG
8 R^3 = DMTr, R^4 = R^5 = TBDMS
9 R^3 = DMTr, R^4 = TBDMS, R^5 = Ph_3Si
10 R^3 = R^4 = R^5 = TBDMS

11 R^3 = R^4 = TBDMS, R^6 = Me

hydroxyl H-phosphonate **4** bound to a solid support and the progress of the reactions was monitored by ^{31}P NMR.[149] Using 3 equivalents of the reagents, they observed complete conversion to phosphite triester **7** within 5 min for BSTFA, 10 min for TMSCl/Et_3N and 30 min for BSA or HMDS.

For us the appealing characteristic of phosphite triesters **6** is the presence of the "3º-like" silyl group, which is bulkier than the 1º β-cyanoethyl group of compound **2** in Scheme 1, thus providing a model compound with a greater steric hindrance around the phosphorus atom which might allow increased selectivity by the chiral sulfurizing reagents. In addition, instead of the trimethylsilyl group of compound **6**, silylation with a *tert*-butyldimethylsilyl or triphenylsilyl group, to give compounds **8** and **9**, respectively, would allow even greater degrees of steric bulk around the phosphorus atom.

Procedures for the synthesis of phosphite triesters **8** and **9** have not been reported, but since H-phosphonate **3** can be converted to phosphite triester **6** with TMSCl/Et_3N, in principle the conversion of H-phosphonate **3** to compounds **8** and **9** can be achieved with TBDMSCl/Et_3N

and Ph_3SiCl/Et_3N, respectively. J. H. van Boom et al. has reported the synthesis of phosphite triester **10**.[150] The compound was synthesized by treating H-phosphonate **5** with 1.5 equivalents of TBDMSCl and 2.6 equivalents of DIPEA in pyridine for 40 min at room temperature. The phosphite triester was not isolated but was converted immediately to phosphonate **11**, by combining with CH_3I (80 equiv) at 50 ºC for 4 h.

4.3 Results and Discussion

4.3.1 Synthesis of phosphite triester 2 and H-phosphonate 3 for chiral sulfuriziation

Phosphite triester **2** was synthesized as reported in Chapter 2, and the crude compound was purified in the glove box by silica gel chromatography to afford a white solid in 94% yield, on the basis of the amount of 3'-*O*-(*tert*-butyldimethylsilyl)-thymidine used. The ^{31}P NMR spectrum of this material in toluene-d_8 exhibited two peaks at 139.7 and 139.3 ppm in a ratio of 50.7:49.3, due to the two diastereomers of phosphite triester **2**. The S_P configuration was assigned to the diastereomer at 139.7 ppm on the basis of the established configuration of its corresponding boranophosphate analogue,[65] which was subsequently converted in a stereoretentive fashion to the S_P diastereomers of phosphite triester **2**. (see Chapter 2, Section 2.3.1.2); and the peak at 139.3 ppm was assigned the R_P configuration.

H-phosphonate **3** was prepared following literature procedures (Scheme 3).[150] 5'-*O*-(*p,p'*-Dimethoxytrityl)thymidine **12** was treated with 2-chloro-4*H*-1,3,2-benzodioxaphosphorin-4-one **13** (2.6 equiv) and pyridine (5.0 equiv) in dioxane for 24 h at rt. After an aqueous workup with triethylammonium bicarbonate and purification by silica gel column chromatography, 5'-*O*-*p,p'*-dimethoxytrityl)thymidine-3'-(H-phosphonate) **14** was obtained as a white solid in 77% yield. Compound **14** (1.1 equiv) was then coupled to 3'-*O*-(*tert*-

Scheme 3. Synthesis of H-phosphonate **3**

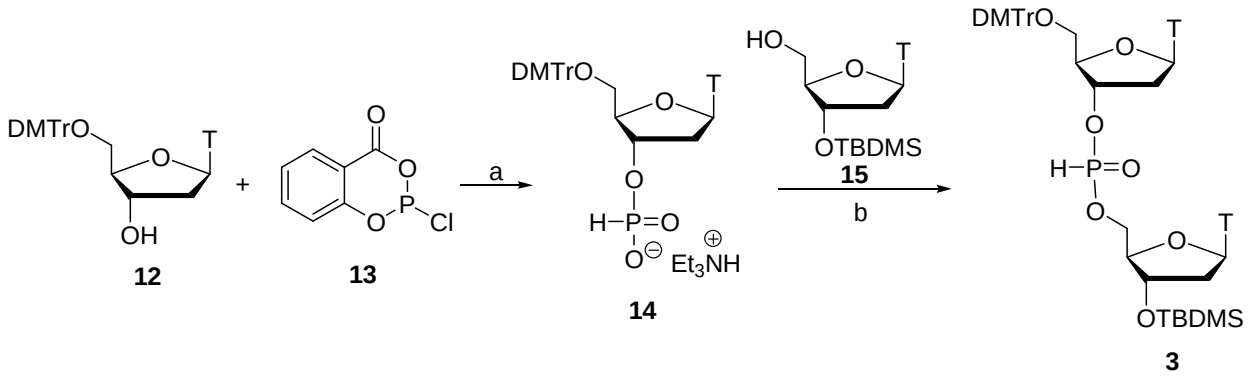

Reagents and conditions: (a) (i) pyridine (5.0 equiv), 1,4-dioxane, rt, 24 h; (ii) aqueous work-up with triethylammonium bicarbonate (TEAB); (b) pyridine, pivaloyl chloride (2.5 equiv, rt, 2 h).

butyldimethylsilyl)thymidine **15** using pivaloyl chloride (2.5 equiv) in pyridine to give H-phosphonate **3** as a white solid in 94% yield after silica gel chromatography. Although H-phosphonate **3** is stable to oxygen, it can undergo hydrolytic cleavage at the H-phosphonate linkage by water and so was stored under nitrogen in the glove box freezer.

The ^{31}P NMR spectrum of H-phosphonate **3** in DMSO-d_6 exhibited peaks at 9.44 ppm and 8.76 ppm that integrated to a ratio of 44.4:55.6, due to the two diastereomers of H-phosphonate **3**. The S_P configuration has been previously assigned to the diastereomer at 9.44 ppm and R_P to the diastereomer at 8.76 ppm.[151]

4.3.2 Method for determining the selectivity of the chiral sulfurizing reagents

Figure 1 illustrates an outline of the method that was used to determine the selectivity of the chiral sulfurizing reagents synthesized in Chapter 3. Details of each step will be presented.

The procedure we developed involves the addition of ~ ¼ equivalent of a sulfurizing reagent to a phosphite triester that consists of a mixture of R_P and S_P diastereomers, which do not interconvert on the reaction time scale. In order to increase the possibility of greater selectivity

Figure 1. Method for determining the selectivity of the chiral sulfurizing reagents

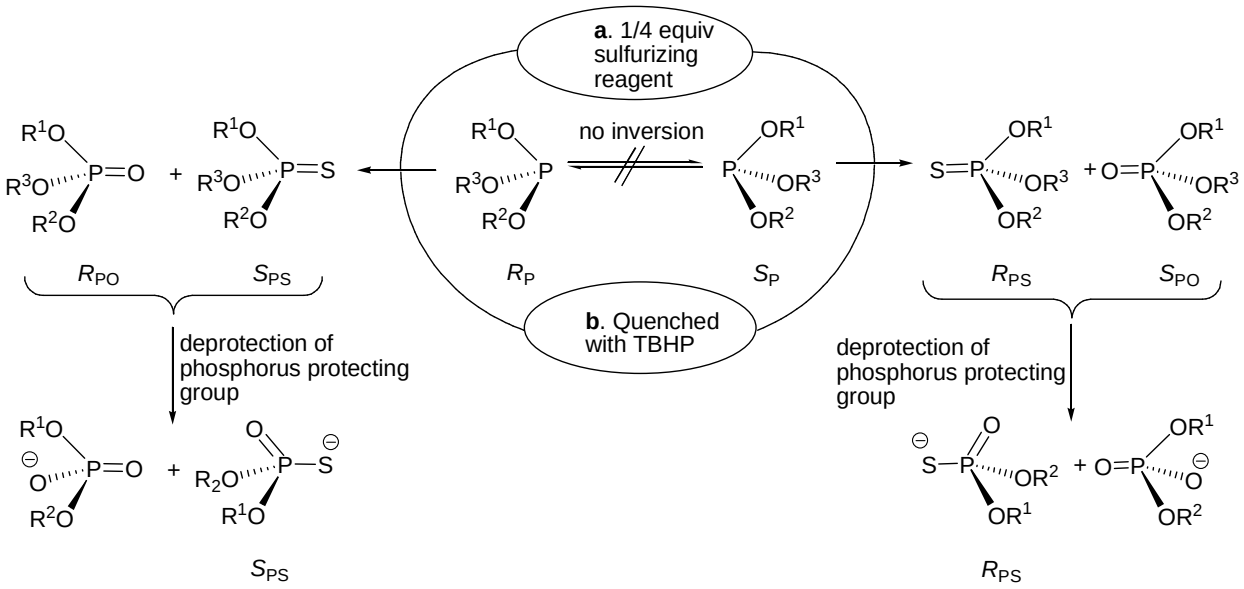

R^1 = 3'-nucleoside, R^2 = 5'-nucleoside and
R^3 = ß-cyanoethyl (for phosphite triester **2**) or silyl groups (for phosphite triesters **6**, **8** and **9**).

by the sulfurizing reagents the reactions were done in the glove box freezer at -32 ºC for 20 h. In principle, any significant selectivity would alter the R_P:S_P reactant ratio as the reaction proceeds, so the use of less sulfurizing reagent would allow a more accurate determination of selectivity. In practice, a reasonable amount of product was needed, and ¼ equivalent seemed to represent a good compromise. After the sulfurization, *tert*-butylhydroperoxide (TBHP) was added to quench the reaction in order to convert the remaining phosphite triester to the phosphite oxide (R_{PO} and S_{PO}). Oxidation of phosphite triesters with TBHP is reported to occur within 5 min at room temperature in solution phase synthesis.[150] The S_{PS}:R_{PS} diasteromeric ratio of the phosphite sulfide after chiral sulfurization can then be compared to the R_P:S_P ratio of the starting phosphite triester to determine the selectivity of the reaction (vide infra). Sulfurization of each diastereomer of phosphite triester **6** has being reported to be a stereoretentive process.[148, 151]

Therefore, since the sulfur atom has the highest priorty (based on Cahn-Ingold-Prelog rules) in the phosphite sulfide, the S_{PS} configuration of the phosphite sulfide will be produced from sulfurizing the R_P configuration of the phosphite triester, and the R_{PS} configuration of the phosphite sulfide will be produced from the S_P phosphite triester. Removal of the protecting groups from the S_{PS} and R_{PS} phosphite sulfides would then give phosphorothioates with S_{PS} and R_{PS} configurations, respectively.

4.3.2.1 Description of a numerical measure of the selectivity of the chiral sulfurization reaction

For a reaction in which a single isomer reacts to give a mixture of stereoisomers (Equation A), the ratio of the two isomers (B and C) in the mixture is often expressed as the enantiomeric excess (ee) if they are enantiomers or diastereomeric excess (de) if they are diastereomers. The ee or de can be derived from the ratio of the products, where B and C are the respective fractions of the enantiomers or distereomers in the mixture, and if B + C = 1, then the ee or de = B – C.

$$A \longrightarrow B + C \qquad \text{(Equation A)}$$

With the progress of asymmetric synthesis, the terms enantiomeric excess (ee) and diastereomeric excess (de) have been expanded to describe enantiostereoselectivity and diasteroselectivity respectively. However, the association between diastereomeric excess (de) and diasteroselectivity has been questioned and it has been suggested that a more appropriate relationship to express the diasteroselectivity of a reaction would be to use the actual ratios of the products formed, that is, the diastereomeric ratio (dr) that can be obtained from analytical methods such as HPLC or NMR.[152]

For instance, in a kinetically controlled reaction where substrate **S** gives a mixture of diastereomers $\mathbf{P}_{\boldsymbol{R}}$ and $\mathbf{P}_{\boldsymbol{S}}$ in ratio of 90:10 (Equation B), since the relative rates of the reaction will determine the product mixture, the diasteroselectivity of the reaction could be reported as dr = 90:10 or as de = 80%.

$$S \longrightarrow P_R + P_S \qquad \text{(Equation B)}$$

dr = 90 : 10

de = 80%

The diastereomer ratio (dr) provides direct information on the relative rates of formation of the *R* and *S* diastereomers (in this case 9:1), and so might be preferred for this reason. The calculated de of 80% does not add any useful information on the steric course of the reaction, but it provides a measure as a single number, which may prove useful for comparison of large amounts of data, as will be seen here. D. Seebach et al. have used the term % diastereomeric selectivity (ds) obtained from the diasteromer ratio (dr), to express the selectivity of the synthesis of 2-*tert*-butyl-5-(1'-hydroxyethyl)-1-aza-3-oxabicylo[3.3.0]-octan-4-one (Scheme 4) - the dr was determined by ^{1}H NMR.[153] In effect, this term seeks to combine the single-number utility of de with the rate-based ratio dr.

Scheme 4. Diastereoselectivity (ds) ratio used to express stereoselectivity

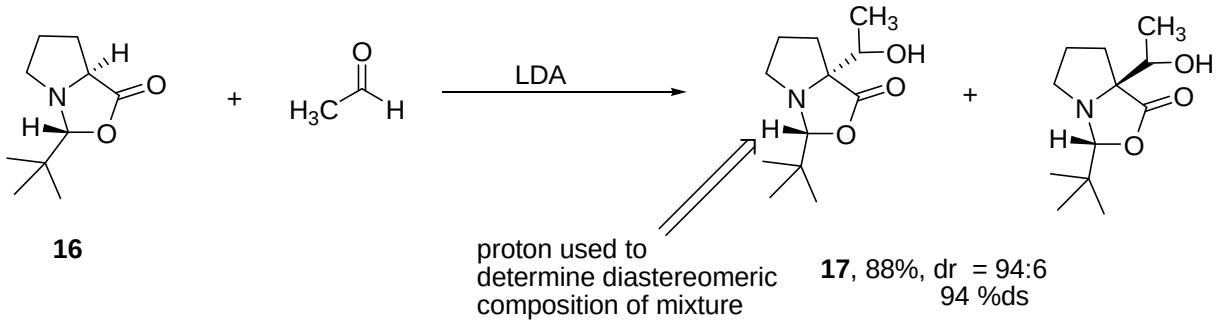

Unlike the reaction above that has a single isomer as the starting substrate, calculating the selectivity of a reaction such as our chiral sulfurization (Section 4.3.2, Figure 1) in which the starting substrate is a mixture of diastereomers, is neither standard nor intuitive. However, the concepts of diastereomeric selectivity (ds) and diastereomer ratio (dr) are useful in this case. Since sulfurization of the two diastereomers of a phosphite triester occurs in a stereoretentive manner,[148, 151] the R_P configuration almost certainly goes to the S_{PS} phosphorothioate and the S_P configuration goes to the R_{PS} phosphorothioate (see Figure 1, configuration change due to the Cahn-Ingold-Prelog rules). The diastereoselectivity for the *R* and *S* configurations are expressed respectively, as $ds_{R(PS)}$ and $ds_{S(PS)}$, where just as in the case described above (i.e. in Scheme 4),

$$ds_{R(PS)} + ds_{S(PS)} = 1. \quad (1)$$

Although it is not strictly required for our analysis, suppose that a sulfurizing reagent were 100% selective for formation of S_{PS} from R_P, then in that case, $ds_{S(PS)}$ = 100% and $ds_{R(PS)}$ = 0%, and we would only expect R_P to react leaving S_P untouched. However, since we assume the sulfurization occurs with complete stereoretention, the selectivity almost certainly refers to the reactive rates of reactivity of the R_P and S_P diastereomers, but in fact we still define $ds_{R(PS)}$ as the selectivity for producing R_{PS}, regardless of the source stereochemistry, and $ds_{S(PS)}$ for producing S_{PS}. This leads to equation (2), and for the case of 100% selectivity, the equation can always be inverted to prevent a zero in the denominator.

$$(R_P / S_P) \times (ds_{S(PS)} / ds_{R(PS)}) = (S_{PS} / R_{PS}) \quad (2)$$

Rearranging (2) gives $(ds_{S(PS)} / ds_{R(PS)}) = (S_{PS} \times S_P)/(R_P \times R_{PS})$ (3)

Substitution of $ds_{S(PS)} = 1 - ds_{R(PS)}$, in equation 3 then gives

$$ds_{R(PS)} = R_{PS} \times R_P /[(S_P \times S_{PS}) + (R_{PS} \times R_P)] \quad (4)$$

Although it is not necessary, subtraction of the $ds_{R(PS)}$:$ds_{S(PS)}$ ratio will give the diastereomeric excess (de) of the reaction (5), and this single value of de will turn out to allow the results to be more easily visualized.

$$de = ds_{R(PS)} - ds_{S(PS)} \quad (5)$$

4.3.3 Optimization of the silylation reaction to produce phosphite triester from H-phosphonate 3 for chiral sulfurization

Since the development of the phosphoramidite and H-phosphonate methods, acetonitrile has been the common solvent used by companies such as Isis Pharmaceuticals,[29] for large scale preparation of oligonucleotides. Reasons for its wide use were mainly due to: (1) it is a polar aprotic solvent that can dissolve the nucleoside monomers and reagents used during the synthesis cycle, (2) although the HPLC-grade reagent contains an average 0.001% water, it is good enough to be used for all reactions in the synthesis cycle, such as the coupling step which requires anhydrous conditions, and (3) acetonitrile is a by-product produced during the production of acrylonitrile, and so was made readily available and the price was relatively low.[154]

However, due to the global financial crisis around mid-2008 there has been a reduction in the demand for acrylonitrile by chemical companies. This led to a shortage of acetonitrile and an increase in its price, thus causing a negative impact on the routine synthesis of oligonucleotides. Other solvents therefore have been investigated, such as acetone as a "washing solvent" between the coupling, capping, oxidation and detritylation reactions of the synthesis cycle.[154] Nevertheless, for our chiral sulfurization reactions ~5 mg phosphite triester will be used in ~ 0.5 mL solvent for each reaction, so given the fact that all the chemistries for oligonucleotide synthesis have already been optimized in acetonitrile and our reactions will not require large

amounts of solvent, acetonitrile was chosen as the solvent for the silylation and sulfurization reactions.

Initial experiments to find the best silylating conditions for the synthesis of phosphite triesters **6** and **8** (Scheme 5), were carried out by simultaneously treating 5 mg each of H-phosphonate **3** with 3 equivalents of BSA (quantity used by B. R. Shaw et al.) and TBDMSCl in anhydrous acetonitrile-d_3 at room temperature. Unlike BSA which does not need any added reagent for it to serve as a silylating reagent, the reaction with TBDMSCl required a base for the conversion of H-phosphonate **3** to phosphite triesters **8**, and so 5 equivalents of Et_3N were used.

Scheme 5. Optimization of the silylation reactions for the synthesis of phosphite triesters **6** and **8** from H-phosphonate **3**

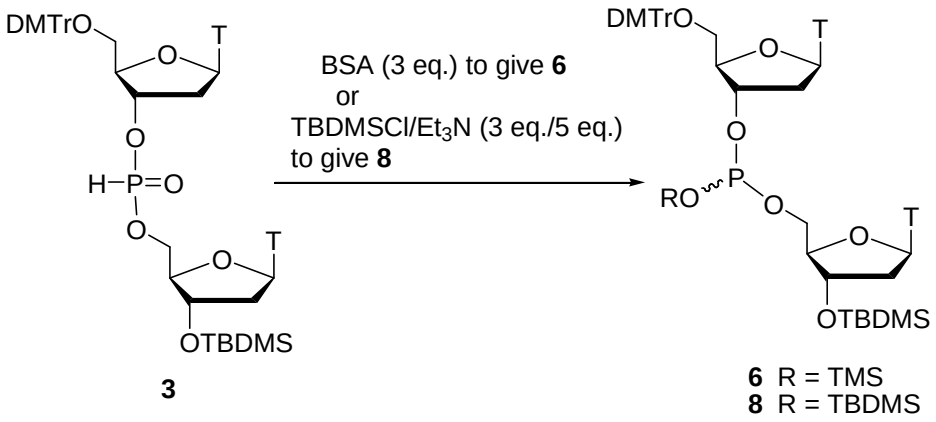

Since H-phosphonate **3** is a mixture of diastereomers, only two peaks corresponding to the R_P and S_P diastereomers of phosphite triesters **6** and **8** were expected after complete silylation. However, after allowing the reaction with BSA to sit with occasional swirling at rt for ~30 min, the ^{31}P NMR spectrum of the reaction solution showed *six* peaks around the phosphite

region (~137 ppm). No change in the NMR was observed after longer reaction time (~ 1day) (Figure 2).

Figure 2. ^{31}P NMR spectrum of the reaction solution of phosphite triester **6**

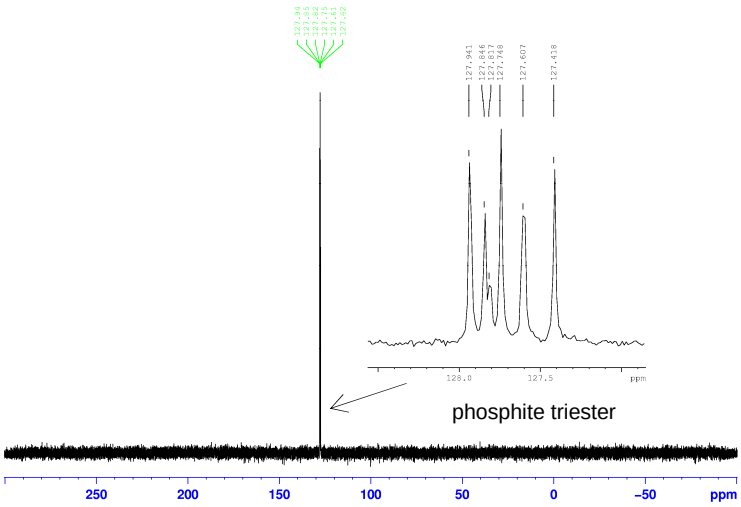

The ^{31}P NMR spectrum of the reaction with TBDMSCl/Et_3N was obtained after ~ 2 h. It showed several peaks in the phosphite triester region and in the H-phosphonate region (~8 ppm). No change in the NMR was observed after ~1 day (Figure 3).

For these two reactions it was initially thought that the various peaks in the ^{31}P NMR spectra were due to exchange of the more labile DMTr group on the H-phosphonate or phosphite triester with the TMS or TBDMS groups from the excess silylating reagents. In order to test this premise, the DMTr group of a sample of H-phosphonate **3** was deprotected with 2% $CHCl_2CO_2H/CH_2Cl_2$. The reaction was done at room temperature for 30 min and the crude compound was purified by silica gel column chromatography to give 5'-hydroxyl H-phosphonate **18** as a white solid in 85% yield (Scheme 6).

Figure 3. ^{31}P NMR spectrum of the reaction solution of phosphite triester **8**

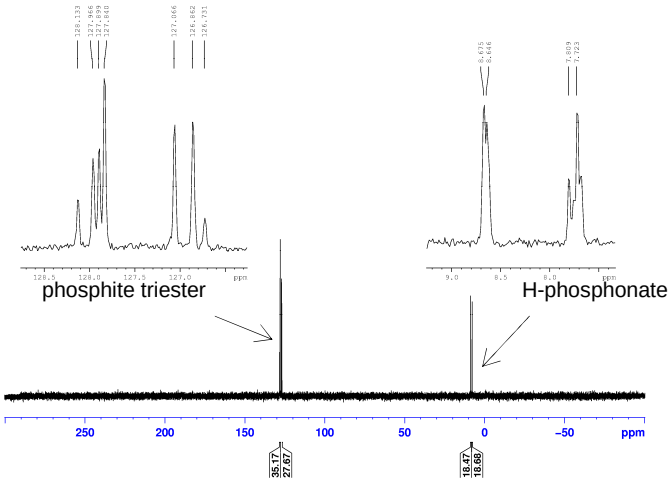

Scheme 6. Synthesis of 5'-hydroxyl H-phosphonate **18**

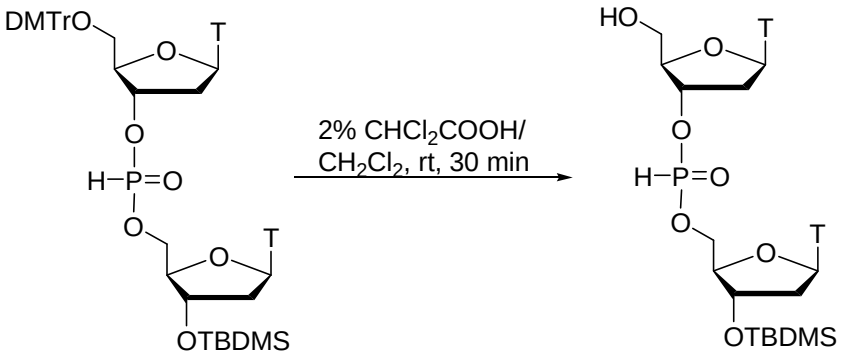

3 **18**

A sample of H-phosphonate **18** (5 mg) was treated with 4 equivalents of BSA in anhydrous acetonitrile-d_3 at room temperature; an additional 1 equivalent of BSA was used instead of the 3 equivalents that were used on H-phosphonate **3** (in Scheme 5) because the free 5'-hydroxyl group of **18** would be protected during the silylation. In principle since the 5'-hydroxyl and the H – P=O groups are the only groups that needed silylation, 3 equivalents of BSA should have been sufficient for the reaction.

After ~30 min of reaction, the ^{31}P NMR spectrum of the solution showed five peaks in the phosphite triester region (Figure 4, NMR A). However, when an additional 3 equivalents of

Figure 4. ^{31}P spectra from silylation of H-phosphonate 18 with 4 eq BSA (A) and 7 eq BSA (B)

A

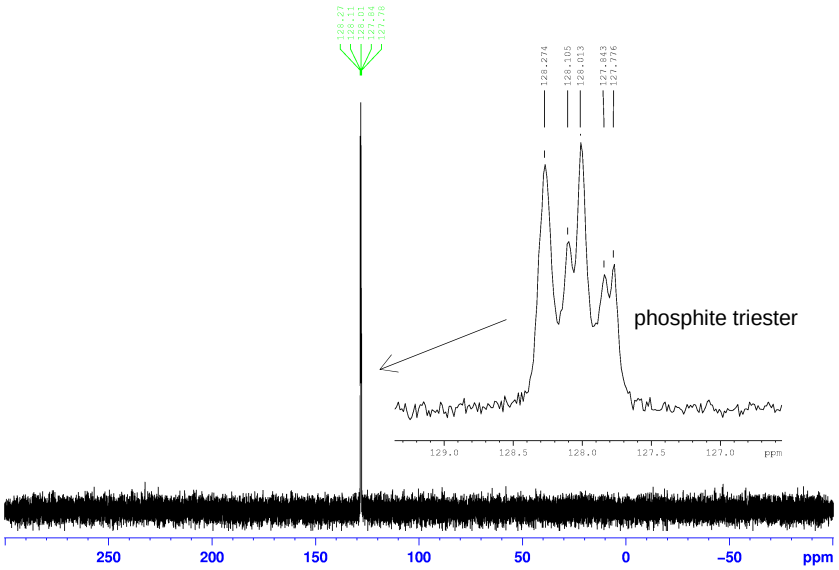

B

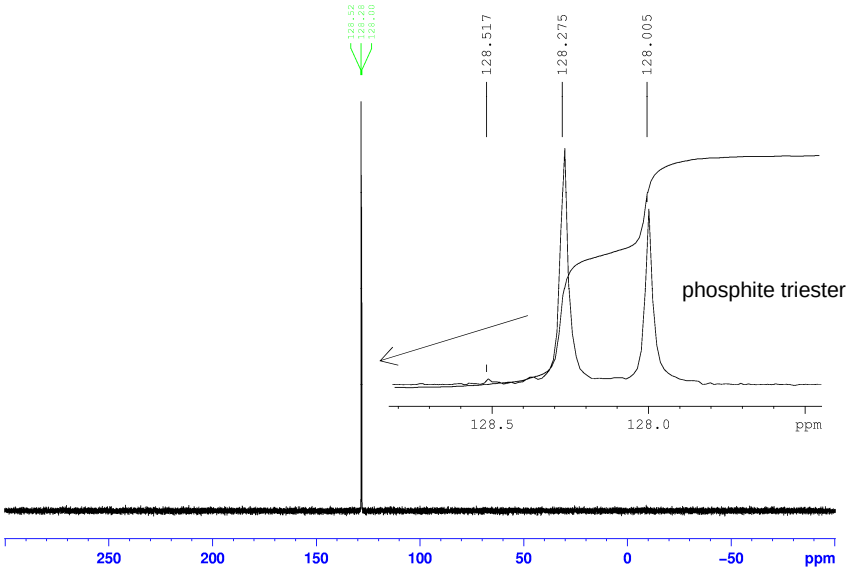

BSA were added to the NMR solution only two peaks at 128.28 ppm and 128.01 ppm in the ^{31}P NMR were observed after ~20 min – the time it took to acquire the spectrum (Figure 4, NMR B). The two peaks integrated to a ratio of 55.8:44.2, which is comparable to the 55.6 (R_P):44.4 (S_P) ratio of its H-phosphonate **3** precursor.

The need for more than 4 equivalents of BSA for complete silylation of H-phosphonate **18** therefore suggested that there were other groups besides the 5' hydroxyl and H – P=O groups that were reacting with the silylating reagent. The amide groups on the thymine moieties could undergo enolization, and so they might be responsible for the various phosphite triester species in Figures 2-4. That is, in addition to silylation at the 5' hydroxyl and H – P=O groups, there could also be a single or double silylation of the thymine moiety on the 3' and/or 5' nucleoside. Scheme 7 shows the possible compounds that might be responsible for the peaks in the NMR spectrum of Figure 4A when insufficient BSA was used - only the R_P diastereomers are shown.

Further reactions with H-phosphonate **3** (used in Scheme 5) indicated that 5 equivalents of BSA were sufficient for complete silylation of all groups (P=O and C=O groups on thymine moieties) on the compound, suggesting that either both nucleobase oxygen atoms are silylated, or excess is needed simply to drive the reaction to completion. The reaction was finished before the ^{31}P NMR could be acquired (~20 min) and the resultant phosphite triester showed only two peaks in the NMR.

From test reactions with TBDMSCl/Et_3N and Ph_3SiCl/Et_3N to synthesize their corresponding phosphite triesters, 5 equivalents of the silylating reagent and 10 equivalents of Et_3N were found to be adequate for complete silylation. The reactions took ~2 h to give a colorless solution with a white precipitate of Et_3NHCl salt.

Scheme 7. Proposed phosphite triesters due to partial silylation of H-phosphonate **3**

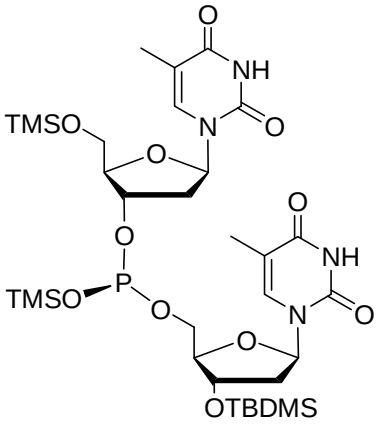

R_P-**19** (no protection at nucleobases)

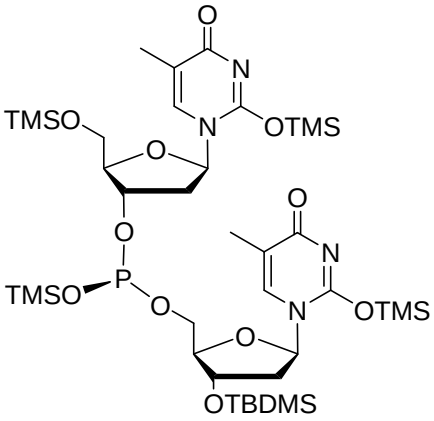

R_P-**20** (protection at both nucleobases)

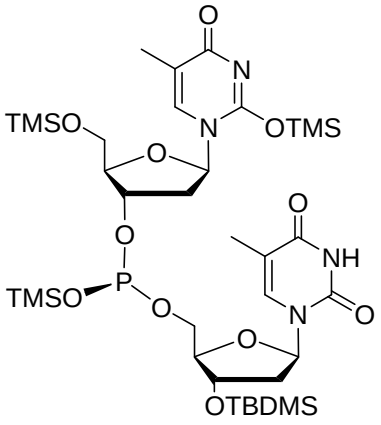

R_P-**21** (protection at
3'-phosphorylated nucleoside)

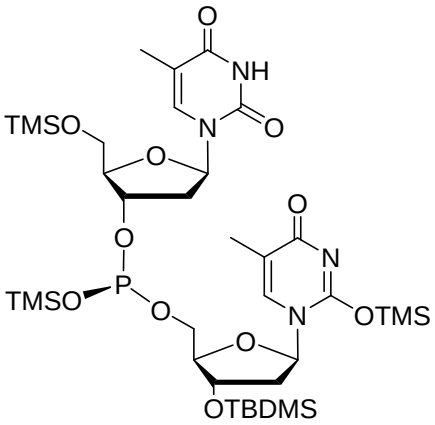

R_P-**22** (protection at
5'-phosphorylated nucleside)

The Et_3NHCl salt produced from silylating with $TBDMSCl/Et_3N$ and Ph_3SiCl/Et_3N is partially soluble in acetonitrile, and so attempts to isolate the phosphite triesters from the ammonium salt were carried out by passing the reaction solutions through a pad of silica gel. The ^{31}P NMR spectra of the solutions collected exhibited several peaks in the phosphite region (~138 ppm) caused by random deprotection of the silyl groups on the thymine moieties, possibly due to adventitious water present on the silica gel. Another method for removing the ammonium salts from the reaction solutions was attempted by evaporating the solvent under reduced

pressure and then redissolving the remaining material in toluene for easy filtration of the salt. However, this method also resulted in random deprotection of the silyl groups on the nucleobase. Therefore, since homogenous solutions of the fully silylated phosphite triesters of TMS (**23**), TBDMS (**24**) and TPS (**25**) (Scheme 8) were needed for screening of the chiral sulfurizing reagents, the Et_3NHCl salts were simply allowed to remain in the reaction solutions during the course of the sulfurization reactions.

Scheme 8. Proposed phosphite triesters due to complete silylation of H-phosphonate **3**

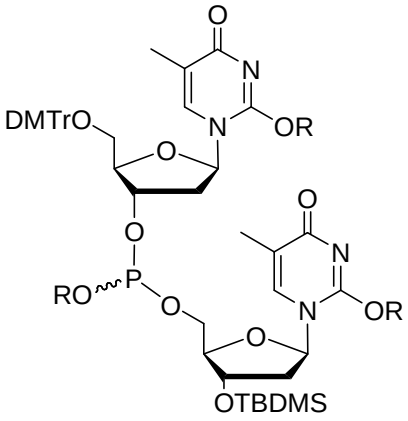

phosphite triester **23**: R = TMS

phosphite triester **24**: R = TBDMS

phosphite triester **25**: R = TPS

4.3.4 Attempts at determining the diastereomer ratios of the starting phosphite triesters and phosphite sulfides by ^{31}P NMR

With the silylation procedure optimized, a procedure (see Experimental Section) was developed for screening the sulfurizing reagents. To find an appropriate method for determining the selectivity of the chiral sulfurization reactions, the starting diastereomer ratios (S_P:R_P) of the

phosphite triesters and their corresponding phosphite sulfide ratios (R_{PS}:S_{PS}) after sulfurization, were first analyzed by ^{31}P NMR spectroscopy.

The starting S_P:R_P ratio of phosphite triester **2** was obtained by ^{31}P NMR using ~10 mg of the sample in toluene-d_8 (Table 1). The assignment of configuration is discussed Section 4.3.1, and the diastereomers corresponding to a ratio of 50.7:49.3 were assigned the S_P and R_P configurations, respectively.

The starting S_P:R_P ratios of phosphite triesters **23**, **24**, and **25** were obtained by first treating H-phosphonate **3** (~10 mg each) with BSA (5 equiv), TBDMSCl/Et_3N (5 equiv/10 equiv) and Ph_3SiCl/Et_3N (5 equiv/10 equiv) respectively (Scheme 9). The reactions were carried

Table 1. ^{31}P NMR analysis of phosphite triesters **2**, and **23-25**[a]

Phosphite triester	Chemical shift (ppm) of diastereomers (Δ ppm)	Diastereomer ratio
2[b]	139.7, 139.3 (0.39)	50.7:49.3 (S_P, R_P)
23	127.76, 127.67 (0.09)	55.9:44.1 (R_P, S_P)[c]
24	127.87, 127.31 (0.56)	56.3:43.8 (R_P, S_P)
25	128.34, 126.89 (1.54)	55.7:44.3 (R_P, S_P)

[a]All ^{31}P NMR spectra were obtained at 22 ºC in CD_3CN with 512 scans on a 400 MHz spectrometer unless specified; [b] data taken from Section 4.3.1 - NMR done in toluene-d_8; [c] ^{31}P NMR peaks not base-line resolved.

out at rt in ~100 μL of CD_3CN for ~2 h, then diluted to ~0.5 mL with CD_3CN and ^{31}P NMR spectra were recorded for each reaction solution (Table 1). In Section 4.3.1, the two diastereomers of H-phosphonate **3** in a ratio of 44.4:55.6 were assigned to the S_P and R_P configurations, respectively, based on literature reports. The conversion of H-phosphonate **3**

Scheme 9. Synthesis of phosphite triesters **23-25** to determine the ^{31}P chemical shifts of the R_P and S_P diastereomers

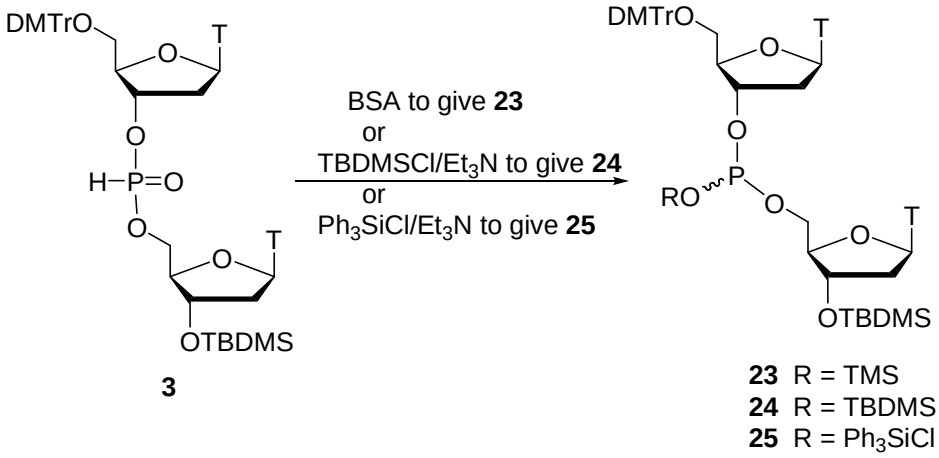

to the phosphite triester **23** has been reported to be a stereoretentive process;[148, 151] therefore, the S_P and R_P configurations were assigned to the two diastereomers of the phosphite triesters **23-25** with the corresponding ratios of ~44:56.

In order to determine the corresponding chemical shifts for the diastereomers when phosphite triesters **2** and **23-25** are converted to their phosphite sulfides, the triesters were treated with excess sulfur at rt (Scheme 10) and the ^{31}P NMR spectra of the resulting phosphite sulfide solutions were recorded (Table 2).

Sulfur is known to react in a stereoretentive manner with chiral phosphite triesters to give their corresponding phosphite sulfides.[148, 151] Single diastereomers of phosphite sulfide **26** were not available for ^{31}P NMR. Therefore since the diastereomer ratio of phosphite sulfide **26** is 50.3:49.7 (i.e. ~1:1) assignment of the configuration to each diastereomer of the mixture could not be achieved with certainty. However, the diastereomers of starting phosphite triester **2** were assigned as 50.7 (S_P):49.3 (R_P), and thus the 50.3:49.7 diastereomer ratio of the phosphite sulfide was tentatively assigned to the (R_{PS})-**26** and (S_{PS})-**26** configurations, respectively. Assignment of

Scheme 10. Synthesis of phosphite sulfides **26-29** to determine the ^{31}P chemical shifts of their R_{PS} and S_{PS} diastereomers

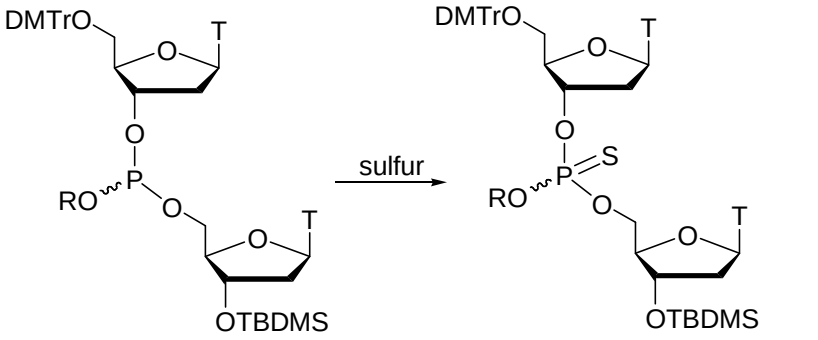

2 R = ß-cyanoethyl
23 R = TMS
24 R = TBDMS
25 R = Ph_3SiCl

26 R = ß-cyanoethyl
27 R = TMS
28 R = TBDMS
29 R = Ph_3SiCl

Table 2. ^{31}P NMR analysis of phosphite sulfides **26-29**[a]

Phosphite sulfides	Chemical shift (ppm) of diastereomers (Δ ppm)	Diastereomer ratio[b]
26	67.04, 66.98 (0.06)	50.3:49.7[c] (R_{PS}:S_{PS})
27	55.38, 55.11 (0.27)	44.0:56.0 (R_{PS}:S_{PS})
28	55.55, 55.49 (0.06)	56.8:43.2[c] (S_{PS}:R_{PS})
29	55.16, 55.05 (0.11)	55.4:44.6[c] (S_{PS}:R_{PS})

[a]All ^{31}P NMR spectra were obtained at ~25 ºC in CD_3CN with 512 scans on a 400 MHz spectrometer; [b] diastereomer ratios are reported in the same order as their chemical shifts, i.e. low field to high field; [c] ^{31}P NMR peaks are not base-line resolved.

configurations to phosphite sulfides **27-29** were made based on their corresponding phosphite triesters with diastereomer ratios of ~44:56. That is, the R_{PS} configuration was assigned to the diastereomers with the corresponding per cent of ~44% and the S_{PS} configuration was assigned to the diastereomers with the corresponding per cent of ~56%.

With the exception of phosphite sulfides **27**, the phosphite sulfides (**26**, **28** and **29**) did not give base-line resolved ^{31}P NMR spectra (Figure 5 shows the ^{31}P NMR of phosphite sulfide **28**). Although careful integration of these spectra gave diastereomer ratios that were similar to

Figure 5. ^{31}P NMR spectrum of phosphite sulfide **28**

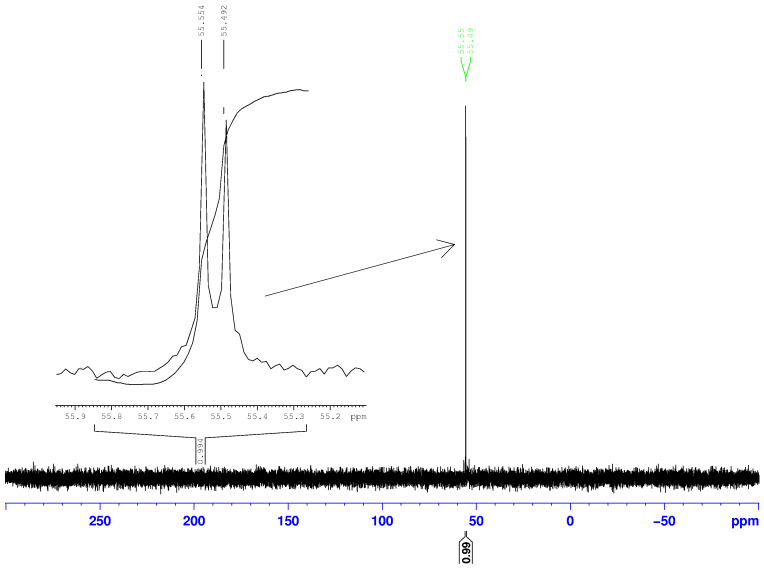

the ratios of their corresponding phosphite triesters in Table 1, the integrations became more difficult and in some cases impossible when screening reactions were carried out using ~¼ equivalent of a sulfurizing reagent. This becomes problematic particularly if there are small selectivities to be determined from the chiral sulfurization reactions. For instance, Figure 6 shows the ^{31}P NMR spectrum of the reaction solution when phosphite triester **24** was treated with ~ ¼ equivalent of sulfur. The sulfurization was carried out in CD_3CN at -32 ºC for 20 h and then quenched with TBHP. In this case integration of the diastereomers of phosphite sulfide **28** could not be carried out, and so an alternative analytical method was clearly needed.

Figure 6. ^{31}P spectrum of the solution from reaction between phosphite triester **24** and ¼ equivalent of sulfur

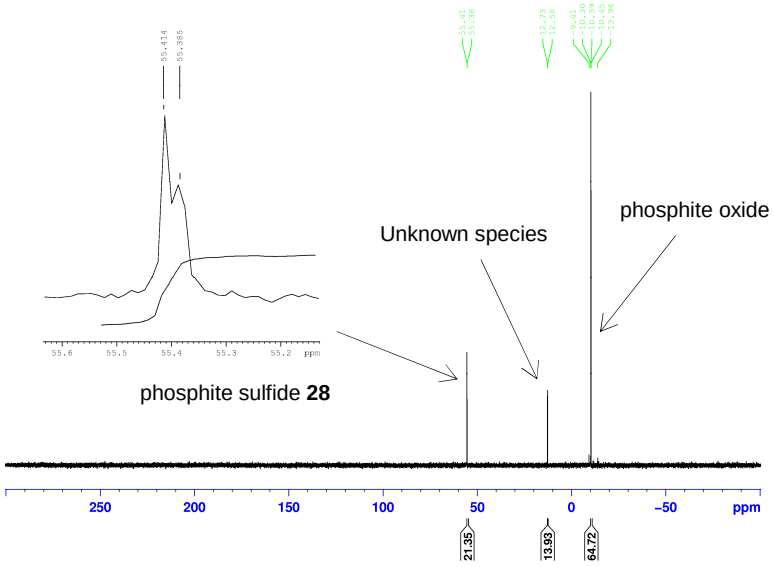

4.3.5 Determination of diastereomer ratios of the phosphite triesters and phosphite sulfides by reverse phase (RP) HPLC

Separations of diastereomeric mixtures of phosphorothioates of chain lengths 2-mer, 3-mer, 4-mer and 5-mer by using reverse phase (RP) HPLC have been reported by W. J. Stec et al. (Figure 7A).[155] The 3-mer, 4-mer, and 5-mer compounds contained one and in some cases two phosphorothioate linkages and a mix of adenosine, guanosine, cytosine, or thymidine. The phosphorothioates were removed from the solid support and all protecting groups on the nucleobases were removed prior to HPLC separation.

Generally, it was found that the 5'-*O*-(*p,p'*-dimethoxytrityl) compounds (**30**) had to be converted to the 5'-hydroxyl compounds (**31**) before any separation could be achieved on a μBondapak C_{18} column (30 cm x 7.8 mm). For instance, the diastereomers of phosphorothioate dinucleotide **32** (Figure 7B) could not be separated (t_r = 12.5 min), but those of its 5'-hydroxyl

Figure 7. Phosphorothioates separated by RP HPLC

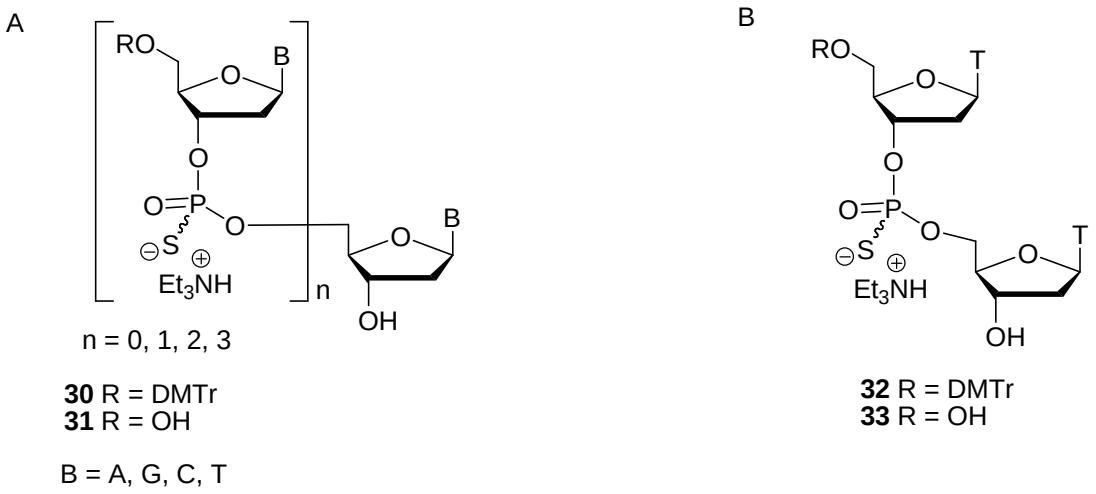

analogue (**33**) were resolved with elution times of 13.4 (assigned to R_P) and 14.2 (S_P) min respectively.[155] The separation was carried out with a linear increase of acetonitrile (1 mL/min), starting with a solvent ratio of 5:95 acetonitrile/triethylammonium acetate (TEAA) and a flow rate of 4 mL/min.

4.3.5.1 RP HPLC protocol for determining diastereomer ratios of phosphite sulfides from chiral sulfurization

The diastereomer ratios of the oxygen sensitive phosphite triesters used for our chiral sulfuriziation reactions could not be determined by HPLC analysis. However, since sulfurization with sulfur is a stereoretentive process, the phosphite triesters were first converted to their phosphite sulfides which were readily analyzed by RP HPLC.

For development of the method for HPLC analysis, samples of phosphite sulfides **26** and **27** (Scheme 11) were synthesized from their corresponding phosphite triesters by complete sulfurization with excess sulfur. Both reactions were carried out at room temperature in ~0.5 mL CD_3CN on a ~5 mg scale. To determine the R_{PS}:S_{PS} ratios of the phosphite sulfides for the

Scheme 11. Phosphite sulfides used to develop HPLC method

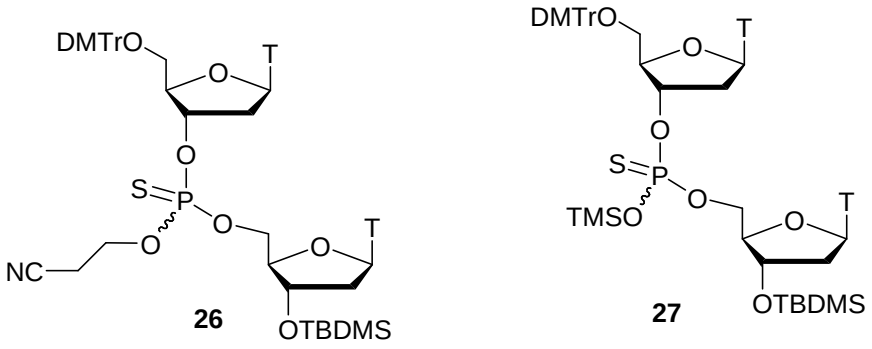

sulfurization reactions, it is necessary for us to analyze the crude reaction solutions, since isolating the phosphite sulfides by methods such as silica gel flash chromatography could alter the diastereomer ratios.

Even though an established HPLC procedure for analysis of 5'-*O*-(*p,p'*-dimethoxytrityl)- and *tert*-butyldimethylsilyl-free phosphorothioate **33** (see Figure 7B) is in the literature, we preferred not to convert phosphite sulfides **26** and **27** to phosphorothioate **33**, since removing all the protecting groups would have to be done in situ. For instance, deprotection of the β-cyanoethyl group of phosphite sulfide **26** requires NH_4OH at 55 ºC, followed by an acid treatment to remove the DMTr and TBDMS groups.

Therefore, after sulfurization the resultant crude solution of phosphite sulfide **26** was used for HPLC analysis without further treatment. However, for phosphite sulfide **27** we have found that the trimethylsilyl groups on the compound can be removed very easily with water and so the compound was treated with 10 μL of saturated triethylammonium bicarbonate (TEAB) for ~½ h to give phosphorothioate **34** (Scheme 12). The diastereomers of phosphorothioate **34** have chemical shifts of 55.27 ppm and 54.95 ppm and integrate to a ratio of 44.6:55.4, which is comparable to the 44.4:55.6 (S_P:R_P) ratio of its H-phosphonate (**3**) precursor.

Scheme 12. Conversion of phosphite triester to phosphorothioate for HPLC analysis

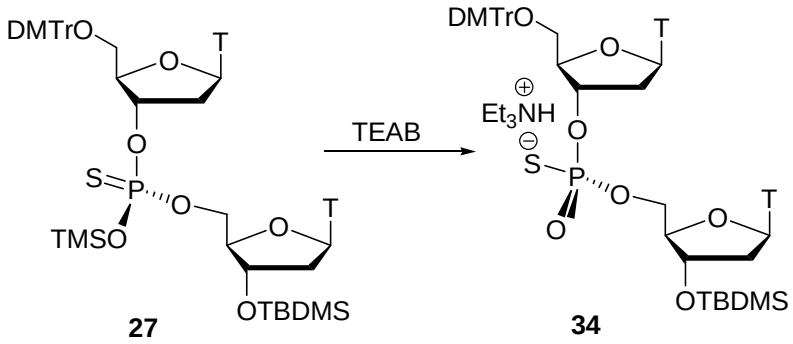

27 **34**

For HPLC analysis of a crude solution that would be typical of our chiral sulfurization, a reaction on a ~5 mg scale was carried out using ¼ equivalent of sulfur (Scheme 13). TBDMSCl/Et_3N was used as the silylating reagent. The sulfurization reaction was carried out at -32 ºC for 20 h in ~0.5 mL CD_3CN, and then quenched with 10 μL (~6 equiv) of TBHP. Saturated TEAB (10 μL) was then added to the reaction solution to convert phosphite sulfide **28** and phosphite oxide **35** to phosphorothioate **34** and phosphodiester **36**, respectively.

Using the crude reaction solutions of phosphite sulfide **26** (Scheme 11), phosphorothioate **34** (Scheme 12) and the mixture of phosphorothioate **34** and phosphodiester **36** (Scheme 13), a

Scheme 13. Sulfurization using ¼ equivalent of sulfur

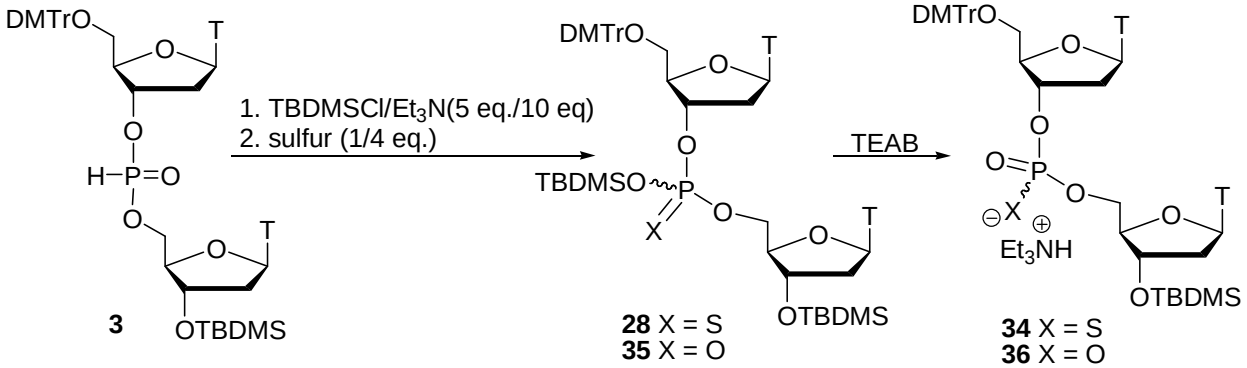

3 **28** X = S **35** X = O **34** X = S **36** X = O

RP HPLC procedure was developed for the determination of diastereomeric ratios of the compounds **26** and **34** (see Experimental Section for details of procedure).

A C_{18} column and a solvent mixture of acetonitrile/water (65/35) were used for the analysis of phosphite sulfide **26**. A C_8 column and mixtures of acetonitrile/TEAA (55/45 and 52/48) were used for analysis of phosphorothioate **34** and the mixture of phosphorothioate **34** and phosphodiester **36**. The two diastereomers of phosphite sulfide **26** eluted at 15.749 and 16.788 min in a ratio of 50.59:49.41% (Figure 8). Single diastereomers of phosphite sulfide **26**

Figure 8. Chromatogram of phosphite sulfide **26**

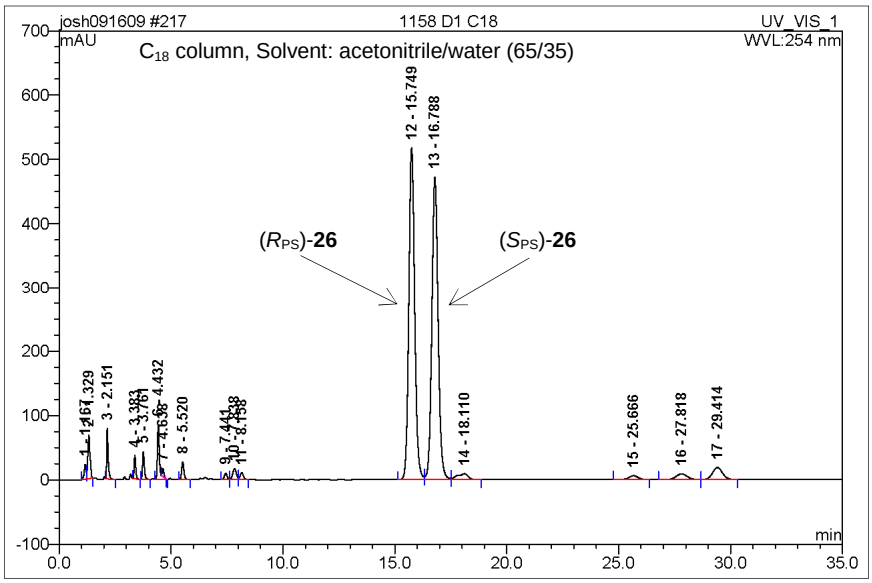

were not available for HPLC analysis, and so an accurate assignment of the configuration to the eluted diastereomers of the mixture could not be made. However, since S_P and R_P were assigned respectively to the diastereomers that gave a ratio of 50.7:49.3 by ^{31}P NMR analysis (Section 3.6), the corresponding eluted diastereomers that gave a ratio of 50.59:49.41 were assigned as (R_{PS})-**26** and (S_{PS})-**26**, respectively. When a solvent mixture of 55/45 acetonitrile/TEAA was

used, the two diastereomers of phosphorothioate **34** eluted at 16.035 and 20.158 min in a ratio of 43.44:56.56% (Figure 9), and were assigned the (R_{PS})-**34** and (S_{PS})-**34** configurations, respectively, based on the configurations assigned to the two diastereomers of the H-phosphonate precursor. Use of a solvent mixture of 52/48 acetonitrile/TEAA resulted in retention times of 23.774 and 30.778 min for (R_{PS})-**34** and (S_{PS})-**34**, respectively.

Figure 9. Chromatogram of phosphorothioate **34**

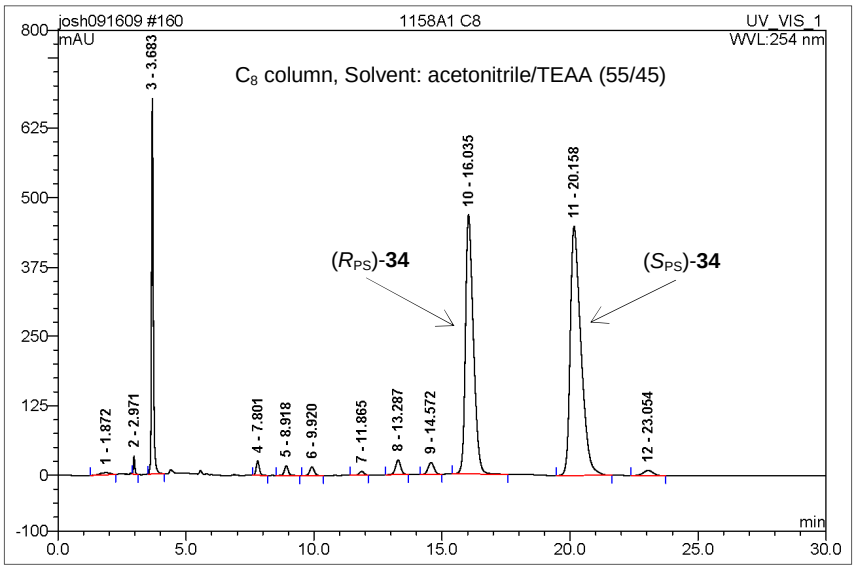

For the analyses, chromatograms were obtained at 254 nm using a diode array detector that can give complete UV spectra (190-400 nm) at any point on a selected peak, thus providing a means of determining the homogeneity of the peak. For instance, the chromatogram for phosphite sulfide **26** and the UV spectra for its two diastereomers are shown in Figure 10. The UV spectra insertions shown for each peak are an overlay of three UV spectra taken at three points on the peak. For example, the UV spectrum inserted for the S_{PS}-**26** peak was comprised of

an overlay of UV spectra taken at 16.65 min (at ½ height of the peak), 16.79 min (at the highest point of the peak), and 16.94 min (at ½ height of the peak).

Figure 10. Chromatogram of phosphite triester **26** and UV spectra of the two diastereomeric peaks

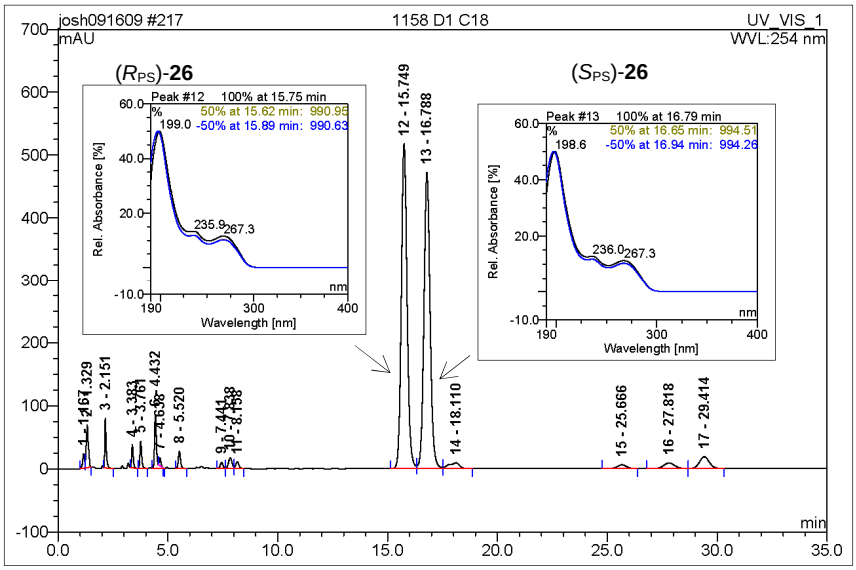

4.3.6 HPLC analysis of crude reaction solutions of all sulfurization reactions

For easy reference, a list of the phosphite triesters and chiral sulfurizing reagents that were used for the sulfurization reactions is shown in Figure 11. Concentrations of the stock solutions of phosphite triester **2**, H-phosphonate **3**, and the sulfurizing reagents that were prepared and the amounts used for each reaction are in the Experimental Section (Table 9). The chiral sulfurizing reagents are labeled as in Chapter 3, i.e. PADS analogues **2a-d** (labeled differently from phosphite triester **2**) and MEDITH analogues **6a-e**.

Figure 11. Summary of all phosphite triesters and chiral sulfurizing reagents used for screening reactions

A Phosphite triesters used for sulfurization reactions

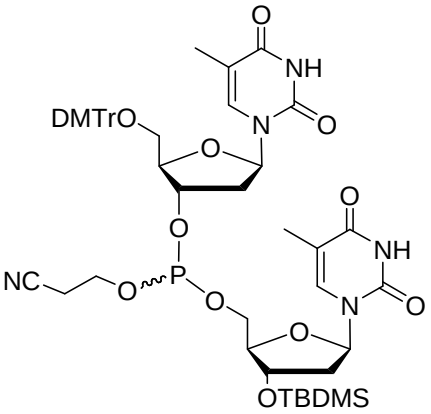

phosphite triester **2**

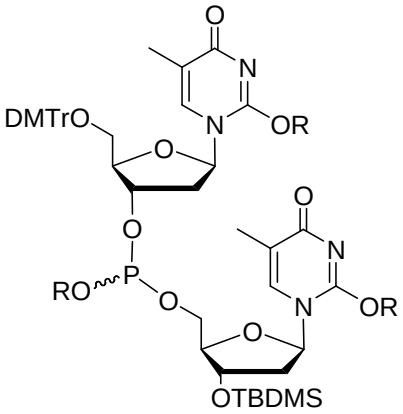

phosphite triester **23**: R = TMS

phosphite triester **24**: R = TBDMS

phosphite triester **25**: R = TPS

B Sulfurizing reagents (labeled as in Chapter 3):

chiral analogues of
Phenylacetyl disulfide (PADS)

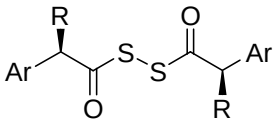

(*R*,*R*) and (*S*,*S*)-**2a**: Ar = Ph and R = Me
(*R*,*R*) and (*S*,*S*)-**2b**: Ar = Ph and R = Et
(*R*,*R*) and (*S*,*S*)-**2c**: Ar = Ph and R = *i*-Pr
(*S*,*S*)-**2d**: Ar = 6-methoxy-2-naphthyl, R = Me

chiral analogues of
5-methyl-3*H*-1,2,4-dithiozol-3-one (MEDITH)

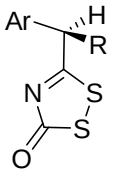

(*R*) and (*S*)-**6a**: Ar = Ph and R = Me
(*R*) and (*S*)-**6b**: Ar = Ph and R = Et
(*R*) and (*S*)-**6c**: Ar = Ph and R = *i*-Pr
(*S*)-**6d**: Ar = 6-methoxy-2-naphthyl, R = Me
(*R*) and (*S*)-**6e**: Ar = 4-*i*-butyl phenyl, R = Me

4.3.6.1 Determination of the % sulfurization of phosphite triesters 2 and 23-25

For the screening reactions, although the concentrations of the stock solutions of all the sulfurizing reagents (see Table 9 in Experimental Section for concentrations) were made up with the intention that the aliquots used (volumes ranged from 16-65 μL) would contained ~25 mol % of the sulfurizing reagents with respect to the amount of phosphite triesters used, ^{31}P NMR

spectra of many of the reaction solutions after sulfurization showed that more than 25% of the phosphite triesters had been sulfurized, thus indicating that more than 25% of the sulfurizing reagents are present in the aliquots use for the reactions. This suggests that inaccurate weights of the reagents were used to make the stock solutions. This could probably be due to the difficulty in accurately weighing the amounts of the reagents (ranging from 2-5 mg) used to prepare the stock solutions. Table 3 shows the approximate per cent of phosphite triesters **2** and **23-25** that

Table 3. Per cent sulfurization of phosphite triesters **2** and **23-25**

	sulfurizing reagents	phosphite triester **2** %	phosphite triester **23** %	phosphite triester **24** %	phosphite triester **25** %
1	sulfur(excess)	100	100	100	100
2	sulfur	16.4	15.0	25.2	29.1
3	PADS	12.9	33.2	17.3	25.1
4	MEDITH	19.0	24.7	24.5	29.8
	chiral PADS analogues				
5	(*R*,*R*)-**2a**	4.7	43.1	31.0	30.8
6	(*S*,*S*)-**2a**	6.1	47.4	31.7	31.9
7	(*R*,*R*)-**2b**	2.4	24.8	22.5	31.6
8	(*S*,*S*)-**2b**	3.1	28.2	20.7	28.0
9	(*R*,*R*)-**2c**	2.1	30.7	40.1	38.3
10	(*S*,*S*)-**2c**	1.4	43.3	39.6	34.4
11	(*S*,*S*)-**2d**	13.6	20.4	20.8	37.7
	chiral MEDITH analogues				
12	(*R*)-**6a**	24.8	43.5	26.2	29.0
13	(*S*)-**6a**	23.1	38.5	27.9	29.4
14[a]	(*R*)-**6a**	20.4	24.2	41.8	25.3
15[a]	(*S*)-**6a**	20.0	24.6	22.5	27.1
16[a]	(*S*)-**6a**	-[c]	24.9	22.5	27.2
17	(*R*)-**6b**	19.8	40.3	22.0	22.8
18	(*S*)-**6b**	25.6	47.2	29.2	28.6
19	(*R*)-**6c**	22.9	40.5	5.5	26.2
20	(*S*)-**6c**	16.1	32.1	2.4	15.1
21[b]	(*R*)-**6c**	23.9	37.2	23.8	31.3
22[b]	(*S*)-**6c**	18.9	37.5	21.2	28.2
23[b]	(*S*)-**6c**	-[c]	-[c]	22.5	-[c]
24	(*S*)-**6d**	26.8	40.0	27.5	28.6
25	(*R*)-**6e**	17.1	29.6	20.4	20.7
26	(*S*)-**6e**	13.8	29.9	13.7	16.1

[a,b] reactions repeated with reagents **6a** and **6c** respectively; [c] no duplicate reaction carried out.

were sulfurized for the reactions carried out. Row 1 shows the % sulfurization of the phosphite triesters that were treated with excess sulfur, in order to determine the diastereomer ratios of the starting phosphite triesters, and rows 2-26 show the %sulfurization for the reactions carried out with the stock solutions of the sulfurizing reagents intended for ~25% sulfurization.

A plot of the % sulfurization versus the sulfurizing reagents shows that the extent of sulfurization of most of the reactions varied between 20-40% (Chart 1). It can also be seen from the chart that phosphite triester **2** is less reactive towards PADS, especially its chiral analogues, and phosphite triester **23** is generally more reactive to many sulfurizing reagents compared to phosphite triesters **24** and **25**.

Chart 1. Per cent sulfurization of phosphite triesters **2** and **23-24**

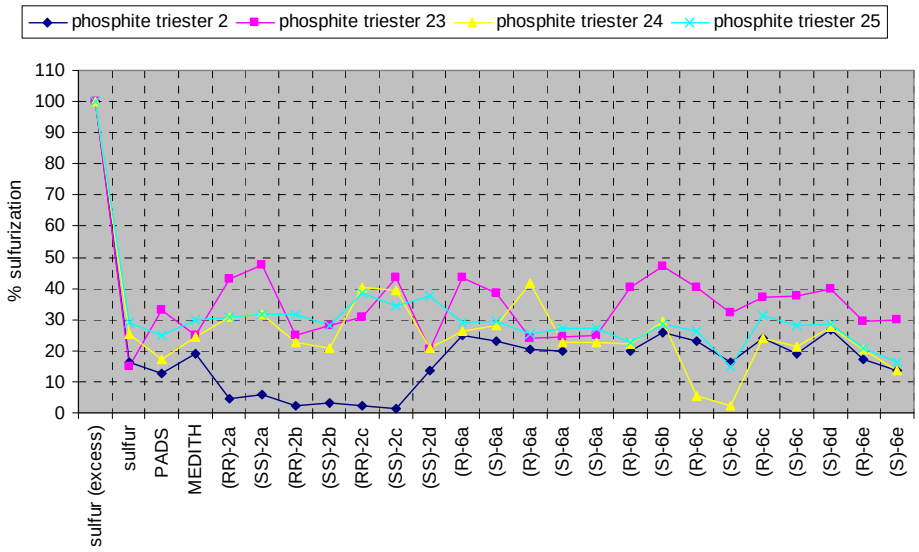

4.3.6.2 R_{PS}:S_{PS} diastereomeric ratios from RP HPLC analysis of crude solutions

The R_{PS}:S_{PS} diastereomer ratios determined by HPLC analysis of the phosphite sulfides **26** and phosphorothioates **34**, which were derived from phosphite triester **2** and phosphite triesters **23-24**, respectively, are shown in Table 4. The reactions were carried out over a period

Table 4. R_{PS}:S_{PS} diastereomeric ratios of all sulfurization reactions

	1	2		3		4		5	
	sulfurizing reagents	Phosphite sulfides from phosphite triester **2**		Phosphorothioate from phosphite triester **23**		Phosphorothioate from phosphite triester **24**		Phosphorothioate from phosphite triester **25**	
		(R_{PS})-**26**	(S_{PS})-**26**	(R_{PS})-**34**	(S_{PS})-**34**	(R_{PS})-**34**	(S_{PS})-**34**	(R_{PS})-**34**	(S_{PS})-**34**
1	Sulfur (excess)	50.59	49.41	43.44	56.56	43.38	56.62	43.36	56.64
2	sulfur	52.12	47.88	43.52	56.48	43.41	56.59	45.63	54.37
3	PADS	52.08	47.92	44.87	55.13	44.2	55.8	45.96	54.04
4	MEDITH	49.09	50.91	44.19	55.81	42.87	57.13	44.96	55.04
	chiral PADS analogues								
5	(*R*,*R*)-**2a**	49.89	50.11	42.72	57.28	40.86	59.14	45.42	54.58
6	(*S*,*S*)-**2a**	51.99	48.01	43.49	56.51	43.07	56.93	43.81	56.19
7	(*R*,*R*)-**2b**	46.85	53.15	42.32	57.68	40.46	59.54	46.42	53.58
8	(*S*,*S*)-**2b**	50.49	49.51	41.87	58.13	43.44	56.56	44.53	55.47
9	(*R*,*R*)-**2c**	49.57	50.53	48.96	51.04	46.37	53.63	43.57	56.43
10	(*S*,*S*)-**2c**	52.81	47.19	45.44	54.56	43.33	56.67	47.27	52.73
11	(*S*,*S*)-**2d**	51.35	48.65	44.01	55.99	41.62	58.38	40.24	59.76
	chiral MEDITH analogues								
12	(*R*)-**6a**	51.13	48.87	42.56	57.44	45.47	54.53	48.8	51.2
13	(*S*)-**6a**	51.14	48.86	42.87	57.13	48.28	51.72	48.62	51.38
14[a]	(*R*)-**6a**	nd[c]	nd[c]	43.68	56.32	46.44	53.56	47.85	52.15
15[a]	(*S*)-**6a**	-[d]	-[d]	43.7	56.3	45.21	54.47	47.53	52.47
16[a]	(*S*)-**6a**	-[d]	-[d]	42.90	57.10	45.36	54.64	48.80	51.20
17	(*R*)-**6b**	51.2	48.8	41.85	58.15	43.51	56.48	47.79	52.21
18	(*S*)-**6b**	51.24	48.76	43.73	56.27	45.82	54.18	49.03	50.97
19	(*R*)-**6c**	50.36	49.64	41.12	58.88	44.08	55.92	45.87	54.13
20	(*S*)-**6c**	50.28	49.72	39.87	60.13	62.30	37.7	45.23	54.77
21[b]	(*R*)-**6c**	49.85	50.15	40.24	59.76	45.05	54.95	45.22	54.78
22[b]	(*S*)-**6c**	49.36	50.64	39.28	60.72	46.17	53.83	45.28	54.72
23[b]	(*S*)-**6c**	-[d]	-[d]	-[d]	-[d]	45.53	54.47	-[d]	-[d]
24	(*S*)-**6d**	50.92	49.08	50.81	49.19	47.81	52.19	49.63	50.37
25	(*R*)-**6e**	50.91	49.09	42.05	57.95	44.94	55.06	45.36	54.64
26	(*S*)-**6e**	50.73	49.27	49.66	50.34	41.92	58.08	44.72	55.28

[a,b] The reactions were repeated with reagents **6a** and **6c** respectively; [c] nd = not determined due to decomposition of the phosphite sulfide; [d] no duplicate reaction carried out.

of ~3-4 months, and when the HPLC instrument was not available the solutions were stored in a freezer at -18 ºC. Most of the solutions were analyzed within one week after the reactions were carried out. Row 1 shows the R_{PS}:S_{PS} diastereomer ratios of the phosphite sulfide and

phosphorothioates after complete sulfurization of phosphite triester **2** and **23**-**25**, respectively, with excess sulfur. Rows 2-26 show the diastereomer ratios of the phosphite sulfide and phosphorothioates after partial sulfurization with the corresponding reagents shown in column 1.

A test of the reproducibility of the chiral sulfurization reactions was carried out by repeating the reactions using the two enantiomers of sulfurizing reagents **6a** and **6c**. The HPLC data for the repeated reactions are shown in rows 14-16 and 21-23, respectively. With the exception of the first reaction with (*S*)-**6c** and phosphite triester **24** (column 4, row 20), an average standard deviation of ±0.46% was calculated for the reactions repeated.

The ^{31}P NMR spectrum of the solution from the first reaction with reagent (*S*)-**6c** and phosphite triester **24** (column 4, row 20) did not show any peaks in the phosphorothioate region. However, from the chromatogram (Figure 12), 2.4% sulfurization of phosphite triester **24** was

Figure 12. Chromatogram from reaction using (*S*)-**6c** and phosphite triester **24**[a]

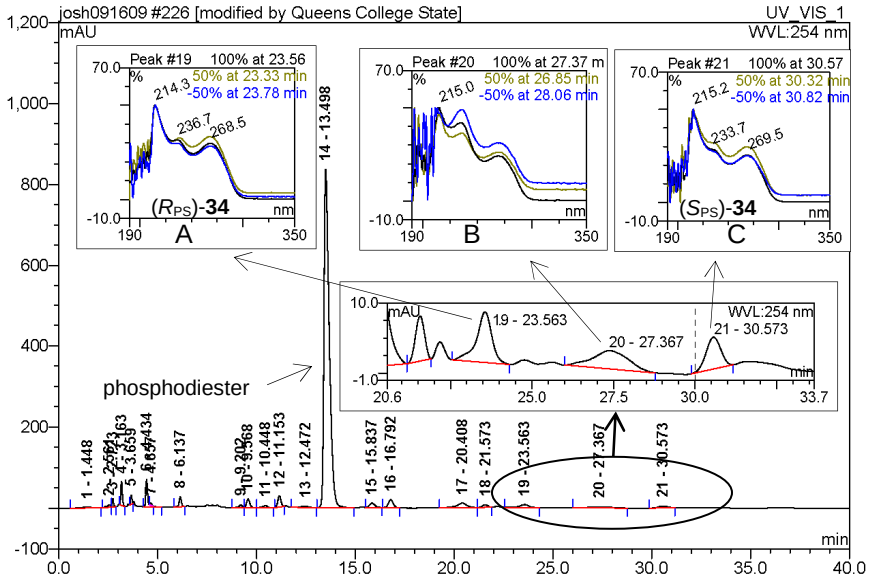

[a] The chromatogram was recorded at 254 nm with 52/48 acetonitrile/TEAA solvent mixture.

observed, on the basis of the ratio of the phosphodiester and phosphorothioate. A diastereomeric ratio of 63.30 (R_{PS})-**34**:37.70 (S_{PS})-**34** was observed for the two diastereomers of the phosphorothioate and this was the reason the reactions with reagents (*R*)-**6c** and (*S*)-**6c** were repeated. Although the base line of the chromatogram (Figure 12) is not uniform and the peaks of the phosphorothioates are very small, the UV spectra of the peaks are similar (see insets A and C in Figure 12) to the UV spectra from the chromatogram of a solution obtained from a reaction between MEDITH (~1/4 equiv) and phosphite triester **24** (Figure 13). The peak at 27.367 min of the chromatogram in Figure 12 is an unknown compound that shows a different UV spectrum. However, since the two repeated reactions (column 4, rows 22 and 23) with (*S*)-**6c** gave (R_{PS})-**34**:(S_{PS})-**34** diastereomeric ratios that are more similar as well as normal yields, the 63.30:37.70 ratio from the first reaction (column 4, row 20) was not considered further.

Figure 13. Chromatogram from reaction using MEDITH (~1/4 equiv) and phosphite triester **24**[a]

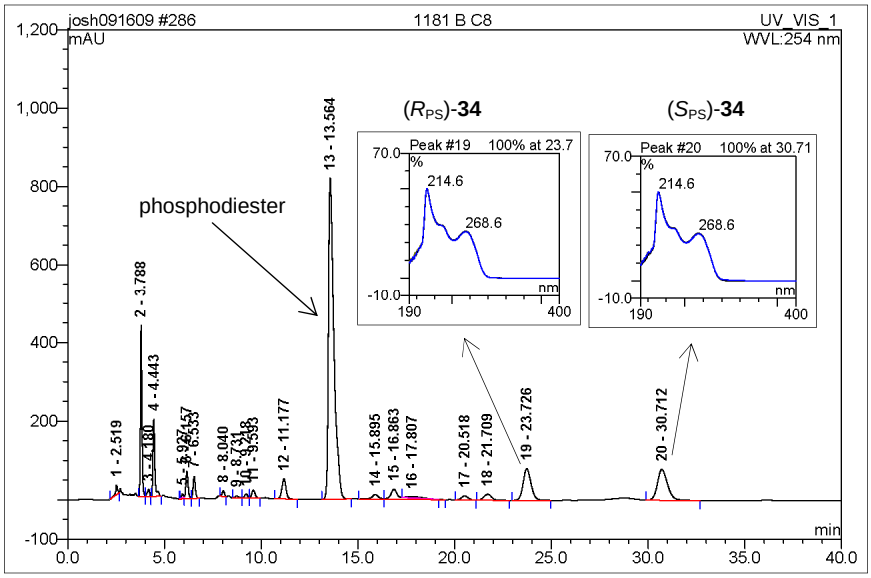

[a] The chromatogram was recorded at 254 nm with 52/48 acetonitrile/TEAA solvent mixture.

It was found that when phosphite triester **2** was treated with any of the MEDITH compounds and the reaction solution was left for more than 1 day, the resultant phosphite sulfide gradually decomposed to an unknown species that did not appear to elute on the HPLC column; no integral in the HPLC corresponded to the ^{31}P NMR integral of the unknown compound which showed a chemical shift ~5 ppm upfield from the phosphite sulfide peaks. Therefore, the HPLC data in Table 4 from the reactions carried out with phosphite triester **2** and the chiral analogues of MEDITH, which exhibited very little selectivity in any case, were considered to be less precise, because the extent of decomposition could not be accurately determined.

4.3.6.3 R_{PS}:S_{PS} diasteromeric ratio predicted if optical purities of sulfurizing reagents (*R*) and (*S*)-6e are 100%

The data in Table 4 might in principle be corrected by taking into account the fact that the sulfurizing reagents are not 100% enantiomerically pure. Inspection of the data led to one set of results as the best test case to determine if the selectivities might change significantly, namely, the sulfurization of triester **23** with (*R*) and (*S*)-**6e**. Each of these sulfurizing reagents is just over 96% enantiomerically pure, but they give relatively different selectivity, 42.05% for (R_{PS})-**34** from S_P-**23** and (*R*)-**6e**, and 49.66% for (R_{PS})-**34** from S_P-**23** and (*S*)-**6e**. An iterative procedure was used to estimate the corrected selectivities according to the following:

%(R_{PS})-**34** from (*R*)-**6e** = actual %(R_{PS})-**34** from (*R*)-**6e** x 98.15% + actual %(R_{PS})-**34** from (*S*)-**6e** x 1.85%

%(R_{PS})-**34** from (*S*)-**6e** = actual %(R_{PS})-**34** from (*R*)-**6e** x 1.75% + actual %(R_{PS})-**34** from (*S*)-**6e** x 98.25%

where the corrected actual %(R_{PS})-**34** values from (*R*)-**6e** and (*S*)-**6e** were changed in order to minimize the differences between the observed and calculated %(R_{PS})-**34** values from (*R*)-**6e** and

(*S*)-**6e**; the calculations were carried out using the Excel Solver routine. The corrected and observed selectivities for (*R*)-**6e** and (*S*)-**6e** are as follows:

corrected %(R_{PS})-**34** from (*R*)-**6e** = 41.90%; observed = 42.05%

corrected %(R_{PS})-**34** from (*S*)-**6e** = 49.80%; observed = 49.66%

As can be seen, if the optical purity of the (*R*)-**6e** and (*S*)-**6e** could be improved to 100%, the diasteremeric ratio only changes by ~0.15%, a change which is well within the uncertainty in the HPLC measurement. We conclude that no significant changes in the selectivities will arise by correcting for the actual enantiomeric purities of the sulfurizing reagents.

4.3.7 Calculated % diastereoselectivity (%$ds_{R(PS)}$:%$ds_{S(PS)}$) ratios for all reactions

Using the %R_{PS}:S_{PS} diastereomeric ratios in Table 4, the % diastereoselectivity ratios (%$ds_{R(PS)}$:%$ds_{S(PS)}$) of the reactions were calculated by the numerical method described in Section 4.3.2.1; i.e. using equations, %$ds_{R(PS)}$ = (R_{PS} x R_P /[(S_P x S_{PS}) + (R_{PS} x R_P)]) x 100 and %$ds_{S(PS)}$ = (1–$ds_{R(PS)}$) x 100 (see results in Table 5). The diastereomeric excesses (de's), which were used to compare the results, are shown in Table 6. The %$ds_{R(PS)}$:%$ds_{S(PS)}$ ratios shown in Table 5 were calculated using the S_P:R_P ratio of each of the starting phosphite triesters (derived from the %R_{PS}:%S_{PS} ratios, respectively, in row 1 of Table 4), as the reference point for zero selectivity; thus showing a 50:50% in row 1 of Table 5 indicating zero selectivity. The % diasteroselectivity (%ds) ratios, achieved from partial sulfurization of phosphite triesters **2** and **23**-**25**, are shown in rows 2-20 of Table 5; the %ds ratio corresponding to reagents **6a** and **6c** is the average from the reactions repeated. The % diastereoselectivity (%ds) ratios were not corrected for enantiomeric purity of the sulfurizing reagents and also for the different per cent sulfurization observed for each reaction (see Table 3 in Section 4.3.6.1).

Table 5. % Diastereoselectivity ratios ($\%ds_{R(PS)}$:$\%ds_{S(PS)}$) for the sulfurization reactions

	sulfurizing reagents	%ds from phosphite triester **2**		%ds from phosphite triester **23**		%ds from phosphite triester **24**		%ds from phosphite triester **25**	
		$\%ds_{R(PS)}$	$\%ds_{S(PS)}$	$\%ds_{R(PS)}$	$\%ds_{S(PS)}$	$\%ds_{R(PS)}$	$\%ds_{S(PS)}$	$\%ds_{R(PS)}$	$\%ds_{S(PS)}$
1	sulfur(excess)	50.00	50.00	50.00	50.00	50.00	50.00	50.00	50.00
2	sulfur	51.53	48.47	50.08	49.92	50.03	49.97	52.30	47.70
3	PADS	51.49	48.51	51.45	48.55	50.83	49.17	52.63	47.37
4	MEDITH	48.50	51.50	50.76	49.24	49.48	50.52	51.62	48.38
	chiral PADS analogues								
5	(*R*,*R*)-**2a**	49.30	50.70	49.27	50.73	47.42	52.58	52.09	47.91
6	(*S*,*S*)-**2a**	51.40	48.60	50.05	49.95	49.68	50.32	50.46	49.54
7	(*R*,*R*)-**2b**	46.26	53.74	48.86	51.14	47.00	53.00	53.09	46.91
8	(*S*,*S*)-**2b**	49.90	50.10	48.40	51.60	50.06	49.94	51.19	48.81
9	(*R*,*R*)-**2c**	48.93	51.07	55.54	44.46	53.02	46.98	50.21	49.79
10	(*S*,*S*)-**2c**	52.22	47.78	52.02	47.98	49.95	50.05	53.94	46.06
11	(*S*,*S*)-**2d**	50.76	49.24	50.58	49.42	48.20	51.80	46.80	53.20
	chiral MEDITH analogues								
12	(*R*)-**6a**[a]	50.54	49.46	49.67	50.33	52.60	47.40	54.99	45.01
13	(*S*)-**6a**[a]	50.55	49.45	49.71	50.29	53.03	46.97	54.98	45.02
14	(*R*)-**6b**	50.61	49.39	48.38	51.62	50.14	49.86	54.46	45.54
15	(*S*)-**6b**	50.65	49.35	50.29	49.71	52.47	47.53	55.68	44.32
16	(*R*)-**6c**[a]	49.52	50.48	47.17	52.83	51.20	48.80	52.21	47.79
17	(*S*)-**6c**[a]	49.23	50.77	46.03	53.97	52.50	47.50	51.92	48.08
18	(*S*)-**6d**	50.33	49.67	57.35	42.65	54.46	45.54	56.28	43.72
19	(*R*)-**6e**	50.32	49.68	48.58	51.42	51.58	48.42	52.02	47.98
20	(*S*)-**6e**	50.14	49.86	56.23	43.77	48.51	51.49	51.38	48.62

[a] The % diastereoselectivity ratio corresponding to the reagent is the average from the reactions repeated.

Table 6. Diastereoselectivity excess (de) for the sulfurization reactions

	sulfurizing reagents	de from phosphite triester **2**	de from phosphite triester **23**	de from phosphite triester **24**	de from phosphite triester **25**
1	sulfur(excess)	0.0	0.0	0.0	0.0
2	sulfur	3.1	0.2	0.1	4.6
3	PADS	3.0	2.9	1.7	5.3
4	MEDITH	-3.0	1.5	-1.0	3.2
	chiral PADS analogues				
5	(*R*,*R*)-**2a**	-1.4	-1.5	-5.2	4.2
6	(*S*,*S*)-**2a**	2.8	0.1	-0.6	0.9
7	(*R*,*R*)-**2b**	-7.5	-2.3	-6.0	6.2
8	(*S*,*S*)-**2b**	-0.2	-3.2	0.1	2.4
9	(*R*,*R*)-**2c**	-2.1	11.1	6.0	0.4
10	(*S*,*S*)-**2c**	4.4	4.0	-0.1	7.9
11	(*S*,*S*)-**2d**	1.5	1.2	-3.6	-6.4
	chiral MEDITH analogues				
12	(*R*)-**6a**[a]	1.1	-0.7 ± 1.1	5.2 ± 1.0	10.0 ± 1.0
13	(*S*)-**6a**[a]	1.1	-0.6 ± 1.1	6.0 ± 2.6	10.0 ± 1.0
14	(*R*)-**6b**	1.2	-3.2	0.3	8.9
15	(*S*)-**6b**	1.3	0.6	4.9	11.4
16	(*R*)-**6c**[a]	-1.0 ± 0.5	-5.7 ± 0.9	2.4 ± 1.0	4.4 ± 0.7
17	(*S*)-**6c**[a]	-1.5 ± 0.9	-7.9 ± 0.3	5.0 ± 0.6	3.8 ± 0.1
18	(*S*)-**6d**	0.7	14.7	8.9	12.6
19	(*R*)-**6e**	0.6	-2.8	3.2	4.0
20	(*S*)-**6e**	0.3	12.5	-3.0	2.8

[a] The average standard deviations are included in the table for the reactions that were repeated

4.3.8 Selectivity through a "match" and "mismatch" between phosphite triesters and sulfurizing reagents

4.3.8.1 Selectivities achieved with achiral reagents: sulfur, PADS and MEDITH

Since phosphite triesters **2** and **23**-**25** each consist of a mixture of diastereomers and a chiral sulfurizing reagent in principle is not needed for selective sulfurization, a comparison was first made between the selectivities achieved by partial sulfuriziation with the achiral reagents: sulfur, PADS, and MEDITH. Chart 2 shows a plot of the diastereomeric excess (de = $\%ds_{R(PS)} - \%ds_{S(PS)}$) achieved with these reagents. A positive de (i.e. greater $\%ds_{R(PS)}$ fractions) suggests that there is a match between the sulfurizing reagent and the S_P diastereomer of the phosphite

triester, and a negative de (i.e. greater %ds$_{S(PS)}$ fraction) suggests a match between the sulfurizing reagent and the R_P diastereomer of the phosphite triester. From Chart 2 it can be seen that sulfur

Chart 2. Selectivity (de) achieved with sulfur, PADS, and MEDITH

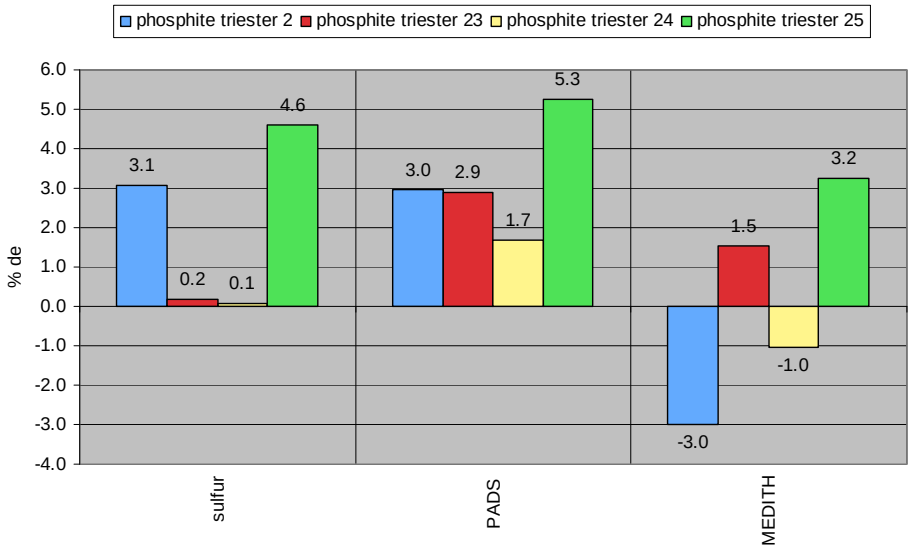

gave de's greater than 1% when reacted with phosphite triesters **2** and **25**; specifically through a match with the S_P diastereomer of the two phosphite triesters. The highest de of 4.6% was achieved from the reaction with phosphite triester **25**. For the reactions with PADS, de's ranging from 1.7-5.3% were achieved through a match with the reagent and the S_P diastereomer of the phosphite triesters; the highest de of 5.3% was achieved from the reaction with phosphite triester **25**. The highest de achieved with MEDITH is 3.2% through a match with the S_P diastereomer of phosphite triester **25**, followed by -3.0% through a match with the R_P diastereomer of phosphite triester **2**. Of the four phosphite triesters used, the compound with the Ph_3Si group (**25**) around the phosphorus gave the highest selectivity through a match with its S_P diastereomer and PADS. On the other hand phosphite triester **2** with the least steric hindrance around the phosphorus atom

(β-cyanoethyl group) gave the highest selectivity through a match with its R_P diastereomer and MEDITH.

4.3.8.2 Comparison of selectivities achieved with achiral and chiral disulfides using diastereomer ratios of starting phosphite triesters as reference point for zero selectivity

To compare the differences in the selectivities achieved with the chiral sulfurizing reagents using the ratio of each of the starting phosphite triesters as the reference point for zero selectivity, the de achieved with achiral PADS and MEDITH were plotted alongside their respective chiral analogues for analysis (Charts 3 and 4, respectively). Chart 3 shows that

Chart 3. Comparison of the selectivities (de) achieved with PADS and its chiral analogues

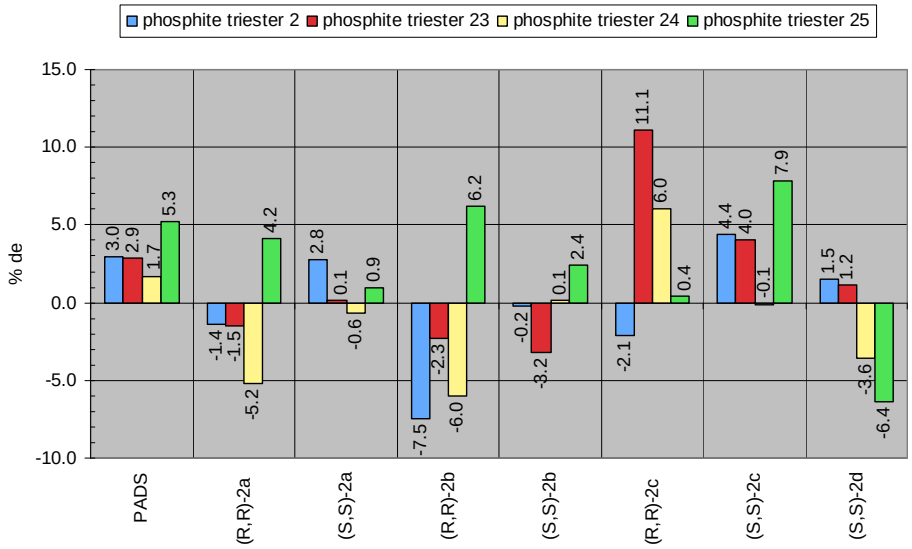

through a match with the S_P diastereomer of phosphite triesters **23-25** a de greater than the 5.3% achieved with PADS was achieved with reagents (*R*,*R*)-**2b**, (*R*,*R*)-**2c**, and (*S*,*S*)-**2c**. The highest de of 11.1% was achieved from the reaction with reagent (*R*,*R*)-**2c** and phosphite triester **23**. This was followed by lower de's of 7.9 and 6.2% from reaction of reagents (*S*,*S*)-**2c** and (*R*,*R*)-**2b**

with phosphite triester **25**, and 6.0% with reagent (*R*,*R*)-**2c** and phosphite triester **24**. PADS did not exhibit selectivity through a match with the R_P diastereomer of any of the phosphite triesters, but chiral reagent (*R*,*R*)-**2b** gave the highest de of -7.5%, through a match with the R_P diastereomer of phosphite triester **2**. This was followed by lower de's of -6.4 and -6.0% from the reactions with reagents (*S*,*S*)-**2d** and (*R*,*R*)-**2b**, and phosphite triesters **25** and **24**, respectively.

Chart 4. Comparison of the selectivities (de) achieved with MEDITH and its chiral analogues[a]

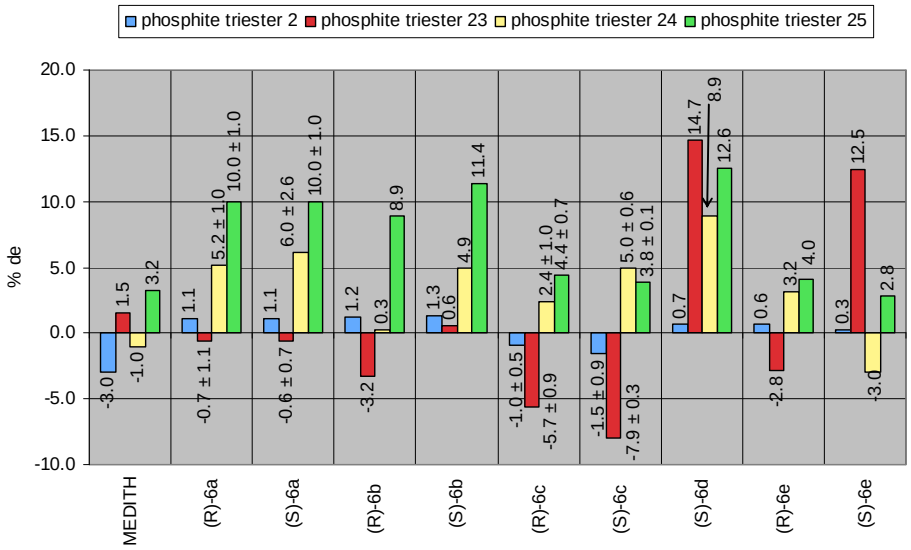

[a] the average standard deviations for the reactions repeated are included in the chart.

A comparison of the selectivities achieved with MEDITH and its chiral anlogues (Chart 4) shows that, through a match with the S_P diastereomer of phosphite triester **23**-**25**, a de significantly greater than the 3.2% achieved with MEDITH was achieved with reagents (*R*)-**6a**, (*S*)-**6a**, (*R*)-**6b**, (*S*)-**6b**, (*S*)-**6d** and (*S*)-**6e**. The highest de of 14.7% was achieved from the reaction with reagent (*S*)-**6d** and phosphite triester **23**. This was followed by a de of ~12.5% from two reactions, namely between reagent (*S*)-**6d** and phosphite triester **25**, and reagent (*S*)-**6e** and phosphite triester **23**. Lower de's ranging from 8.9-11.4% were achieved from the reactions

with reagents (*R*)-**6a**, (*S*)-**6a**, (*R*)-**6b** and (*S*)-**6b**, and phosphite triester **25**; and a de of 8.9% was achieved from a reaction with reagent (*S*)-**6d** and phosphite triester **24**. No significant selectivity was achieved from any of the reactions with phosphite triester **2**. However, a de greater than the -3.0%, which was achieved through a match with the R_P diastereomer of phosphite triester **2** and achiral MEDITH, was achieved with reagent (*R*)-**6b**, (*R*)-**6c** and (*S*)-**6c** through a match with the R_P diastereomer of phosphite triester **23**; de's ranges from -3.2 to -7.9%.

A comparison of selectivities achieved with chiral analogues of PADS (Chart 3) and chiral analogues of MEDITH (Chart 4) shows that the latter reagents generally gave greater selectivities. For instance, reagent (*S*)-**6d** gave the highest selectivity (14.7% de) through a match with the S_P diastereomer of phosphite triester **23** and through a match with the R_P diastereomer of the same phosphite triester, reagent (*S*)-**6c** gave selectivity of -7.9% de. It can also be seen from the two charts that, with the exception of the reaction with (*S,S*)-**2d** (last entry in Chart 3), the other achiral and chiral disulfides matched best with the S_P diastereomer of phosphite triester **25** (with the Ph_3Si group), with five chiral analogues of MEDITH (i.e., (*R*)-**6a**, (*S*)-**6a**, (*R*)-**6b**, (*S*)-**6b**, and (*S*)-**6d**) giving de's ranging from 8.9-12.6%, as opposed to the highest de (7.9%) achieved with the PADS chiral analogue (*S,S*)-**2c**.

4.3.8.3 Comparison of selectivities achieved with chiral disulfides using selectivities of achiral disulfides as reference point for zero selectivity

In order to easily visualize the differences in selectivities achieved with the chiral analogues of PADS and MEDITH from their achiral analogues, the selectivities achieved with the achiral disulfides on each phosphite triester were used as the reference point for zero selectivity (see results in Table 7). The % diastereoselectivity ratios ($\%ds_{R(PS)}$:$\%ds_{S(PS)}$) of the reactions were calculated using the equations in Section 4.3.7 (i.e., $\%ds_{R(PS)} = (R_{PS} \times R_P / [(S_P \times$

S_{PS}) + (R_{PS} x R_P)]) x 100 and $\%ds_{S(PS)} = (1–ds_{R(PS)}) \times 100$); however, the R_P and S_P fractions in the equation were substituted with the selectivities achieved with the achiral disulfides (i.e., S_{PS} and R_{PS} fractions, respectively). The diastereomeric excesses (de's) of the reactions are shown in Table 8. A plot of the de's achieved with the chiral analogues of PADS is shown in Chart 5,

Table 7. % Diastereoselectivity ratios ($\%ds_{R(PS)}$:$\%ds_{S(PS)}$) using selectivities achieved with achiral disulfides as point of reference

	sulfurizing reagents	%ds from phosphite triester **2**		%ds from phosphite triester **23**		%ds from phosphite triester **24**		%ds from phosphite triester **25**	
		$\%ds_{R(PS)}$	$\%ds_{S(PS)}$	$\%ds_{R(PS)}$	$\%ds_{S(PS)}$	$\%ds_{R(PS)}$	$\%ds_{S(PS)}$	$\%ds_{R(PS)}$	$\%ds_{S(PS)}$
1	PADS	50.00	50.00	50.00	50.00	50.00	50.00	50.00	50.00
2	(*R*,*R*)-**2a**	47.81	52.19	47.82	52.18	46.59	53.41	49.46	50.54
3	(*S*,*S*)-**2a**	49.91	50.09	48.60	51.40	48.85	51.15	47.83	52.17
4	(*R*,*R*)-**2b**	44.78	55.22	47.41	52.59	46.18	53.82	50.46	49.54
5	(*S*,*S*)-**2b**	48.41	51.59	46.95	53.05	49.23	50.77	48.56	51.44
6	(*R*,*R*)-**2c**	47.44	52.56	54.10	45.90	52.19	47.81	47.58	52.42
7	(*S*,*S*)-**2c**	50.73	49.27	50.58	49.42	49.12	50.88	51.32	48.68
8	(*S*,*S*)-**2d**	49.27	50.73	49.13	50.87	47.37	52.63	44.19	55.81
9	MEDITH	50.00	50.00	50.00	50.00	50.00	50.00	50.00	50.00
10	(*R*)-**6a**[a]	52.04	47.96	48.91	51.09	53.12	46.88	53.38	46.62
11	(*S*)-**6a**[a]	52.05	47.95	48.95	51.05	53.55	46.45	53.37	46.63
12	(*R*)-**6b**	52.11	47.89	47.61	52.39	50.66	49.34	52.84	47.16
13	(*S*)-**6b**	52.15	47.85	49.53	50.47	52.99	47.01	54.08	45.92
14	(*R*)-**6c**[a]	51.01	48.99	46.41	53.59	51.72	48.28	50.59	49.41
15	(*S*)-**6c**[a]	50.73	49.27	45.27	54.73	53.02	46.98	50.30	49.70
16	(*S*)-**6d**	51.83	48.17	56.61	43.39	54.97	45.03	54.67	45.33
17	(*R*)-**6e**	51.82	48.18	47.82	52.18	52.10	47.90	50.40	49.60
18	(*S*)-**6e**	51.64	48.36	55.47	44.53	49.03	50.97	49.76	50.24

[a] The % diastereoselective ratio corresponding to the reagent is the average of the reactions repeated

Table 8. Diastereoselectivity excess (de) using selectivities achieved with achiral disulfides as point of reference

	sulfurizing reagents	de from phosphite triester **2**	de from phosphite triester **23**	de from phosphite triester **24**	de from phosphite triester **25**
1	PADS	0.0	0.0	0.0	0.0
2	(*R*,*R*)-**2a**	-4.4	-4.4	-6.8	-1.1
3	(*S*,*S*)-**2a**	-0.2	-2.8	-2.3	-4.3
4	(*R*,*R*)-**2b**	-10.4	-5.2	-7.6	0.9
5	(*S*,*S*)-**2b**	-3.2	-6.1	-1.5	-2.9
6	(*R*,*R*)-**2c**	-5.1	8.2	4.4	-4.8
7	(*S*,*S*)-**2c**	1.5	1.2	-1.8	2.6
8	(*S*,*S*)-**2d**	-1.5	-1.7	-5.3	-11.6
9	MEDITH	0.0	0.0	0.0	0.0
10	(*R*)-**6a**[a]	4.1	-2.2 ± 1.1	6.2 ± 1.0	6.8 ± 1.0
11	(*S*)-**6a**[a]	4.1	-2.1 ± 0.7	7.0 ± 2.6	6.7 ± 1.0
12	(*R*)-**6b**	4.2	-4.8	1.3	5.7
13	(*S*)-**6b**	4.3	-0.9	6.0	8.2
14	(*R*)-**6c**[a]	2.0 ± 0.5	-7.2 ± 0.9	3.4 ± 1.0	1.2 ± 0.7
15	(*S*)-**6c**[a]	1.5 ± 0.9	-9.5 ± 0.3	6.0 ± 0.6	0.6 ± 0.1
16	(*S*)-**6d**	3.7	13.2	9.9	9.3
17	(*R*)-**6e**	3.6	-4.4	4.2	0.8
18	(*S*)-**6e**	3.3	10.9	-1.9	-0.5

[a] The average standard deviation are included in the table for the reactions that were repeated

and the plot of the de's achieved with the chiral analogues of MEDITH is shown in Chart 6. The % de was calculated in the same way as in Charts 3 and 4, i.e. % de = $\%ds_{R(PS)}$–$\%ds_{S(PS)}$. Compared with the R_{PS}:S_{PS} ratio achieved with the achiral reagent, a positive value achieved from a chiral analogue in the charts indicates that there in an increase in selectivity through a match with the S_P diastereomer of the phosphite triester, and a negative value indicates that there is a switch in the selectivity through a match with the R_P diastereomer of the phosphite triester. From Chart 5 it can be seen that many of the chiral reagents generally resulted in a switch of selectivity through a match with the R_P diastereomer of the phosphite triesters. Through a match with the S_P diasteromer of the phosphite triester **23**, reagent (*R*,*R*)-**2c** gave the highest increase of 8.2%. This was followed by lower increases of 4.4 and 2.6% de, achieved from the reactions

Chart 5. Differences in de achieved with chiral analogues of PADS from de achieved with PADS

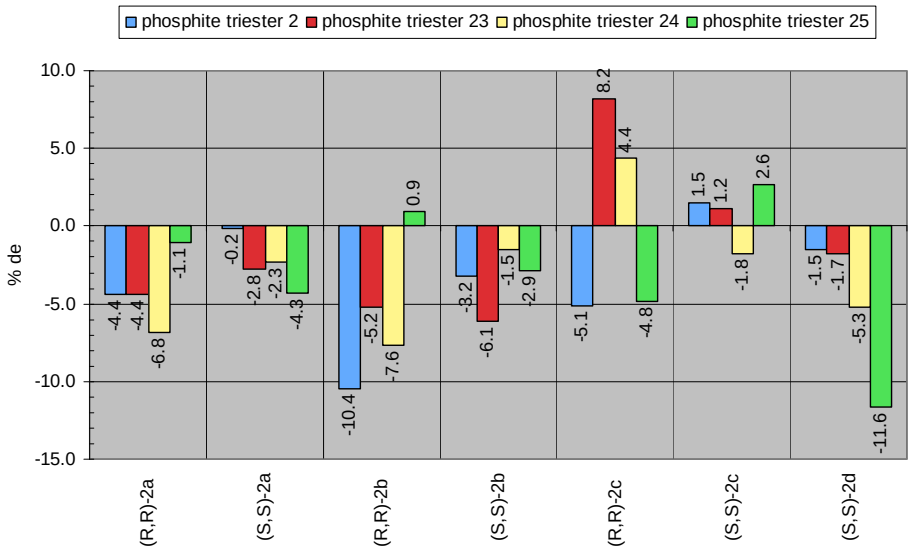

between reagents (*R*,*R*)-**2c** and (*S*,*S*)-**2c**, and phosphite triesters **24** and **25**, respectively. Through a match with the R_P diastereomer of phosphite triester **25** and reagent (*S*,*S*)-**2d**, the highest increase of -11.6% de was achieved. This was followed by -10.4% de from the reaction with reagent (*R*,*R*)-**2b** and phosphite triester **2**, followed by a wide range of about -1.0 to -7.6% de from the other reagents.

For the differences in selectivities achieved with the chiral analogues of MEDITH, using the selectivity of achiral MEDITH as the reference point for zero selectivity (Chart 6), it can be seen that through a match with the S_P diastereomer of the phosphite triesters, higher selectivities than those obtained with MEDITH were generally achieved with many of the chiral reagents. The highest increase of 13.2% de was achieved with reagent (*S*)-**6d**, through a match with the S_P diastereomer of phosphite triester **23**. A lower increase of 10.9% de was achieved with reagent (*S*)-**6e** through a match with the S_P diastereomer of phosphite triester **23** and, 9.9 and 9.3% with

Chart 6. Differences in de achieved with chiral analogues of MEDITH from de achieved with MEDITH[a]

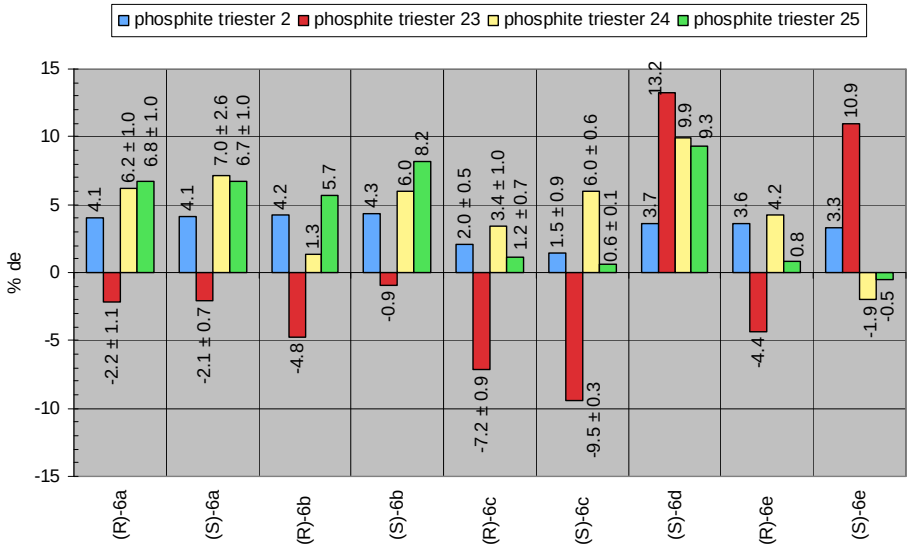

[a] the average standard deviations for the reactions repeated are included in the chart.

reagent (*S*)-**6d** through a match with the S_P diastereomer of phosphite triester **24** and **25**, respectively. With the exception of reagents (*S*)-**6d** and (*S*)-**6e**, the other reagents resulted in a switch in selectivities through a match with the R_P diastereomer of phosphite triester **23**. The highest de of -9.5% was achieved with reagent (*S*)-**6c**, followed by -7.2% with reagent (*R*)-**6c** and de's ranging from ~-1.0 to -4.8% with the other chiral reagents.

4.4 Conclusion

For screening the chiral analogues of phenylacetyl disulfide (PADS) and 5-methyl-3*H*-1,2,4-dithiazol-3-one (MEDITH), in addition to the dithymidine phosphite triester prepared by the phosphoramidite method, phosphite triesters with different degrees of steric hindrance around the phosphorus were successfully prepared via the H-phosphonate method, using BSA, TBDMSCl/Et_3N, and Ph_3SiCl/Et_3N. Because silylation occurs at the H – P=O group and on the thymine bases, it is important to use ≥ 5 equiv of the silylating reagents and for the reactions

with TBDMSCl and TPSCl, 10 equiv of Et_3N to obtain completely silylated phosphite triesters. After sulfurization, analysis of the R_{PS}:S_{PS} diastereomeric ratios of the resulting phosphite sulfides or phosphorothioates were successfully determined by RP HPLC; ^{31}P NMR did not give sufficient resolution of peaks or accuracy of peak integration to be useful.

A numerical procedure was developed to express the diastereoselectivity ($\%ds_{R(PS)}$ and $\%ds_{S(PS)}$) of the sulfurization reactions, regardless of the source of stereochemistry, and the % diastereomeric excess (% de = $\%ds_{R(PS)}$–$\%ds_{S(PS)}$) was used to compare selectivities of the reactions. It was found that the actual selectivity for giving the R_{PS} diastereomer of phosphorothioate **34** is greater. The chiral analogues of MEDITH were found to be generally more selective than the chiral analogues of PADS, but the selectivities were not predictable. Through a match with the S_P diastereomer of phosphite triester **23** (with the TMS group around the phosphorus atom), the highest actual selectivity (de of 14.7%) was achieved with MEDITH analogue (*S*)-**6d** (naproxen derivative) to give phosphorothioate (R_{PS})-**34**, followed by 12.5% with (*S*)-**6e** (ibuprofen derivative). Through a match with the R_P diastereomer of the same phosphite triester (**23**), the MEDITH analogue (*S*)-**6c** (isopropyl group at the α position) gave the highest actual selectivity (de of -7.9%).

An evaluation of the benefit from chirality reveals that the chiral analogues of PADS are generally more selectivity to the R_P diastereomer of the phosphite triesters to give S_{PS} of phosphite sulfide **26** and phosphorothioate **34**, whereas the chiral analogues of MEDITH were found to be generally more selectivity to the S_P diastereomer to the phosphite triesters. Through a match with the R_P diastereomer of the phosphite triester **25** (with the Ph_3Si group around the phosphorus atom), the PADS analogue (*S,S*)-**2d** (naproxen derivative) gave the highest de of -11.6%. Through a match with the S_P diastereomer of phosphite triester **23** (with the TMS group

around the phosphorus atom), the highest de of 13.2% was achieved with MEDITH analogue (*S*)-**6d** (naproxen derivative), followed by 10.9% with MEDITH analogue (*S*)-**6e** (ibuprofen derivative).

Since the best actual selectivities were achieved with MEDITH analogues (*S*)-**6d** (naproxen derivative of MEDITH) and (*S*)-**6e** (ibuprofen derivative of MEDITH), a suggestion for future work is to use achiral analogues of the disulfides with larger aromatic groups.

4.5 Experimental Section

General information. ^{1}H and ^{13}C NMR specra were recorded on a Bruker 400 MHz spectrometer with tetramethylsilane as an external standard. ^{31}P NMR spectra were recorded on a Bruker 400-MHz spectrometer with an external capillary containing 85% H_3PO_4 in CD_3CN. 5'-*O*-(*p,p'*-Dimethoxytrityl)thymidine **12** and 3'-*O*-(*tert*-butyldimethylsilyl)thymidine **15** were synthesized as discussed in chapter 2. Triethylamine and pyridine were distilled from calcium hydride and collected under nitrogen. 2-Chloro-4H-1,3,2-benzodioxaphosphorin-4-one was used directly from the supplier. Acetonitrile and 1,4-dioxane were distilled under nitrogen from calcium hydride. Tetrahydrofuran was dried prior to use by distillation from sodium-benzophenone. Water (HPLC grade, submicron filtered), dichloromethane, hexanes, and acetic acid were used directly from suppliers. Flash column chromatography was done using 230-400 mesh silica gel from Silicycle. Thin-layer chromatography was done on aluminum-backed silica gel F (200-µm) plates (Analtech).

Synthesis of phosphite triester 2. The synthesis of phosphite triester **2** was done on a 0.6 g scale in the same manner as described in Chapter 2. The crude compound was taken into the glove box and purified by using a short column of silica gel (~20 g of silica gel in a 60 mL coarse frit) and eluent mixture of THF/hexane (2:1). All fractions with R_f of 0.55 (THF/hexane

2:1) were evaporated under reduced pressure to afford phosphite triester **2** as a white foam (0.60 g, 94% yield). ^{1}H NMR (400 MHz, CD_3CN, two diastereomers): δ 9.37 (br s, NH, 4H), 7.48-7.26 (m, ArH/4 x H-6, 22H), 6.91-6.88 (m, ArH, 8H), 6.30 (m, 2 x ^{T1}H-1', 2H), 6.19 (m, 2 x ^{T2}H-1', 2H), 5.03 (m, 2 x ^{T1}H-3', 2H), 4.41 (m, 2 x ^{T2}H-3', 2H), 4.12 (m, 2 x ^{T1}H-4', 2H), 4.08-3.91 (m, 2 x ^{T2}H-4', 2 x ^{T2}H-5', 2 x ^{T2}H-5", 2 x CH_2OP, 10H), 3.79 (s, 2 x CH_3O, 6H), 3.78 (s, 2 x CH_3O, 6H), 3.35 (m, 2 x ^{T1}H-5', 2 x ^{T1}H-5", 4H), 2.65 (br t, *J* = 5.9 Hz, 2 x CH_2CN, 4H), 2.44 (m, 2 x ^{T1}H-2', 2 x ^{T1}H-2", 4H), 2.19 (m, 2 x ^{T2}H-2', 2 x ^{T2}H-2", 4H), 1.83 (m, 2 x CH_3C-5, 6H), 1.52 (d, *J* = 1.1 Hz, CH_3C-5, 3H), 1.50 (d, *J* = 1.1 Hz, CH_3C-5, 3H), 0.91 (s, 2 x (CH_3)$_3$CSi, 18H), 0.12 (s, (CH_3)$_2$Si, 6H), 0.10 (s, (CH_3)$_2$Si, 6H). ^{31}P NMR (161 Mz, CD_3CN, two diastereomers): δ 140.41, 140.38. HRMS (ESI): Calcd for $C_{50}H_{61}N_5O_{13}PSi$ $[M-H]^-$: 998.3773, found 998.3777.

Preparation of triethylammonium bicarbonate buffer. Et_3N (56 mL, 0.41 mol) was added to 144 mL of deionized H_2O, resulting in a two-layer solution. With vigorous stirring, pieces of dry ice (CO_2) were added to the solution until a homogeneous solution of pH ~ 8 was attained, as determined with Alkacid® test paper. The slightly yellow solution obtained was stored at rt.

Preparation of 0.1 M triethylammonium acetate (TEAA) buffer for HPLC analysis. At rt, Et_3N (13.9 mL, 0.1 mol) was added to a vigorously stirred solution of 950 mL HPLC grade H_2O and 5.6 mL of acetic acid. After ~20 min, acetic acid was added dropwise to the solution until the pH was 7.0 as determined using an Accumet® Basic pH meter (Fisher Scientific). The solution was stored in a sealed bottle and kept at rt and protected from ambient light.

Synthesis of 5'-*O*-(*p,p'*-dimethoxytrityl)thymidine 3'-(H-phosphonate) 14. Compound **14** was synthesized by following the literature procedure used for the synthesis of the

5'-*O*-(*tert*-butyldimethylsilyl) analogue of compound **14**.[150] Under nitrogen, a solution of 2-chloro-4H-1,3,2-benzodioxaphosphorin-4-one (1.0326 g, 5.0985 mmol) dissolved in 5 mL of 1,4-dioxane was added dropwise over ~3 min to a rapidly stirred solution of 5'-*O*-(*p,p'*-dimethoxytrityl)thymidine **12** (2.0107 g, 3.6921 mmol) and pyridine (0.8080 g, 10.2149 mmol) in 40 mL of 1,4-dioxane. The flask was rinsed with 5 mL of 1,4-dioxane and transferred to the reaction solution. After the solution was stirred at rt for ~20 min, 0.5 mL of water was added, and the mixture was diluted with 60 mL of CH_2Cl_2/Et_3N (99/1). The solution was washed with 25 mL of 2 M triethylammonium bicarbonate (TEAB). The organic layer was extracted and the aqueous layer was extracted with 2 x 25 mL CH_2Cl_2. The combined organic layers were dried with anhydrous $MgSO_4$, filtered, and evaporated on the rotovap to give an orange gum. The product was purified by silica gel chromatography using a 0 to 9% gradient of MeOH in 0.5% Et_3N/CH_2Cl_2 (50 g silica gel in a column of diameter 50 mm). All fractions with R_f of 0.24 (10% $MeOH/CH_2Cl_2$) were combined and evaporated on a vacuum line to afford compound **14** as a white foam (2.01 g, 77% yield). ^1H, ^{13}Cm, and ^{31}P NMRs corresponded to NMR spectra recorded with an authentic sample from ChemGene.

Synthesis of H-phosphonate 3. Compound **3** was synthesized by following the literature procedure used for the synthesis of the 5'-*O*-(*tert*-butyldimethylsilyl) analogue of compound **3**.[150] Under nitrogen, compound **14** (0.8339 g, 0.1.1749 mmol) and 3'-*O*-(*tert*-butyldimethylsilyl)thymidine **15** (0.4114 g, 1.1540 mmol) were co-evaporated with 12 mL of pyridine to remove water and then redissolved in 10 mL of pyridine. With stirring, pivaloyl chloride (0.3290 g, 2.7285 mmol) was added dropwise over ~1 min. The reaction solution was stirred at rt for 1 h, and then evaporated on the vacuum line to give a white foam. The foam was dissolved in THF and eluted through a short column of silica gel (~10 g silica gel in a 60 mL

course frit) with the aid of THF. The UV-active material that came through with the solvent front was collected and evaporated on a vacuum line to give the crude product as a white foam. The compound was purified by silica gel chromatography using a 0 to 6% gradient of MeOH in CH_2Cl_2 (60 g silica gel in a column of diameter 50 mm). The appropriate fractions with R_f of 0.6 (10% MeOH/CH_2Cl_2) were combined, and the solvents were evaporated on a vacuum line to afford H-phosphonate **3** as a white foam (0.76 g, 70 %). The ^{1}H and ^{31}P NMR spectra of the compounds correspond to the NMR spectra reported in the literature.[151]

Procedure used for screening the chiral sulfurizing reagents

The procedure used for screening the chiral sulfurizng reagents is outlined in Chart 7.

Chart 7. Procedure used for screening sulfurizing reagents

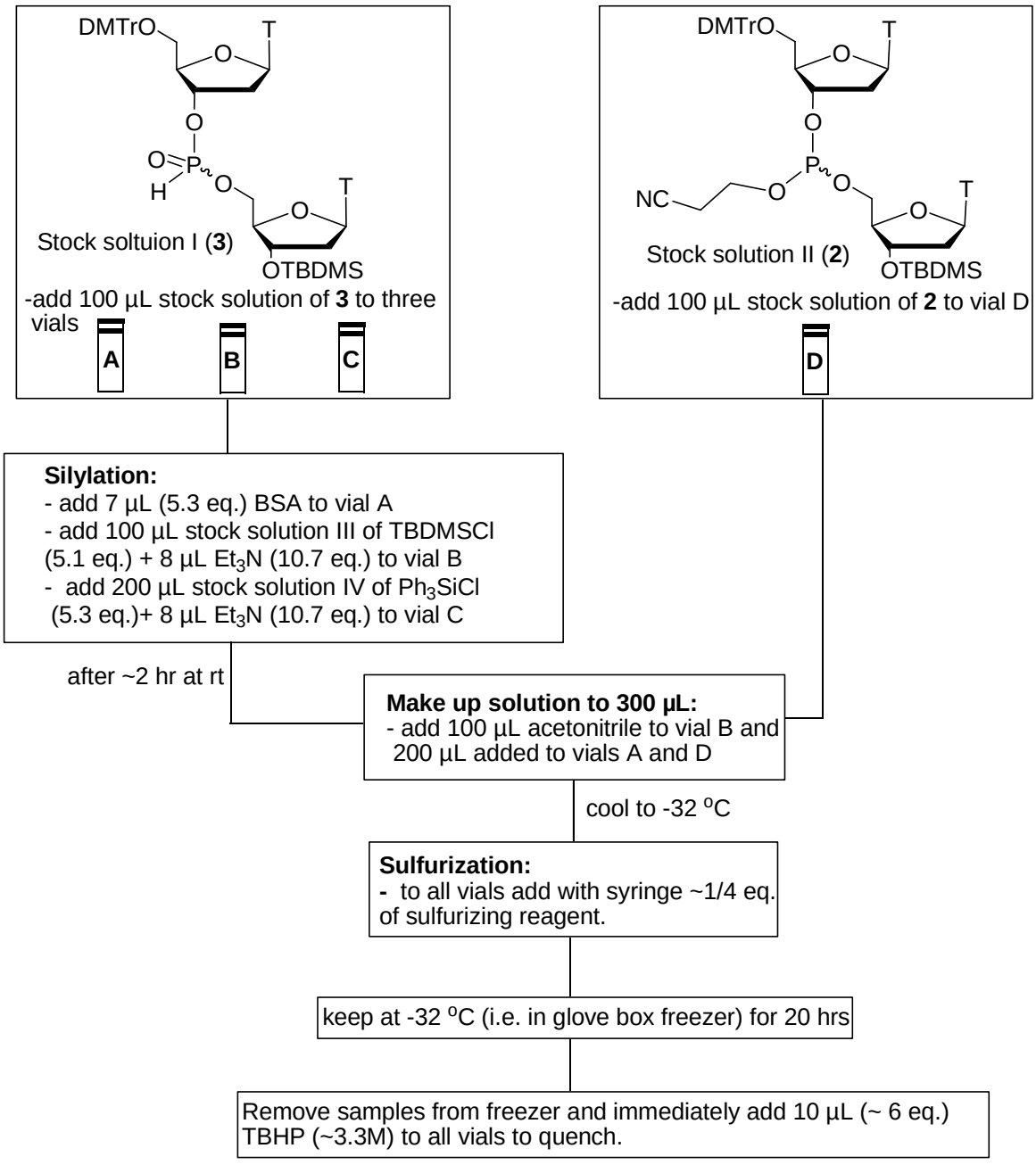

H-Phosphonate **3** and phosphite triester **2** synthesized from a single batch were used for all screening reactions. Since phosphite triester **2** and phosphite triesters **23-25** are sensitive to oxygen, the screenings of the chiral sulfurizing reagents were carried out in a nitrogen-filled glove box. Both enantiomers of a chiral sulfurizing reagent were screened simultaneously; however, the chart only shows the procedure for screening one enantiomer of the reagent.

For the screening reactions the following stock solutions were made up in acetonitrile:

(1) H-phosphonate **3** (Solution I): 0.054 M (1500 μL)

(2) Phosphite triester **2** (Solution II): 0.052 M (500 μL)

(3) Silylating reagents: (a) TBDMSCl (Solution III): 0.27 M (1250 μL)

(b) Ph_3SiCl (Solution IV): 0.14 M (2500 μL)

Solutions I and II were stored in the glove box freezer (at -32 ºC) and solutions III and IV were stored at rt. All stock solutions were used up within two weeks and fresh solutions were made for subsequent experiments in similar concentrations. Solutions of the sulfurizing reagents were prepared ~ ½ h before they were used; they were made up to concentrations ranging from ~0.02-0.09 M (quantities for each experiment are shown below in Table 6).

Following from Chart 7, 100 μL each of Solution I (~5 mg of H-phosphonate **3**, ~ 0.005 mmol) was placed into vials A, B and C and 100 μL of Solution II (~5 mg of Phosphite triester **2**, ~ 0.005 mmol) was placed in vial D. A magnetic stir bar was placed into each vial and at room temperature the following silylating reagents were added by microsyringes to the solutions in vials A, B and C:

Vial A: 7 μL of BSA (0.028 mmol, 5.3 equiv)

Vial B: 100 μL of Solution III (0.027 mmol, 5.1 equiv TBDMSCl) and 8 μL of Et_3N (0.057 mmol, 10.7 equiv)

Vial C: 200 μL of Solution IV (0.028 mmol, 5.3 equiv Ph_3SiCl) and 8 μL of Et_3N (0.057 mmol, 10.7 equiv)

After allowing the reaction solutions to sit with occasional swirling for 2 h, a clear and colorless solution was obtained in vial A and a colorless solution with white precipitate (Et_3NHCl salt) was obtained in vials B and C. Vials A, B, C and D were then placed into the glove box freezer (-32 ºC) and stirred using a magnetic stirrer placed at the bottom of the freezer. Stirring all solutions continuously was difficult due to the interference caused by the bottom of the freezer (~1½" thick) between the stirrer and the vials, and vials needed to be jolted regularly for stirring to continue. After ~15-20 min in the freezer, with stirring, ~ ¼ equivalent of a chiral sulfurizing reagent was added to each vial over ~2 min. The vials were closed quickly and the solutions stirred in the freezer for ~1 h. Stirring was stopped after 1 h and the solutions were kept at -32 ºC for another 19 h. After a total of 20 h reaction time, each vial was then taken out and 10 μL (~6 equiv) of a ~3.3 M solution of *tert*-butylhydrogen peroxide (TBHP) was immediately added to oxidize the remaining phosphite triester present in the reaction solution. After allowing the solutions to sit at rt for ~15-20 min, a yellow solution was obtained in vial A; dark orange solutions were obtained in vials B and C, and a colorless solution was formed in vial D.

Table 9. Concentrations of the stock solutions of H-phosphonate **2**, phosphite triester **3**, and sulfurizing reagents that were prepared and the quantities used for each reaction

	H-phosphonate **2**		phosphite triester **3**		sulfurizng reagents				
	[conc.][a]	mmol used	[conc.][a]	mmol used		[conc.][a]	mmol used	mol% of reagent w.r.t **2**[b]	mol% of reagent w.r.t **3**[b]
1	0.0544	0.0054	0.0524	0.0052	sulfur(excess)	0.0740	0.0081	149.51	155.36
2	0.0544	0.0054	0.0524	0.0052	sulfur	0.0740	0.0013	24.46	25.42
3	0.0596	0.0060	0.0539	0.0054	PADS	0.0660	0.0015	24.37	26.94
4	0.0596	0.0060	0.0539	0.0054	MEDITH	0.0900	0.0014	24.17	26.72
					chiral PADS analogues				
5	0.0544	0.0054	0.0524	0.0052	(*R,R*)-**2a**	0.0560	0.0014	25.71	26.72
6	0.0544	0.0054	0.0524	0.0052	(S,S)-**2a**	0.0560	0.0014	25.71	26.72
7	0.0535	0.0053	0.0524	0.0052	(*R,R*)-**2b**	0.0580	0.0013	24.95	25.46
8	0.0535	0.0053	0.0524	0.0052	(S,S)-**2b**	0.0710	0.0014	26.55	27.10
9	0.0538	0.0054	0.0511	0.0051	(*R,R*)-**2c**	0.0560	0.0014	26.04	27.39
10	0.0538	0.0054	0.0511	0.0051	(S,S)-**2c**	0.0530	0.0013	24.64	25.92
11	0.0538	0.0054	0.0510	0.0051	(S,S)-**2d**	0.0220	0.0013	24.55	25.89
					chiral MEDITH analogues				
12	0.0543	0.0054	0.0531	0.0053	(*R*)-**2a**	0.0210	0.0013	24.73	25.30
13	0.0543	0.0054	0.0531	0.0053	(*S*)-**2a**	0.0220	0.0013	24.29	24.85
14	0.0596	0.0060	0.0539	0.0054	(*R*)-**2a**	0.0270	0.0015	24.92	27.55
15	0.0596	0.0060	0.0539	0.0054	(*S*)-**2a**	0.0310	0.0015	24.45	27.03
16	0.0574	0.0057	-[c]	-[c]	(*S*)-**2a**	0.0310	0.0015	25.38	-[c]
17	0.0543	0.0054	0.0531	0.0053	(*R*)-**2b**	0.0470	0.0013	24.22	24.77
18	0.0543	0.0054	0.0531	0.0053	(*S*)-**2b**	0.0530	0.0013	24.38	24.94
19	0.0535	0.0053	0.0524	0.0052	(*R*)-**2c**	0.0770	0.0013	24.48	24.98
20	0.0535	0.0053	0.0524	0.0052	(*S*)-**2c**	0.0640	0.0013	25.13	25.65
21	0.0571	0.0057	0.0539	0.0054	(*R*)-**2c**	0.0660	0.0014	24.28	25.72
22	0.0571	0.0057	0.0539	0.0054	(*S*)-**2c**	0.0640	0.0014	24.66	26.13
23	0.0571	0.0057	-[c]	-[c]	(*S*)-**2c**	0.0640	0.0014	24.66	-[c]
24	0.0538	0.0054	0.0510	0.0051	(*S*)-**2d**	0.0230	0.0013	23.53	24.81
25	0.0571	0.0057	0.0539	0.0054	(*R*)-**2e**	0.0550	0.0014	24.08	25.51
26	0.0571	0.0057	0.0539	0.0054	(*S*)-**2e**	0.0630	0.0014	24.28	25.72

[a] concentration of stock solution prepared (M); [b] expected % of sulfurizing reagent, with respect to (w.r.t) H-phosphonate **2** or phosphite triester **3**, from aliquot used (volumes ranges from 16-65 μL); [c] no duplicate reaction carried out.

RP HPLC analysis of phosphite sulfide 26 and phosphorothioate

The column used for analyzing phosphite sulfide **26** solution (Table 10, entry 1) is a Dionex Acclaim® PolarAdvantage II C_{18} column (5 μm, 120A°, 4.6 x 150 mm). Phosphorothioate **34** (entry 2) and the mixture of phosphorothioate **34** and phosphodiester **36** solutions (entry 3) were analyzed on a Dionex Acclaim® 120 C_8 column (5 μm, 120A°, 4.6 x 250 mm).

Table 10. RP HPLC analysis of phosphite sulfide **26** and phosphorothioate **34**[a]

	Compounds[b]	Solvents	Elution time (min)	Diastereomer ratios (%)[e, f]
1	phosphite sulfide **26** (excess sulfur used)	Acetonitrile:water 65:35	15.749, 16.788 15.745, 16.788	50.59 (R_{PS}):49.41 (S_{PS}) 50.59 (R_{PS}):49.41 (S_{PS})
2	phosphorothioate **34** (excess sulfur used)	Acetonitrile:TEAA[d] 55:45	16.035, 20.158	43.44 (R_{PS}):56.56 (S_{PS})
3	Mixture of phosphorothioate **34** + phosphodiester **36**[c] (1/4 eq. sulfur used)	Acetonitrile:TEAA[d] 55:45 52:48	16.206, 20.408 24.250, 31.504 23.774, 30.778 23.910, 30.956	43.60 (R_{PS}):56.40 (S_{PS}) 43.41 (R_{PS}):56.59 (S_{PS}) 43.44 (R_{PS}):56.56 (S_{PS}) 43.61 (R_{PS}):56.39 (S_{PS})

[a] All analyses were done at 30 ºC with a flow rate of 1.0 mL/min; [b] from a 0.5 mL reaction solution 3 μL was injected into HPLC; [c] elution times for the phosphodiester (not shown in table) are 9.860 min using 55/45 solvent mix and 13.808 min using 52/48 solvent mix; [d] TEAA concentration is ~0.1 M (pH 7.0); [e] diastereomer ratios are in the same order as their elution times; [f] to test the reproducibility of the columns, two injections were made for phosphite sulfide **26** and three injections for the mixture of phosphorothioate **34** + phosphodiester **36** using the 52/48 solvent mixture.

Before running any analysis, the column was first equilibrated with the solvent mixture for ~30-40 min. For each analysis, ~3 μL of the ~0.5 mL reaction solution was injected into the HPLC.

Chromatograms were taken for a period of 35 min for phosphite sulfide **26** and 30 min for phosphorothioate **34**. For the mixture of phosphorothioate **34** and phosphodiester **36**, chromatograms were taken for a period of 30 min when the 55/45 acetonitrile/TEAA mixture was used and 40 min when the 52/48 solvent mixture was used. A simple test of the reproducibility of the C_{18} column was carried out by injecting two samples of the phosphite sulfide **26** solution in the HPLC, which resulted in identical ratios of 50.59:49.41. Using the solvent mixture of 52/48 acetonitrile/TEAA, a test of the reproducibility of the C_8 column was carried out by injecting three samples of the mixture of phosphorothioate **34** and phosphodiester **36** in the HPLC (one sample injected ~1 week after). These three analyses gave comparable ratios of 43.41:56.59, 43.44:56.56 and 43.61:56.39.

References

1. Uhlmann, E.; Peyman, A. *Chem. Rev.* **1990**, *90*, 543-584.

2. Zamecnik, P. C.; Stephenson, M. L. *Proc. Natl. Acad. Sci. USA* **1978**, *75*, 280-284.

3. Stephenson, M. L.; Zamecnik, P. C. *Proc. Natl. Acad. Sci. USA* **1978**, *75*, 285-288.

4. Matsukura, M.; Shinozuka, K.; Zon, G.; Mitsuya, H.; Reitz, M.; Cohen, J. S.; Broder, S. *Proc. Natl. Acad. Sci. USA* **1987**, *84*, 7706-7710.

5. Sepp-Lorenzino, L.; Ruddy, M. *Clin. Pharmacol. Ther.* **2008**, *84*, 628-632.

6. Scanlon, K. J. *Curr. Pharm. Biotechnol.* **2004**, *5*, 415-420.

7. Fire, A. Z. *Angew. Chem., Int. Ed.* **2007**, *46*, 6966-6984.

8. Grimm, D.; Kay, M. A. *J. Clin. Invest.* **2007**, *117*, 3633-3641.

9. Novina, C. D.; Sharp, P. A. *Nature* **2004**, *430*, 161-164.

10. Mello, C. C.; Conte, D. *Nature* **2004**, *431*, 338-342

11. Elbashir, S. M.; Harborth, J.; Lendeckel, W.; Yalcin, A.; Weber, K.; Tuschi, T. *Nature* **2001**, *411*, 494-498.

12. Alberts, B., *Essential Cell Biology*. 2nd ed.; Garland Science: New York, 2004; pp 229-263.

13. Rayburn, E. R.; Zhang, R. *Drug Discov. Today* **2008**, *13*, 513-521.

14. Manoharan, M. *Curr. Opin. Chem. Biol.* **2004**, *8*, 570-579.

15. Chiu, Y.-L.; Rana, T. M. *RNA* **2003**, *9*, 1034-1048.

16. Jiang, M.; Milner, J. *Oncogene* **2002**, *21*, 6041-6048.

17. Sepp-Lorenzino, L.; Ruddy, M. K. *Nature* **2008**, *84*, 628.

18. Stein, C. A. *Pharmacol. Ther.* **2000**, *85*, 231-236.

19. Agrawal, S.; Kandimalla, E. R. *Nat. Biotechnol.* **2004**, *22*, 1533-1538.

20. Bhattacharjee, R. N.; Akira, S. *Mini Rev. Med. Chem.* **2006**, *6*, 287-291.

21. Ashman, R.; Lenert, P. *Immunol. Res.* **2007**, *39*, 4-14.

22. Caruthers, M. H. *Acc. Chem. Res.* **1991**, *24*, 278-284.

23. Beaucage, S. L.; Caruthers, M. H. *Tetrahedron Lett.* **1981**, *22*, 1859-1862.

24. McBride, L. J.; Caruthers, M. H. *Tetrahedron Lett.* **1983**, *24*, 245-248.

25. Sinha, N. D.; Beirnat, J.; Koster, H. *Tetrahedron Lett.* **1983**, *24*, 5843-5846.

26. Froehler, B. C., *Methods in Molecular Biology. Protocols for Oligonucleotides and Analogues*. Agrawal, S., Ed.; Publisher: Totowa, New Jersey: 1993; Vol. 20, pp 63-80.

27. Stawinski, J.; Kraszewski, A. *Acc. Chem. Res.* **2002**, *35*, 952-960.

28. Iyer, R. P.; Egan, W.; Regan, J. B.; Beaucage, S. L. *J. Am. Chem. Soc.* **1990**, *112*, 1253-1254.

29. Cheruvallath, Z. S.; Carty, R. L.; Moore, M. N.; Capaldi, D. C.; Krotz, A. H.; Wheeler, P. D.; Turney, B. J.; Craig, S. R.; Gaus, H. J.; Scozzari, A. N.; Cole, D. L.; Ravikumar, V. T. *Org. Proc. Res. Dev.* **2000**, *4*, 199-204.

30. Stec, W. J.; Wilk, A. *Angew. Chem., Int. Ed. Engl.* **1994**, *33*, 709-722.

31. Hacia, J. G.; Wold, B. J.; Dervan, P. B. *Biochemistry* **1994**, *33*, 5367-5369.

32. Agrawal, S. *Nucleosides Nucleotides* **1995**, *14*, 985-989.

33. Yu, D.; Kandimalla, E. R.; Roskey, A.; Zhao, Q.; Chen, L.; Chen, J.; Agrawal, S. *Bioorg. Med. Chem.* **2000**, *8*, 275-284.

34. Stec, W. J.; Grajkowski, A.; Koziolkiewicz, M.; Uznanski, B. *Nucleic Acids Res.* **1991**, *19*, 5883-5888.

35. Wang, L.; Chen, S.; Xu, T.; Taghizadeh, K.; Wishnok, J. S.; Zhou, X.; You, D.; Deng, Z.; Dedon, P. C. *Nat. Chem. Biol.* **2007**, *3*, 709-710.

36. Eckstein, F. *Nat. Chem. Biol.* **2007**, *3*, 689-690.

37. Stec, W. J.; Grajkowski, A.; Kobylanska, A.; Karwowski, B.; Koziolkiewicz, M.; Misiura, K.; Okruszek, A.; Wilk, A.; Guga, P.; Boczkowska, M. *J. Am. Chem. Soc.* **1995**, *117*, 12019-12029.

38. Stec, W. J.; Karwowski, B.; Boczkowska, M.; Guga, P.; Koziolkiewicz, M.; Sochacki, M.; Wieczorek, M. W.; Blaszczyk, J. *J. Am. Chem. Soc.* **1998**, *120*, 7156-7167.

39. Wilk, A.; Grajkowski, A.; Phillips, L. R.; Beaucage, S. L. *J. Am. Chem. Soc.* **2000**, *122*, 2149-2156.

40. Oka, N.; Yamamoto, M.; Sato, T.; Wada, T. *J. Am. Chem. Soc.* **2008**, *130*, 16031-16037.

41. Seeman, J. I. *Chem. Rev.* **1983**, *83*, 83-134.

42. Perlikowska, W.; Gouygou, M.; Daran, J. C.; Balavoine, G.; Mikolajczyk, M. *Tetrahedron Lett.* **2001**, *42*, 7841-7846.

43. Perlikowska, W.; Gouygou, M.; Mikolajczyk, M.; Daran, J. C. *Tetrahedron: Asymmetry* **2004**, *15*, 3519-3529.

44. Baechler, R. D.; Mislow, K. *J. Am. Chem. Soc.* **1970**, *92*, 3090-3093.

45. Tang, W.; Zhang, X. *Chem. Rev.* **2003**, *103*, 3029-3070.

46. Nozaki, K.; Sakai, N.; Nanno, T.; Higashijima, T.; Mano, S.; Horiuchi, T.; Takaya, H. *J. Am. Chem. Soc.* **1997**, *119*, 4413-4423.

47. Cobley, C. J.; Gardner, K.; Klosin, J.; Praquin, C.; Hill, C.; Whiteker, G. T.; ZanottiGerosa, A.; Petersen, J. L.; Abboud, K. A. *J. Org. Chem.* **2004**, *69*, 4031-4040.

48. Fujii, M.; Ozaki, K.; Sekine, M.; Hata, T. *Tetrahedron* **1987**, *43*, 3395-3407.

49. Fujii, M.; Ozaki, K.; Kume, A.; Sekine, M.; Hata, T. *Tetrahedron Lett.* **1986**, *27*, 3365-3368.

50. Mizuguchi, M.; Makino, K. *Patent written in Japanese* **1996**, JP 08245665, 10 pp.

51. Mizuguchi, M.; Makino, K. *Nucleosides Nucleotides* **1996**, *15*, 407-417.

52. Bajwa, G. S.; Bentrude, W. G. *Tetrahedron Lett.* **1978**, *5*, 421-424.

53. Bentrude, W. G.; Sopchik, A. E.; Gajda, T. *J. Am. Chem. Soc.* **1989**, *111*, 3981-3987.

54. Hayakawa, Y.; Hirabayashi, Y.; Hyodo, M.; Yamashita, S.; Matsunami, T.; Cui, D. M.; Kawai, R.; Kodama, H. *Eur. J. Org. Chem.* **2006**, 3834-3844.

55. Huang, Y. D.; Yu, J. H.; Bentrude, W. G. *J. Org. Chem.* **1995**, *60*, 4767-4773.

56. Hommer, H.; Gordillo, B. *Phosphorus, Sulfur Silicon Relat. Elem.* **2002**, *177*, 465-470.

57. Schaller, H.; Weimann, G.; Lerch, B.; Khorana, H. G. *J. Am. Chem. Soc.* **1963**, *85*, 3821-3827.

58. Claesen, C. A. A.; Segers, R. P. A. M.; Tesser, G. I. *Recl. Trav. Chim. Pays-Bas* **1985**, *104*, 119-122.

59. Agrawal, S.; Christodoulou, L.; Gait, M. J. *Nucleic Acids Res.* **1986**, *14*, 6227-6245.

60. Schaller, H.; Weimann, G.; Lerch, B.; Khorana, H. G. *J. Am. Chem. Soc.* **1963**, *85*, 3821-3827.

61. Hayakawa, Y.; Kataoka, M. *J. Am. Chem. Soc.* **1998**, *120*, 12395-12401.

62. Eleuteri, A.; Capaldi, D. C.; Krotz, A. H.; Cole, D. L.; Ravikumar, V. T. *Org. Proc. Res. Dev.* **2000**, *4*, 182-189.

63. Ogilvie, K. K.; Thompson, E. A.; Quilliam, M. A.; Westmore, J. B. *Tetrahedron Lett.* **1974**, 2865-2868.

64. Ogilvie, K. K. *Can. J. Chem.* **1973**, *51*, 3799-3807.

65. Jin, Y.; Just, G. *Tetrahedron Lett.* **1998**, *39*, 6429-6432.

66. Iyer, R. P.; Phillips, L. R.; Egan, W.; Regan, J. B.; Beaucage, S. L. *J. Org. Chem.* **1990**, *55*, 4693-4699.

67. Hersh, W. H.; Fong, R. H. *Organometallics* **2005**, *24*, 4179-4189.

68. Vedejs, E.; Donde, Y. *J. Org. Chem.* **2000**, *65*, 2337-2343.

69. Hersh, W. H.; Xu, P.; Simpson, C. K.; Grob, J.; Bickford, B.; Hamdani, M. S.; Wood, T.; Rheingold, A. L. *J. Org. Chem.* **2004**, *69*, 2153-2163.

70. Oka, N.; Wada, T.; Saigo, K. *J. Am. Chem. Soc.* **2003**, *125*, 8307-8317.

71. Humbel, S.; Bertrand, C.; Darcel, C.; Bauduin, C.; Jugé, S. *Inorg. Chem.* **2003**, *42*, 420-427.

72. Reynolds, D. W.; Lorenz, K. T.; Chiou, H. S.; Bellville, D. J.; Pabon, R. A.; Bauld, N. L. *J. Am. Chem. Soc.* **1987**, *109*, 4960-4968.

73. Hayakawa, Y.; Kawai, R.; Hirata, A.; Sugimoto, J.; Kataoka, M.; Sakakura, A.; Hirose, M.; Noyori, R. *J. Am. Chem. Soc.* **2001**, *123*, 8165-8176.

74. Brown, H. C.; McDaniel, O. H.; Haflinger, *Determination of Organic Structures by Physical Methods*. Academic Press: New York, 1955; Vol. 1, p 573, 581.

75. Rahman, M. M.; Liu, H.-Y.; Eriks, K.; Prock, A.; Giering, W. P. *Organometallics* **1989**, *8*, 1-7.

76. Stein, C. A.; Cheng, Y.-C. *Science* **1993**, *261*, 1004-1012.

77. Dias, N.; Stein, C.A. *Mol. Cancer Ther.* **2002**, *1*, 347-355.

78. Efimov, V. A.; Kalinkina, A. L.; Chakhmakhcheva, O. G.; Schmaitz Hill, T.; Jayaraman, K. *Nucleic Acids Res.* **1995**, *23*, 4029-4033.

79. Zhang, Z.; Nichols, A.; Alsbeti, M.; Tang, J. X.; Tang, J. Y. *Tetrahedron Lett.* **1998**, *39*, 2467-2470.

80. Song, Q.; Wang, Z.; Sanghvi, Y. S. *Nucleosides, Nucleotides Nucleic Acids* **2003**, *22*, 629-633.

81. Kamer, P. C. J.; Roelen, H. C. P. F.; van den Elst, H.; van der Marel, G. A.; van Boom, J. H. *Tetrahedron Lett.* **1989**, *30*, 6757-6760.

82. Roelen, H. C. P. F.; Kamer, P. C. J.; van den Elst, H.; van der Marel, G. A.; van Boom, J. H. *Recl. Trav. Chim. Pays-Bas* **1991**, *110*, 325-331.

83. Vu, H.; Hirschbein, B. L. *Tetrahedron Lett.* **1991**, *32*, 3005-3008.

84. Rao, M. V.; Reese, C. B.; Zhao, Z. *Tetrahedron Lett.* **1992**, *33*, 4839-4842.

85. Stec, W. J.; Uznanski, B.; Wilk, A.; Hirschbein, B. L.; Fearon, K. L.; Bergot, B. J. *Tetrahedron Lett.* **1993**, *34*, 5317-5320.

86. Rao, M. V.; Macfarlane, K. *Tetrahedron Lett.* **1994**, *35*, 6741-6744.

87. Xu, Q.; Musier-Forsyth, K.; Hammer, R. P.; Barany, G. *Nucleic Acids Res.* **1996**, *24*, 1602-1607.

88. Arterburn, J. B.; Perry, M. C. *Tetrahedron Lett.* **1997**, *38*, 7701-7704.

89. Zhang, Z.; Nichols, A.; Tang, J. X.; Alsbeti, M.; Tang, J. Y. *Nucleosides Nucleotides* **1997**, *16*, 1585 - 1588.

90. Zhang, Z.; Nichols, A.; Tang, J. Y. *Tetrahedron Lett.* **1999**, *40*, 2095-2098.

91. Tang, J.-T.; Han, Y.; Tang, J. X.; Zhang, Z. *Org. Proc. Res. Dev.* **2000**, *4*, 194-198.

92. Ju, J.; McKenna, C. E. *Bioorg. Med. Chem. Lett.* **2002**, *12*, 1643-1645.

93. Zhang, Z.; Han, Y.; Tang, J. X.; Tang, J. *Tetrahedron Lett.* **2002**, *43*, 4347-4349.

94. Cheruvallath, Z. S.; Kumar, R. K.; Rentel, C.; Cole, D. L.; Ravikumar, V. T. *Nucleosides, Nucleotides Nucleic Acids* **2003**, *22*, 461-468.

95. Krotz, A. H.; Gorman, D.; Mataruse, P.; Foster, C.; Godbout, J. D.; Coffin, C. C.; Scozzari, A. N. *Org. Proc. Res. Dev.* **2004**, *8*, 852-858.

96. Hyodo, M.; Sato, Y.; Yamashita, S.; Hattori, A.; Kambe, E.; Kataoka, M.; Hayakawa, Y. *Tetrahedron* **2005**, *61*, 965-970.

97. Krotz, A. H.; Hang, A.; Gorman, D.; Scozzari, A. N. *Nucleosides, Nucleotides Nucleic Acids* **2005**, *24*, 1293-1299.

98. Wyrzykiewicz, T. K.; Cole, D. L. *Bioorg. Chem.* **1995**, *23*, 33-41.

99. Cheruvallath, Z. S.; Sasmor, H.; Cole, D. L.; Ravikumar, V. T. *Nucleosides, Nucleotides Nucleic Acids* **2000**, *19*, 533-543.

100. The usual name quoted in the literature, 3-methyl-1,2,4-dithiazolin-5-one, appears to us to be in error; the parent ring system is fully unsaturated (hence the "ol" ring termination) and the position of the unsaturation is indicated by giving the *H* the lowest available number.

101. Kodomari, M.; Fukuda, M.; Yoshitomi, S. *Synthesis* **1981**, 637-638.

102. Tamami, B.; Kiasat, A. R. *Synth. Commun.* **1998**, *28*, 1275-1280.

103. Jia, X.-S.; Liu, X.-T.; Li, Q.; Huang, Q.; Kong, L.-L. *J. Chem. Res.* **2006**, 547-548.

104. Nagasawa, K.; Yoshitake, S.; Amiya, T.; Ito, K. *Synth. Commun.* **1990**, *20*, 2033-2040.

105. Flack, H. D. *Acta Crystallogr., Sect. A: Found. Crystallogr.* **1983**, *39*, 876-881.

106. Flack, H. D.; Bernardinelli, G. *Chirality* **2008**, *20*, 681-690.

107. Pettersson, K. *Ark. Kemi* **1956**, *10*, 283-96.

108. Aaron, C.; Dull, D. L.; Schmiegel, J. L.; Jaeger, D.; Ohashi, Y.; Mosher, H. S. *J. Org. Chem.* **1967**, *32*, 2797-2803.

109. Clark, D. R.; Mosher, H. S. *J. Org. Chem.* **1970**, *35*, 1114-1118.

110. Wang, M.-X.; Lu, G.; Ji, G.-J.; Huang, Z.-T.; Meth-Cohn, O.; Colby, J. *Tetrahedron: Asymmetry* **2000**, *11*, 1123-1135.

111. Wu, Z.-L.; Li, Z.-Y. *Tetrahedron: Asymmetry* **2001**, *12*, 3305-3312.

112. Kinbara, K.; Kobayashi, Y.; Saigo, K. *J. Chem. Soc., Perkin Trans. 2* **1998**, 1767-1775.

113. Kinbara, K.; Kobayashi, Y.; Saigo, K. *J. Chem. Soc., Perkin Trans 2* **2000**, 111-119.

114. Koshima, H.; Nakagawa, T.; Matsuura, T. *Tetrahedron Lett.* **1997**, *38*, 6063-6066.

115. Lemmerer, A.; Bathori, N. B.; Bourne, S. A. *Acta Crystallogr., Sect. B: Struct. Sci.* **2008**, *64*, 780-790.

116. Volonterio, A.; Bravo, P.; Capelli, S.; Meille, S. V.; Zanda, M. *Tetrahedron Lett.* **1997**, *38*, 1847-1850.

117. Rout, G. C.; Seshasayee, M.; Subrahmanyan, T.; Aravamudan, G. *Acta Crystallogr., Sect. C: Cryst Struct. Commun.* **1983**, *39*, 1387-1389.

118. Paul, C.; Srikrishnan, T. *J. Chem. Crystallogr.* **2004**, *34*, 211-217.

119. Niyomura, O.; Kitoh, Y.; Nagayama, K.-I.; Kato, S. *Sulfur Lett.* **1999**, *22*, 195-207.

120. Niyomura, O.; Kato, S.; Inagaki, S. *J. Am. Chem. Soc.* **2000**, *122*, 2132-2133.

121. Bereman, R. D.; Baird, D. M.; Bordner, J.; Dorfman, J. R. *Polyhedron* **1983**, *2*, 25-30.

122. Beyer, L.; Richter, R.; Seidelmann, O. *J. Prakt. Chem.* **1999**, *341*, 704-726.

123. Li, F.; Yin, H. D.; Hong, M.; Zhai, J.; Wang, D. Q. *Acta Crystallogr., Sect. E: Struct. Rep. Online* **2006**, *E62*, o1417-o1418.

124. Erben, M. F.; Della Vedova, C. O.; Willner, H.; Trautner, F.; Oberhammer, H.; Boese, R. *Inorg. Chem.* **2005**, *44*, 7070-7077.

125. Erben, M. F.; Della Vedova, C. O.; Willner, H.; Boese, R. *Eur. J. Inorg. Chem.* **2006**, 4418-4425.

126. Higashi, L. S.; Lundeen, M.; Seff, K. *J. Am. Chem. Soc.* **1978**, *100*, 8101-8106.

127. Colman, E.-.; Harpp, D. N. *J. Sulfur Chem.* **2004**, *25*, 291-316.

128. Eliel, E. L.; Wilen, S. H.; Mander, L. N., *Stereochemistry of Organic Compounds*. Wiley-Interscience: New York, 1994.

129. Imrie, C.; Cook, L.; Levendis, D. C. *J. Organomet. Chem.* **2001**, *637-639*, 266-275.

130. Frisch, M. J.; Trucks, G. W.; Schlegel, H. B.; Scuseria, G. E.; Robb, M. A.; Cheeseman, J. R.; Montgomery, Jr., J. A.; Vreven, T.; Kudin, K. N.; Burant, J. C.; Millam, J. M.; Iyengar, S. S.; Tomasi, J.; Barone, V.; Mennucci, B.; Cossi, M.; Scalmani, G.; Rega, N.; Petersson, G. A.; Nakatsuji, H.; Hada, M.; Ehara, M.; Toyota, K.; Fukuda, R.; Hasegawa, J.; Ishida, M.; Nakajima, T.; Honda, Y.; Kitao, O.; Nakai, H.; Klene, M.; Li, X.; Knox, J. E.; Hratchian, H. P.; Cross, J. B.; Bakken, V.; Adamo, C.; Jaramillo, J.; Gomperts, R.; Stratmann, R. E.; Yazyev, O.; Austin, A. J.; Cammi, R.; Pomelli, C.; Ochterski, J. W.; Ayala, P. Y.; Morokuma, K.; Voth, G. A.; Salvador, P.; Dannenberg, J. J.; Zakrzewski, V. G.; Dapprich, S.; Daniels, A. D.; Strain, M. C.; Farkas, O.; Malick, D. K.; Rabuck, A. D.; Raghavachari, K.; Foresman, J. B.; Ortiz, J. V.; Cui, Q.; Baboul, A. G.; Clifford, S.; Cioslowski, J.; Stefanov, B. B.; Liu, G.; Liashenko, A.; Piskorz, P.; Komaromi, I.; Martin, R. L.; Fox, D. J.; Keith, T.; Al-Laham, M. A.; Peng, C. Y.; Nanayakkara, A.; Challacombe, M.; Gill, P. M. W.; Johnson, B.; Chen, W.; Wong, M. W.; Gonzalez, C.; and Pople, J. A.; *Gaussian 03W, Revision D.01*, Gaussian, Inc., Wallingford CT, 2004.

131. Hersh, W. H. unpublished results.

132. Fisher, L. E.; Caroon, J. M.; Stabler, S. R.; Lundberg, S.; Zaidi, S.; Sorensen, C. M.; Sparacino, M. L.; Muchowski, J. M. *Can. J. Chem.* **1994**, *72*, 142-145.

133. Allegretti, M.; Bertini, R.; Cesta, M. C.; Bizzarri, C.; Di Bitondo, R.; Di Cioccio, V.; Galliera, E.; Berdini, V.; Topai, A.; Zampella, G.; Russo, V.; Di Bello, N.; Nano, G.; Nicolini, L.; Locati, M.; Fantucci, P.; Florio, S.; Colotta, F. *J. Med. Chem.* **2005**, *48*, 4312-4331.

134. Yde, B.; Yousif, N. M.; Pedersen, U.; Thomsen, I.; Lawesson, S.-O. *Tetrahedron* **1984**, *40*, 2047-2052.

135. Bishop, J. E.; Dagam, S. A.; Rapoport, H. *J. Org. Chem.* **1989**, *54*, 1876-1883.

136. Polshettiwar, V.; Kaushik, M. P. *Tetrahedron Lett.* **2006**, *47*, 2315-2317.

137. Shalaby, M. A.; Grote, C. W.; Rapoport, H. *J. Org. Chem.* **1996**, *61*, 9045-9048.

138. Zumach, G.; Kühle, E. *Angew. Chem., Int. Ed. Engl.* **1970**, *9*, 54-63.

139. Goerdeler, J.; Nandi, K. *Chem. Ber.* **1975**, *108*, 3066-3070.

140. Goerdeler, J.; Nandi, K. *Chem. Ber.* **1981**, *114*, 549-563.

141. Chen, L.; Thompson, T. R.; Hammer, R. P.; Barany, G. *J. Org. Chem.* **1996**, *61*, 6639-6645.

142. Roy, S. K.; Tang, J.-Y. *Sulfurizing reagent: 3-Aryl-1,2,4-dithiazoline-5-one*. US 6,500,944 B2, Dec. 31, 2002, 2002.

143. Davulcu, A. H.; McLeod, D. D.; Li, J.; Katipally, K.; Littke, A.; Doubleday, W.; Xu, Z.; McConlogue, C. W.; Lai, C. J.; Gleeson, M.; Schwinden, M.; Parsons, R. L., Jr. *J. Org. Chem.* **2009**, *74*, 4068-4079.

144. Tsuchihashi, G. *Tetrahedron Lett.* **1982**, *23*, 5427-5430.

145. Ebbers, E. J.; Ariaans, G. J. A.; Bruggink, A.; Zwanenburg, B. *Tetrahedron: Asymmetry* **1999**, *10*, 3701-3718.

146. Zalkow, L. H.; Glinski, J. A.; Gelbaum, L. T.; Moore, D.; Melder, D.; Powis, G. *J. Med. Chem.* **1988**, *31*, 1520-1526.

147. Kume, A.; Fugii, M.; Sehine, M.; Hata, T. *J. Org. Chem.* **1984**, *49*, 2139-2143.

148. Sergueeva, Z. A.; Sergueev, D. S.; Shaw, B. R. *Tetrahedron Lett.* **1999**, *40*, 2041-2044.

149. Sergueev, D. S.; Shaw, B. R. *J. Am. Chem. Soc.* **1998**, *120*, 9417-9427.

150. de Vroom, E.; Dreef, C. E.; van den Elst, H.; van der Marel, G. A.; van Boom, J. H. *Recl. Trav. Chim. Pays-Bas* **1988**, *107*, 592-595.

151. Seela, F.; Kretschmer, U. *J. Org. Chem.* **1991**, *56*, 3861-3869.

152. Gawley, R. E. *J. Org. Chem.* **2006**, *71*, 2411-2416.

153. Seebach, D.; Boes, M.; Naef, R.; Schweizer, W. B. *J. Am. Chem. Soc.* **1983**, *105*, 5390-5398.

154. Gaytan, P. *BioTechniques* **2009**, *47*, 701-702.

155. Stec, W. J.; Zon, G. *J. Chromatogr.* **1985**, *326*, 263-280.